



UNIVERSITY OF
LIVERPOOL

Interplay of MicroRNAs and Ion Channels Differentially Expressed Between Tracheal and Articular Chondrocytes

*Thesis submitted in accordance with the requirements of the University of Liverpool for the
degree of Doctor in Philosophy by:*

Lina Abdul Kadir BSc. MRes.

Department of Musculoskeletal Biology, Institute of Ageing and Chronic Disease, Faculty of
Health & Life Sciences, University of Liverpool, William Henry Duncan Building, 6 West
Derby Street, Liverpool, L7 8TX

January 2021

DEDICATION

This thesis is dedicated to my late grandmother who always believed in me, prayed for me, and encouraged me to keep learning. May Allah rest her soul in peace.

اهداء لجدتي رحمها الله التي دائما دعمتني و شجعتني في كل مجالات حياتي

ABSTRACT

Cartilage is made up of a single cell type, chondrocytes, which synthesise the extracellular matrix in which they reside in. Despite being non-excitabile cells, chondrocytes' cell membrane is rich in ion channels. The expression profiles and physiological roles of ion channels in articular chondrocytes are well characterised compared to tracheal chondrocytes, where little is known. The Ca^{2+} -activated chloride channel (CaCC), Ano1 and the voltage-gated Ca^{2+} Channel, $\text{Ca}_v3.2$ are essential for normal tracheal cartilage formation. Deletion of Ano1 and $\text{Ca}_v3.2$ leads to the deformation of cartilage rings and premature death of mice. MicroRNAs (miRNAs) have also been implicated in the deformation of cartilage rings and the pathogenesis of tracheomalacia, which is characterised by the collapsibility of the trachea. miRNA regulation of ion channels in chondrocytes has not been previously shown. In this study, I aim to identify the tracheal chondrocyte transcriptome and channelome using RNA-sequencing and compare to that of articular chondrocytes. I also aim to elucidate the interplay of miRNA and ion channels between tracheal and articular chondrocyte and investigate the effect of miRNAs on chondrocyte function.

Chondrocytes were isolated from rat tracheal and articular cartilage with collagenase digestion. Deep RNA sequencing of chondrocytes was performed to unbiasedly detect their transcriptome and channelome. miRNA upstream regulators were bioinformatically identified and validated with qPCR quantification. To interrogate the role of selected miRNAs, chondrocytes were transfected with miR-141-3p and its effect on chondrocyte physiology was assessed using functional assays. Patch-clamp

electrophysiology was used to characterise the single channel fingerprints of ion channel subtypes and pharmacological agents were used to validate their identity.

Tracheal and articular chondrocytes were shown to share a similar transcriptome and channelome; however distinct differences in ion channel subtypes were observed. miR-141-3p, identified amongst the top upstream regulators ($p < 0.00002$), had a putative target site in the 3'-UTR region of the volume regulated anion channel (VRAC), *Lrrc8a* and caused its downregulation in both chondrocyte types (T: $p < 0.000002$, A: $p < 0.00001$) whereas the inhibition of miR-141-3p caused its upregulation (T: $p < 0.006$, A: $p < 0.005$). miR-141-3p depolarised the resting membrane potential (RMP) of tracheal chondrocytes ($p < 0.01$) and decreased their proliferation ($p < 0.007$). It also increased the migration of tracheal chondrocytes ($p < 0.01$) which was decreased with the addition of CaCC antagonist, CaCCinh-A01 (20 μM). Patch-clamp electrophysiology detected VRAC currents in tracheal chondrocytes which were inhibited with the VRAC antagonist DCPIB (40 μM) at -100 mV (K_D : 3.28 ± 0.008 μM ; $p < 0.05$).

In this thesis, one of the first detailed molecular and electrophysiological studies of tracheal chondrocytes was undertaken. Together these data show for the first time the elucidation of the tracheal chondrocyte channelome and the novel interplay of miR-141-3p and ion channels in chondrocyte physiology that leads to functional changes that affect chondrocytes' RMP, proliferation and migration.

ACKNOWLEDGEMENTS

First and foremost, I would like to express my sincere gratitude to my supervisors Prof. Richard Barrett-Jolley & Dr. Kasia Goljanek-Whysall for conceiving this project and their assistance at every stage of this research project. I am indebted for their immense knowledge, invaluable advice, and continuous support during my PhD studies. I would also like to express my deepest appreciation to The University of Liverpool; these studies would never have taken place without the funding they have provided.

I would like to offer a special thanks to Dr. Fiona O'Brien who has continually encouraged me in my academic research and daily life. As well as my lab colleagues Dr. Caroline Staunton, Dr. Rhiannon Morgan, Dr. Numan Celik and Dr. Omar Haidar for their friendship and a cherished time spent together. Thank you to my friends and peers Euan and Adam for making me laugh and keeping me well fed and caffeinated throughout my PhD. I would also like to thank everyone who has helped and supported me over the course of my studies; too many to personally mention here.

I am extremely grateful for my Mum and Dad for their continuous and unparalleled love, prayers, and support throughout all my studies. I would not be where I am without their sacrifices and encouragement. Thank you for always believing in me. I am also deeply thankful for my siblings Abdul, Mahmood, and Mariam for always being there for me and Milo and Nova for making me happy. I am extremely grateful and indebted to my partner Ali for his unwavering love, kindness, and encouragement. Thank you for keeping me sane and helping me through the dark times. I would not have been able to do this without you.

Last but not least I would also like to extend my deepest gratitude to my friends Bushra, Kira, Misso, and Noor for their profound belief in my abilities, love, and encouragement throughout our friendship, it means so much.

LIST OF ABBREVIATIONS

3'-UTR	3'-Untranslated Region
Acan	Aggrecan
AGO	Argonaute
Anos	Anoctamins
ASIC	Acid Sensing Ion channels
BK	Large conductance calcium-activated potassium channel
BMP	Bone morpho-genetic proteins
BPS	British Pharmacological Society
<i>C. elegans</i>	<i>Caenorhabditis elegans</i>
CaCC	Calcium-activated Chloride Channels
CaCCinh-A01	6-(1,1-Dimethylethyl)-2-[(2-furanylcarbonyl)amino]-4,5,6,7-tetrahydrobenzo[b] thiophene-3-carboxylic acid
CAGE	Cap analysis gene expression
cDNA	Circular DNA
ceRNA	Competing endogenous RNA
Col10a	Collagen type 10 α 1
Col2a1	Collagen type 2 α 1
DCPIB	4-[(2-Butyl-6,7-dichloro-2-cyclopentyl-2,3-dihydro-1-oxo-1H-inden-5-yl)oxy]butanoic acid
DGCR8	DiGeorge Syndrome Critical Region 8
DMEM	Dulbecco's modified Eagle's medium

ds-cDNA	Double stranded circular DNA
DTT	Dithiothreitol
ECM	Extracellular matrix
ENaC	Epithelial sodium channel
EPYC	Epiphycan
EST	Expressed sequence tag
Exp5	Exportin 5
FAK	Focal adhesion kinase
FCS	Foetal calf serum
FGF	Fibroblast growth factor
FPKM	Fragments per kilobase of transcript per million mapped reads.
<i>g</i>	Conductance
GERD	Gastroesophageal reflux disease
HDAC4	Histone deacetylase 4
IGF	Insulin growth factor
IGF-1	Insulin growth factor 1
Ihh	Indian hedgehog
IL1-β	Interleukin-1 β
IPA	Ingenuity pathway analysis
IUPHAR	International union of basic and clinical pharmacology
IV	Current-voltage curve
K_{2P}	Two-pore domain potassium channel
K_{ATP}	ATP- sensitive potassium channels

K_D	Dissociation constant
K_{IR}	Inward rectifier potassium channel
K_V	Voltage-gated Potassium channel
lncRNA	Long non-coding RNA
Lrrc8	Leucine rich repeat containing 8
MAP	Molecular activity predictor
miRDIP	MicroRNA data integration portal
miRNA	MicroRNA
Mmp	Matrix metalloproteinases
MSCs	Mesenchymal stem cells
NGS	Next generation sequencing
NMDAR	Ionotropic glutamate receptors
nt	Nucleotide
OA	Osteoarthritis
PAC	Proton-activated chloride channel
PCA	Principal component analysis
PDGF	Platelet-derived growth factor
PFA	Paraformaldehyde
piRNA	Piwi-interacting RNA
P_o	Open probability
pri-RNA	Primary miRNA
PTHrP	Parathyroid hormone-related protein
qPCR	Quantitative polymerase chain reaction

RA	Rheumatoid arthritis
RISC	RNA-induced silencing complex
RMP	Resting membrane potential
RNase	Ribonuclease
RNA-Seq	RNA sequencing
RUNX2	Runt-related transcription factor 2
RVD	Regulated volume decrease
RVI	Regulated volume increase
SAGE	Serial analysis of gene expression
Shh	Sonic hedgehog
siRNA	Small interfering RNA
SK	Small conductance calcium-activated potassium channel
SNPs	Single nucleotide polymorphisms
TDMD	Target-directed miRNA degradation
TEA	Tetraethylammonium
TGF-β	Transforming growth factor- β
TGFβ4	Transforming growth factor- β 4
TIMPS	Tissue inhibitors of Mmps
TM	Tracheomalacia
Tm	Melting temperature
TNFα	Tumour necrosis factor α
TRAF5	Tumour necrosis factor receptor-associated factor 5
TRP	Transient receptor potential channel

TRPA	Transient receptor potential ankyrin channel
TRPC	Transient receptor potential canonical channel
TRPM	Transient receptor potential melastatin channel
TRPML	Transient receptor potential mucolipin channel
TRPN	Transient receptor potential no mechanoreceptor potential C channel
TRPP	Transient receptor potential polycystin channel
TRPV	Transient receptor potential vanilloid channel
TRPV4	Transient receptor potential vanilloid 4 channel
VGCC	Voltage-gated calcium channel
VGSC	Voltage-gated sodium channel
V_m	Membrane potential
VRAC	Volume regulated anion channel
V_{REV}	Reversal potential
Wnt	Wingless factor

LIST OF FIGURES

Figure 1.1: The structure of hyaline articular and tracheal cartilage.	5
Figure 1.2: Embryonic development of cartilage.	9
Figure 1.3: Canonical pathway of miRNA biogenesis and processing.	32
Figure 2.1: Workflow of RNA-sequencing sample preparation and library construction.	47
Figure 3.1: Workflow of RNA-sequencing analysis.	65
Figure 3.2: Representative immunofluorescence of chondrocyte markers in tracheal and articular chondrocytes.	70
Figure 3.3: Differential expression of chondrocyte markers between tracheal and articular chondrocytes.	72
Figure 3.4: Principal component analysis (PCA) of global RNA-Seq gene expression between tracheal and articular chondrocytes.	73
Figure 3.5: Top Canonical pathways and upstream regulators identified using IPA.	77
Figure 3.6: Chondrocyte pathways with Molecular Activity Predictor (MAP) overlay.	79
Figure 3.7: Venn diagram of differential ion channel gene expression between tracheal and articular chondrocytes.	81
Figure 3.8: Heat map of the ion channel differential gene expression in tracheal and articular chondrocytes.	82
Figure 3.9: RNA-seq differential expression of ligand-gated ion channel genes.	85
Figure 3.10: RNA-seq differential expression of voltage-gated ion channel genes.	89
Figure 3.11: RNA-seq differential expression of potassium ion channel genes.	92
Figure 3.12: RNA-seq differential expression of 'other' ion channel genes.	94
Figure 3.13: RNA-seq differential expression of chloride ion channels genes.	96
Figure 3.14: Summary of chondrocyte channelome.	97
Figure 3.15: Relative gene expression of chloride ion channel genes in rat tracheal and articular chondrocytes.	100

Figure 4.1: Relative expression of miRNAs identified as upstream regulators between tracheal and articular chondrocytes obtained using qPCR quantification.	126
Figure 4.2: Gene ontology analysis of miR-141-3p targets.	131
Figure 4.3: Representative immunofluorescence of tracheal chondrocytes transfected with miR-141-3p.	134
Figure 4.4: qPCR quantification of relative expression of miR-141-3p levels following transfection of tracheal and articular chondrocytes with miR-141-3p.	135
Figure 4.5: qPCR quantification of relative expression of ion channel genes in tracheal and articular chondrocytes following transfection with miR-141-3p.	138
Figure 4.6: Comparison of expression levels of ion channel genes between tracheal and articular chondrocytes following transfection with miR-141-3p using qPCR quantification.	139
Figure 5.1: RMP measurement of tracheal chondrocytes transfected with miR-141-3p mimic and antagomiR.	159
Figure 5.2: Ki67 immunocytochemistry staining of tracheal and articular chondrocytes following transfection with miR-141-3p mimic and antagomiR.	163
Figure 5.3: Proliferation of tracheal and articular chondrocytes assessed with Ki67 immunocytochemistry staining.	166
Figure 5.4: Rate of migration of tracheal chondrocytes transfected with miR-141-3p assessed with wound scratch assay.	168
Figure 6.1: Comparison of the RMP between tracheal and articular chondrocytes under normal physiological conditions.	186
Figure 6.2: Representative Single channel activity of a chloride-like ion channel in cell-attached patch-clamp mode.	189
Figure 6.3: K-means clustering of single channels measured using different recording solutions.	190
Figure 6.4: Representative Single channel activity of a non-specific cation-like ion channel in cell-attached patch-clamp mode.	192
Figure 6.5: Representative Single channel activity of a sodium-like ion channel in cell-attached patch-clamp mode.	193

Figure 6.6: Representative Single channel activity of a potassium-like ion channel in cell-attached patch-clamp mode.	194
Figure 6.7: Representative Single channel activity of VRAC channel in cell-attached patch-clamp mode.	195
Figure 6.8: The effect of low pH on RMP of tracheal and articular chondrocytes.	199

LIST OF TABLES

Table 1.1: Ion channels expressed in chondrocytes.	20
Table 2.1: First strand cDNA synthesis for mRNA quantification using qPCR.	50
Table 2.2: First strand cDNA synthesis for miRNA quantification using qPCR.	51
Table 2.3: Reagents used per reaction of qPCR run for mRNA and miRNA.	51
Table 2.4: qPCR conditions for mRNA and miRNA quantification.	52
Table 2.5: Ionic composition of solutions used during electrophysiology recordings.....	55
Table 2.6: Liquid junction potentials calculated for the electrophysiological solutions.	56
Table 3.1: Chondrocyte markers identified from the literature.	61
Table 3.2: Ano primers designed by Primerdesign Ltd., UK.	67
Table 3.3: Ion channel primers designed using Primerblast NCBI.	68
Table 4.1: miRNA primers designed by Qiagen, UK.	121
Table 4.2: Ion channel gene primers for qPCR quantification designed by Primerdesign Ltd., UK and Primerblast NCBI.....	122
Table 4.3: miR-141-3p negative control, mimic and antagomiR primers designed by Qiagen, UK.	122
Table 4.4: miRNA upstream regulators identified from RNA-seq data using IPA upstream regulator analysis (Qiagen, UK).	124
Table 5.1: Summary of the effect of miR-141-3p mimic and antagomiR transfection on the RMP, proliferation and migration of tracheal and articular chondrocytes.	169
Table 6.1: pH-sensitive ion channels significantly differentially expressed in tracheal chondrocytes in comparison to articular chondrocytes.	198
Table A.1: Genes differentially expressed between tracheal and articular chondrocytes.....	228
Table A.2: Top 50 significantly differentially expressed genes identified using DESEQ2 analysis between tracheal and articular chondrocytes.....	228

CONTENTS

DEDICATION.....	i
ABSTRACT	ii
ACKNOWLEDGEMENTS.....	iv
LIST OF ABBREVIATIONS	v
LIST OF FIGURES.....	x
LIST OF TABLES.....	xiii
CONTENTS.....	xiv
1 INTRODUCTION.....	1
1.1 CARTILAGE AND CHONDROCYTES.....	2
1.1.1 <i>Cartilage</i>	2
1.1.2 <i>Chondrocyte role and function</i>	7
1.1.3 <i>Chondrogenesis</i>	8
1.1.4 <i>ECM production and regulation by chondrocytes</i>	11
1.1.5 <i>Diseases of cartilage</i>	11
1.2 ION CHANNELS	15
1.2.1 <i>Definition and classification of ion channels</i>	15
1.2.2 <i>Ion channel families</i>	16
1.2.3 <i>Role of ion channels in chondrocyte physiology and disease</i>	18
1.3 MICRORNA-MEDIATED REGULATION OF GENE EXPRESSION	28
1.3.1 <i>MicroRNA biogenesis, nomenclature, and regulation</i>	29
1.3.2 <i>MicroRNAs in cartilage physiology and disease</i>	35
1.4 AIMS.....	40
2 MATERIALS AND METHODS	42
2.1 TISSUE COLLECTION AND CELL PREPARATION.....	43
2.1.1 <i>Animals</i>	43
2.1.2 <i>Tracheal Chondrocytes</i>	43

2.1.3	<i>Articular Chondrocytes</i>	44
2.2	IMMUNOFLUORESCENCE	44
2.3	RNA-SEQUENCING.....	45
2.3.1	<i>RNA extraction</i>	45
2.3.2	<i>RNA preparation and library construction</i>	46
2.4	QUANTITATIVE POLYMERASE CHAIN REACTION (qPCR)	48
2.4.1	<i>RNA extraction</i>	48
2.4.2	<i>First strand cDNA synthesis</i>	49
2.4.3	<i>Quantitative Polymerase Chain Reaction (qPCR)</i>	50
2.5	ELECTROPHYSIOLOGY	53
2.5.1	<i>Single-channel electrophysiological recordings</i>	53
2.5.2	<i>Equilibrium potentials</i>	54
2.6	STATISTICAL ANALYSIS	56
3	COMPARISON BETWEEN TRACHEAL AND ARTICULAR CHONDROCYTE TRANSCRIPTOME AND CHANNELOME.....	57
3.1	INTRODUCTION.....	58
3.1.1	<i>RNA-sequencing for transcriptome profiling</i>	58
3.1.2	<i>Chondrocyte markers</i>	60
3.1.3	<i>Ion channels in chondrocytes</i>	62
3.1.4	<i>Aims</i>	62
3.2	METHODS	63
3.2.1	<i>Immunofluorescence</i>	63
3.2.2	<i>RNA sequencing</i>	63
3.2.3	<i>Ingenuity Pathway Analysis (IPA)</i>	65
3.2.4	<i>Quantitative polymerase reaction (qPCR)</i>	66
3.2.5	<i>Identifying differentially expressed ion channel genes</i>	69
3.3	RESULTS.....	69

3.3.1	<i>Expression of chondrocyte markers in isolated tracheal and articular chondrocytes. .</i>	69
3.3.2	<i>Assessment of global tracheal and articular chondrocyte differential gene expression</i>	
	71	
3.3.3	<i>Top canonical pathways identified between tracheal and articular chondrocytes.</i>	74
3.3.4	<i>Expression of ion channel families in tracheal and articular chondrocytes.....</i>	80
3.3.5	<i>Validation of chloride ion channel expression between tracheal and articular chondrocytes.....</i>	98
3.4	DISCUSSION	100
3.4.1	<i>Chondrocyte characterisation</i>	101
3.4.2	<i>Tracheal and articular chondrocyte transcriptome</i>	104
3.4.3	<i>Tracheal and articular chondrocyte channelome</i>	108
4	MICRORNA REGULATION OF ION CHANNELS IN TRACHEAL AND ARTICULAR CHONDROCYTES	
	113	
4.1	INTRODUCTION.....	114
4.1.1	<i>Role of microRNAs in ion channel regulation and channelopathies</i>	115
4.1.2	<i>MicroRNA target prediction</i>	116
4.1.3	<i>IPA ingenuity upstream regulator analysis.....</i>	117
4.1.4	<i>Aims.....</i>	117
4.2	METHODS	118
4.2.1	<i>MicroRNA target prediction and Gene ontology analysis</i>	118
4.2.2	<i>qPCR quantification of microRNAs and ion channel genes.....</i>	119
4.2.3	<i>Transfection of tracheal and articular chondrocytes with miR-141-3p mimic and antagomiR</i>	119
4.3	RESULTS.....	123
4.3.1	<i>MicroRNA expression between tracheal and articular chondrocytes.....</i>	123
4.3.2	<i>Gene ontology of miR-141-3p predicted downstream targets.....</i>	126
4.3.3	<i>Tracheal and articular chondrocyte transfection with miR-141-3p.....</i>	132

4.3.4	<i>Ion channel genes targeted by miR-141-3p following transfection.....</i>	133
4.4	DISCUSSION.....	140
4.4.1	<i>Comparison of miRNA expression in tracheal and articular chondrocytes.....</i>	140
4.4.2	<i>Gene ontology of miR-141-3p predicted downstream targets.....</i>	142
4.4.3	<i>Ion channels genes targeted by miR-141-3p in tracheal and articular chondrocytes</i>	145
5	THE EFFECT OF MIR-141-3P ON CHONDROCYTE PHYSIOLOGY	150
5.1	INTRODUCTION.....	151
5.1.1	<i>Role of Ion channels in migration and proliferation</i>	152
5.1.2	<i>Chondrocyte proliferation and migration.....</i>	153
5.1.3	<i>Role of miR-141-3p in proliferation and migration</i>	155
5.1.4	<i>Aims.....</i>	156
5.2	METHODS	157
5.2.1	<i>RMP measurement.....</i>	157
5.2.2	<i>Ki67 proliferation assay.....</i>	157
5.2.3	<i>Migration assay.....</i>	158
5.3	RESULTS.....	158
5.3.1	<i>RMP of tracheal chondrocytes transfected with miR-141-3p.....</i>	158
5.3.2	<i>Proliferation of tracheal and articular chondrocytes transfected with miR-141-3p...</i>	160
5.3.3	<i>Migration of tracheal chondrocytes transfected with miR-141-3p</i>	166
5.4	DISCUSSION.....	168
5.4.1	<i>Effect of miR-141-3p on RMP of tracheal chondrocytes.....</i>	169
5.4.2	<i>Effect of miR-141-3p on tracheal and articular chondrocyte proliferation</i>	171
5.4.3	<i>Effect of miR-141-3p on tracheal chondrocytes migration.....</i>	175
6	ELECTROPHYSIOLOGICAL COMPARISON BETWEEN TRACHEAL AND ARTICULAR CHONDROCYTES.....	180
6.1	INTRODUCTION:.....	181
6.1.1	<i>RMP of tracheal and articular chondrocytes</i>	181

6.1.2	<i>pH in tracheal and articular chondrocytes environment</i>	182
6.1.3	<i>Aims</i>	183
6.2	METHODS	184
6.2.1	<i>Single-channel cell-attached patch clamp recordings</i>	184
6.2.2	<i>RMP recordings under normal and acidic pH conditions</i>	184
6.2.3	<i>Pharmacological agents</i>	184
6.2.4	<i>Statistical Analysis</i>	185
6.3	RESULTS	185
6.3.1	<i>Comparison of the RMP between tracheal and articular chondrocytes</i>	185
6.3.2	<i>Ion channels functionally expressed in tracheal chondrocytes</i>	186
6.3.3	<i>Expression of VRAC in tracheal chondrocytes</i>	191
6.3.4	<i>The effect of pH on the RMP in both tracheal and articular chondrocytes</i>	196
6.4	DISCUSSION	200
6.4.1	<i>RMP of tracheal and articular chondrocytes</i>	200
6.4.2	<i>Tracheal chondrocyte channelome</i>	202
6.4.3	<i>The expression of VRAC in tracheal chondrocytes</i>	207
6.4.4	<i>The effect of extracellular acidic pH on tracheal and articular chondrocytes</i>	208
7	GENERAL DISCUSSION	212
7.1	MAIN FINDINGS	213
7.1.1	<i>Tracheal and articular chondrocytes: similar or different?</i>	214
7.1.2	<i>miRNA and ion channel interplay in chondrocytes</i>	217
7.1.3	<i>Importance of maintaining the physiological chondrocyte environment</i>	222
7.2	FUTURE PERSPECTIVES	224
7.3	CONCLUSION	225
8	APPENDIX	226
9	REFERENCES	231

1

Introduction

1

Cartilage is essential for everyday life and if impaired, the quality of life would be greatly reduced. Cartilage is vital for support in the trachea and provides smooth articulation and shock absorption in joints. Tracheal cartilage has been overshadowed by articular cartilage and has not been as thoroughly studied as articular cartilage in the joints. The single cell type found in cartilage, the chondrocyte, is the main focus of these studies as chondrocytes synthesise and maintain cartilage. The articular chondrocyte ion channel fingerprint has been extensively investigated. However, despite the importance of ion channels in cell physiology, the electrophysiological characteristics of tracheal chondrocytes remains unclear. This is of particular importance as ion channels are vital for normal tracheal cartilage development and their deletion leads to malformation of tracheal cartilage rings and hence, disease (Rock et al., 2008a). miRNAs have been shown to target ion channel genes and epigenetically regulate their expression. This interplay of ion channels and miRNA also has a role in disease propagation. This thesis aims to address the questions regarding the role of ion channels and miRNAs in tracheal chondrocytes and compare to articular chondrocytes.

1.1 Cartilage and chondrocytes

1.1.1 Cartilage

Cartilage is the most abundant connective tissue in the body. It is a firm and flexible avascular connective tissue that has a high fluid content and is an anaerobic tissue that requires low oxygen consumption (Zhou et al., 2004). Cartilage is categorised into three types, fibro, elastic, and hyaline. Different types of cartilage show different

protein expression patterns and histological characteristics. Fibro cartilage, which forms mostly as a response to injury is characterised by the high content of collagenous fibres and type I collagens in the extracellular matrix (ECM) (Benjamin and Evans, 1990). Elastic cartilage, which is the least abundant cartilage in the body is identified by the presence of elastic fibres in the ECM (Anderson, 1964) and hyaline cartilage, the most abundant cartilage in the body, is characterised by the predominance of glycosaminoglycans and type II collagen in the ECM (Mendler et al., 1989). For this doctoral thesis, the focus will be on hyaline cartilage, specifically hyaline cartilage of the joints and trachea.

The structure of hyaline articular and tracheal cartilage is similar. However, there are slight differences that reflect the function of these two cartilages. Both cartilage types can be divided into multiple layers. The arrangement of these cartilage layers and their ECM content differs between the two cartilages. Articular cartilage can be divided into three layers, the superficial zone, the middle zone, and the deep zone (**Figure 1.1A**). The ECM content and arrangement of these zones is important as these ECM proteins can be used as markers to identify the cartilage type and differentiate between the stages of cartilage development from Mesenchymal Stem Cells (MSCs) during chondrogenesis, which will be discussed later.

The superficial zone is the thinnest outermost layer of articular cartilage. It is covered in synovial fluid that contains lubricin which provides a gliding surface for joints to articulate (Jay et al., 2001). The superficial zone is abundant in flattened

chondrocytes that lie parallel to the joint surface (**Figure 1.1A**). These chondrocytes synthesise large amounts of collagen compared to proteoglycans, making the superficial zone the highest water content zone in articular cartilage (Buckwalter et al., 1997). The collagen fibrils and fibres in this zone are tightly packed and arranged parallel to the joint surface in order to provide greater tensile and shear strength. The superficial zone of cartilage acts as a protective layer and is followed by the middle zone.

The chondrocytes in the middle zone have a more spheroid shape and are arranged perpendicular to the joint surface (Aydelotte and Kuettner, 1988) (**Figure 1.1A**). They have a lower density, but synthesise more proteoglycans, with aggrecan dominating the matrix (Aydelotte et al., 1988). The collagen fibres in the middle zone are thicker than the superficial zone and their arrangement is more random and oblique (Sophia Fox et al., 2009). Finally, in the deep zone, chondrocytes are arranged parallel to the collagen fibres and are perpendicular to the joint surface (**Figure 1.1A**). The collagen fibres in the deep zone are also arranged perpendicular to the joint surface in a radial disposition (Sophia Fox et al., 2009). They have the largest diameter compared to other zones along with the highest proteoglycan content, and the lowest water concentration (Buckwalter and Mankin, 1998). The deep zone provides the greatest resistance to compressive force and is followed by the tide mark that separates cartilage from calcified cartilage which later forms into bones (Askew and Mow, 1978) (**Figure 1.1A**). In the trachea this is not the case as cartilage forms C-shaped rings that provide support.

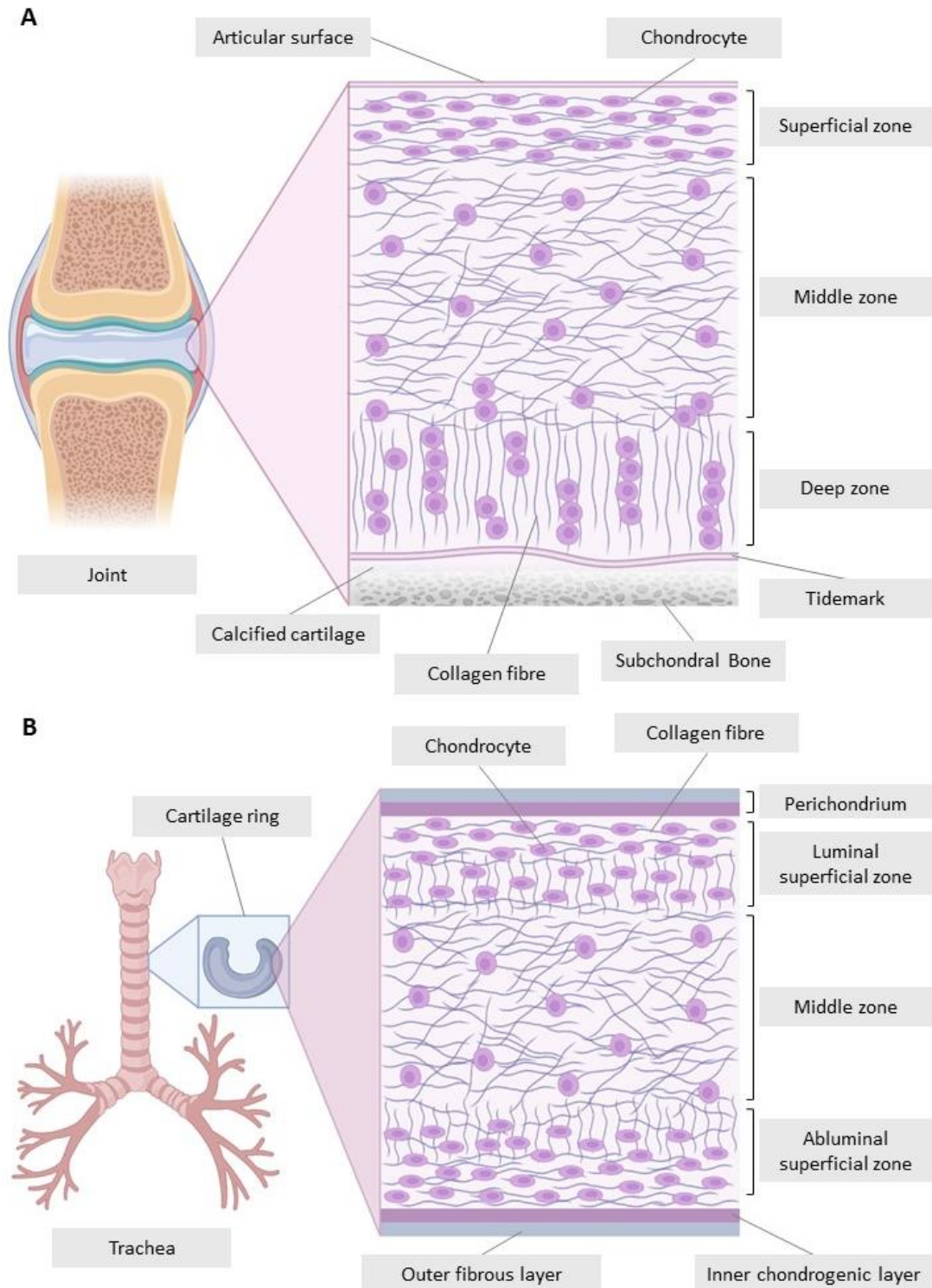


Figure 1.1: The structure of hyaline articular and tracheal cartilage. A) Articular cartilage consists of the superficial zone, the middle zone, and the deep zone followed by the tide mark, calcified cartilage, and subchondral bone. B) Tracheal cartilage comprises of the perichondrium which contains an outer fibrous layer and an inner chondrogenic layer followed by the luminal superficial zone, the middle zone and the abluminal superficial zone. The arrangement of collagen fibres and chondrocyte density differ depending on the zone in each cartilage type.

Tracheal cartilage is protected by the perichondrium, which consists of two separate layers: an outer fibrous layer and an inner chondrogenic layer (**Figure 1.1B**). The chondrogenic layer remains undifferentiated and can later form chondrocytes (Bairati et al., 1996). The perichondrium is followed by the luminal superficial zone, which is rich in collagens, mainly type II. The collagens in the superficial zone are arranged parallel to the surface and layered at right angles to each other (Roberts et al., 1997) (**Figure 1.1B**). The superficial zone has a higher density of chondrocytes that are flattened and parallel to the surface. Similar to articular cartilage, the luminal superficial layer is also followed by the middle zone which has a lower density of chondrocytes that are rounder in shape and a higher density of proteoglycans (Roberts et al., 1997) (**Figure 1.1B**). The arrangement of the collagen fibres in the middle zone is less evident and the collagen fibres are arranged predominantly perpendicular to the luminal and abluminal surfaces (Roberts et al., 1997).

However, unlike articular cartilage, the middle zone of tracheal cartilage is followed by the abluminal superficial zone (**Figure 1.1B**), which is similar to the luminal superficial zone but shows less clear layering of collagen fibres. The cartilage in the trachea functions to provide structural support as well as resilience to friction and the layering of collagen fibres supports this function. Compromise of the tracheal cartilage rings can be fatal. Factors such as epigenetic inhibition of vital genes by miRNAs can lead to cartilage ring deformation and tracheal collapse (Gradus et al., 2011).

The role and function that chondrocytes play in different cartilage types and their genetic identity complements and enhances the function of the cartilage that they reside in. Hence it is important to understand how these chondrocytes differ genetically to gain the ability to enhance their cartilage function.

1.1.2 Chondrocyte role and function

Cartilage health and growth is dependent on the important role that chondrocytes play in the synthesis, development, maintenance and repair of the ECM that surround them (Sophia Fox et al., 2009). Chondrocytes only occupy 1-5% of total cartilage tissue. They are metabolically active and have a low density because they turnover large volumes of ECM components compared to cell volume ratio (Akkiraju and Nohe, 2015a). Despite the avascular, anaerobic nature of cartilage, chondrocytes are resilient, and they obtain their nutrients and metabolites through diffusion from the synovium in articular cartilage and from the perichondrium in tracheal cartilage (Akkiraju and Nohe, 2015a).

Chondrocytes in both tracheal and articular cartilage are surrounded by a pericellular matrix in structures known as chondrones. Chondrocytes continue to proliferate and migrate through gaps in these chondrones until they mature (Poole, 1997). These chondrones are embedded in the ECM and are rich in collagen VI. This enables chondrocytes to resist loading in dynamic compression, which is important in articular cartilage as the cartilage needs to be able to withstand heavy loads in the joints. The resilience and ability of chondrocytes to adapt to the forces experienced

in cartilage is striking and contributes to the cartilage function. In order to further understand chondrocytes and gain knowledge of their identity in relation to their function in their respective cartilage environment, an understanding of how chondrocytes form from MSCs is required.

1.1.3 Chondrogenesis

Chondrocytes originate from the condensation, proliferation, differentiation, and maturation of MSCs in a process known as chondrogenesis (**Figure 1.2**). Chondrogenesis is a well-orchestrated process that is mediated by signals initiated through cell-cell and cell-matrix interactions in order to form chondrocytes. Chondrogenesis was first described by (Fell, 1925) and is dependent on various growth and differentiation factors as well as the activation of signalling pathways that affect the transcription of specific genes. The different factors that regulate chondrogenesis can be used as markers to identify the stage of cell transition and phenotype. Despite the identification of signalling molecules and pathways necessary for chondrogenesis, the understanding of the molecular events that regulate this intricate process is still ongoing.

The process of chondrogenesis is initiated with the condensation of MSCs into chondroprogenitor cells. The ECM of MSCs prior to condensation is rich in hyaluronan and collagen type I and collagen type II α (Sandell et al., 1994). As the MSCs condense into chondroprogenitor cells, the expression of collagen I is lost and the expression of the nuclear transcription factor, Sox9, a master regulator of chondrogenesis is

enhanced (Ng et al., 1997). Sox9 is expressed early in chondrogenesis and is required to further drive the expression of collagen II α 1 (Ng et al., 1997, Goldring et al., 2006b). Additionally, Sox9 promotes the expression of cartilage-specific genes such as Col2a1 which encodes the collagen type II alpha 1 peptide, which is also needed for the formation of cartilage (Eames et al., 2003). Moreover, the activation of the signalling molecule, sonic hedgehog (Shh), which is a member of the hedgehog family of proteins along with bone morpho-genetic proteins (BMPs) also causes the upregulation of Sox9 (Monsoro-Burq, 2005). This in turn causes the activation of other growth factors such as transforming growth factor- β (TGF- β), fibroblast growth factor (FGF), and Wingless factors (Wnt).

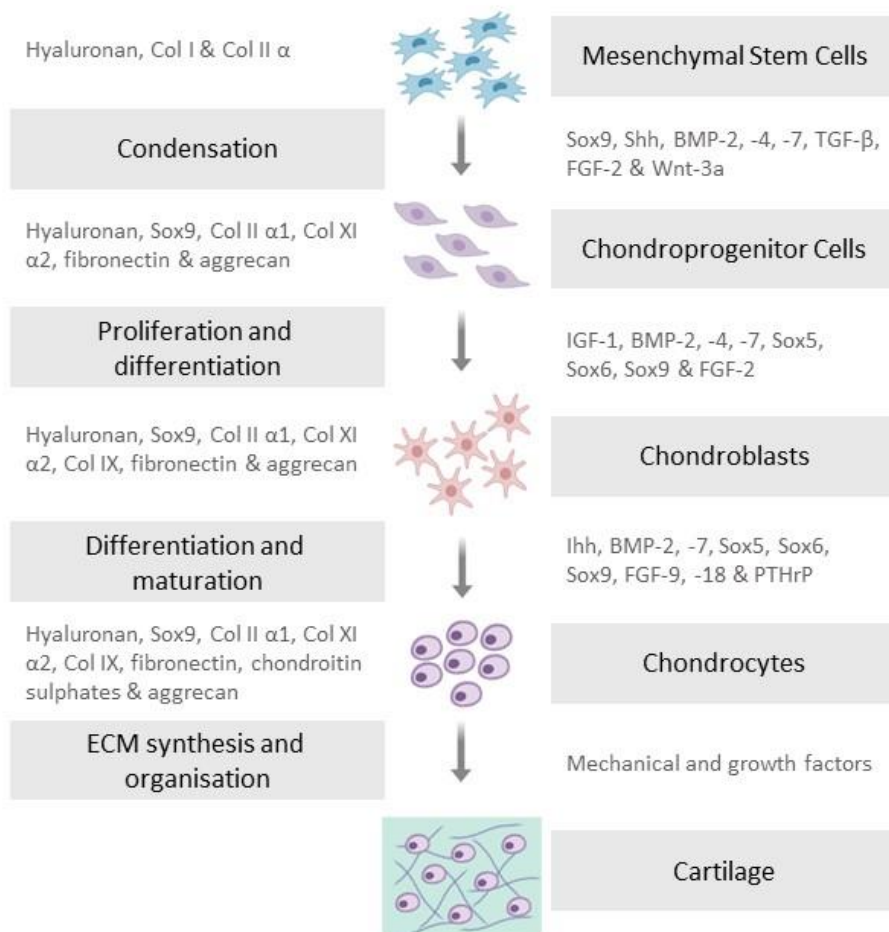


Figure 1.2: Embryonic development of cartilage. The process of chondrogenesis is regulated by various growth factors and signalling pathways.

TGF- β , BMP, FGF and Wnt pathways interplay together to promote the expression of ECM proteins and growth factors that further drive the process of chondrogenesis and cartilage formation. TGF- β stimulates the synthesis of proteoglycans, fibronectin, and collagen II α 1, all essential for cartilage formation (Goldring et al., 2006b, Morales, 1991, Fukumoto et al., 2003). Whereas BMPs play a part in the synthesis of collagen II α 1 as well as aggrecan (Indrawattana et al., 2004). It is the balance of FGF and BMP signalling that determines the rate of proliferation of chondroprogenitor cells and their differentiation into chondroblasts (Minina et al., 2002).

Furthermore, Insulin-like growth factor (IGF) also stimulates proliferation of the chondroprogenitor cells and aids their differentiation into chondroblasts along with BMPs and FGFs (Fukumoto et al., 2003). IGF enhances the synthesis of proteoglycans and collagen II α which further drives the process of chondrogenesis (Guenther et al., 1982, Luyten et al., 1988, Osborn et al., 1989). Other members of the Sox family, Sox5 and Sox6, are not expressed in chondrocyte condensation but are expressed during the chondrocyte differentiation (Lefebvre et al., 1998b). They are also required for the expression of collagen IX, aggrecan, as well as collagen II α 1 during chondrocyte differentiation (Smits et al., 2001). Finally, the expression of Indian hedgehog (Ihh), also a member of the hedgehog family, controls the maturation of chondrocytes from chondroblasts and causes the upregulation of parathyroid hormone-related protein (PTHrP), which works as a feedback mechanism to regulate the process. It is these mature chondrocytes that synthesise and maintain the ECM proteins that form cartilage.

1.1.4 ECM production and regulation by chondrocytes

Chondrocytes synthesise the ECM that facilitates compressional and tensile forces in articular cartilage and structural support in tracheal cartilage. The ECM components they synthesize, and turnover include collagens, glycoproteins, glycosaminoglycans such as chondroitin sulphates, proteoglycans, and hyaluronan (Archer and Francis-West, 2003). Chondrocytes synthesise collagen II, IX and XI. Collagens are the most abundant macromolecule in the ECM and make up two thirds of the dry weight of cartilage (Eyre, 2004). Collagens stabilise the matrix of cartilage and provide tensile and shear strength in the tissue. Collagen II, known as the collagen of cartilage, makes up 90 – 95% of the collagens in cartilage and gets arranged into fibrils and fibres that get interwoven with the proteoglycan, aggrecan (Bhosale and Richardson, 2008a). These proteoglycans function to trap large volumes of fluid that allows the cartilage to be compressible and make it an ideal tissue to resist forces. Chondrocytes organise collagens, proteoglycans, and other non-collagenous proteins uniquely and the structure of cartilage and its ECM composition differs slightly depending on the type, zone, and area of residence (Boutell et al., 2000, McKee et al., 2019). Dysregulation of the ECM structure, composition and abundance in cartilage leads to cartilage diseases.

1.1.5 Diseases of cartilage

The most prevalent disease of cartilage is osteoarthritis (OA). OA results in the progressive degradation of articular cartilage and is characterised by the erosion of the articular surface (Chen et al., 2017). The breakdown of proteoglycans leads to a

reduction in compressive stiffness of cartilage and accelerates the breakdown of collagen II, which has a half-life of several decades to 400 years and is irreplaceable once lost (Eyre et al., 2006). In addition, the environment that chondrocytes reside in controls their metabolic activity and plays a role in the progression of the disease. Pro-inflammatory cytokines and growth factors play a role in the synthesis and degradation of the ECM (van den Berg, 1999). As well as that epigenetic regulation of cartilage genes by miRNAs also leads to the progression of OA (Malemud, 2018a). miRNAs have been shown to regulate chondrocyte signalling pathways in OA such as the MAPK, SMAD, BMP, and NF- κ B (Li et al., 2018b, Li et al., 2018a). Additionally, miRNAs also regulate chondrocyte apoptosis and the enzymes that lead to the breakdown of cartilage such as matrix metalloproteinases (Mmps) and ADAMTSs (Jin et al., 2014, Yamasaki et al., 2009, Ji et al., 2016).

Once chondrocytes hypertrophy, they start to express collagen X (Zheng et al., 2003). This marks the terminal differentiation of chondrocytes that regulates the expression of proteolytic enzymes such as Mmps and ADAMTSs that degrade the proteoglycan and collagen network (Porter et al., 2005, Murphy and Lee, 2005). The activation of transcriptional regulators such as Runt-Related Transcription Factor 2 (RUNX2) further induces hypertrophy and enhances the production of proteolytic enzymes that digest the articular cartilage ECM (Chen et al., 2020). Mmp-1 and Mmp-13 which are collagenases, break down the cartilage network (Murphy and Lee, 2005). Whereas ADAMTSs breakdown proteoglycans (Porter et al., 2005). These proteolytic enzymes are regulated by activators such as cathepsin B and inhibitors such as tissue inhibitors

of Mmps (TIMPs). It is the imbalance of these factors that leads to OA. Moreover, repeated assault and injury to articular cartilage further enhances Mmp production and so enhances the cartilage breakdown.

Inflammatory cytokines, such as interleukin-1 β (IL-1 β), tumour necrosis factor- α (TNF- α), and interleukin-6 (IL-6), are known to be upregulated during OA progression, they get secreted by chondrocytes and play a role in the disruption of cartilage homeostasis, through increasing Mmp expression and inhibiting the production of Mmp inhibitors (Wojdasiewicz et al., 2014). These inflammatory cytokines also affect ion channel expression in OA and rheumatoid arthritis (RA). TNF α and IL1 β were shown to cause alterations in chondrocyte's membrane proteins (Jeremiasse et al., 2020). They were also shown by my group to increase calcium-activated potassium channel expression at the transcriptomic level (Haidar et al., 2020).

As explained above, the cartilage ECM undergoes alterations during OA pathogenesis, these changes also include changes in the osmotic environment driven by increased water content and composition of its ionic environment. As well as that the cartilage water content also increases (Mow et al., 1999, Venn and Maroudas, 1977, Mankin and Thrasher, 1975). Chondrocytes attempt to adjust to these changes and maintain their homeostasis by altering the transport of ions across their membrane and thus increase their cell volume (Lewis et al., 2011b, Hdud et al., 2014). Despite chondrocytes recognizing the loss of ECM proteins and actively changing their membrane proteins and producing collagen II and proteoglycans, the ratio

between the ECM protein production compared to proteolytic enzyme production is imbalanced and results in complete loss of cartilaginous tissue overtime. Moreover, cellular attempts to repair the tissue results in aberrant osteoblast like differentiation, forming osteophytes or fibroblastic differentiation and inducing fibrosis or stiffening of the joints (Hashimoto et al., 2002, Findlay and Atkins, 2014, Remst et al., 2015).

In the trachea, defects to the cartilage rings cause tracheomalacia (TM), which was first described in 1963 by (Baxter and Dunbar, 1963) as an uncommon condition in which the tracheal wall is soft and pliable. TM is characterised by the collapse of the trachea during respiration. Its symptoms can range from minor expiratory stridor with typical barking cough to severe respiratory distress (Filler et al., 1982). It is often misdiagnosed as it presents with asthma-like symptoms; TM can be classified into congenital or acquired disorder (Baxter and Dunbar, 1963). Congenital TM results due to abnormal formation of the cartilage rings whereas acquired TM occurs when there is a degeneration of normal cartilage that supports the trachea. Some of the causes of acquired TM are infections, tumours and trauma (Baxter and Dunbar, 1963). If the ECM of cartilage is deformed, then the cartilage rings will not be able to resist heavy loads or provide strength and structure to the trachea. Membrane proteins such as ion channels and transporters have been shown to be implicated in TM, whereby their deletion can lead to the malformation of the cartilage rings (Rock et al., 2008a). Ion channels and their role in chondrocytes in health and disease will be discussed in the next section.

1.2 Ion channels

Despite being 'non-excitabile' cells, chondrocytes express a diverse collection of ion channels that are vital for chondrocyte homeostasis. These ion channels play a role in regulating chondrocyte membrane potential, proliferation, migration, volume regulation and their ability to synthesise ECM proteins (Barrett-Jolley et al., 2010a). Emerging evidence implicates ion channels in diseases of the cartilage (TM and OA). Ion channel expression is altered in articular cartilage in OA and RA and is vital for tracheal cartilage support (Haidar et al., 2020, Jeremiasse et al., 2020, Lin et al., 2014b, Rock et al., 2008a). Ion channels constitute a large superfamily, however despite their importance in tracheal cartilage as demonstrated above, very little is known about the members that may be expressed in tracheal chondrocytes. An overview of the role of ion channels in chondrocytes and how they contribute to the pathogenesis of cartilage disease will be discussed below.

1.2.1 Definition and classification of ion channels

Ion channels are transmembrane proteins that are essential for a variety of cellular functions. They facilitate the movement of ions into and out of the cell (Hodgkin and Huxley, 1952a) and play a vital role in setting the resting membrane potential (RMP). Ion channels usually consist of a central aqueous pore with one or more subunits that surround it. The opening of ion channels and hence their activation, usually occurs through a conformational change of the ion channel pore (Catterall, 1995) that allows the flow of ions such as K^+ , Na^+ , Ca^{2+} , Mg^{2+} and Cl^- . There are multiple stimuli that can control the opening of the ion channel pore, also known as ion channel gating; these

are specific to each ion channel and can include voltage changes across the membrane (voltage-gated ion channels), mechanical stress (mechanically-gated ion channels) or chemical stimuli such as binding of a ligand (ligand-gated ion channels) (Sachs, 1991, Unwin, 1993).

1.2.2 Ion channel families

According to the International Union of Basic and Clinical pharmacology (IUPHAR) and the British Pharmacological Society (BPS) database for ion channels, there are three main classes of ion channels: ligand-gated ion channels, voltage-gated ion channels and 'other' ion channels (**Table 1.1**). This classification is based on the ion channels' mode of activation and correlates to structural similarities and common ancestors between the ion channel families (Yu et al., 2005). These three classes of ion channels are subsequently classified into different ion channel families, which are further subdivided into ion channel subtypes (Alexander et al., 2019). Ligand-gated ion channels are comprised of the inhibitory, anion-selective GABA_A and glycine receptors and the excitatory cation-selective nicotinic acetylcholine, 5-HT₃, ionotropic glutamate and P2X receptors (Alexander et al., 2019). The binding of a neurotransmitter to an orthosteric site triggers a conformational change of these receptors and hence results in their opening/activation (Unwin, 1993). Meanwhile the binding of endogenous or exogenous modulators to allosteric sites of these channels regulates their gating. Ligand-gated ion channels mediate fast synaptic transmission (in milliseconds) at neuromuscular junctions and in the nervous system (Changeux, 2010).

Voltage-gated ion channels are a superfamily of channels that are characterised by their rapid response to changes in the RMP, resulting in the permeation of select ions. They play a pivotal role in the propagation of action potentials and the promotion of neurotransmitter secretion in neurones and muscles (Moran et al., 2015) as well as the secretion of hormones, sensation of the environment, gene expression, and cell division (Yu and Catterall, 2004). The ion channel families included in the voltage-gated ion channel superfamily are the voltage-gated sodium, potassium, proton and calcium channels; calcium-activated, two-pore domain, and inwardly rectifying potassium channels; cyclic nucleotide regulated channels, CatSper channels, two pore channels; ryanodine receptors and transient receptor potential channels (Alexander et al., 2019).

Finally, the last classification of ion channels is the 'other' ion channels, this includes ion channel families that do not fit into the ligand-gated or voltage-gated ion channel categories. These 'other' ion channels also do not share structural properties with the two previous categories and have evolved separately (Yu et al., 2005). The 'other' ion channel category consists of ClC, Maxi and calcium-activated chloride channels; volume regulated anion channels, CFTR, connexins and pannexins; Orai channels, sodium leak channels, piezo channels and aquaporins (Alexander et al., 2019). These channels are involved in a variety of processes such as systemic water homeostasis, cell migration, cell volume regulation, membrane excitability, cell proliferation, epithelial electrolyte transport, muscle contraction and regulation of neuronal excitability (Alexander et al., 2019). Many of the major ion channel families have been

detected in articular chondrocytes. Family members of the voltage-gated, ligand-gated, and 'other' ion channel categories have been observed in articular chondrocytes over the years; the expression of these channel and their roles in chondrocyte physiology and disease will be discussed below.

1.2.3 Role of ion channels in chondrocyte physiology and disease

A number of studies, including those from my group have shown the functional presence of the ever-expanding list of ion channels in chondrocytes (**Table 1.1**). The RMP of any cell is determined by the compliment of ion channels expressed by these cells – in the case of chondrocytes, ion channels shown in **Table 1.1** regulate the RMP. In excitable cells, the expression of ion channels is vital for the firing of action potentials and regulation of the RMP is essential for excitability in these cells. In general, the RMP of cells is essential for its function and signalling within the cell's microenvironment. For years it was debated whether the RMP was important for the control of non-excitabile cell function, which the basic answer for such question is 'yes'. Most non-excitabile cells have a dynamic membrane potential despite not having an action potential firing phenotype which sub-serves a range of essential biological functions (Abdul Kadir et al., 2018). Similarly, for chondrocytes, the RMP is vital for their ability to produce the ECM. Studies have shown that modifying the RMP through ion channel inhibition compromised their ability to produce ECM mRNA and proteins (Wu and Chen, 2000, Mouw et al., 2007). Hence the RMP is important for the chondrocyte microenvironment and will be further discussed in chapter 4.

Chondrocytes exist in a unique microenvironment. The ECM which chondrocytes synthesise and are embedded in, contributes to the net charge of the cartilage tissue, and drives the osmotic and ionic gradients (Urban et al., 1993). The ECM is able to resist and maintain the osmotic gradient. This results in hydrostatic pressure that contributes to the ability of cartilage to withstand biomechanical stresses and strains (Sanchez-Adams et al., 2014). Chondrocytes have an unusual ionic environment as they are surrounded by proteoglycans that are negatively charged. This fixed charge density attracts a large number of cations such as Na^+ in addition to water, creating high extracellular osmolarity and contributing to the low pH environment of chondrocytes (Urban et al., 1993). The high extracellular $[\text{Na}^+]$ creates a steep inward gradient for Na^+ entry into chondrocytes through the Na^+/K^+ -ATPase pump in these cells. Hence the function of ion channels is important in chondrocytes as they regulate the volume changes of chondrocytes and help to maintain their viability in such harsh environments.

Chondrocytes are subjected to high dynamic loads during physical activity (Eckstein et al., 1999). Under pressure, cartilage decreases in volume by exuding fluids (McCutchen, 1962). This causes changes in the water content of the interstitial component of cartilage and thus causes changes in the extracellular osmotic potential (Sivan et al., 2006). These changes are reversible upon relaxation and so chondrocytes are regularly exposed to increasing and decreasing osmotic forces (Mow et al., 1992). These changes are modulated by the regulatory volume increase

Table 1.1: Ion channels expressed in chondrocytes.

Ion channel	General role	Subtype	Role in chondrocytes	Reference
Sodium Channels				
Epithelial sodium channel (ENaC)	Essential for the clearance of the respiratory airways. Regulates blood pressure and extracellular fluid volume in the kidney. Also regulates cell's osmolarity.	α - and β -subunits	Mechanotransduction	(Shakibaei and Mobasheri, 2003, Trujillo et al., 1999a)
Voltage-gated sodium channel (VGSC)	Regulates the voltage changes across the plasma membrane.	NaV β 1 and 2, NaV1.2, NaV1.3, NaV1.6 & NaV1.7	Mechanotransduction and ECM maintenance	(Sugimoto et al., 1996b, Wu and Chen, 2000, Asmar, 2017)
Potassium Channels				
Voltage-gated Potassium channel (K _v)	Critical for the repolarization of the membrane following an action potential.	K _v 1.4 & K _v 1.6	Maintenance of the RMP	(Mobasheri et al., 2005, Clark et al., 2010b)
ATP- sensitive potassium channel (K _{ATP})	Modulates cellular excitability.	K _{ir} 6.x	Coupling cellular activity to metabolic state	(Mobasheri et al., 2007)

Inward rectifier potassium channel (K _{ir})	Stabilizes the RMP.	K _{ir} 2.2	Maintenance of the RMP	(Clark et al., 2011b)
Large conductance calcium-activated potassium channel (BK)	Regulates excitability. Contributes to after-hyperpolarisation activity.	Kcnma1 & kcnmb1	Coupling of membrane stretch to regulated volume decrease (RVD)	(Long and Walsh, 1994, Mobasheri et al., 2010)
Small conductance calcium-activated potassium channel (SK)	Regulates excitability and response to pressure.	-	Intracellular calcium regulation	(Mobasheri et al., 2007, Wright et al., 1996)
Two-pore domain potassium channel (K _{2p})	Maintenance of the RMP in different smooth muscle cells and neurones.	Task-2, Twik-1 & Twik-2	Regulation of the RMP	(Clark et al., 2011b)

Calcium Channels				
Voltage-gated calcium channel (VGCC)	Involved in calcium signalling and cell excitability.	Ca _v 1.2 & Ca _v 3.2	Calcium signalling and ECM maintenance	(Shakibaei and Mobasheri, 2003, Poiraudau et al., 1997b, Wu and Chen, 2000, Shao et al., 2005)
Non-selective Cations				

Transient receptor potential vanilloid channel (TRPV)	Plays a role in mechanosensing, osmosensing and thermosensing. Plays a role in calcium homeostasis.	Trpv4, Trpv5 & Trpv6	Osmoregulation and calcium signalling regulation	(Phan et al., 2009, Gavenis et al., 2009, Clark et al., 2010a)
Chloride Channels				
Maxi channel	Involved in cell volume and apoptosis regulation.	Maxi-Cl	Control of RMP	(Tsuga et al., 2002, Sugimoto et al., 1996b, Sumiyoshi et al., 2010)
Volume regulated anion channel (VRAC)	Involved in volume regulation.	Lrrc8a, b, c, d & e	Regulates the RVD and the RMP	(Okumura et al., 2009)
Calcium-activated chloride channel (CaCC)	Involved in calcium signalling.	Ano1 and Ano2	Essential for the formation of cartilage rings	(Rock et al., 2008a)
ClC channel	Stabilizes the RMP.	ClC-7	Maintains chloride currents that are activated by extracellular acidification.	(Kurita et al., 2015)
'Other' Channels				
Aquaporins	Involved in cell volume regulation.	Aqp-1, Aqp-3	Regulates cell volume	(Mobasheri and Marples, 2004, Mobasheri et al., 2004)

Acid sensing ion channels (ASIC)	pH sensing.	Asic1	Intracellular pH regulation	(Sánchez et al., 2006, Song et al., 2020)
Ionotropic glutamate receptors (NMDAR)	Role in mechanosensing.	-	Response to mechanical stimulation	(Millward-Sadler et al., 2001, Salter et al., 2004)
Connexins	Mediates ATP and Ca ²⁺ exchange in the joint.	Connexin 43	Mechano-coupling	(Knight et al., 2009, Zhang et al., 2014)
Piezo	Mechanotransduction.	Piezo1 & Piezo2	Calcium signalling in response to mechanical stimuli.	(Lee et al., 2017, Beech and Xiao, 2018)

(RVI) and regulatory volume decrease (RVD), which are mechanisms controlled by ion channels. RVD occurs when chondrocytes recover their volume after swelling via osmosis following exposure to a hypotonic challenge. When a chondrocyte takes up water, it causes the efflux of ions and hence decreases its intracellular osmolarity until it is in equilibrium with the extracellular environment. On the other hand, when chondrocytes recover their volume following a shrinkage due to a hypertonic challenge, RVI occurs (Lewis et al., 2011c). Ion channels and transporters that have been shown to be linked to the RVI include the $\text{Na}^+/\text{K}^+/\text{2Cl}^-$ co-transporter (Lytle, 1997) and the Na^+/H^+ transporter (Hughes et al., 2010), whereas RVD is mediated by the transient receptor potential vanilloid type 4 channel (TRPV4) (Phan et al., 2009), where it was shown that TRPV4 null mice were unable to exhibit a RVD response (Clark et al., 2010a).

Transient receptor potential (TRP) channels are a family of non-selective cation channels that are involved in nociception, temperature, mechano- and osmosensation (Becker et al., 2005, Phan et al., 2009, Feetham et al., 2014). TRP channels regulate the intracellular Ca^{2+} concentrations in non-excitabile cells. They are divided into 6 subfamilies: canonical (TRPC), vanilloid (TRPV), melastatin (TRPM), ankyrin (TRPA), mucolipin (TRPML), polycystin (TRPP), and no mechanoreceptor potential C (TRPN) (Matta and Zakany, 2013). TRP channels have been shown to be implicated in OA; articular chondrocytes isolated from OA patients expressed various TRP channels (Gavenis et al., 2009). TRPA1 was shown to mediate acute inflammation in OA (Moilanen et al., 2015). Whereas, TRPV5 facilitates calcium influx and inhibits

chondrocyte autophagy in a rat OA model (Wei et al., 2017) and TRPV6 acts as a chondroprotective factor where its deletion causes cartilage fibrillation, loss of proteoglycans and severe OA changes (Song et al., 2017). In chondrocytes, TRPV4 is not only essential in RVI but it also plays a role in chondrocyte mechanotransduction (O'Connor et al., 2014) and is a regulator of Sox9 and hence chondrogenesis (Muramatsu et al., 2007) whereby its mutation causes skeletal malformations due to the inhibition of BMP signalling pathway (Leddy et al., 2014). Other channels that transport cations such as Na⁺ which is attracted by the negatively charged chondrocyte environment are the Epithelial sodium channel (ENaC) which also plays a role in the RVI (Trujillo et al., 1999b, Bondarava et al., 2009).

ENaCs were first shown to be expressed in chondrocytes by (Trujillo et al., 1999a) and were later functionally identified by my own group (Lewis et al., 2013a). ENaC is a heteromeric channel, that forms from up to four subunits: α , β , δ , and γ (Canessa et al., 1994). ENaCs are known to regulate blood volume and pressure in the cardiac system (Canessa et al., 1994) and in the kidney, they play a role in sodium reabsorption (Rossier et al., 2002). In articular chondrocytes, ENaC is thought to play a role in mechanotransduction and contribute to the maintenance of the RMP, which may aid in the regulation of ECM synthesis and prevent apoptosis (Wright et al., 1996, Shakibaei et al., 2001, Shakibaei and Mobasher, 2003). The abundance of the α and β subunits of ENaC were shown to be altered in human chondrocytes from RA patients and were significantly higher compared to control. However, in OA patients, the α and β subunits of ENaC were absent compared to control (Trujillo et al., 1999a).

ENaCs were also shown to co-localise with other ion channels such as the voltage-gated calcium channels (VGCC) and β 1 integrin in differentiating chondrocytes (Shakibaei and Mobasher, 2003).

Calcium signalling is important in chondrocytes during skeletal development. VGCC play a major role in calcium signalling in chondrocytes and are classified into Cav1.x, Cav2.x and Cav3.x (x denoting the subtype) (Matta et al., 2015b). Cav1.2 and Cav3.2 subunits were detected in chondrocytes of developing murine embryos (Shao et al., 2005), they enable a rapid elevation of cytosolic Ca^{2+} levels by IGF-1 in articular chondrocytes (Poiraudou et al., 1997a). This cytosolic calcium influx is necessary for the regulation of ECM synthesis of aggrecan and type II collagen in articular chondrocytes (Xu et al., 2009a). The inhibition of VGCC with the drugs nifedipine and verapamil inhibits proliferation and abrogates chondrogenesis (Fodor et al., 2013), it also reduces the RMP of chondrocytes by 18% (Wohlrab et al., 2001). VGCC are also important in tracheal chondrocyte, whereby Cav3.2 was shown to be essential in tracheal cartilage formation. Mice null for Cav3.2 had altered Sox9 expression and disrupted cartilage ring formation (Lin et al., 2014b). Cav3.2 was also found to be involved in signalling pathways triggering mechanical load-induced OA; where mice null for Cav3.2 exhibited significantly lower articular cartilage damage than controls (Lin et al., 2014b). Specific inhibitors of the VGCC also reduced the expression of MMP-1, -3 and -13 in osteoarthritic canine chondrocytes (Boileau et al., 2005). The importance of calcium signalling in chondrocytes is evident as there are multiple

channels that get activated by calcium that are vital for normal cartilage physiology, such as the calcium activated chloride channels (CaCC).

CaCC were first recognised in *Xenopus Oocytes* by (Miledi, 1982, Barish, 1983). However, the molecular identity underlining this current was not discovered until 2008 by three different groups (Caputo et al., 2008, Schroeder et al., 2008, Yang et al., 2008) which showed TMEM16A as a strong candidate. TMEM16 proteins are also known as anoctamins (Anos). They are a family of 10 proteins, with Ano1 and Ano2 being the most studied. CaCC currents were also generated by Ano6 and Ano7, whereas Ano5, 8, 9, and 10 did not produce measurable currents and their role as CaCC is debated (Schreiber et al., 2010). CaCC are expressed in various tissues among which are sensory receptors, smooth muscles, neuronal tissues, and different epithelial organs. They are also involved in various diseases such as cancers and airway malformations (Kunzelmann et al., 2011). The importance of chloride channels in the airway is well established, with CFTR being vital for physiological functioning of the airway. CaCC are of strong interest as they were ideal druggable targets to control physiological functions or correct defects such as cystic fibrosis (Rock et al., 2009). Aside from their importance in cystic fibrosis and being functional alternatives to CFTR, CaCC proved to be essential for the functioning of the trachea.

Deletion of Ano1 and Ano2 causes severe malformation of the cartilage rings and death of mice 1 month post birth due to TM (Rock et al., 2008a). Another family of chloride channels that are important in chondrocytes are the volume regulated anion

channels (VRAC). They play a role in the volume regulation of chondrocytes (Okumura et al., 2009). VRACs consist of 5 subunits Lrrc8a, b, c, d, and e. With Lrrc8a being essential for the formation of the channel (Qiu et al., 2014, Voss et al., 2014). Other chloride channels such as ClC, which form a large family of voltage-dependent chloride channels, are also essential in chondrocytes as they play a role in OA (Poroca et al., 2017). ClC-7 gets downregulated as OA progresses and its knockdown decreases the acid sensitive currents and results in enhanced cell death in a human chondrocyte cell line (Kurita et al., 2015).

Thus, chondrocyte ion channels have widespread importance in physiology and disease. nevertheless, it is important to note that ion channels not only regulate chondrocytes RMP, volume changes and progression of diseases but they too are regulated by multiple factors. These factors include pharmacological agents as well as epigenetically factors such as miRNAs which will be discussed in the section below. This regulation of ion channels by miRNAs too plays a role in chondrocyte physiology and disease.

1.3 MicroRNA-mediated regulation of gene expression

MicroRNAs, also known as miRNAs or miRs, play a vital role in the regulation of gene expression in several biological processes including cell proliferation, differentiation, and cell death (Hwang and Mendell, 2006). They are short non-coding RNA that are evolutionarily conserved, present in virtually all eukaryotes, signifying their important role in biological processes. Here, the role of miRNAs in both tracheal and

articular chondrocytes will be discussed and their role in chondrocyte physiology, cartilage diseases and ion channels will be investigated.

1.3.1 MicroRNA biogenesis, nomenclature, and regulation

MicroRNAs are evolutionarily conserved short non-coding RNAs that are usually 18 - 22 nucleotides long (Bartel, 2004b). They bind to complementary sequences within their target mRNAs leading to post-transcriptional changes and modification of gene expression. Generally, miRNAs base pair to regions within the 3'- untranslated region (3'-UTR) of protein coding mRNA that are complimentary. The interaction of miRNAs with their target(s) usually leads to translational repression or cleavage of these target mRNA (Meijer et al., 2013). miRNAs were first observed in 1993 by Ambrose and colleagues when the characterisation of genes that control the timing of larval development in *Caenorhabditis elegans* (*C. elegans*) revealed a regulatory small non-coding RNA, known as lin-4 (Lee et al., 1993). It was not until later on in 2000, when another non-coding RNA, let-7 was discovered in *C. elegans* by Ruvkun's group (Reinhart et al., 2000) that miRNA started to gain attention from scientists. This led to the exploration of the role of miRNAs and what was previously thought to be junk RNA was recognised as functional. Soon after, other homologs were found in other bilateral animals, including mammals and these two regulatory RNAs were found to represent a class of small endogenous RNAs found in worms, flies, and mammals (Lagos-Quintana et al., 2001, Griffiths-Jones et al., 2008).

Approximately a quarter of miRNA genes in humans are found in the introns of pre-mRNAs (Bartel, 2004b), this makes it convenient for the coordinated expression of miRNA and protein, explaining the conserved sites between miRNA and targeted mRNA (Bartel, 2004b, Aravin et al., 2003). Canonical miRNAs are usually transcribed as single miRNAs from introns of coding or non-coding transcripts. However, there is a class of miRNAs, mirtrons, that originate from a non-canonical biogenesis pathway (Ruby et al., 2007, Okamura et al., 2007). Sometimes several miRNA loci that are located close to each other get transcribed together forming a polycistronic cluster (Lee et al., 2002). Nearly all the miRNAs are conserved in closely related animals such as human and mouse (Friedman et al., 2009). Other small RNAs have also been discovered in plants, fungi, and animals, such as small interfering RNA (siRNA) (Carthew and Sontheimer, 2009) and piwi-interacting RNA (piRNA) (Ozata et al., 2019), which also act as guide RNAs. However, miRNAs differ in their biogenesis.

Most miRNAs are transcribed as an RNA stem-loop by RNA polymerase II/III that results in a hairpin structure of several hundred to thousand nucleotide (nt) long double-stranded miRNA precursor known as primary miRNA (pri-miRNA) (**Figure 1.3**) (Lee et al., 2002). This pri-miRNA gets processed by the nuclear RNase III enzyme, Drosha, which forms a complex with its cofactor DiGeorge Syndrome Critical Region 8 (DGCR8), resulting in the pri-miRNA cleavage into a shorter (70 - 90 nt) hairpin named pre-miRNA that contains a 2 nt 3' overhang that serves as a recognition site for the second processing step (**Figure 1.3**) (Lee et al., 2003). Next, the pre-miRNA is exported to the cytoplasm by exportin 5 (Exp5) which binds to small RNAs that bear

a short 3' overhang and a terminal stem-loop (Lund et al., 2004). Exp5 depends on a co-factor known as Ran, a GTPase that only binds in the GTP bound form (Bohnsack et al., 2004). Once the Exp5/Ran-GTP/pre-miRNA complex passes through the nuclear pore, Ran-GTP gets hydrolysed, and the pre-miRNA gets released (**Figure 1.3**). In contrast to canonical miRNA, mirtrons, originate from an alternative non-canonical pathway that omits Drosha cleavage and arise as by-products of intron splicing. Mirtrons enter the canonical biogenesis pathway at the Exp5 level (Westholm and Lai, 2011). This thesis will not focus on mirtrons and reference to miRNAs will be referring to canonical miRNAs unless otherwise stated.

In the cytoplasm, Dicer - the RNase III endonuclease, makes a cleavage ~ 20-nt upstream of the 2-nt 3' overhang recognition site of the pre-miRNA releasing a double stranded miRNA duplex that has a 5' phosphate and a 2 nt 3' overhang (**Figure 1.3**). This duplex gets unravelled by an RNA helicase and one strand of the duplex is loaded into the Argonaute (AGO) protein, which along with other proteins, forms the RNA-induced silencing complex (RISC) (**Figure 1.3**). Usually the guide strand (either the 5' or 3' strand, depending on which end of the pre-miRNA they are derived from) forms the mature miRNA while the passenger strand gets degraded, however in some cases the passenger strand can be stable and functional (Yang et al., 2011c). Hence the stability of the miRNA strand determines which miRNA gets produced. This mature miRNA binds to target sequences partially or completely complementary in mRNA at the 3'-UTR and results in either the mRNA degradation, translational repression or mRNA deadenylation (Meijer et al., 2013). Hundreds of genes can be

targeted by one mature miRNA and one gene can be targeted by several different miRNAs, making miRNAs powerful regulators of post-translational gene expression.

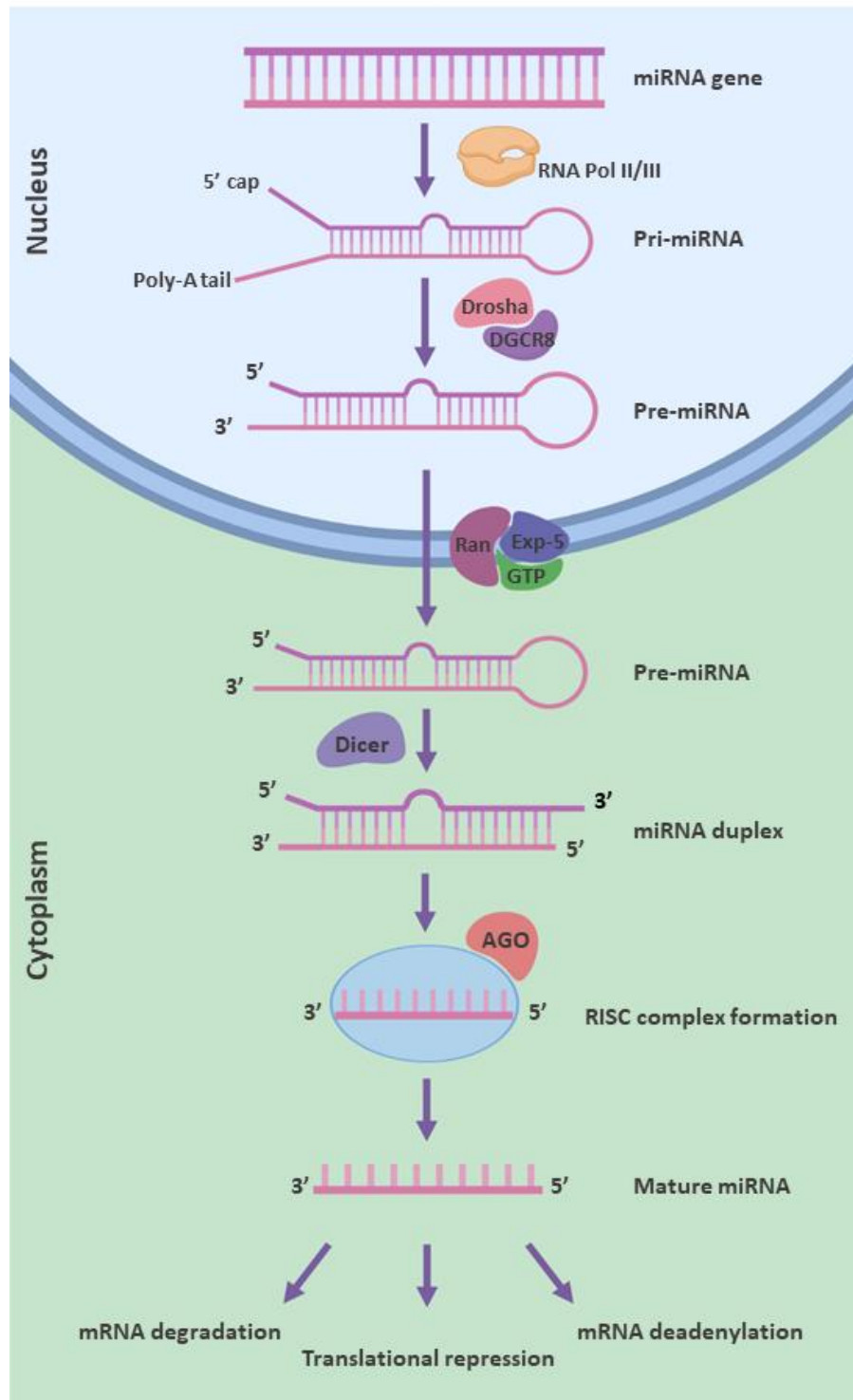


Figure 1.3: Canonical pathway of miRNA biogenesis and processing. miRNA processing through a series of endonucleolytic maturation steps. Figure adapted from (Winter et al., 2009)

The regulation of miRNAs can occur at any step of their biogenesis. miRNAs can be regulated by different physiological triggers such as different cell cycle stages, growth factors and neuronal signalling which have an effect on miRNA turnover, causing their rapid degradation (Ghini et al., 2018, Gulyaeva and Kushlinskiy, 2016, Zhang et al., 2012). miRNAs can also be regulated by different ribonucleases (RNases); as in contrast to their precursors, miRNAs have unprotected 5' and 3' ends that can be targeted by these enzymes. However, it was shown that miRNAs can be made more stable by methylation or uridylation which deters the activity of exoribonucleases (Ramachandran and Chen, 2008). Another form of miRNA regulation can occur through the miRNA: target interaction, where the miRNA target affects the miRNA activity. Two mechanisms of this regulation have been proposed. The competing endogenous RNA (ceRNA) (Thomson and Dinger, 2016) and the target-directed miRNA degradation (TDMD) mechanism (Rüegger and Großhans, 2012).

The ceRNA mechanism proposes that endogenous RNAs with shared miRNA binding sites compete with one another for the binding of the miRNA and binding of the RISC complex. Specific RNAs can impair miRNA activity by sequestering the miRNA-RISC complex and hence upregulating target mRNA gene expression (Thomson and Dinger, 2016). Whereas in the TDMD mechanism, the RNA target promotes degradation of its miRNA, whereby binding of highly complementary RNAs, either target mRNAs or non-coding RNAs, and destabilise the miRNA (Baccarini et al., 2011, Marcinowski et al., 2012, Ameres et al., 2010). This triggers post-transcriptional modification of the miRNA and causes tailing (addition of non-templated nucleotides at the 3' end of the

miRNA) and 3' to 5' trimming (shortening) (Ameres et al., 2010) as well as unloading from AGO (De et al., 2013), all leading to the decay of the highly complementary miRNA.

The nomenclature of mature miRNA usually starts with the prefix 'miR-' followed by a number, which identifies the miRNA, for example, miR-181. However, some miRNAs such as lin-4 and let-7 are an exception. In order to identify the designated species that the miRNA belongs to, a short letter prefix is used, for example 'hsa-' refers to *Homo sapiens*, while 'rno-' refers to *Rattus norvegicus*. Moreover, a letter suffix is used to identify miRNA paralogous sequences that differ at one or two positions, for example, miR-30a, miR-30b and miR-30c. Whereas a number suffix indicates miRNAs with identical sequences but at different loci, for example, miR-1-2. In order to identify which strand gets incorporated into the RISC complex and which gets degraded as it is less stable, an asterisk was previously used to distinguish the less stable strand, for example, miR-143*. However now a clearer nomenclature is used which identifies each strand by the arm of the pre-miRNA that it is derived from. For example, miRNAs that originate from the 5' arm of the pre-miRNA adopt a '5p' suffix and those derived from the 3' arm adopt a '3p' suffix, regardless of being the guide or passenger strand. Therefore, miR-141 can either be miR-141-5p or miR-141-3p (Griffiths-Jones et al., 2006).

The expression profile of miRNAs and their function varies between different cell types, tissues, developmental stages, and cellular environments, with some miRNA

being specific and enriched in the tissues they are expressed in. This provides a mechanism of gene regulation in which miRNA abundance can allow for customised expression of proteins in different cell types depending on function whilst achieving a uniform expression level within each cell type. Several miRNA with profound effects on skeletal development and cell function have been studied, with many affecting chondrogenesis. These miRNAs will be discussed below.

1.3.2 MicroRNAs in cartilage physiology and disease

MicroRNAs play a vital role in all aspects of cartilage physiology such as the regulation of ECM proteins, chondrocyte differentiation, growth factor regulation, chondrocyte proliferation and disease (Gibson and Asahara, 2013). miRNAs have been shown to be essential for normal skeletal development, whereby the tissue specific deletion of Dicer, the RNase III endonuclease needed for miRNA biogenesis, causes a decrease in chondrocyte proliferation, and accelerates hypertrophy of chondrocytes, leading to severe growth retardation in Dicer null mice (Kobayashi et al., 2008). A highly expressed miRNA that has been widely studied in cartilage is miR-140 (Papaioannou et al., 2013, Miyaki et al., 2010). Numerous studies have been carried out on this miRNA after it was shown to have cartilage specific expression in zebrafish and mice embryos (Wienholds et al., 2005, Tuddenham et al., 2006). miR-140 is expressed in the intronic sequence of the *Wwp2* gene (Yang et al., 2011b). In zebrafish, miR-140 was shown to disrupt Platelet-derived growth factor (PDGF) signalling thus affecting palatogenesis and producing defects resembling cleft palate (Eberhart et al., 2008). This was supported in humans where there were significantly higher numbers of

missense mutations in the coding regions and the 3'-UTR region of the PDGF receptors of patients with cleft palate compared to matched controls, with one case having mutations adjacent to and affecting the miR-140 binding site (Rattanasopha et al., 2012).

In mice, the knockout of miR-140 caused reduced longitudinal growth of the skull and growth defects of endochondral bones (Miyaki et al., 2010). Knockout of miR-140 also caused altered differentiation of chondrocytes due to the targeting of the *dnpep* gene that modulates the BMP signalling pathway by miR-140. This results in the mice having craniofacial deformities and dwarfism (Nakamura et al., 2011). miR-140 null mice also showed progressive cartilage fibrillation and proteoglycan loss, which are characteristics of early OA (Miyaki et al., 2010). Further studies have implicated miR-140 in the disease progression of OA, whereby miR-140 was shown to be downregulated in human OA cartilage compared to normal cartilage (Tardif et al., 2009). In addition, Histone deacetylase 4 (HDAC4), an enzyme that regulates chondrocyte hypertrophy through the inhibition of Runx2, a driver of hypertrophy, was shown to be a target of miR-140. HDAC4 is specifically expressed in non-hypertrophic chondrocytes and plays a role in the proliferation and differentiation of chondrocytes. Targeting of HDAC4 by miR-140 inhibits its expression thus eliminating the inhibition of Runx2, driving the chondrocytes into hypertrophy and progressing OA (Tuddenham et al., 2006). miR-140 was also shown to target other genes associated with OA including ADAMTS5, an enzyme that is involved in the degradation of articular cartilage (Miyaki et al., 2010), SP1, associated with

maintaining chondrocyte proliferation (Yang et al., 2011b), and Mmp-13, an enzyme that degrades collagens and other ECM proteins (Tardif et al., 2009, Tuddenham et al., 2006). The expression of miR-140 is regulated in cartilage whereby Sox9 is upstream of miR-140 expression (Nakamura et al., 2012). Sox9 along with related family members, Sox5 and Sox6 enhanced miR-140 expression (Yamashita et al., 2012) demonstrating the Sox9 dependent miR-140 expression.

Not all miRNA regulation in cartilage is detrimental, Let-7 was shown to be required for normal chondrocyte proliferation in the growth plate (Papaioannou et al., 2013). Another miRNA, miR-675, rescues the expression of collagen II, which in the absence of Sox9 in articular chondrocytes is blocked. This proposes a mechanism through which miR-675 mediates the Sox9 regulation of collagen II in articular chondrocytes and promotes its expression (Dudek et al., 2010). Studies have also shown that the expression of miR-675 is tightly regulated by HuR, an RNA binding and stress response protein. HuR suppresses miR-675 expression by inhibiting Drosha processing (an RNase III enzyme important in miRNA biogenesis), however when it is relocated from the nucleus to the cytoplasm in response to stress, it no longer inhibits Drosha and hence rapidly stimulates miR-675 expression (Keniry et al., 2012). This response to stress may explain the increased expression of miR-675 in chondrocytes from OA patients.

Other miRNAs have also been shown to target ECM proteins through Sox9. miR-145 targets Sox9 and hence regulates the expression of cartilage ECM genes indirectly.

The overexpression of miR-145 suppresses Sox9 and as a consequence, suppresses Col2a1, Acan, Col9a2, and Col11a1 ECM gene expression (Yang et al., 2011a) while stimulating the expression of Runx2 and Mmp-13, which are associated with hypertrophy and OA (Martinez-Sanchez et al., 2012). In contrast, miR-125 targets ADAMTS4 and Mmp-13 and reduces their expression (Matsukawa et al., 2013, Yu et al., 2015b) and miR-27a was shown to be decreased in OA chondrocytes where its inhibition causes increased Mmp-13 expression (Tardif et al., 2009). Sox9 is also targeted by miR-101 which was shown to reverse the IL-1 β -induced downregulation of collagen II and Acan. In addition, overexpression of miR-101 reduced cartilage destruction in OA induced mouse knee joint (Kim et al., 2013). Whereas miR-1 was shown to repress Acan expression but only in hypertrophic chondrocytes (Sumiyoshi et al., 2010) and miR-29a and b directly target and suppress type II collagen expression (Yan et al., 2011). As well as that miR-181a, highly expressed in chicken chondrocytes, was shown to directly target and suppress Acan (Sumiyoshi et al., 2013). miR-199a and miR-193 have also been shown to influence the expression of cartilage ECM genes. These two miRNAs inhibit the expression of Col2a1 and Acan when they're overexpressed (Ukai et al., 2012). However, the deletion of a cluster of miRNAs, which include miR-199a and miR-214 results in severe deformity in skeletal development (Watanabe et al., 2008) suggesting that the role of miRNAs in cartilage physiology is complicated and contradictions need to be elucidated further.

Another miRNA that fuels the imbalance of anabolic and catabolic mechanism in cartilage is miR-455-3p, which was shown to target the translation of Smad2, which

signals through the Smad 2/3 pathway, which has been shown to have anabolic consequences (promoting the expression of Collagen II and Acan). An increase in the expression of miR-455 was observed in OA cartilage and is thought to promote the TGF- β Smad 1/5/8 pathway (which has catabolic consequences by enhancing the expression of Mmp-13 and Col10a1) by suppressing the Smad 2/3 pathway and hence promoting cartilage catabolism and the degradation response of chondrocytes (Swingler et al., 2012).

miR-146a and b are key miRNAs involved in regulating the inflammatory response. miR-146a was amongst the top miRNAs to be downregulated in patients with advanced OA and its overexpression in human chondrocytes reduced the IL-1 β -induced TNF α production suggesting that this miRNA is a negative regulator of inflammation in OA (Jones et al., 2009). miR-146a was expressed abundantly in early-stage human OA cartilage and its expression is reduced as OA advances (Yamasaki et al., 2009). miR-146a was also found to target downstream Smad4 which induced VEGF expression and increased articular chondrocyte apoptosis (Li et al., 2012). In addition, expression of miR-34a was upregulated in rat primary chondrocytes after IL-1 β stimulation. Silencing of miR-34a prevented the IL-1 β induced collagen II α 1 downregulation and apoptosis in rat chondrocytes (Abouheif et al., 2010) IL-1 β contributes to OA progression (Hashimoto et al., 2008, Daheshia and Yao, 2008, Kobayashi et al., 2005) and the balance of TGF- β signalling and IL-1 β is crucial for cartilage homeostasis whereby TGF- β counteracts the IL-1 β upregulation of Mmp-13 and downregulation of ECM proteins (Takahashi et al., 2005). On the other hand, the

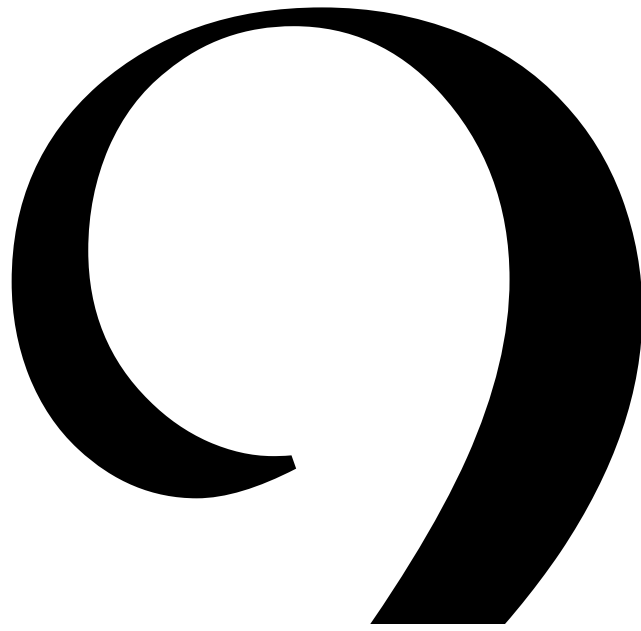
stimulation of Collagen II and Acan by TGF- β is abrogated by IL-1 β (Roman-Blas et al., 2007).

miRNA also have a role in tracheal cartilage formation. Several miRNAs such as miR-140, miR-675, miR-145, miR-199, miR-125 and miR-30a/c are expressed in tracheal tissue (Gradus et al., 2011). miRNAs can cause the deformation of cartilage rings and result in TM. miR-125 and miR-30a/c, have been shown to target snail1 which is a FGF signalling effector in growth plate pre-hypertrophic chondrocytes that represses the transcription of Acan and Col2a1. These two miRNAs repress Snail1 and enable the full functional differentiation of Col2a1 in tracheal chondrocytes and hence they are essential for normal tracheal development. The inhibition of miR-125 and miR-30a/c has been shown to upregulate Snail1 and cause poor deposition of the ECM which leads to abnormal cartilage ring formation and TM (Gradus et al., 2011). TM also occurs due to the targeting of ion channels by miRNAs.

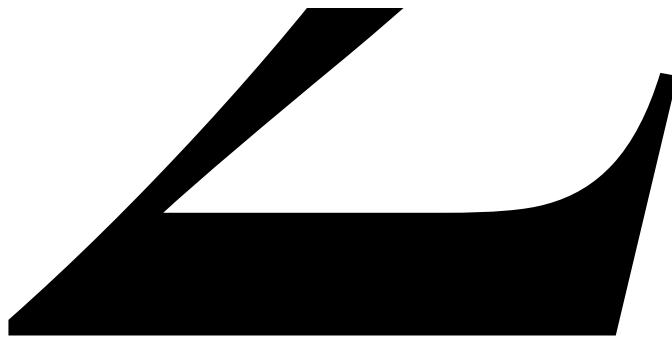
1.4 Aims

There are several aims to this doctoral thesis exploring the interplay of miRNAs and ion channels differentially expressed between tracheal and articular chondrocytes. Firstly, the unbiased characterisation of the tracheal chondrocyte transcriptome and channelome using RNA-sequencing and comparison to that of articular chondrocytes will be achieved. Specifically, identifying similarities and differences in ion channel gene expression and using bioinformatic tools to investigate the upstream regulators (miRNA) driving the gene expression between the two chondrocyte types. Following

that, these upstream regulators will be validated using quantitative polymerase chain reaction and their effect on ion channel genes differentially expressed between tracheal and articular chondrocytes will be studied. Subsequently the effect of these upstream regulators on tracheal and articular chondrocyte function will be investigated through transfection of these upstream regulators. Finally, the functional fingerprint of tracheal chondrocyte channelome will be validated using electrophysiology and pharmacological agents and the effect of changing the environment of these chondrocytes on the constitutively active ion channels and the resting membrane potential will be investigated.



Materials and Methods



2.1 Tissue collection and cell preparation

2.1.1 Animals

Male Wistar rats were purchased from Charles River (UK) and kept under standard 12hr/12hr light/dark conditions with unlimited access to water and a normal chow diet. Healthy male Wistar rats (6-10 weeks old, weighing between 200-300g) were euthanized using Schedule 1 methods, through a lethal dose of pentobarbitone followed by cervical dislocation.

2.1.2 Tracheal Chondrocytes

The trachea was isolated ensuring that the connective tissue and the trachealis muscle were removed, and was cut into small pieces. The tissue was incubated overnight with type II collagenase (from *Clostridium histolyticum*, 265 collagen digestion units/mg, Invitrogen, UK) in serum-free Dulbecco's modified Eagle's medium (DMEM) supplemented with 1 g/L glucose, pyruvate, 4 mM glutamine, 0.5% Amphotericin B and 1% penicillin/streptomycin solution. The filtered cell suspension was centrifuged at 318 x *g* (1400 rpm) for 5 minutes. The supernatant was removed, and the pellet was re-suspended in serum-free DMEM. This step was repeated, and the pellet was re-suspended in DMEM with 10% Foetal Calf Serum (FCS) and grown in a monolayer culture for no more than four passages. Cells were kept at 37 °C, 5% CO₂ in humidified air and passaged every two to three days to maintain cells at 70-80% confluence.

2.1.3 Articular Chondrocytes

Articular cartilage was isolated by removing the femoral head off the rat femur and cutting off the *ligamentum teres*. In order to isolate articular chondrocytes, the femoral head was incubated overnight with type II collagenase as stated above and cells were grown in a monolayer culture for no more than four passages. Cells were kept at 37 °C, 5% CO₂ in humidified air and passaged every two to three days to maintain cells at 70-80% confluence.

2.2 Immunofluorescence

Rat tracheal and articular chondrocytes were seeded onto coverslips at a density of 2.5×10^4 per ml. The cells were fixed with 4% paraformaldehyde (PFA) in PBS for 10 minutes and washed with 100 mM Glycine solution for 10 minutes. Following that they were washed with 0.05% Triton X-100 in PBS for 10 minutes and rinsed with PBS, three times, 5 minutes each. To block non-specific binding, the cells were incubated with antibody buffer solution (2-10% donkey/goat serum, 1% bovine serum albumin and 0.05% Triton X-100) for 60 minutes. After that, the cells were incubated with primary antibodies at 4 °C overnight. After incubation, the chondrocytes were washed with PBS containing 0.05% Triton-X100 three times, 10 minutes each and were incubated with secondary antibody at room temperature for 1-2 hours. Negative controls involved primary and secondary antibody omission. Following incubation with secondary antibody, the cells were washed with PBS containing 0.05% Triton-X100 three times, 10 minutes each. The chondrocytes were post-fixed with 4% PFA in PBS for 5 minutes. The coverslips were mounted with Vectashield

Hard Set Antifade Mounting Medium containing DAPI (Vector laboratories, UK). Images were acquired using the Zeiss LSM 800 confocal microscope. Images were acquired using x40 or x63 oil immersion objective and analysed using the ImageJ software.

2.3 RNA-sequencing

2.3.1 RNA extraction

Total RNA was extracted from rat tracheal and articular chondrocytes using the RNeasy mini kit (Qiagen, UK) according to the manufacturer's instructions. Tracheal and articular chondrocytes were harvested with trypsinization at passage 1 and centrifugation at 300 x *g* for 5 minutes. Cells were disrupted with the addition of 350 μ l of buffer RLT plus and homogenized using a blunt 20G needle. Following that, the cells were transferred to genomic DNA eliminator spin columns and centrifuged for 30 s at 8000 x *g*. For the purification of RNA molecules longer than 200 nucleotides, the genomic DNA eliminator spin columns were discarded and 350 μ l of ethanol was added to the flowthrough.

The samples were transferred to RNeasy MinElute spin columns and centrifuged for 15 s at 8000 x *g*. 700 μ l of buffer RW1 was added and centrifuged for 15 s at 8000 x *g*. Following that, 500 μ l of buffer RPE was added and the samples were centrifuged for 15 s at 8000 x *g*. Then 500 μ l of 80% ethanol was added and centrifuged for 2 minutes at 8000 x *g*. The RNeasy MinElute spin columns were centrifuged at full speed for 5 minutes with the lids open. Finally, 28 μ l of RNase free water (Sigma

Aldrich, UK) was added to the RNeasy MinElute spin columns and centrifuged for 1 minute at full speed to elute the RNA. RNA concentration and purity were estimated according to the 260/280 and 260/230 ratio recorded using Nanodrop2000 (Thermofisher Scientific, UK).

2.3.2 RNA preparation and library construction

Following the RNA extraction, samples were prepped for sequencing as shown in **Figure 2.1**. RNA integrity was assessed using a TapeStation 2200 (Agilent Technologies) and samples with RIN > 9.6 were used. As total RNA consists of rRNA, long nc-mRNA, mRNA and various ncRNA, it is important to purify the RNA species of interest from the total RNA (for this project, mRNA was the RNA species of interest as well as the ncRNAs, miRNAs). This is usually carried out through the enrichment or the depletion of the total RNA. Poly-A selection and enrichment were performed to sequence mRNA; 500 ng of polyA enriched mRNA was used for sequencing (**Figure 2.1**). PolyA tail enrichment was carried out by annealing oligo-(dT) magnetic beads onto the RNA. Samples were assessed for quality control and the sequence library was prepared by Eurofins Scientific, Luxembourg.

RNA was broken down into small fragments and converted into double stranded circular DNA (ds-cDNA) in order to increase the coverage during sequencing. Following that, sequence adapters were added to the samples, which were amplified by PCR. The samples were assessed for quality control and sequenced using the Illumina protocol and sequencer. Once the samples were sequenced with a flow cell,

quality scores were assigned to each base of the sequenced fragments to ensure that there were no false positives. The sequence reads were refined through the removal of the sequence adaptors, trimming the reads, and filtering the data to discard garbage reads that do not pass the quality control process (low quality base calls and artefacts). RNA-seq data was provided in the FASTQ format, ready to be analysed.

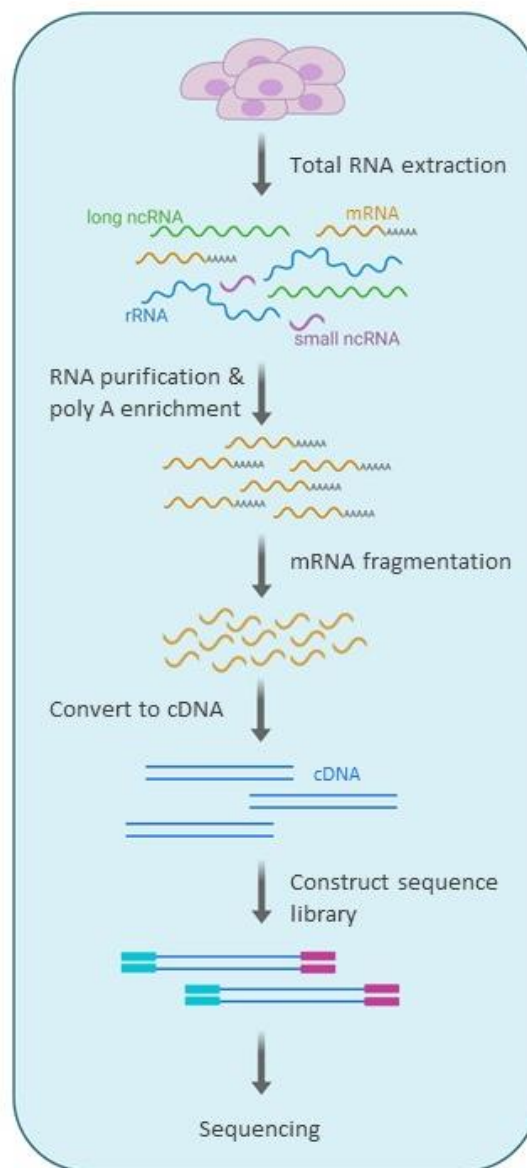


Figure 2.1: Workflow of RNA-sequencing sample preparation and library construction. Process of RNA-seq detailing RNA preparation, library construction, RNA fragmentation and ligation of sequence adaptors.

2.4 Quantitative Polymerase Chain Reaction (qPCR)

2.4.1 RNA extraction

Total RNA was extracted from rat tracheal and articular chondrocytes as described above. For the isolation of total RNA that includes 18 nucleotides upwards, the RNeasy mini kit (Qiagen, UK) was used according to the manufacturer's instructions. For the purification of total RNA containing small RNAs such as miRNAs, 525 μ l of 100% ethanol was added to the flowthrough from the genomic DNA eliminator spin columns following centrifugation for 30 s at 8000 x *g*. The samples were transferred to RNeasy MinElute spin columns and centrifuged for 15 s at 8000 x *g*. Following that 500 μ l buffer RPE was added, and the samples were centrifuged for 15 s at 8000 x *g*. An additional 500 μ l of buffer RPE was added to the samples and centrifuged for 2 minutes at 8000 x *g*. The RNeasy MinElute spin columns were centrifuged at full speed for 5 minutes with the lids open. Finally, 28 μ l of RNase free water (Sigma Aldrich, UK) was added to the RNeasy MinElute spin columns and centrifuged for 1 minute at full speed to elute the RNA. RNA concentration and purity were estimated as previously described using Nanodrop 2000 (ThermoFisher Scientific, UK).

Total RNA extraction to include small RNAs such as miRNA was also performed using TRIzol reagent (Invitrogen, UK) to extract RNA from tracheal and articular chondrocytes. Chondrocytes were seeded in 6-well plates and left to grow overnight. The cells were lysed with 500 μ l of TRIzol reagent (Invitrogen, UK) followed by the addition of 100 μ l of chloroform (Sigma Aldrich, UK) and the samples were mixed by hand. The samples were incubated at room temperature for 5 minutes and

centrifuged at 12000 x *g* for 10 minutes at 4 °C. The samples split into three phases: the lower red phenol-chloroform phase, the interphase, and the aqueous phase. The aqueous phase, which contains the RNA was transferred into new tubes. In order to precipitate the RNA, 250 µl of 100% isopropanol (Sigma Aldrich, UK) was added and mixed by hand. The samples were incubated for 30 minutes and centrifuged at maximum speed (17000 x *g*) for 20 minutes at 4 °C. The supernatant was removed and 500 µl of 70% ethanol (Sigma Aldrich, UK) was added to wash the RNA and samples were incubated for 30 minutes at room temperature. Following that the samples were centrifuged at 12000 x *g* for 2 minutes at 4 °C. The supernatant was removed, and the pellet was left to air dry for 5 - 15 minutes and re-suspended in 20 – 30 µl of RNase-free water (Sigma Aldrich, UK). RNA concentration and purity were estimated as previously described using Nanodrop2000 (Thermofisher Scientific, UK).

2.4.2 First strand cDNA synthesis

Isolated total RNA was used to synthesise first-strand cDNA. For qPCR quantification of mRNA, the reaction was prepared as shown in **Table 2.1**. Template RNA was diluted to 500 ng with RNase-free water (Sigma Aldrich, UK) and random hexamers (Invitrogen, UK) were incubated at 65 °C in a thermocycler (Applied Biosystems, USA) for 10 minutes. Following that, 5x first strand buffer (RT buffer) (Invitrogen, UK), dithiothreitol (DTT) (Invitrogen, UK), dNTPs (a mix of dATP, dCTP, dGTP, and dTTP in water; Qiagen, UK), Superscript II Reverse Transcriptase (Invitrogen, UK) and RNase inhibitor, Riblock (Thermofisher Scientific, UK) were incubated at 42 °C for 60 minutes in a thermocycler (Applied Biosystems, USA) as shown in **Table 2.1**. The cDNA was

diluted 1 in 10 by adding 180 μ l of RNase free water (Sigma Aldrich, UK) to the 20 μ l reaction mix.

Table 2.1: First strand cDNA synthesis for mRNA quantification using qPCR.

Component	Volume per reaction (μ l)
First reaction 10 minutes at 65 °C	
Template RNA (500 ng)	Variable
RNase-free water	Variable
Random hexamers	1 μ l
Second Reaction 60 minutes at 42 °C	
RT buffer	4 μ l
DTT	2 μ l
dNTP	1 μ l
Superscript II	1 μ l
RNase inhibitor	1 μ l

For qPCR quantification of miRNA, the miScript RT II kit (Qiagen, UK) was used as shown in **Table 2.2**. 5x miScript HiSpec buffer, 10x miScript Nucleic mix, RNase-free water, miScript Reverse transcriptase mix (Qiagen, UK) and template RNA (100 ng) were added as shown in **Table 2.2** and incubated for 60 minutes at 37 °C, the samples were incubated for a further 5 minutes at 95 °C to deactivate the reverse transcriptase. The cDNA was diluted 1 in 10 by adding 180 μ l of RNase free water (Sigma Aldrich, UK) to the 20 μ l reaction mix.

2.4.3 Quantitative Polymerase Chain Reaction (qPCR)

For the qPCR quantification of mRNA, cDNA was used as a template, RNase-free water, the gene primers, and Faststart Essential DNA Green Master (Roche, UK) were

also used. Whereas for the qPCR quantification of miRNAs, cDNA was used as a template, universal primers, Faststart Essential DNA Green Master (Roche, UK) and microRNA primers were used. The composition of qPCR reaction mix per reaction for mRNA and miRNAs is outlined in **Table 2.3**. Three technical replicates and at least 3 biological replicates were used. The qPCR was performed with 45 cycles on a Roche Light Cycler 96 system (Roche, UK). The qPCR protocol used is shown in **Table 2.4**.

Table 2.2: First strand cDNA synthesis for miRNA quantification using qPCR.

Component	Volume per reaction (μ l)
Incubate for 60 minutes at 37 °C followed by 5 minutes at 95 °C	
5x miScript HiSpec Buffer	4 μ l
10x miScript Nucleic mix	2 μ l
RNase-free water	Variable
miScript Reverse Transcriptase mix	2 μ l
Template RNA (100 ng)	Variable

Table 2.3: Reagents used per reaction of qPCR run for mRNA and miRNA.

Component	mRNA	microRNA
	Volume (μ l)	
Universal primers	-	0.7
microRNA primers	-	0.7
Forward primer	1	-
Reverse primer	1	-
Faststart Essential DNA Green Master	10	5
cDNA template	5	5
RNase-free water	3	-

Table 2.4: qPCR conditions for mRNA and miRNA quantification.

qPCR Condition	mRNA		miRNA	
	Temperature (°C)	Time (s)	Temperature (°C)	Time (s)
Preheating	95	600	95	600
Denaturation	95	10	95	10
Annealing	58 - 60	10	55	10
Extension	72	10	72	10
Cycles	45	45	45	45
Melt Curve (end of 45 cycles)	95	10	95	10
	65	60	65	60
	97	1s (5 readings/ continuous °C)	97	1s (5 readings/ continuous °C)

2.5 Electrophysiology

Chondrocytes were passaged with x1 Trypsin-EDTA (Sigma Aldrich, UK) and re-suspended in FCS-free DMEM and plated onto glass bottom dishes coated with Poly-D-Lysine (MatTek, UK). The cells were incubated for 30-60 minutes at 37 °C in order to lightly adhere to the dishes. Cells were freshly prepared for each experiment and were used up to passage 4.

2.5.1 *Single-channel electrophysiological recordings*

Single-channel electrophysiological recordings were performed through cell-attached patch clamp using an Axopatch 200a amplifier (Axon Instruments, USA). Low-pass filtering was set to 1 kHz and the data was digitized at 5 kHz with a Digidata 1200A interface. Patch pipettes were fabricated using fire-polished 1.5 mm o.d. borosilicate glass capillary tubes (Sutter Instrument, USA, supplied by INTRACEL, UK). They were pulled using a two-step electrode puller (Narishige, Japan) and when filled with recording solutions had a resistance of approximately 5-8 M Ω depending on the patch-clamp method used. All electrophysiological solutions are listed in **Table 2.5**. Single-channel all-points amplitude histograms were created in WinEDR (John Dempster, University of Strathclyde) or QuB (Qin et al., SUNY, Buffalo, NY, USA). Amplitudes were taken at various holding potentials and used to create current-voltage (IV) curves. Reversal potential and slope conductance (g) were then calculated from the equation of the fitted line and open probabilities (P_o) were analysed using the QuB software (Qin et al., SUNY, Buffalo, NY, USA) or the WinEDR software (John Dempster, University of Strathclyde). Liquid junction potentials were calculated using

JpCalc (Barry & Lynch, 1991) and are shown in **Table 2.6** for the relevant extracellular and intracellular solutions.

2.5.2 *Equilibrium potentials*

The selectively permeable membrane of cells separates charged ions and results in equilibrium potentials. The differential distribution of ions in the intracellular and extracellular solutions indicate where the equilibrium potential for each ion lies and can be calculated for each ion within a solution using the Nernst equation (**Equation 2.1**).

$$E = -58 * z * \log\left(\frac{[I]_{in}}{[I]_{out}}\right) \quad \text{Equation 2.1}$$

Where E is the equilibrium potential of the ion, z is the valency of the ion and $[I]_{in}$ and $[I]_{out}$ are the intracellular and extracellular concentrations of the ion, respectively. When an ion channel is selectively permeable to one ion only, E equates the reversal potential (V_{rev}) of the channel at which the channel current is zero. V_{rev} can then be compared to the experimentally measured value taken from the IV curve.

Table 2.5: Ionic composition of solutions used during electrophysiology recordings. The pH adjustments were made with HCl and NaOH. All extracellular solutions were pH 7.4 and all intracellular solutions were pH 7.2 unless stated otherwise.


Reagents	Physiological solution (mM)		High K ⁺ /Ca ²⁺ -free solution (mM)		K ⁺ -free solution (mM)		Acidic solution (pH 6.5) (mM)	
	Intracellular	Extracellular	Intracellular	Extracellular	Intracellular	Extracellular	Intracellular	Extracellular
Na	0	140	0	0	100	145	0	140
K	141	5	141	141	0	0	141	5
Ca	0	2	0	0	0	1.5	0	2
Cl	27	148	27	27	41	147.5	27	148
Mg	1	1	1	1	1	1	1	1
Gluconic acid	115	0	115	115	0	0	115	0
Cs	0	0	0	0	40	0	0	0
EGTA	5	0	5	5	0.5	0	5	0
Glucose	0	5	0	0	0	0	0	5
HEPES	10	10	10	10	3	3	0	0
Me	0	0	0	0	100	0	0	0
SO₃	0	0	0	0	100	0	0	0
MES	0	0	0	0	0	0	10	10

Table 2.6: Liquid junction potentials calculated for the electrophysiological solutions. Calculations were performed using JpCalc (Barry and Lynch, 1991b).

Solution	Junction potential (mV)
Physiological and acidic pH solution	-
High K ⁺ / Ca ²⁺ - free solution	3.5 mV
K ⁺ -free solution	-

2.6 Statistical analysis

Statistical analysis was performed using GraphPad Prism 8 (GraphPad Software, USA) and Minitab (Minitab Ltd, UK). Statistical tests are reported in the figure legends. All values are reported as mean \pm SEM, with sample size = n unless stated otherwise. Statistical significance defined as $p < 0.05$.

A large, stylized black number '3' that serves as a decorative background for the text. The top loop is open on the left, and the bottom loop is open on the right.

3

Comparison between
tracheal and articular
chondrocyte transcriptome
and channelome

3.1 Introduction

Understanding the transcriptome of cells is essential as it allows for an unbiased insight into the functional elements of the genome and an understanding of the development of cells and tissues under normal physiological conditions and how these may change in disease states. Articular cartilage has been well studied over the past few decades, with an extensive focus on diseases such as OA and RA. However, tracheal cartilage has been somewhat neglected and the transcriptome of tracheal cartilage and its 'channelome' are yet to be investigated. Since articular and tracheal cartilage express one cell type, chondrocytes, their transcriptome may be very similar. However, the influence of the environment around them and the function of the cartilage they synthesise and reside in may drive some differences. Therefore, in this chapter, a comparison between the articular and tracheal chondrocyte transcriptome will be undertaken to gain a better understanding of these cells and their function in physiology and disease. This will be achieved using RNA sequencing, which will provide an unbiased investigation into these cells' transcriptome.

3.1.1 RNA-sequencing for transcriptome profiling

Over the past decade, transcriptomics became a general phenotyping tool, with several methods used in the past to deduce and quantify the transcriptome. The complete set of RNA transcripts in a cell and the quantity in which they are present is referred to as the transcriptome of a cell. The development of high-throughput next-generation sequencing (NGS) in the early 2000s revolutionized transcriptomics by enabling RNA analysis through the sequencing of complementary DNA (cDNA) (Wang et al., 2009). This method, known as RNA sequencing (RNA-Seq), had distinct

advantages over previous approaches and has revolutionized our understanding of the complex and dynamic nature of the transcriptome.

RNA-Seq provides a more thorough and quantitative view of gene expression, allowing the detection of novel transcripts. As well as that allele-specific expression, and alternative splicing can be easily detected with RNA-seq (Kukurba and Montgomery, 2015). Unlike other methods, RNA-seq is not limited to only detecting transcripts that correspond to existing genomic sequences, it can also be used to detect sequence variations such as single nucleotide polymorphisms (SNPs) (Wilhelm et al., 2008). Moreover, RNA-Seq has very minimal background signal compared to other methods such as DNA microarrays (Wang et al., 2009). RNA-seq also has a large dynamic range of expression levels over which transcripts can be detected as it does not have an upper quantification limit (Mortazavi et al., 2008). The expression levels detected by RNA-seq are highly accurate as RNA-seq exhibits high reproducibility of technical and biological replicates. It also uses less RNA sample and is cheaper than methods previously used with prices decreasing with time (Wang et al., 2009).

RNA-seq offers a variety of different applications and analysis pipelines. Coupled with bioinformatic tools, it provides a strong platform for studying the transcriptome. Hence in the present study, RNA-seq quantification that relies on mapping the transcripts against a reference genome was chosen as the method of transcriptome quantification. Through this, various parameters could be detected and measured. For example, genes that are typically used as cell markers could be compared. In the case of this project, genes identified as chondrocyte markers shared between

tracheal and articular chondrocytes will be compared as well as those specific to each cell type.

3.1.2 Chondrocyte markers

In order to accurately assess the transcriptome of a cell, characterisation of the cell type under the conditions that are optimal for the study needs to be undertaken. There are no real 'markers' for cells, however, the genes expressed by cells can give a specific indication to which cell lineage they belong to, how mature they are and in the case of chondrocytes, what stage they are at in the chondrogenesis process. Some of the genes that can be used as chondrocyte markers are genes that are essential for the function of chondrocytes. Such genes include: Sox9, Col2a1 and Runx2 (Ng et al., 1997, Goldring et al., 2006a). These genes are core for the function of chondrocytes and without them, chondrocytes are not able to produce normal cartilage. Other genes that can be used as markers of chondrocytes are ECM genes such as Acan that are synthesised by chondrocytes (Bhosale and Richardson, 2008b). Surface markers such as Cd44, Cd9 and Cd151 can also be used in addition to the markers stated above (Hamada et al., 2013, Xu et al., 2020, Sumiyoshi et al., 2016).

Genes that are not part of the chondrogenic profile can be used to confirm the identity of chondrocytes such as Col1a1 (Dessau et al., 1980). As well as that, genes expressed at different stages of the chondrogenesis pathway can help to identify the maturity of the cells and would therefore make useful markers for chondrocytes. Also, genes that play a role in the anabolism and catabolism of cartilage, such as Mmps and ADAMTSs are also useful markers of chondrocytes as the balance of these

genes contributes to the healthy functioning of cartilage and their imbalance leads to diseases such as OA (Murphy and Lee, 2005, Porter et al., 2005, Bi, 2018). **Table 3.1** summarises the genes that are generally used as chondrocyte markers. As well as chondrocyte markers, chondrocytes express a variety of membrane proteins including different ion channel families and subtypes that make up their channelome. These ion channels are essential for the functioning of chondrocytes and are involved in the regulation of multiple biological processes such as cell volume control, proliferation, and migration, among others.

Table 3.1: Chondrocyte markers identified from the literature.

<i>Chondrocyte marker</i>	<i>Role of gene</i>	<i>Reference</i>
Acan	ECM protein	(Kiani et al., 2002)
Sox9	Chondrogenesis master regulator	(Henry et al., 2012)
Sox5	Chondrocyte differentiation	(Lefebvre et al., 2001)
Sox6	Chondrocyte differentiation	(Lefebvre et al., 2001)
Col1a1	Expressed in MSCs	(Sandell et al., 1994)
Col2a1	ECM protein	(Mendler et al., 1989)
Cd44	Surface marker	(Hamada et al., 2013)
Cd9	Surface marker	(Sumiyoshi et al., 2016)
Cd151	Surface marker	(Fujita et al., 2006)
Epyc	ECM organisation	(Onnerfjord et al., 2012)
Adamts5	Proteolytic enzyme	(Akkiraju and Nohe, 2015a)
Mmp13	Proteolytic enzyme	(Akkiraju and Nohe, 2015a)

3.1.3 Ion channels in chondrocytes

All living cells exhibit electrical properties and possess a membrane potential (Abdul Kadir et al., 2018). However, only a few cells are considered excitable and are able to fire action potentials, such as neurones and muscle cells. Other cells such as chondrocytes are considered inexcitable, yet despite this they still express a diverse collection of ion channels which influence their membrane potential (Abdul Kadir et al., 2018). The chondrocyte channelome of articular chondrocytes has been well established (Mobasheri et al., 2019, Barrett-Jolley et al., 2010b). Whereas the tracheal chondrocyte channelome remains to be elucidated. Identifying the tracheal chondrocyte channelome would not only aid in the understanding of these cells under physiological and disease conditions but would also offer a valuable list of druggable targets that can be used to tackle tracheal cartilage diseases and support regenerative medicine advances.

3.1.4 Aims

Despite the many similarities between chondrocytes from tracheal and articular cartilage. The comparison between their transcriptome and channelome remains to be investigated. Factors that would influence the similarities and differences between the two chondrocyte types such as the function of the cartilage that these chondrocytes reside in and their environment, have not been studied and will likely influence the genes they express. It may be that these chondrocytes express slightly different genes in order to accommodate for their cartilage-specific function. Therefore, in this chapter, the aim is to characterise the tracheal chondrocyte transcriptome and compare it to that of the established articular chondrocyte.

Specifically, identifying similarities and differences in ion channel gene expression, elucidating differences in biological pathways between the two cell types and identifying upstream regulators driving these differences. Furthermore, identifying the ion channels expressed in both cell types and detecting similarities and difference between the channelomes of these two cartilage phenotypes will be undertaken. This will be carried out using RNA-seq.

3.2 Methods

3.2.1 Immunofluorescence

Immunocytochemistry was carried out as previously described in chapter 2.2. Chondrocytes were stained with anti-CD44 (ab6124; Abcam), anti-aggrecan (ab36816; Abcam), anti-Sox9 (ab185966; Abcam) and anti-collagen II a1 (ab185430; Abcam) primary antibodies. AF594 (A11037; Life Technologies) and AF488 (A11029; Life Technologies) were used as secondary antibodies. AF488 was excited at 488 nm and emission spectra were recorded between 500-600 nm; AF594 was excited at 594 nm and emission was recorded between 575-700 nm and DAPI was excited at 374 nm and emission was recorded at 748 nm.

3.2.2 RNA sequencing

RNA extraction and RNA-seq was conducted as previously reported in chapter 2. For the analysis of the RNA-seq data, UseGalaxy.org, an open-source web-based bioinformatics platform for data intensive biomedical research was used. As shown in **Figure 3.1**, a reference-based transcriptome assembly was used to analyse the

dataset in this project. In order to map the transcriptome, bowtie2 was used to align the sequencing reads to the reference genome sequences, in this case the *Rattus norvegicus* genome (Rnor_6.0 (GCA_000001895.4)). Aligning the read fragments to the *Rattus norvegicus* genome fragments helps to determine the location (chromosome and position) of the fragments in the genome. The genome is initially broken down into fragments as it allows the alignment of reads even if they are not exact matches to the reference genome. Once the reads per gene were determined, cufflinks was used to assemble the transcripts, estimate their abundances and test for the differential expression and regulation in the samples.

Cufflinks estimates the relative abundance of the transcripts based on how many reads support each transcript. Following that cuffdiff, part of the cufflinks package was used in order to find significant changes in the transcript expression, splicing, and promotor use. This gives an output to many different parameters such as gene ID, Fragments Per Kilobase of transcript per Million mapped reads (FPKM), log₂ fold change and *p*-value as well as *q*-value. The output data was then further analysed using the Ingenuity Pathway Analysis (Qiagen, UK). Once the differentially expressed genes between tracheal and articular chondrocytes were determined, R studio was used to generate principal component analysis (PCA) plots. This was done for both the entire datasets and a subset containing channels only. The channels subset of data used for the majority of analysis here was created by subsetting the global data set with MATLAB. This also enabled the categorisation of these ion channel families and the comparison of their expression levels between the trachea and articular chondrocytes.

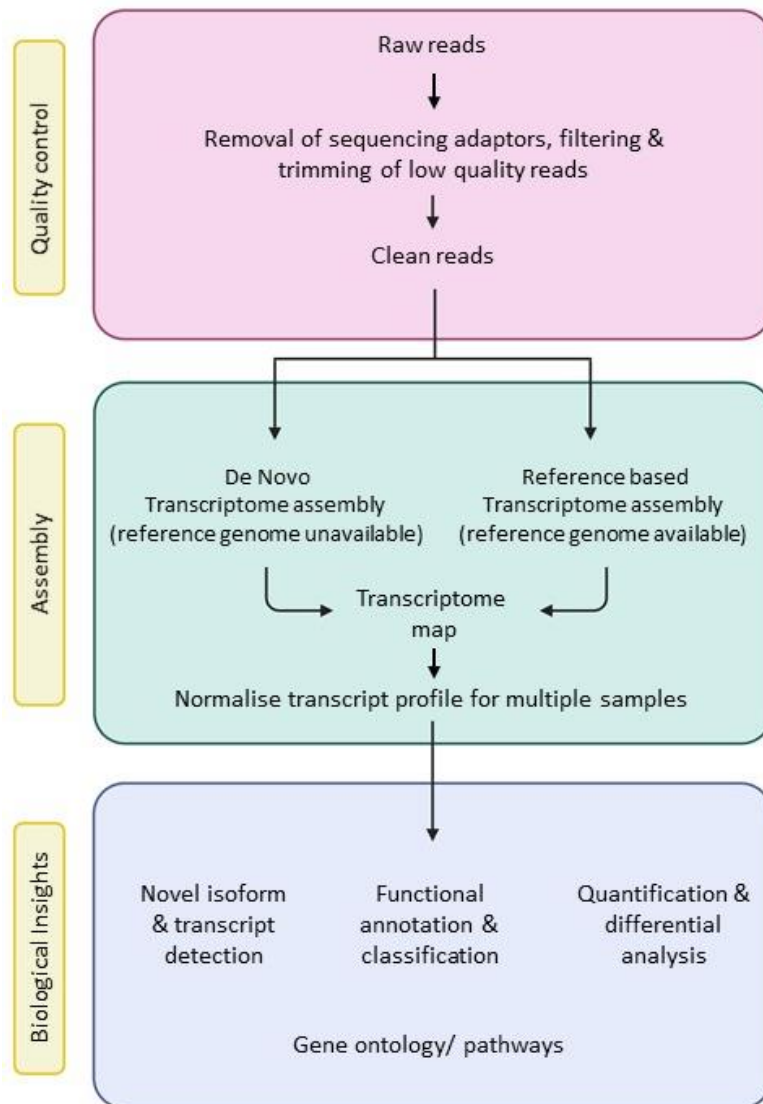


Figure 3.1: Workflow of RNA-sequencing analysis. Representation of the RNA-seq data processing through bioinformatics. Raw reads obtained are subjected to quality control assessment. The clean reads are used for transcriptome assembly, ready to be further analysed.

3.2.3 Ingenuity Pathway Analysis (IPA)

Ingenuity Pathway Analysis (IPA) (Qiagen, UK) was used to further analyse the RNA-seq data. It was used to predict downstream effects, molecular interactions and new targets using the RNA-seq data. A core analysis was conducted and a cut off of 0.05 was set for the expression p -value. Direct and indirect interactions were included in

the analysis. In addition, a miRNA target filter was also used to obtain a list of miRNAs that were upstream regulators in the RNA-seq data. IPA was used to predict upstream regulators and canonical pathways involved in chondrocytes as well as the causal networks.

3.2.4 Quantitative polymerase reaction (qPCR)

qPCR analysis was carried out as described in chapter 2.4. Accession numbers of ion channel genes were sourced from the NCBI gene database (<https://www.ncbi.nlm.nih.gov/gene/>). Primers for Ano genes were designed and validated by Primerdesign Ltd, UK (**Table 3.2**). Primerblast NCBI was used to design the primer sequences for Lrrc8 ion channel genes as well as Clcn7 and Cacna1g (**Table 3.3**). Primers were designed to span the exon-exon junction and to cover as many of the isoforms/ variants as possible. The optimal primers were chosen based on melting temperature (T_m), self-complementarity, and the sequence of the primers. Primers were purchased from Sigma-Aldrich, UK.

Table 3.2: Ano primers designed by Primerdesign Ltd., UK.

<i>Gene</i>	<i>Accession number</i>	<i>Species</i>	<i>Sequence (5' → 3')</i>	<i>Size (bp)</i>	<i>Melting Tm (°C)</i>
Ano1	NM_00110756	Rat	F: CATCCCTGCCTCCATTGTGG R: GGTGATGTTGTGTCTCTGGTCA	106	57.7 57.7
Ano2	XM_00876329	Rat	F: TCAACGTCAGCCAGCTGAA R: GGGTGGCTCTCGATAATCTTTG	98	56.2 56.3
Ano3	XM_01759233	Rat	F: AGGGTGCCCTTCAGGAAAA R: GAACCATTGGGTTTTGGGACA	115	55.3 56.1
Ano4	NM_00110677	Rat	F: AGCAGAAGGATTACAGATGGAGAA R: CCTGAAAGGCATCCGTACATTC	130	57.1 56.9
Ano5	XM_00622926	Rat	F: TTGCCGCAAGATGACCTTC R: CTCGTTTGATTTTCTCCGCGAC	117	57.9 58
Ano6	NM_00110810	Rat	F: CCAAGCTGGCTTTTATCATTGTTA R: CTCCTCTTGATCTTGCTTTTCG	113	55.9 57.3
Ano7	NM_00100407	Rat	F: GAGTGACAACCAGGACACCTTC R: GCACTCAATACACCTTCTGCCA	141	58.3 58.3
Ano8	XM_01760040	Rat	F: CTGCGTCTGGAGTCCTGGA R: CACTGTCTTCATCCATGCCTTG	92	57.6 57.1
Ano9	XM_01759024	Rat	F: CACTGTCAAGTTCTTCATCCTGC R: GCCACTGAGATGGCACTCC	148	57.5 57.1
Ano10	XM_236774.8	Rat	F: GGCATTGAAGTCGGATGTTGAC R: CAGGAACAACCTCCAAGTAATCATCAA	106	57.7 57.8

Table 3.3: Ion channel primers designed using Primerblast NCBI.

<i>Gene</i>	<i>Accession number</i>	<i>Species</i>	<i>Sequence (5' → 3')</i>	<i>Size (bp)</i>	<i>Melting Tm (°C)</i>
Lrrc8a	NM_001127244.2	Human	F: GGGTTGAACCATGATTCCGGTGAC R: GAAGACGGCAATCATCAGCATGAC	133	72.9 70.7
Lrrc8b	NM_001134476.2	Human	F: ACCTGGATGGCCCACAGGTAATAG R: ATGCTGGTCAACTGGAACCTCTGC	126	69.5 71.4
Lrrc8c	NM_032270.5	Human	F: ACAAGCCATGAGCAGCGAC R: GGAATCATGTTTCTCCGGGC	132	66.7 67.7
Lrrc8d	NM_001134479.2	Human	F: ATGGAGGAGTGAAGTCTCCTGTCTG R: CTTCCGCAAGGGTAAACATTCCTG	126	68.8 70.7
Lrrc8e	NM_001268284.3	Human	F: ACCGTGGCCATGCTCATGATTG R: ATCTTGTCCTGTGTACCTGGAG	62	73.2 66.5
Clcn7	NM_031568.2	Rat	F: GCCATGGCCAACGTTTCTAA R: AAGTGCAGAATGAGACTGGCG	156	59.11 60.94
Cacna1g	NM_001308302	Rat	F: ATGACAGTGAAGGTGGTGGC R: CCAGGATGTCTGATGACGGAG	115	60.25 59.97
Hprt1	NM_012583	Rat	F: TCCTCCTCAGACCGCTTTTC R: ATCACTAATCACGACGCTGGG	78	59.39 60.20

3.2.5 Identifying differentially expressed ion channel genes.

To identify ion channel genes that were differentially expressed between the tracheal and articular chondrocytes from the RNA-seq dataset, MATLAB was used. Ion channel genes were identified from the International Union of Basic and Clinical Pharmacology database (IUPHAR-DB) (Sharman et al., 2009) and separated out from the RNA-seq dataset. Following the identification of the ion channel genes, an interactive tool for comparing lists using Venn Diagrams, Venny 2.1 (<https://bioinfogp.cnb.csic.es/tools/venny/index.html>) was used to create a Venn diagram of the ion channel genes shared between tracheal and articular chondrocytes. A heatmap of the ion channel gene expression between tracheal and articular samples was also created using R studio and a hierarchical clustering of the samples and ion channel genes was performed using MATLAB.

3.3 Results

3.3.1 Expression of chondrocyte markers in isolated tracheal and articular chondrocytes.

To confirm cell phenotype and ensure that the population of isolated cells (passage 1) were mature chondrocytes, chondrocyte markers were used. First, a list of markers used to classify chondrocytes was identified from the literature (**Table 3.1**). Next, immunofluorescence was used to identify functional expression of some of these markers in tracheal and articular chondrocytes as observed in **Figure 3.2**. Aggrecan (**Figure 3.2A &E**), Col2a1 (**Figure 3.2B & F**), Sox9 (**Figure 3.2C &G**) and Cd44 (**Figure**

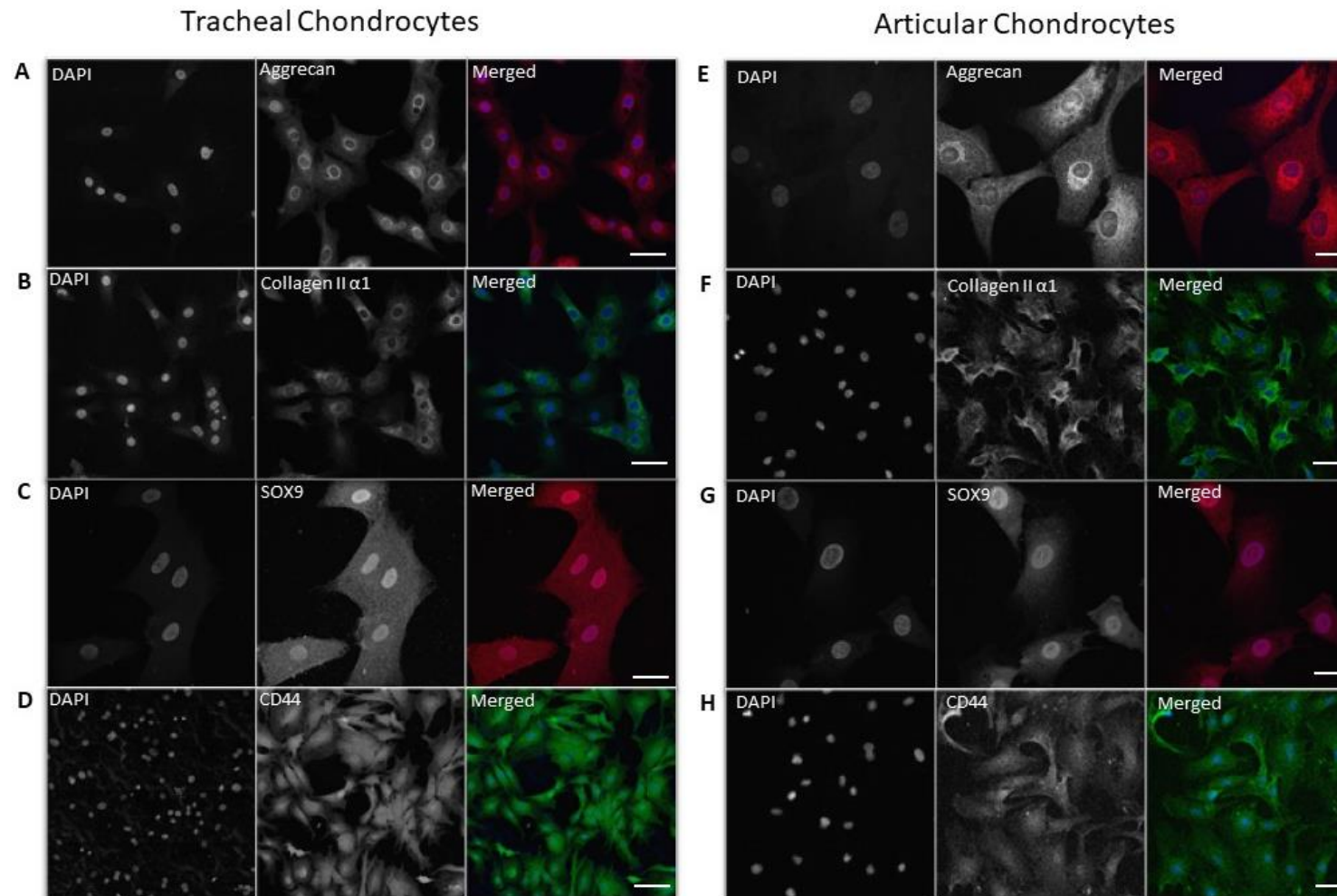


Figure 3.2: Representative immunofluorescence of chondrocyte markers in tracheal and articular chondrocytes. Representative immunostaining of tracheal and articular chondrocytes with chondrocyte markers: Aggrecan (A and E), Collagen II α 1 (B and F), Sox9 (C and G) and Cd44 (D and H). Images obtained using a Zeiss LSM 800 confocal microscope at x20 magnification. Scale bar: 100 μ m.

3.2D & H), were shown to be expressed. Finally, to validate the expression of these chondrocyte markers and others (**Table 3.1**), differential gene expression of these markers between tracheal and articular chondrocytes was determined from the RNA-seq data. Interestingly several of these genes were significantly decreased in tracheal chondrocytes compared to articular chondrocytes (**Figure 3.3**). These genes include Sox5 ($p < 0.00005$), Col2a1 ($p < 0.03$), Epyc ($p < 0.00005$), Adamts5 ($p < 0.00005$) and Mmp13 ($p < 0.00005$). However, Acan ($p < 0.00005$) and Runx2 ($p < 0.01$) were significantly increased in tracheal chondrocytes (**Figure 3.3**).

3.3.2 Assessment of global tracheal and articular chondrocyte differential gene expression

To provide an initial assessment of how similar or different the global gene expression patterns between tracheal and articular chondrocytes, PCA analysis of the RNA-Seq dataset was performed in R studio. This revealed that over 50% of the variability between the genes expressed by tracheal and articular chondrocytes was captured in the first three principal components (**Figure 3.4A**). Dimensionality reduction with PCA showed that in both the first and second principal components there was a clear difference between the two chondrocyte types (**Figure 3.4B**). This was also seen between the second and third principal components (**Figure 3.4C**). However, clustering of the first and third principal component indicated that there was a slight overlap between the tracheal and articular chondrocyte genes (**Figure 3.4D**). To identify which genes were most different between the two global RNA-Seq datasets, differential analysis with DESEQ2 was performed (Love et al., 2014). This identified 528 genes to be significantly differentially expressed by a factor of 3 (log₂ fold

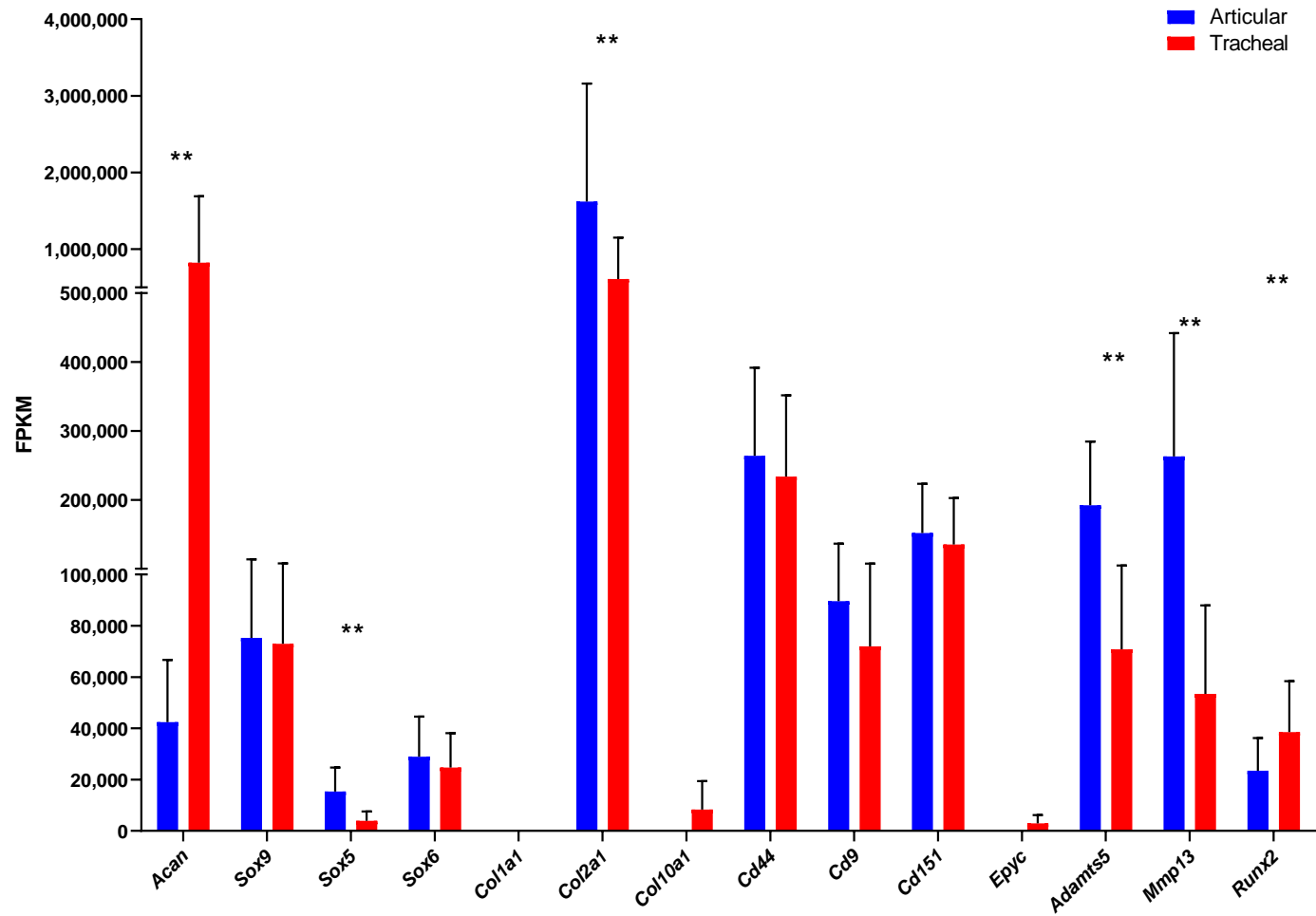


Figure 3.3: Differential expression of chondrocyte markers between tracheal and articular chondrocytes. Chondrocyte markers were identified from RNA-Seq data (AC n=3; TC n=5). ** q -value of 0.001. FDR (q -value) was determined using the Benjamini Hochberg correction.

change) or more (adjust p-value: $p < 0.05$). The top 50 of these genes are shown in the appendix (**Table A.2**). Following this, IPA (Qiagen, UK) was used to examine this differential gene expression between tracheal and articular chondrocytes.

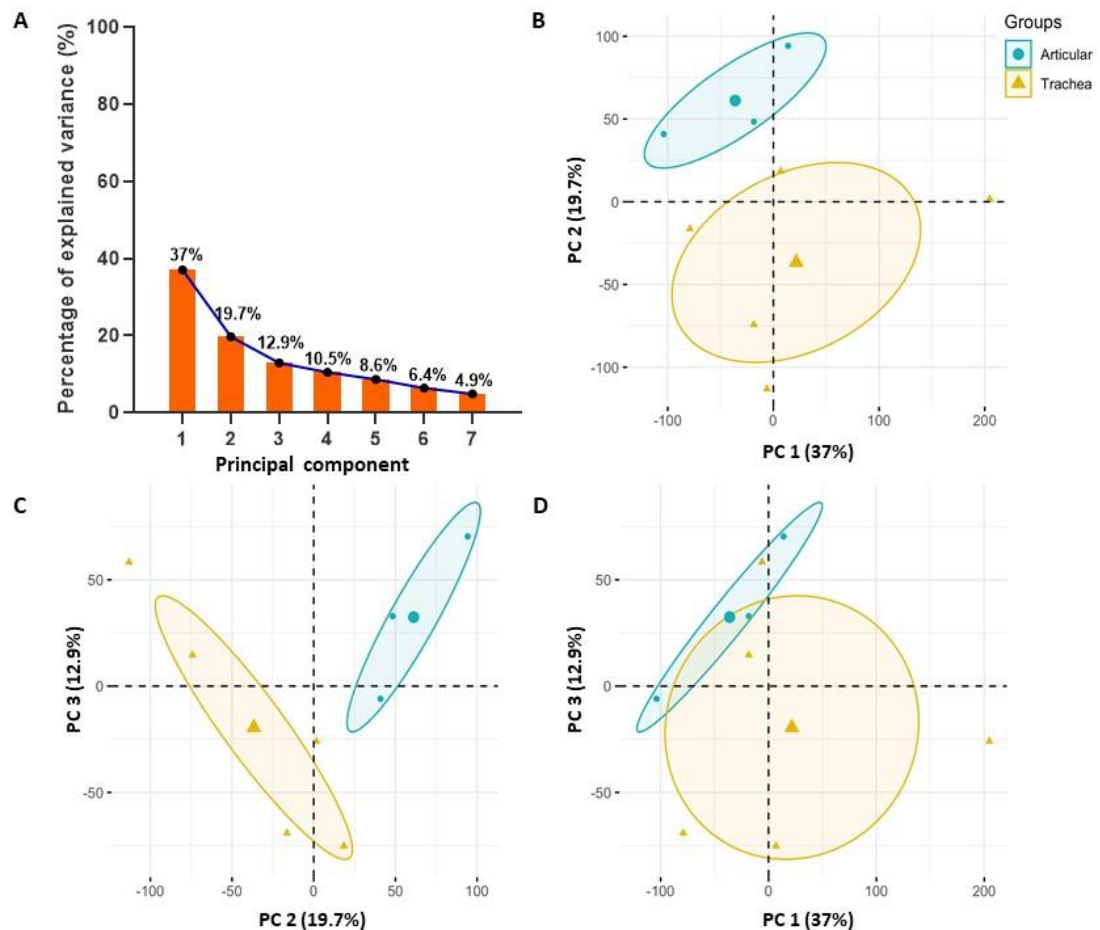


Figure 3.4: Principal component analysis (PCA) of global RNA-Seq gene expression between tracheal and articular chondrocytes. 32650 genes were identified and subjected to dimensionality reduction with PCA in R Studio. A) Over 50% of the variability between the two chondrocyte types was captured within the first three principal components. B) Clustering of tracheal and articular chondrocyte gene expression between the first and second principal components. C) Clustering of tracheal and articular chondrocyte gene expression between the second and third principal components. D) Clustering of tracheal and articular chondrocyte gene expression between the first and third principal components. The 95% confidence intervals for unsupervised clustering are shown in yellow for tracheal chondrocyte samples ($n=5$) and blue for articular samples ($n=3$).

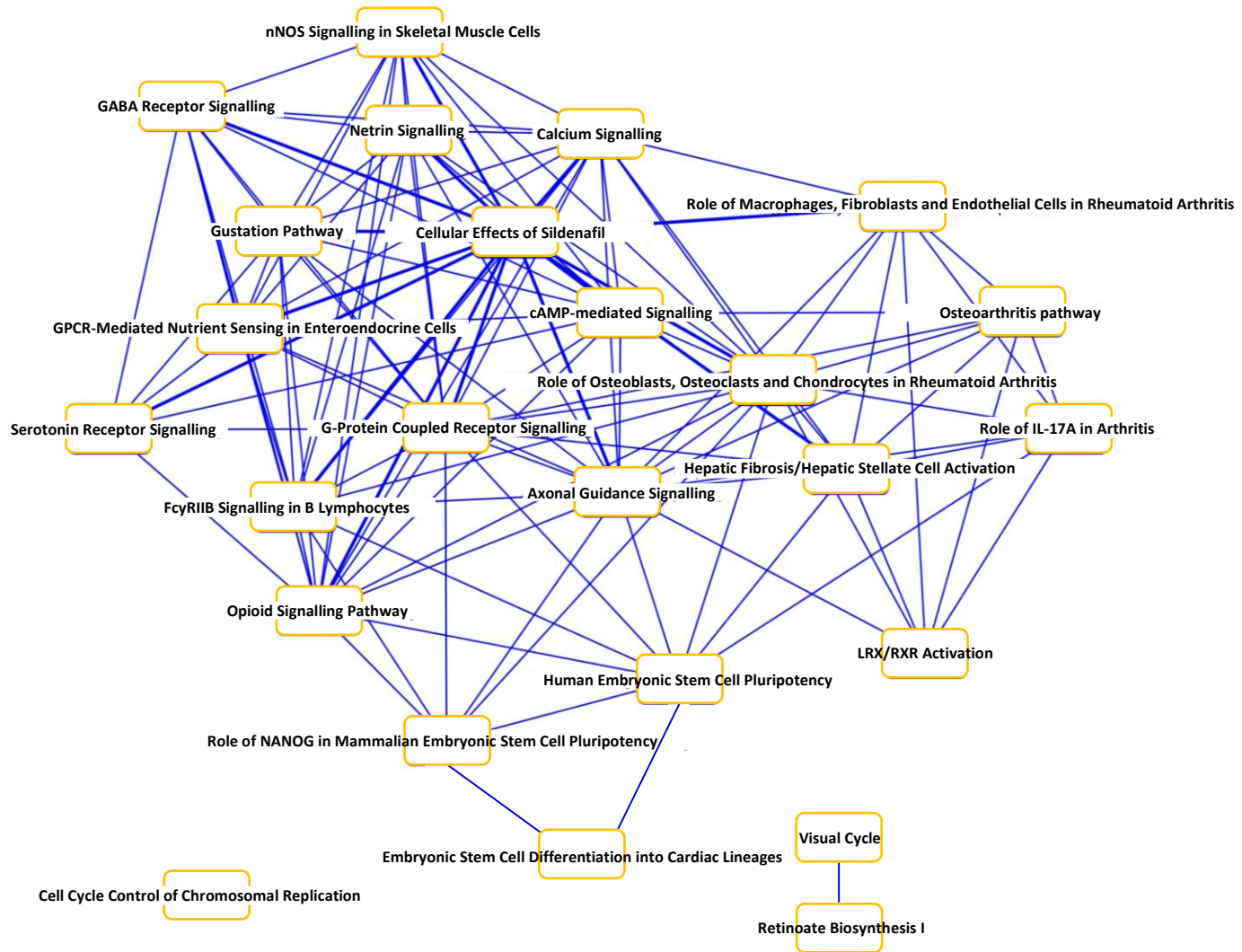
3.3.3 Top canonical pathways identified between tracheal and articular chondrocytes.

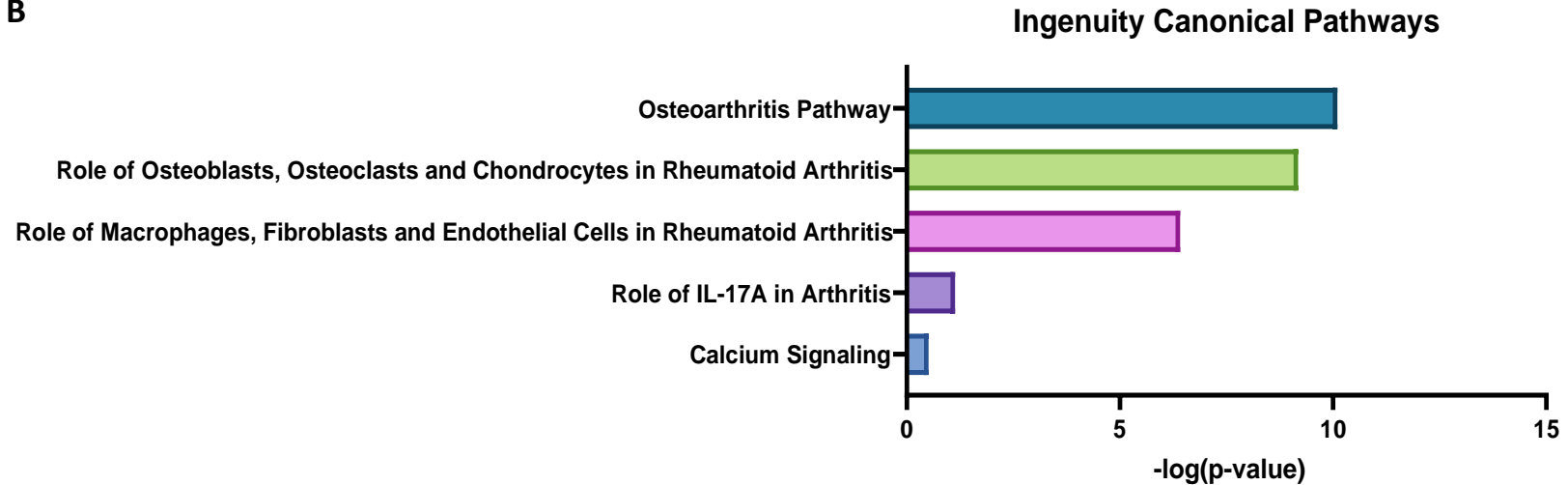
Global RNA-Seq analysis detected 32650 genes to be expressed by tracheal and articular chondrocytes. An unbiased approach was used to gain a clearer view into the function of these genes, the role they play in chondrocyte canonical pathways and the targets they regulate. A core analysis was carried out in IPA (Qiagen, UK) and upstream regulators and top canonical pathways were identified. Through this, 546 pathways were identified with the top 25 pathways shown in **Figure 3.5A**. A closer look into these pathways identified the osteoarthritis pathway to be amongst the top 5 pathways differentially expressed between tracheal and articular chondrocytes (**Figure 3.5B**). Other pathways relating to chondrocytes were also identified such as ‘the role of osteoblasts, osteoclasts and chondrocytes in Rheumatoid Arthritis’, ‘the Role of Macrophages, Fibroblasts and Endothelial Cells in Rheumatoid Arthritis’, and ‘the Role of IL-17A in Arthritis’ (**Figure 3.5B**). Aside from investigating the top canonical pathways, genes differentially expressed between the two chondrocyte types that were upstream regulators were examined, many of which were found to be miRNAs, some of the top ones are highlighted in **Figure 3.5C**.

To determine the role of the differentially expressed genes in the top chondrocyte canonical pathways, the genes differentially expressed between tracheal and articular chondrocytes were mapped onto the pathways using the Molecular Activity Predictor (MAP) function in IPA. Mapping the genes onto the osteoarthritis pathway in chondrocytes highlights some important genes that are differentially expressed between tracheal and articular chondrocytes (**Figure 3.6A**). The most notable genes

are Runx2 and Sox9, which seem to be central to the development of OA and get targeted by upstream regulators which lead to the downstream processes that lead to cartilage catabolism and disease. Mapping the genes onto the OA pathway, shows that most of the genes seem to be predicted to be inhibited (blue), with a few that were predicted to be activated (orange) (**Figure 3.6A**). MAP analysis was also conducted on the Rheumatoid Arthritis in chondrocytes pathway (**Figure 3.6B**).

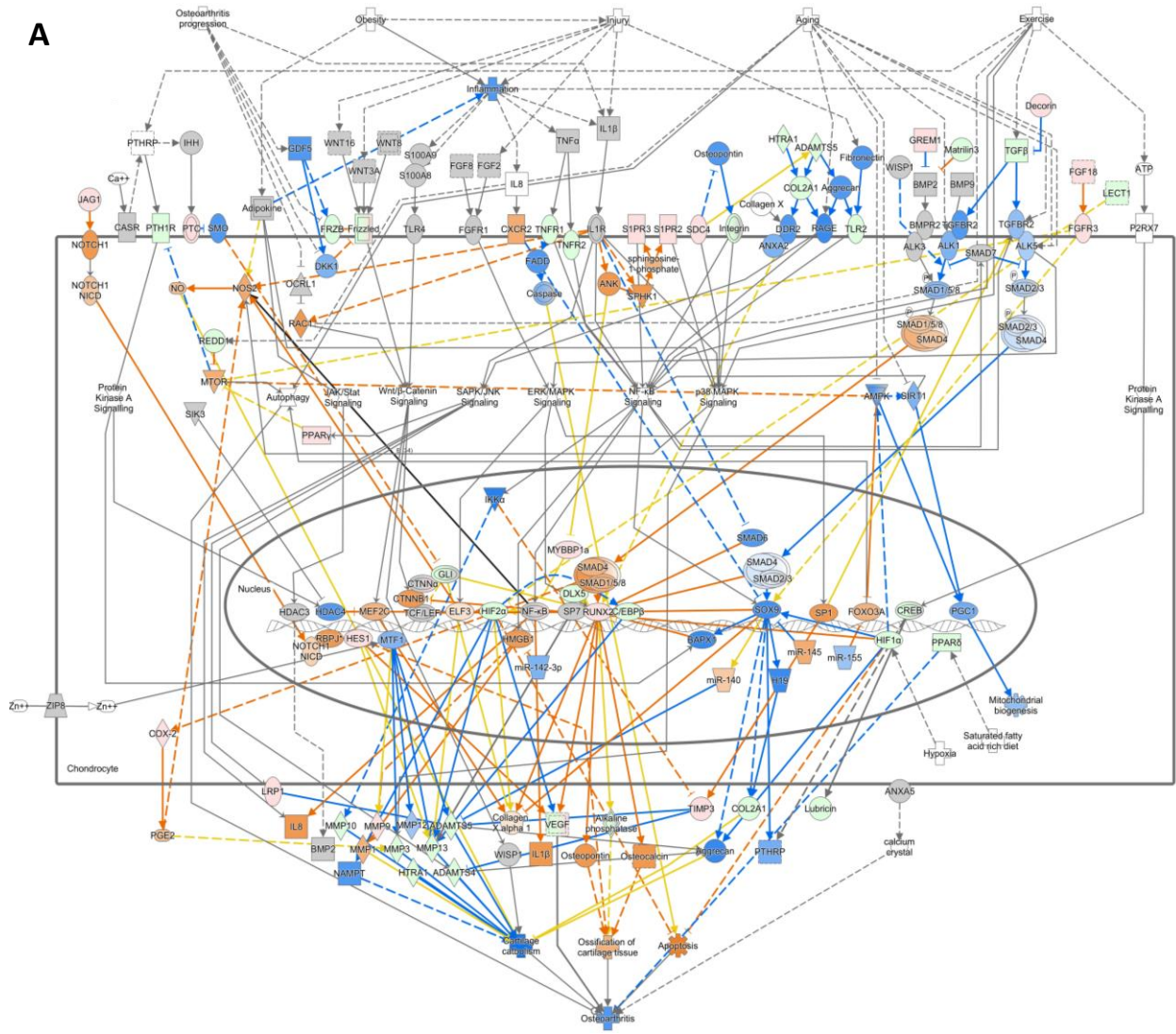
A



B**C**

Predicted Upstream Regulators	P-value	Z-value
miR-141-3p	0.00003	-0.065
miR-181a-5p	0.0002	0.363
miR-29	0.03	-1.509

Figure 3.5: Top Canonical pathways and upstream regulators identified using IPA. A) Overlapping canonical pathways and their connection to each other. B) Key predicted pathways generated by IPA comparing tracheal chondrocytes to articular chondrocytes. C) Key predicted upstream regulators identified through IPA comparing the two chondrocyte types.



More extreme in dataset

- Increased measurement (Red circle)
- Decreased measurement (Green circle)

More confident

- Predicted activation (Orange circle)
- Predicted Inhibition (Blue circle)

Glow Indicates activity when opposite of measurement

- Red glow
- Green glow

Predicted Relationships

- Leads to activation (Orange line)
- Leads to inhibition (Blue line)
- Findings inconsistent with state of downstream molecule (Yellow line)
- Effect not predicted (Grey line)

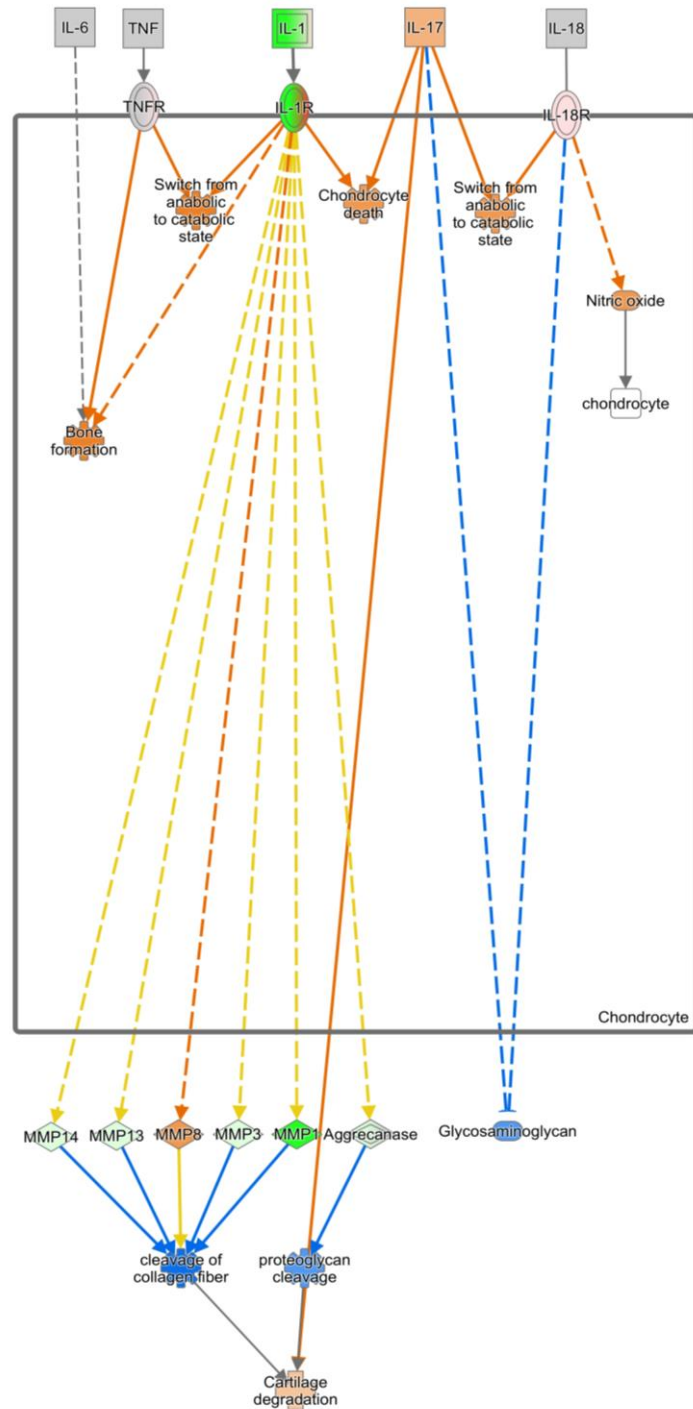
B

Figure 3.6: Chondrocyte pathways with Molecular Activity Predictor (MAP) overlay. A) Osteoarthritis pathway in the chondrocyte. B) Rheumatoid Arthritis pathway in the chondrocyte. Genes that have increased (red) or decreased (green) measurements from the RNA-seq dataset are predicted to be activated (orange) or inhibited (blue). The strength of the prediction is represented by the opacity of the colour. The predicted relationship between the molecules are shown in the key. Orange leads to activation, blue leads to inhibition, yellow indicates findings inconsistent with the state of downstream molecule and grey indicates effect not predicted.

3.3.4 Expression of ion channel families in tracheal and articular chondrocytes

In order to identify the ion channel gene expression in tracheal chondrocytes and compare to that of articular chondrocytes, ion channel genes were identified from the RNA-seq dataset using MATLAB. This identified a total of 190 ion channel genes that showed expression in either tracheal or articular chondrocytes or both (**Figure 3.7**). Further investigating the expression of these genes revealed that 164 ion channel genes were shared between the two chondrocyte types and 8 were exclusive to tracheal chondrocytes while 18 ion channel genes were expressed in articular chondrocytes only (**Figure 3.7**). Out of the 164 genes shared between the tracheal and articular chondrocytes, 89 genes were shown to be significantly different in either the tracheal or articular chondrocytes, 19 of which are highlighted in the box (**Figure 3.7**). For example, the VGCC, *Cacna1g* and the CaCC, *Ano1* had significantly higher expression in tracheal cartilage ($p < 0.00005$ for both). Whereas the CaCC *Ano2* was only expressed in tracheal cartilage ($p < 0.00005$). However, the CIC channel *Clcn7* was also expressed in both chondrocyte types but showed no significant difference (**Figure 3.7**).

To further validate and compare the ion channel gene expression between the two chondrocyte types, a heatmap of the ion channel gene expression (Log₂ fold change values) between the tracheal and articular chondrocyte unpooled samples was created to visually observe the differences (**Figure 3.8**). Hierarchical clustering of the samples detected the difference between the two chondrocyte types and clustered

tracheal chondrocytes together and articular chondrocyte samples together (Figure 3.8).

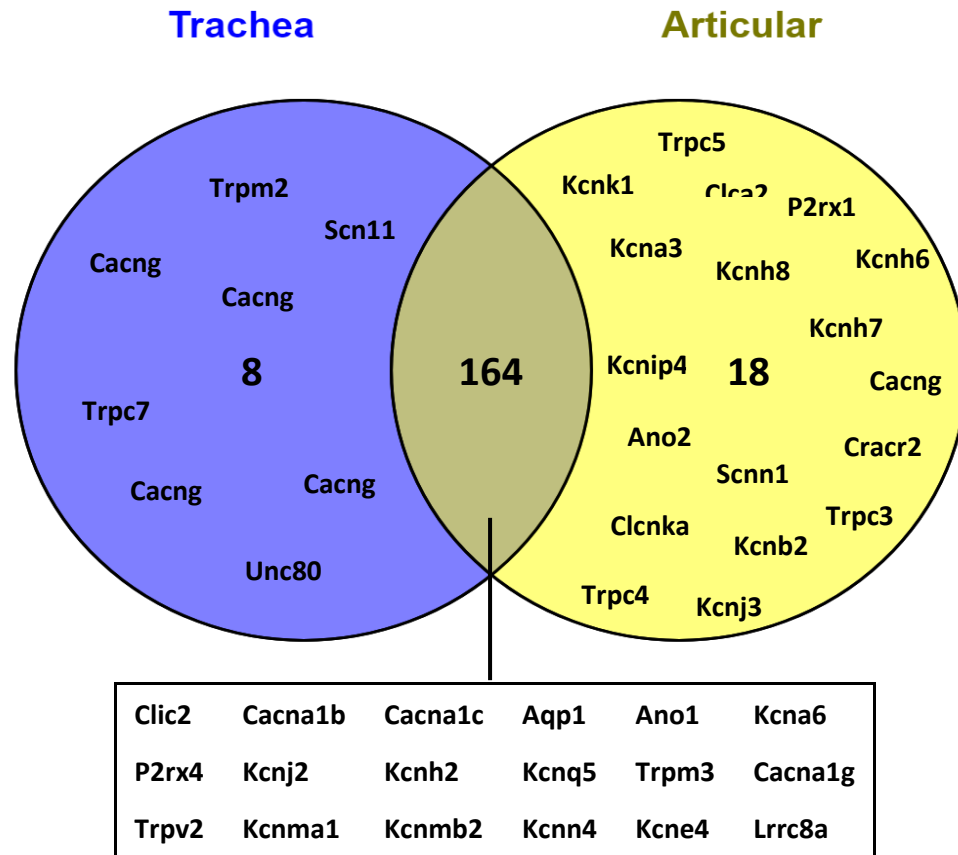


Figure 3.7: Venn diagram of differential ion channel gene expression between tracheal and articular chondrocytes. A total of 190 ion channel genes were found to be expressed in the RNA-seq dataset. Out of those, 8 genes were expressed in tracheal chondrocytes only and 18 were expressed in articular chondrocytes only. 164 ion channel genes were shared between tracheal and articular chondrocytes. Some ion channel genes significantly different between tracheal and articular chondrocytes are shown in the box.

The heatmap also showed that the ion channel gene expression in tracheal and articular chondrocytes was very similar and mostly conserved. However, there were notable differences in the ion channel subtype genes. In order to investigate these differences, ion channel genes were grouped into families and subfamilies according to the International Union of Basic and Clinical pharmacology (IUPHAR) and the British Pharmacological Society (BPS) database (Alexander et al., 2019). These subtypes were plotted between tracheal and articular chondrocytes.

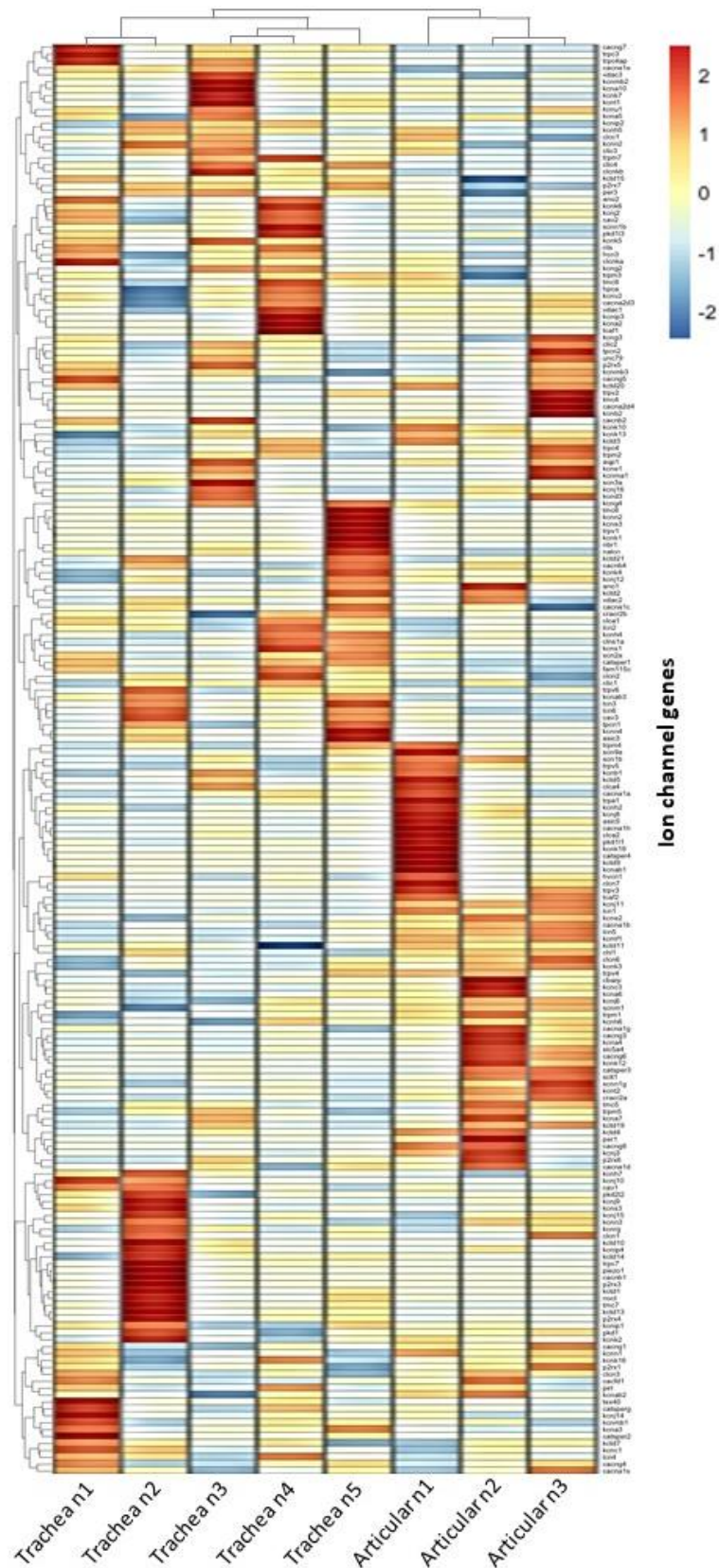
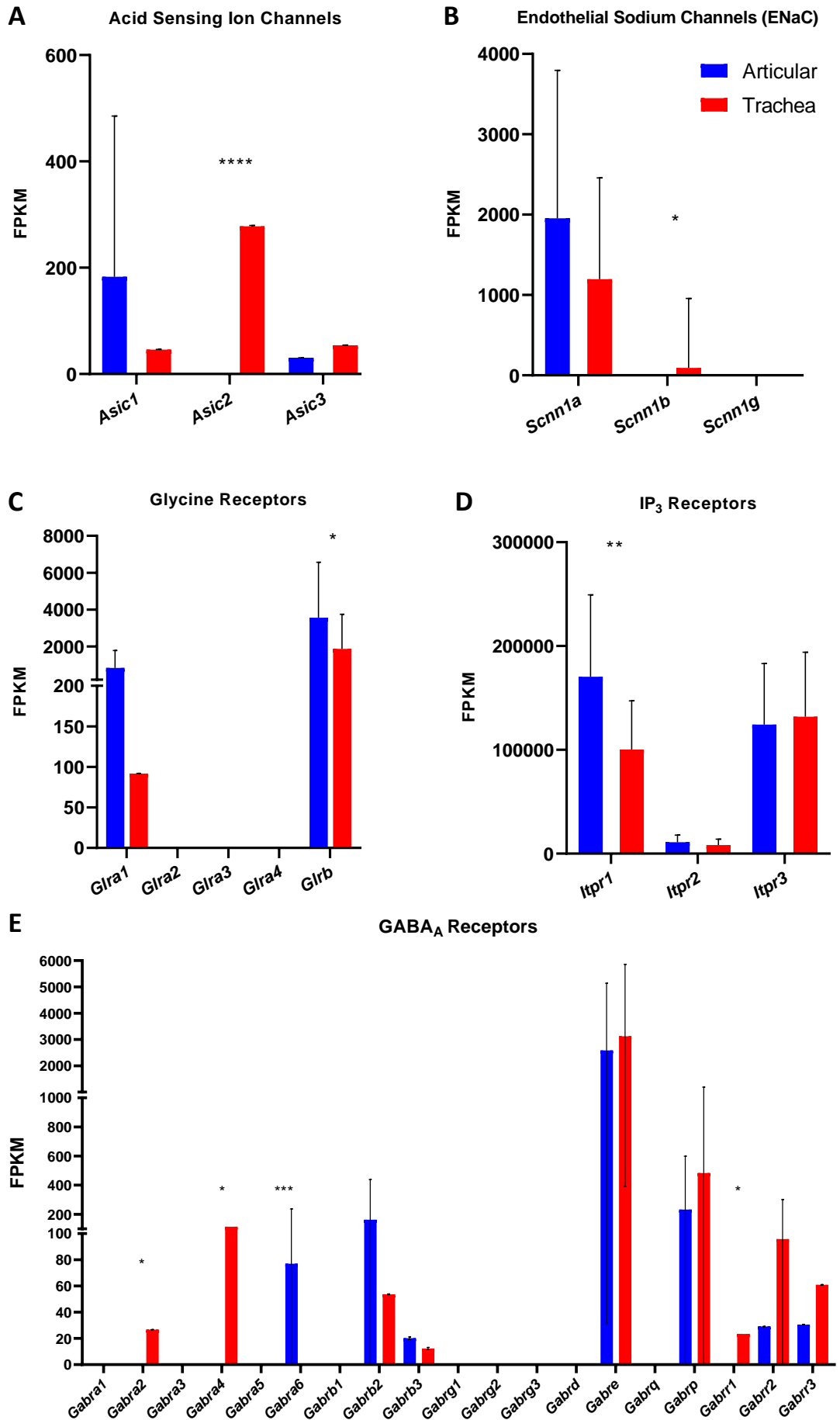
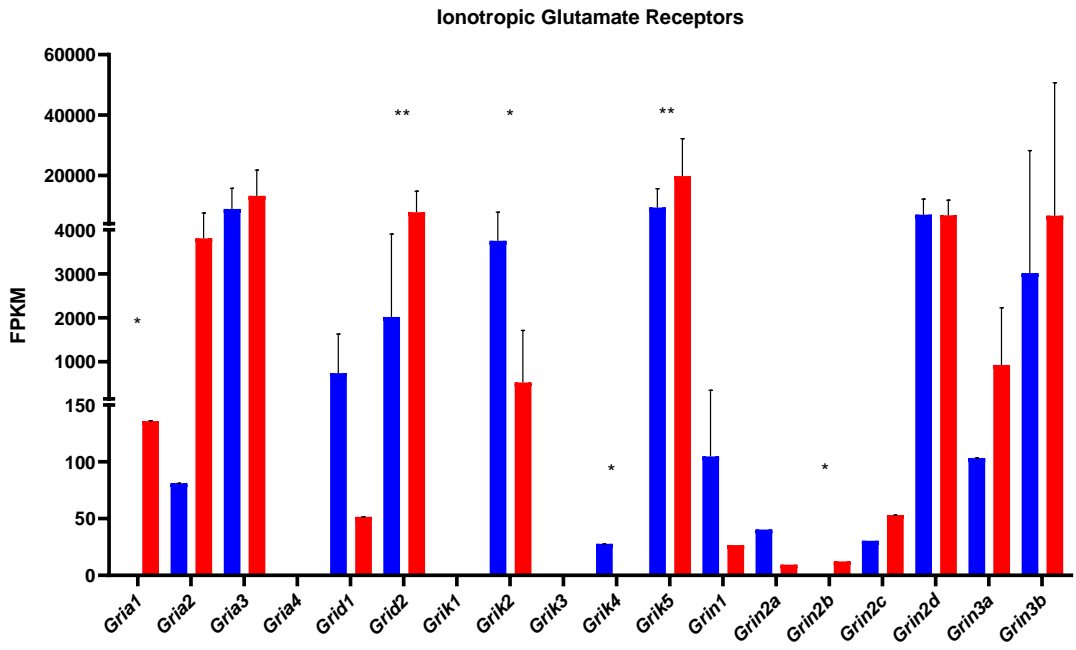


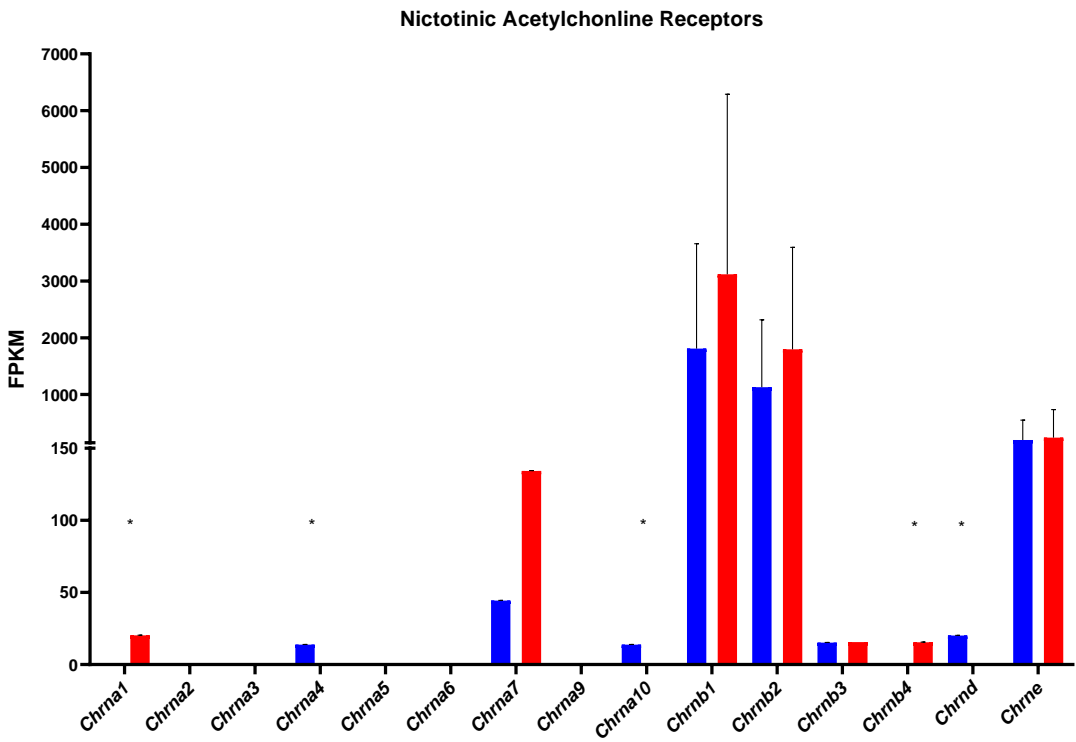
Figure 3.8: Heat map of the ion channel differential gene expression in tracheal and articular chondrocytes. Ion channel genes shown on the right-hand side and tracheal (n=5) and articular (n=3) chondrocyte samples shown on bottom axis. Legend corresponds to the fold change Values. Samples were clustered using MATLAB and graph was created using R studio.



F



G



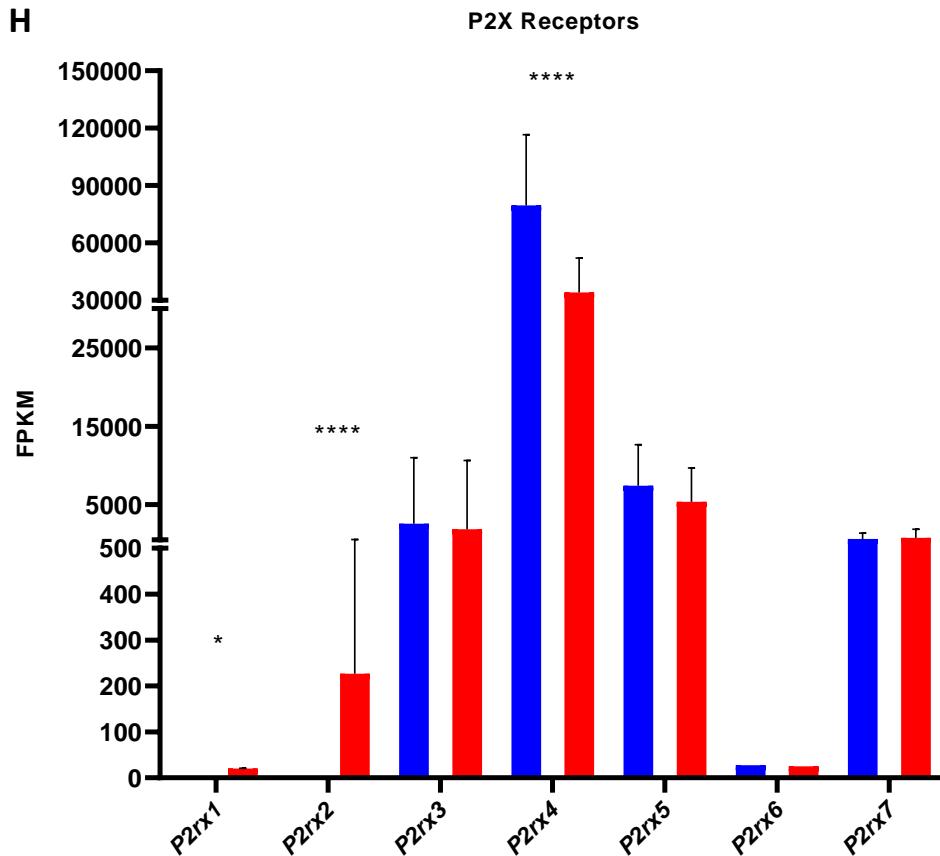
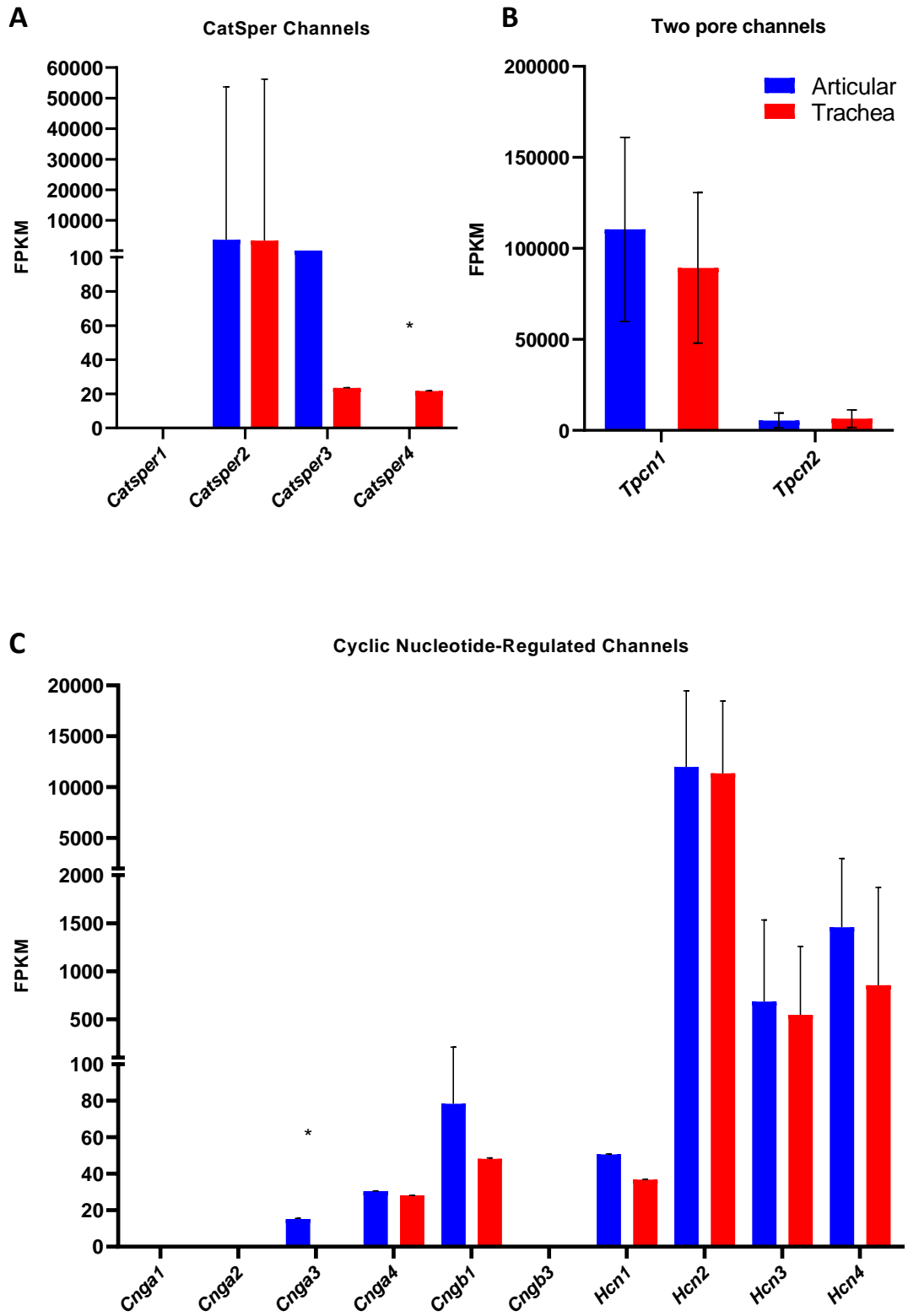
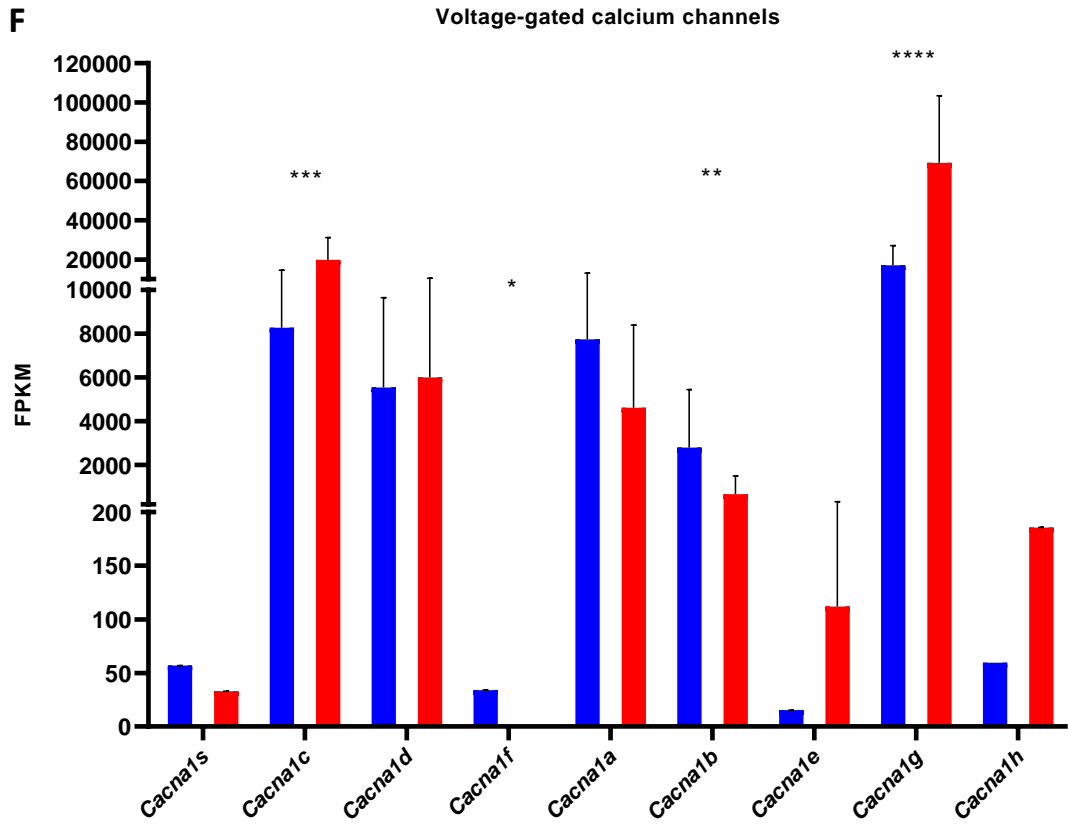
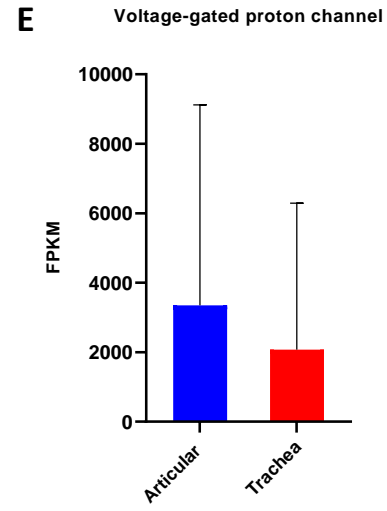
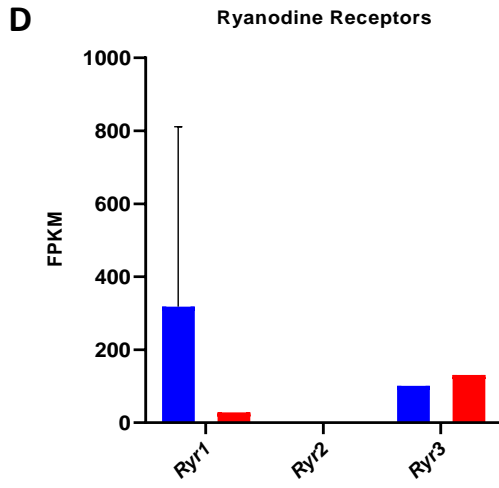


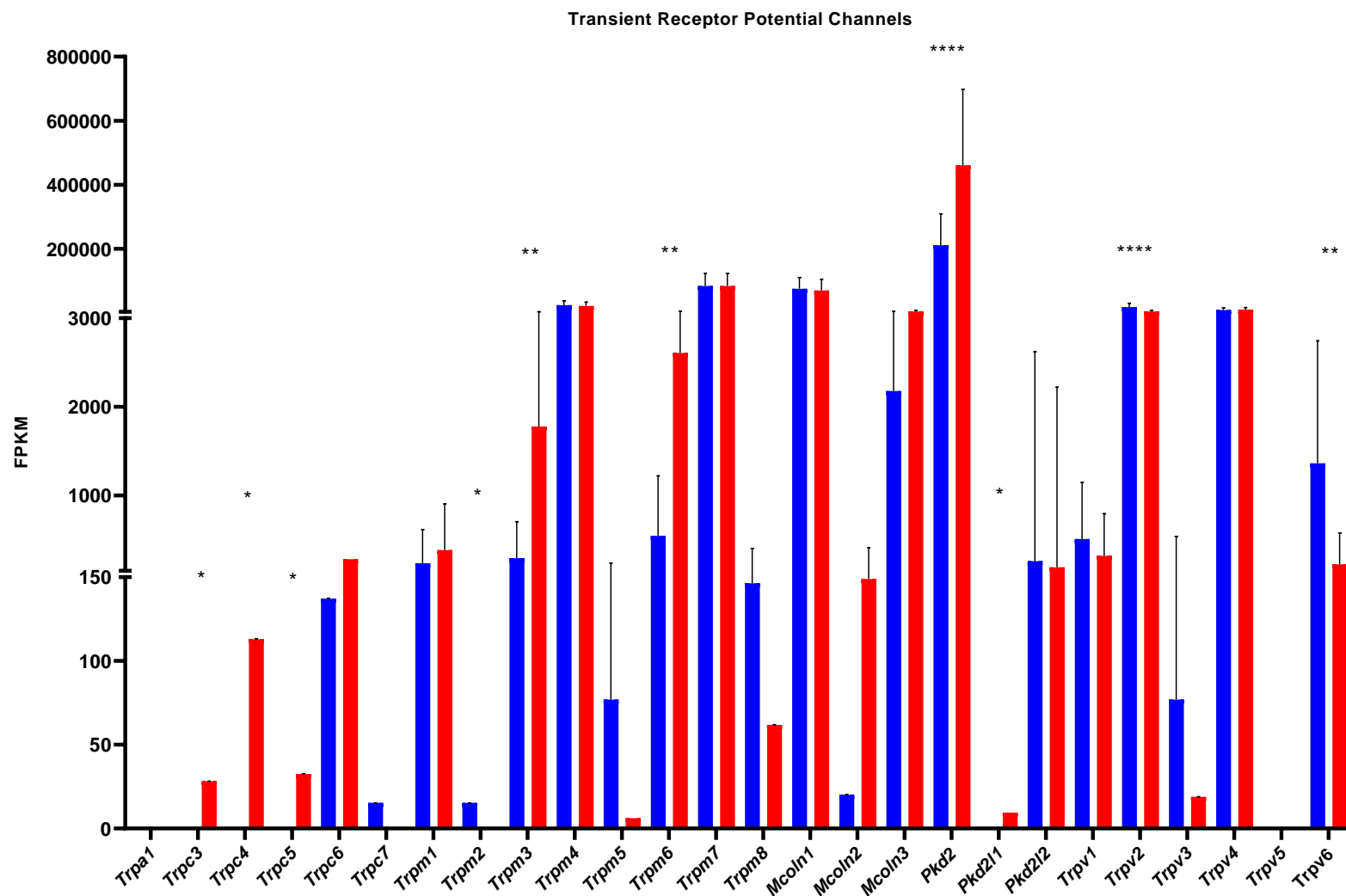
Figure 3.9: RNA-seq differential expression of ligand-gated ion channel genes. Expression of A) Acid-sensing ion channels. B) Endothelial Sodium channels (ENaC) C) Glycine receptors D) IP₃ receptors E) GABA_A receptors F) Ionotropic glutamate receptors G) Nicotinic Acetylcholine receptors and H) P2X receptors was observed. Graphs were created using GraphPad Prism 8. Bars represent mean FPKM values. Error bars represent 95% confidence limits. * denotes $p < 0.05$, ** denotes $p < 0.01$, *** $p < 0.001$ and **** $p < 0.0001$.

Out of the ten ligand-gated ion channels (Alexander et al., 2019) 8 were found to be expressed in tracheal and articular chondrocytes (**Figure 3.9**). These ligand-gated ion channels had 22 significantly different subtypes between the two chondrocyte types (**Figure 3.9A-H**). Eight voltage-gated ion channels (Alexander et al., 2019) excluding potassium channels were also found to be expressed in the two chondrocyte types (**Figure 3.10**). Of those voltage-gated ion channels, 19 subtypes were shown to be significantly different (**Figure 3.10A-H**). The RNA-seq dataset also identified the





G



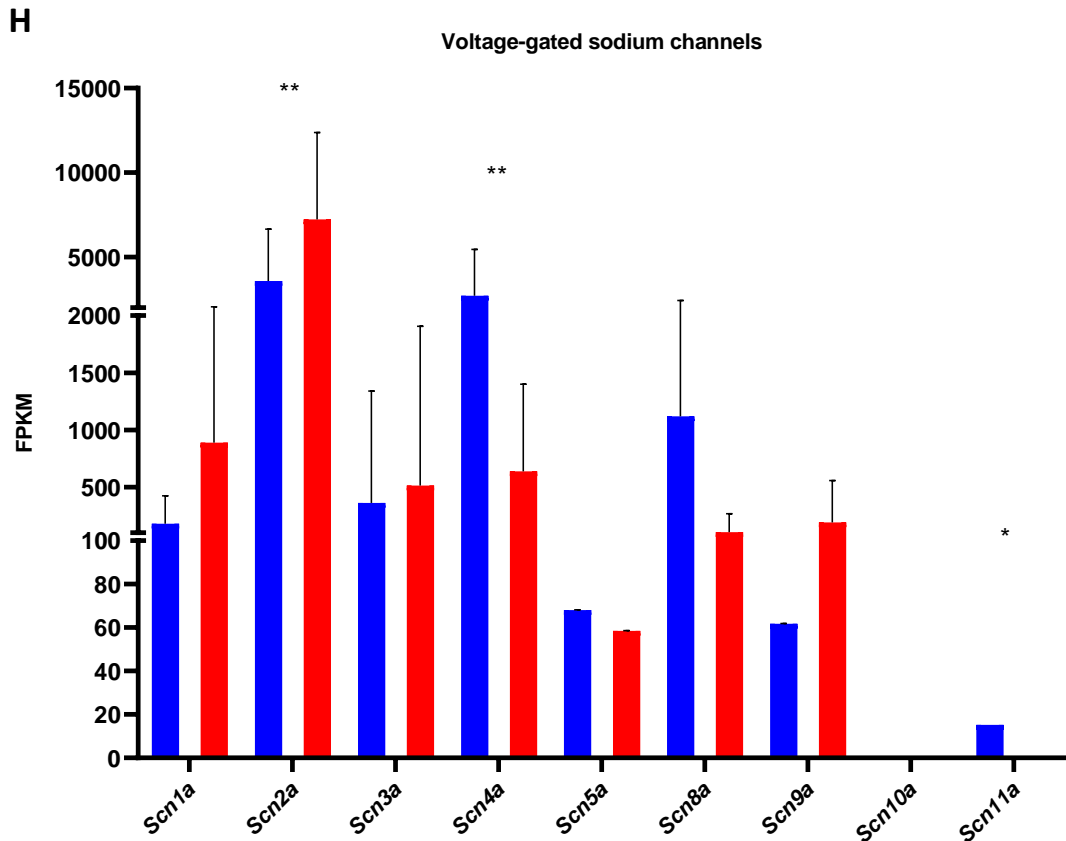
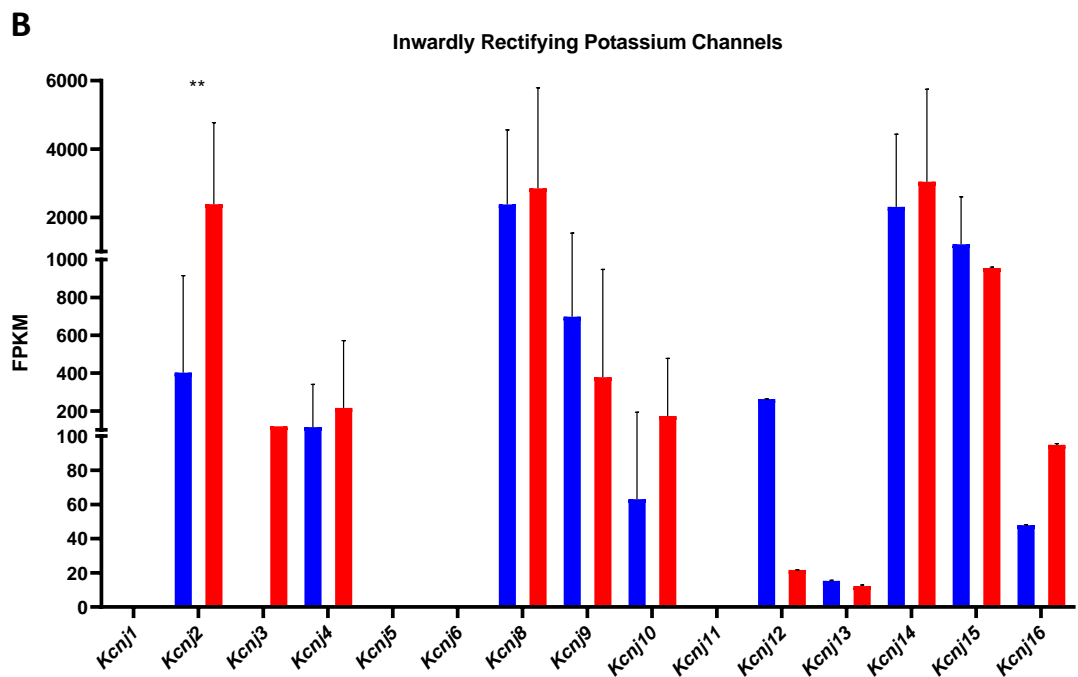
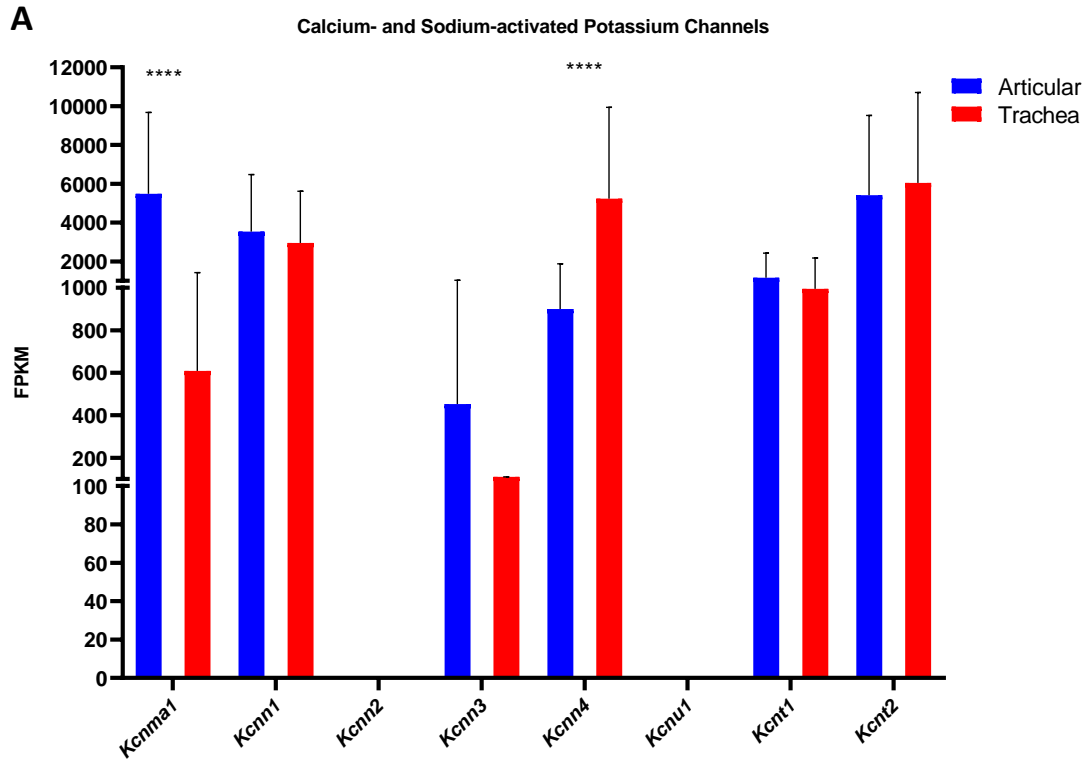


Figure 3.10: RNA-seq differential expression of voltage-gated ion channel genes. Expression of A) CatSper channels B) Two pore channels C) Cyclic nucleotide regulated channels D) Ryanodine receptors E) Voltage-gated proton channel F) Voltage-gated calcium channels G) Transient Receptor Potential Channels and H) Voltage-gated sodium channels was observed. Graphs were created using GraphPad Prism 8. Bars represent mean FPKM values. Error bars represent 95% confidence limits. * denotes $p < 0.05$, ** denotes $p < 0.01$, *** $p < 0.001$ and **** $p < 0.0001$.

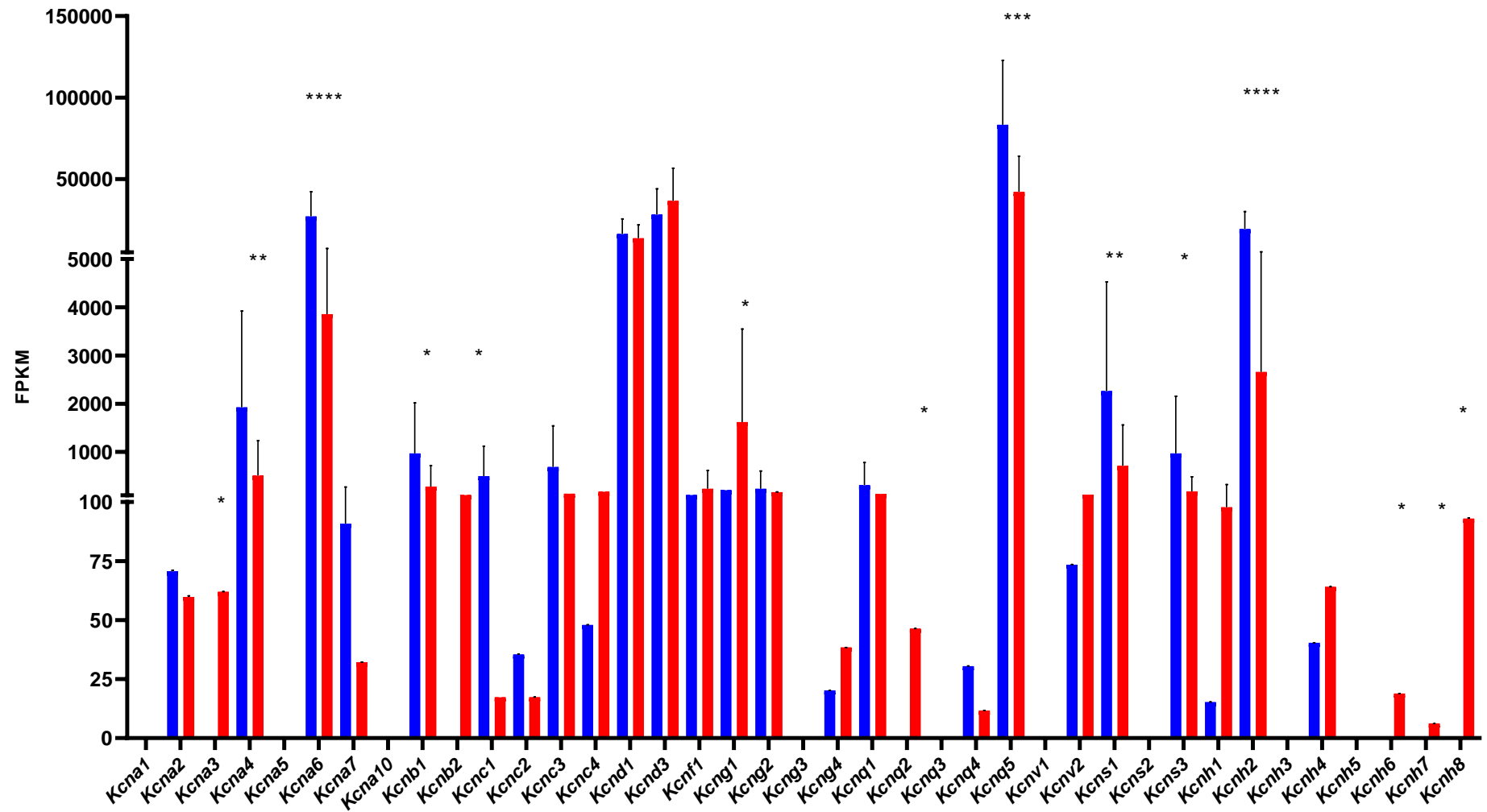
expression of four potassium channel families (Alexander et al., 2019), of which 22 subtypes were shown to be significantly different (**Figure 3.11A-D**). Next the expression of six ‘other’ ion channels (Alexander et al., 2019) was detected which had 16 significantly different subtypes (**Figure 3.12A-F**). Finally, four chloride ion channels (Alexander et al., 2019) were shown to be expressed between the two chondrocyte types. These chloride channels showed 10 significantly different subtypes (**Figure 3.13A-D**). Combining the transcriptomic expression of these ion channel families

provided the information for an updated articular chondrocyte channelome and the establishment of the novel tracheal chondrocyte channelome (**Figure 3.14**).



C

Voltage-gated potassium Channels



D

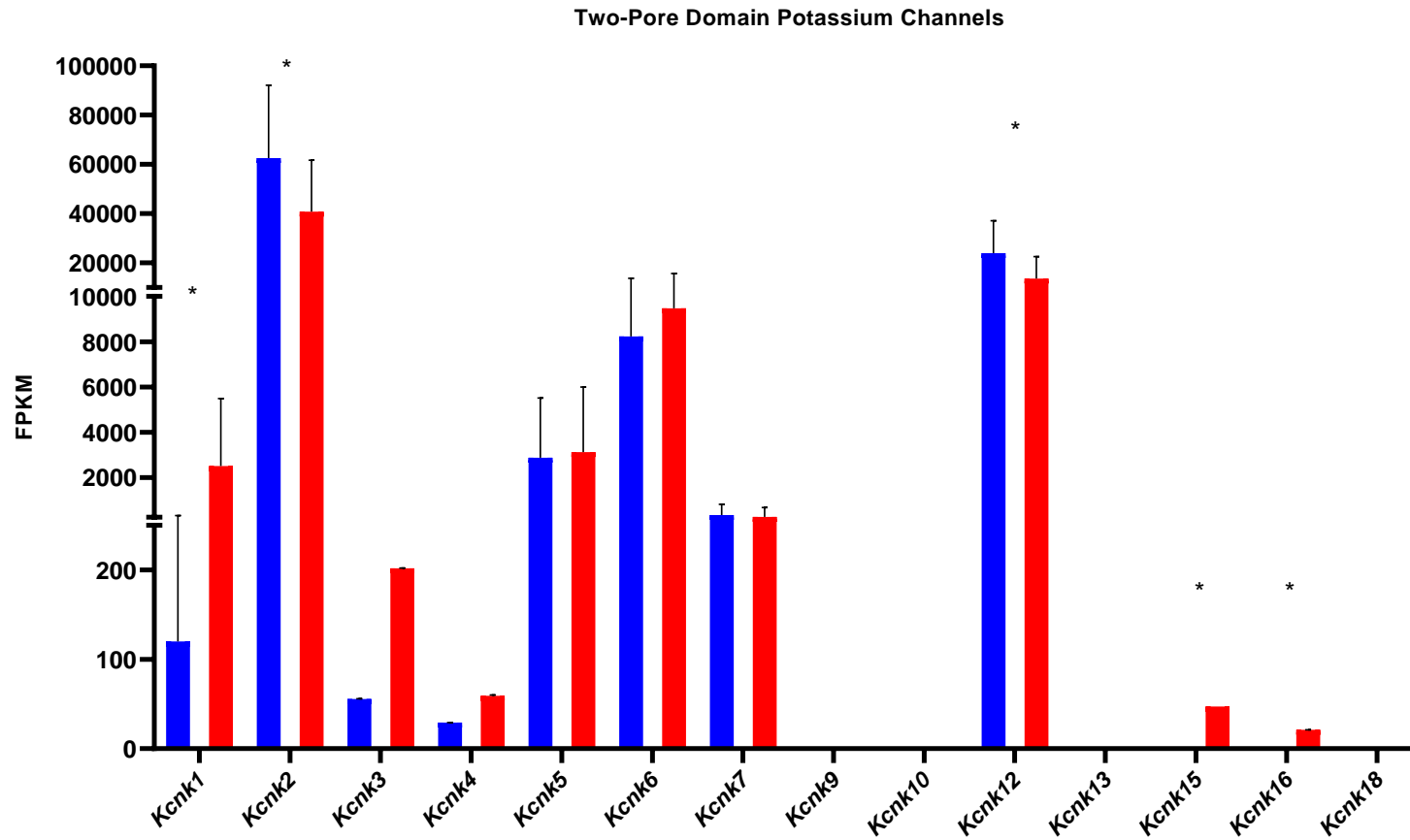
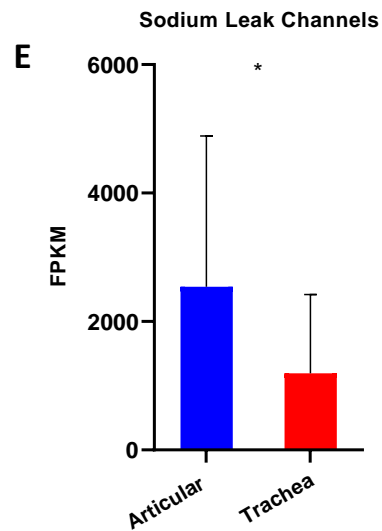
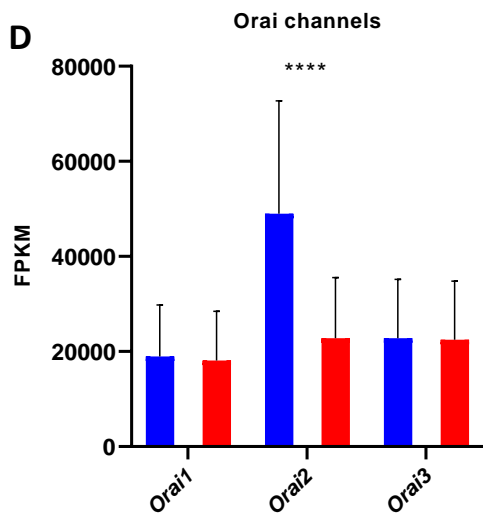
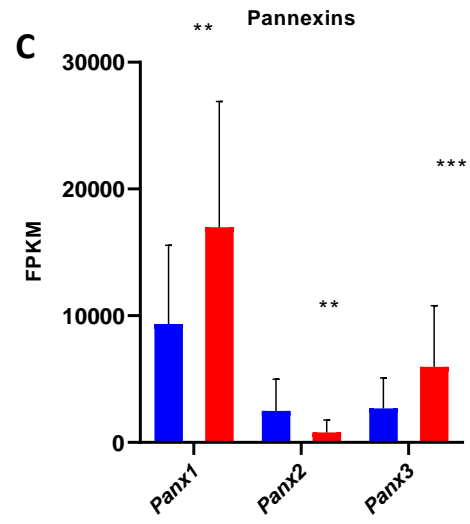
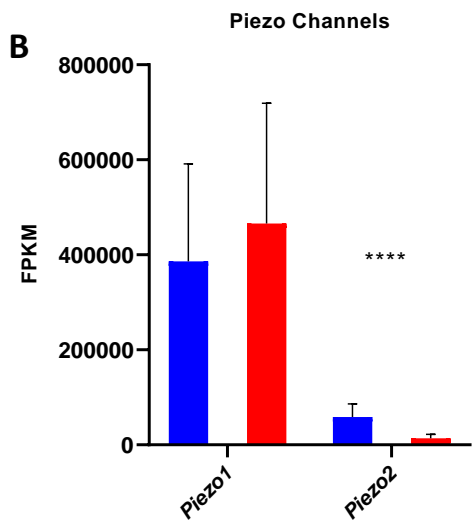
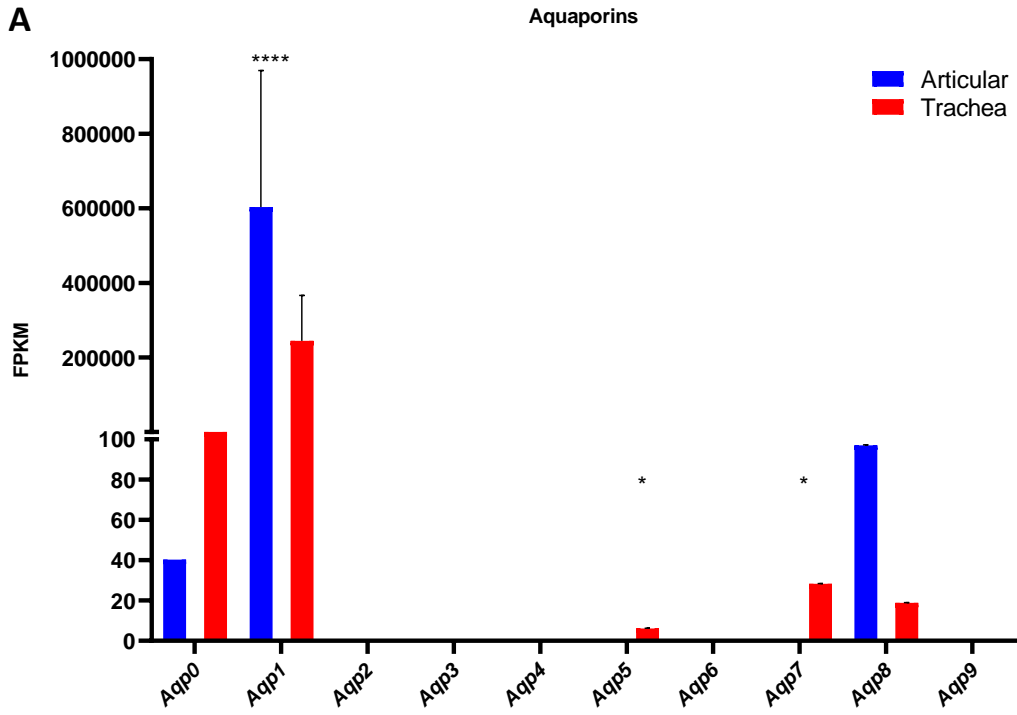


Figure 3.11: RNA-seq differential expression of potassium ion channel genes. Expression of A) Calcium- and Sodium-activated potassium channels B) Inwardly rectifying potassium channels C) Voltage-gated potassium channels and D) Two-pore domain potassium channels was observed. Graphs were created using GraphPad Prism 8. Bars represent mean FPKM values. Error bars represent 95% confidence limits. * denotes $p < 0.05$, ** denotes $p < 0.01$, *** $p < 0.001$ and **** $p < 0.0001$.



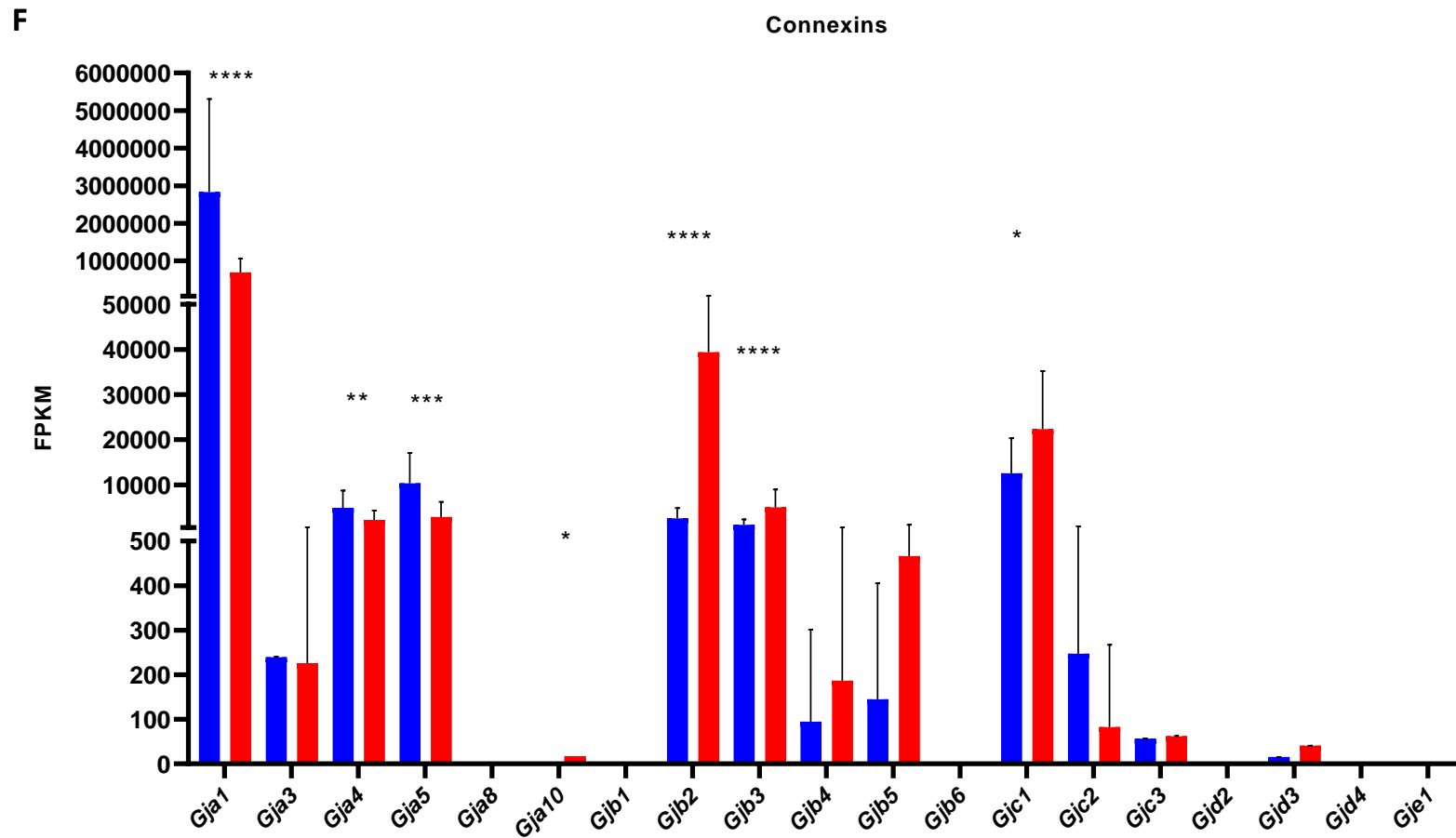
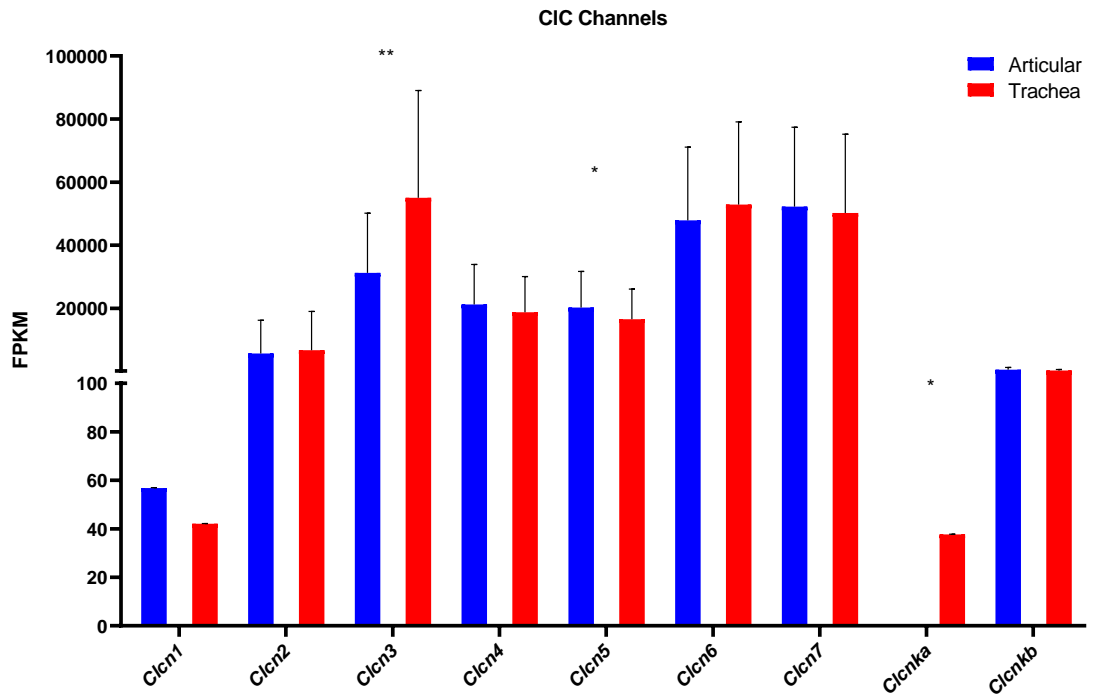
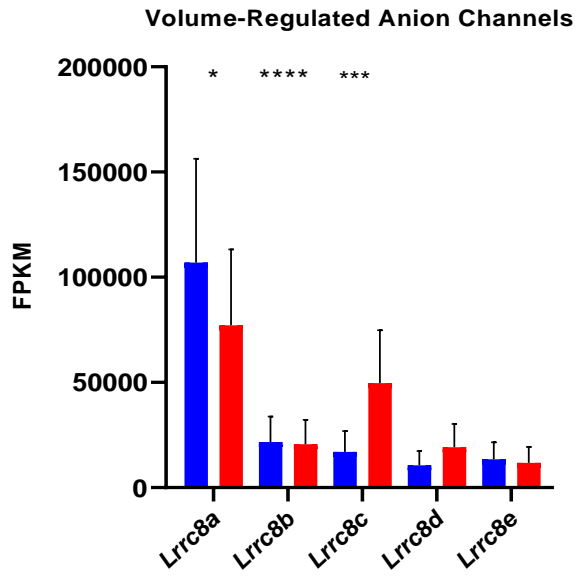


Figure 3.12: RNA-seq differential expression of 'other' ion channel genes. Expression of A) Aquaporins B) Piezo channels C) Pannexins D) Orai channels E) Sodium leak channels and F) Connexins was observed. Graphs were created using GraphPad Prism 8. Bars represent mean FPKM values. Error bars represent 95% confidence limits. * denotes $p < 0.05$, ** denotes $p < 0.01$, *** $p < 0.001$ and **** $p < 0.0001$.

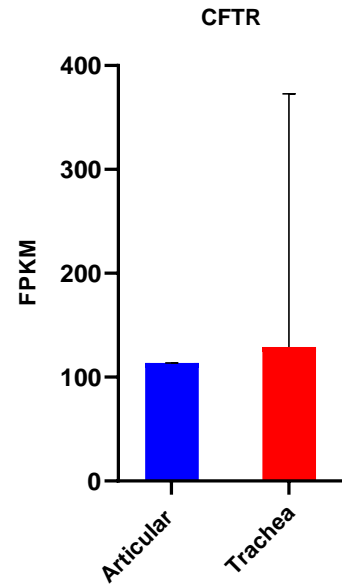
A



B



C



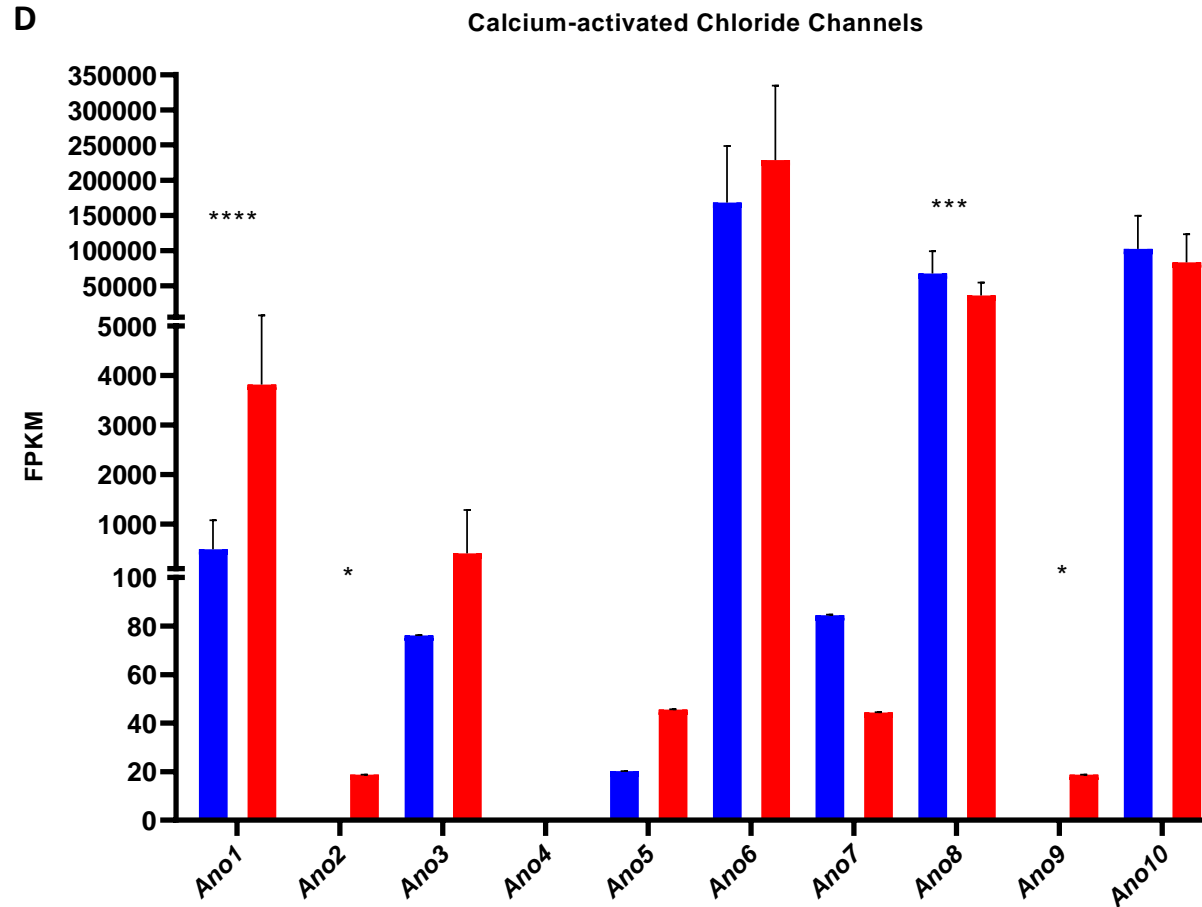


Figure 3.13: RNA-seq differential expression of chloride ion channels genes. Expression of A) CIC channels B) Volume-regulated anion channels C) CFTR channel and D) Calcium-activated chloride channels was observed. Graphs were created using GraphPad Prism 8. Bars represent mean FPKM values. Error bars represent 95% confidence limits. * denotes $p < 0.05$, ** denotes $p < 0.01$, *** $p < 0.001$ and **** $p < 0.0001$.

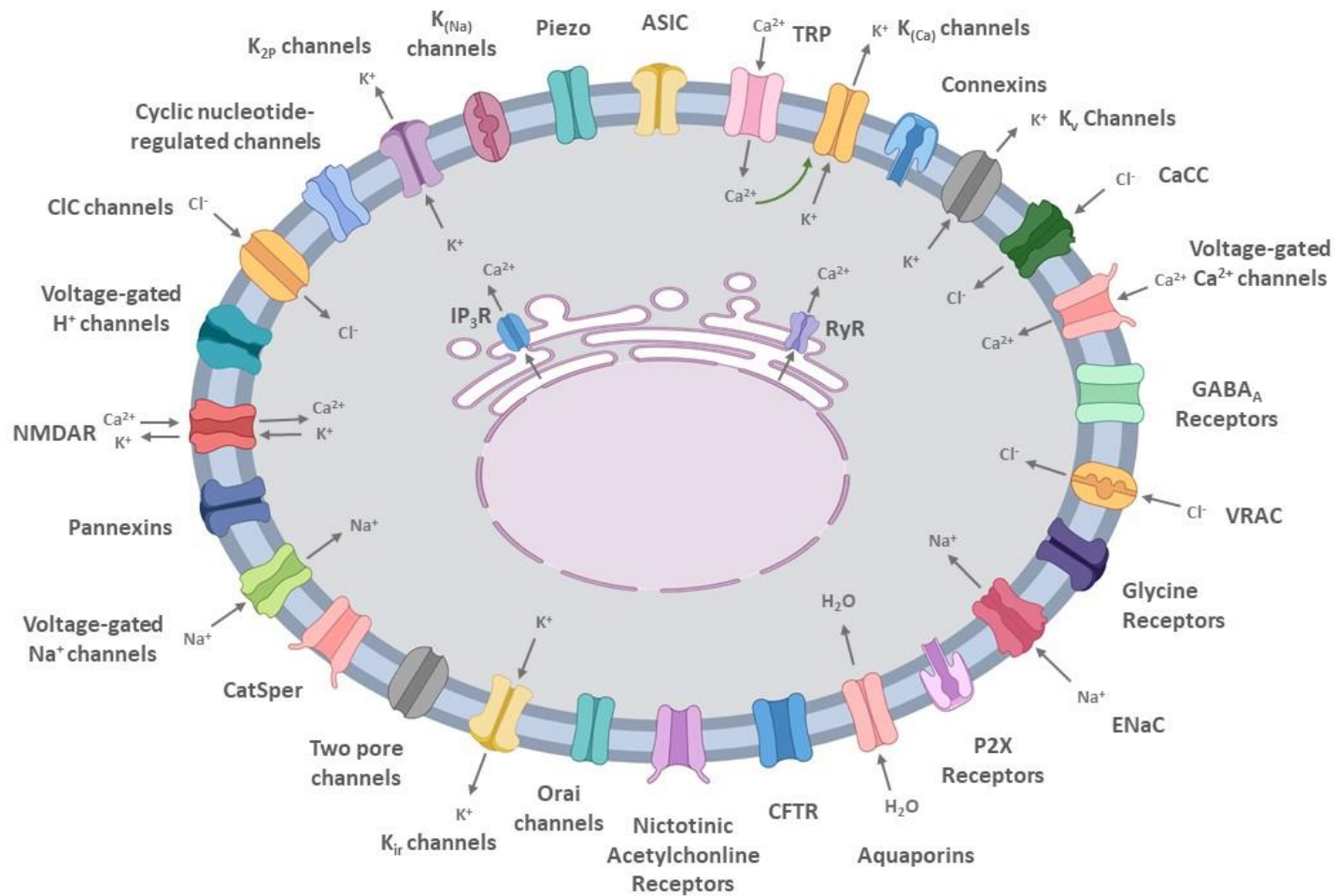
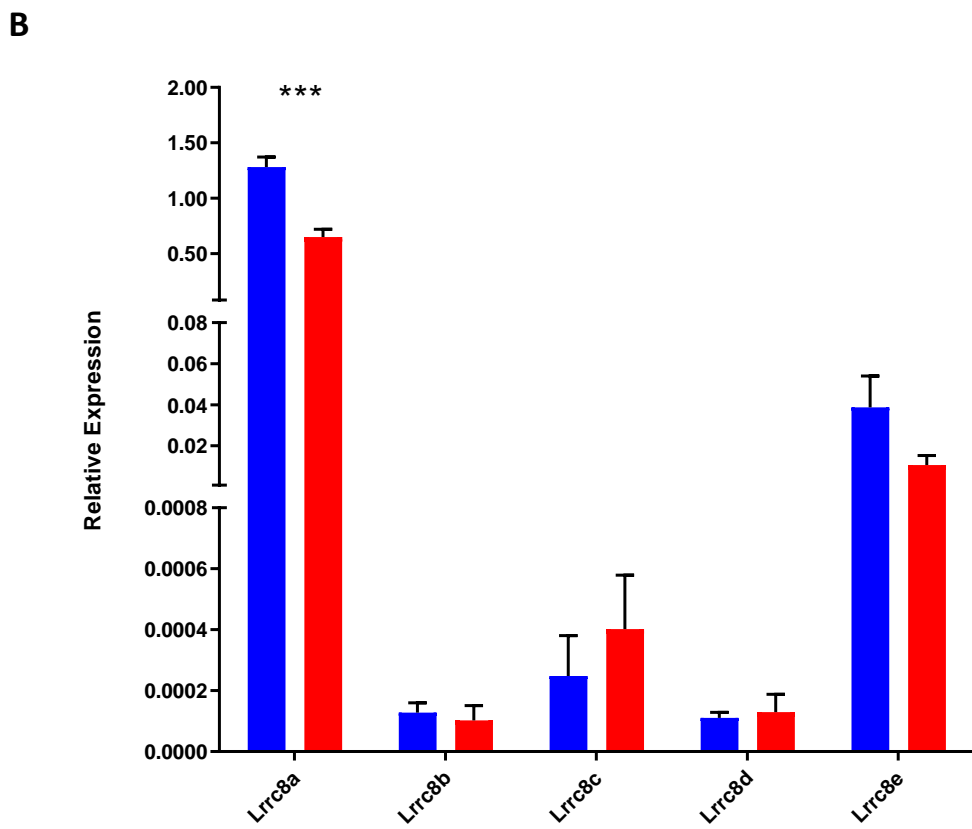
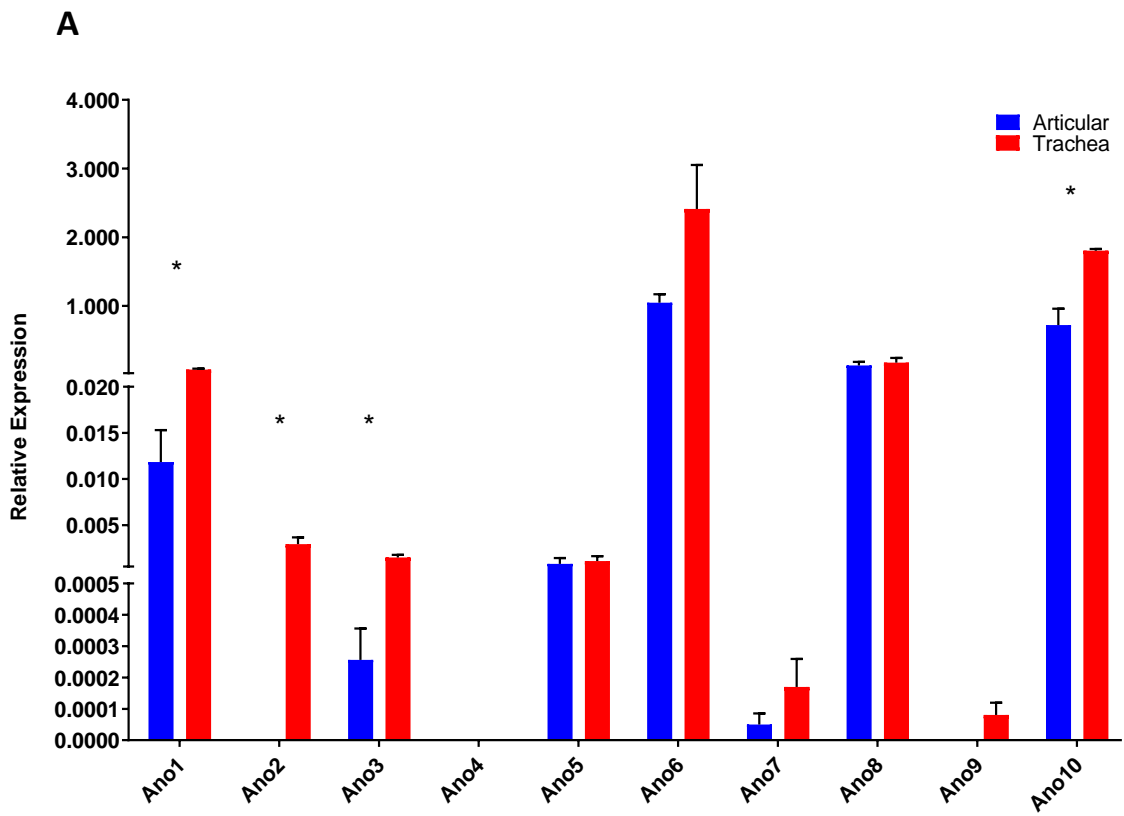


Figure 3.14: Summary of chondrocyte channelome. Tracheal and articular chondrocytes share most ion channel families but express different subtypes of ion channels.

3.3.5 Validation of chloride ion channel expression between tracheal and articular chondrocytes

As described in section 1.2.3, chloride channels have previously been implicated in diseases of cartilage and are of interest. Hence the transcriptomic expression of chloride channels was further validated through qPCR analysis (**Figure 3.15**). The expression of these ion channel genes using qPCR correlated with the transcriptomic expression of RNA-seq. For example, *Ano1* was also shown to have significantly higher expression in tracheal chondrocytes in comparison to articular chondrocytes ($p < 0.05$) as well as *Ano2*, *Ano3* and *Ano10* ($p < 0.05$ for all) (**Figure 3.15A**). VRAC channel relative expression also correlated with the transcriptomic expression, with *Lrrc8a* also being significantly higher in articular chondrocytes ($p < 0.005$) (**Figure 3.15B**). However, the expression of the ClC ion channel gene *Clcn7* did not show significant difference between the two chondrocyte types (**Figure 3.15C**). The qPCR expression of the VGCC, *Cacna1g* was also investigated, and this too showed significantly higher expression in tracheal chondrocytes as in the transcriptomic data ($p < 0.05$) (**Figure 3.15D**).



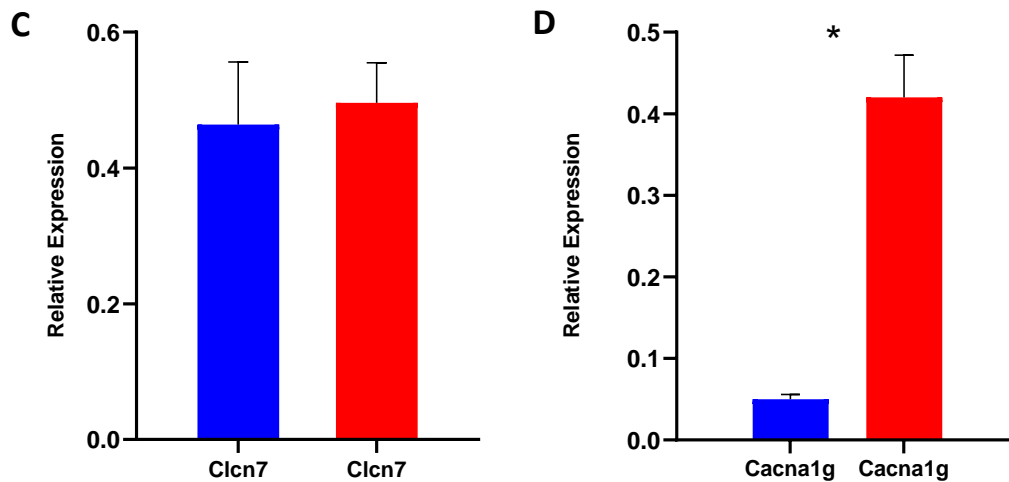


Figure 3.15: Relative gene expression of chloride ion channel genes in rat tracheal and articular chondrocytes. Expression of A) Ano gene family. B) Lrrc8 gene family. C) Clcn7 (ClC-7) gene and D) Cacna1g gene in tracheal and articular chondrocytes. All genes were normalised against Hprt1 as a reference. Bars indicate mean and error bars represent SEM of n=3 biological samples. Graphs were created using GraphPad Prism 8 and analysed using an unpaired t-test. * denotes $p < 0.05$ and *** denotes $p < 0.001$.

3.4 Discussion

In this chapter, the tracheal chondrocyte transcriptome and channelome were assessed using an unbiased approach with RNA-seq and compared to that of the articular chondrocyte. Different bioinformatic analyses were used to ascertain the similarities and differences between the two chondrocyte types. This revealed that there were many similarities between the two chondrocyte types as had been expected; with many canonical pathways being identified, amongst which, the role of chondrocytes in OA being in the top 5 pathways. In addition, novel ion channel gene expression of many of the ion channel genes was identified in tracheal chondrocytes as well as articular chondrocytes, with many subtypes showing significant differential expression. This was validated with qPCR analysis and showed that the expression of these genes was correlated with that of the transcriptome

expression. Though many similarities were observed between the two chondrocyte types, some differences were detected which will be discussed below.

3.4.1 Chondrocyte characterisation

An approach that was used to characterise the tracheal and articular chondrocytes was to use a range of different chondrocyte makers identified from the literature and investigate their expression in chondrocytes using immunocytochemistry and transcriptomic expression from the RNA-seq data. Immunocytochemistry of the tracheal and articular chondrocytes did not show an observable difference of aggrecan, collagen II a1, Sox9, and Cd44 expression between the two chondrocyte types (**Figure 3.2**).

Aggrecan (Acan), was used as a marker of chondrocyte function as Acan is an ECM protein only synthesised by chondrocytes (Kiani et al., 2002). The expression of aggrecan was significantly higher in tracheal chondrocytes compared to articular chondrocytes ($p < 0.00005$), this difference in expression between the two chondrocyte types has not been previously reported in the literature. However, tracheal chondrocytes may express more aggrecan as a mechanism to adapt to the tracheal cartilage function – to provide support to the windpipe as aggrecan is vital for structural support and ECM stabilisation (Kiani et al., 2002). The deletion of aggrecan has been observed to cause deformation of tracheal cartilage rings that is lethal (Lauing et al., 2014, Watanabe et al., 1994). This raises questions as to why aggrecan deletion seems to be lethal in tracheal cartilage in comparison to articular cartilage. These questions could be investigated in the future through knockdown

studies and comparison of the ECM composition between the two chondrocyte types.

Interestingly the expression of epiphycan (*Epyc*) was observed only in tracheal chondrocytes and was not expressed in articular chondrocytes. *Epyc* has been previously shown to be specific to cartilage of the ribs and trachea (Onnerfjord et al., 2012). This indicates that the populations of chondrocytes isolated were pure, uncontaminated and cartilage specific. However, another study showed its expression in the deep zones of articular cartilage whereby its deletion exacerbates OA progression (Nuka et al., 2010). *Epyc*'s unique expression in chick and mouse cartilage suggests a key role in chondrocyte differentiation and cartilage stability (Shinomura and Kimata, 1992, Kurita et al., 1996). Future work is needed to fully understand these discrepancies in *Epyc* expression.

The transcription factor Sox9 and its relatives Sox5 and Sox6 were also used as markers as Sox9 is a master regulator of cartilage formation and regulates the expression of collagen II $\alpha 1$ (Bell et al., 1997, Bi et al., 1999, Lefebvre et al., 1998a). Sox5 was shown to be significantly higher in articular chondrocytes ($p < 0.00005$). It is not clear why Sox5 expression is higher in articular chondrocytes. Sox5 was thought to be redundant however it has been shown to enhance the expression of aggrecan by potentiating Sox9 binding to its site (Han and Lefebvre, 2008). As aggrecan expression was more significant in tracheal chondrocytes, it was surprising that articular chondrocytes had higher levels of Sox5. Future studies to determine if Sox5

expression is also higher at the protein level would further investigate these discrepancies in Sox5 expression.

Collagen II a1 (Col2a1) expression was used as a marker as Col2a1 is a hallmark collagen of cartilage and is also synthesised by chondrocytes (Mendler et al., 1989). Col2a1 expression was shown to be significantly higher in articular chondrocytes ($p < 0.03$). To identify if the chondrocytes were mature and differentiated, the expression of Col1a1 was inspected (**Figure 3.3**). This showed no expression in either tracheal or articular chondrocytes confirming that the population of chondrocytes that was isolated is not showing a fibroblastic or osteogenic phenotype (Von Der Mark et al., 1977, Marlovits et al., 2004, Dessau et al., 1978).

Col10a1 expression was also identified and showed very little expression in tracheal and almost undetectable expression in articular chondrocytes (**Figure 3.3**). Col10a1 was used as a marker for chondrocyte hypertrophy to ensure that the mature chondrocytes used for this study were not becoming hypertrophic and developing into calcified bone. The minimal expression of col10a1 indicates that the chondrocytes may be becoming more mature at which point they start to synthesise Col10a1 (Pullig et al., 2000, Drissi et al., 2005). In addition, the expression of Col10a1 could be due to the expression of Runx2, which regulates Col10a1 expression (Zheng et al., 2003) and was shown to be significantly higher in tracheal chondrocytes in comparison to articular chondrocytes ($p < 0.01$), which was reflected in the Col10a1 expression (**Figure 3.3**). This will be further discussed in chapter 7.

Surface markers such as Cd44 were also used as markers as they have been previously reported to characterise chondrocytes in the literature (Hamada et al., 2013). Cd9 and Cd151, markers of OA, were also used as they have been shown to activate proteolytic enzymes in OA (Fujita et al., 2006, Sumiyoshi et al., 2016). Adamts5 and Mmp-13, which are proteolytic enzymes involved in OA, were shown to be significantly higher in articular chondrocytes ($p < 0.00005$ for both). This was expected as OA occurs in articular cartilage (Akkiraju and Nohe, 2015a). However, the effect of inflammation and expression of these proteolytic enzymes has not been previously studied in tracheal cartilage. Future studies would perhaps investigate the effect of factors upregulated in OA progression on tracheal chondrocytes.

3.4.2 Tracheal and articular chondrocyte transcriptome

In this chapter, RNA-seq was the chosen method to study the transcriptomics of tracheal and articular chondrocytes as it is the best method on the market for assessing the transcriptome of cells. Initial transcriptomic studies were performed using hybridization-based technologies; these were relatively low cost and provided a high-throughput option (Schena et al., 1995). However, they had some limitations which include: the requirement of prior knowledge of the sequences being tested, the presence of cross-hybridisation artifacts when similar sequences were being analysed and the inability to accurately quantify low expressed or high expressed genes (Schena et al., 1995, Shendure and Ji, 2008). In contrast, sequence-based methods were developed; these methods include the generation of expressed sequence tag (EST) libraries, which was relatively low-throughput and not ideal for quantifying transcripts, leading to other tag-based methods such as serial analysis of

gene expression (SAGE) and cap analysis gene expression (CAGE) which were developed to enable higher throughput and more precise quantification of expression levels (Velculescu et al., 1995, Shiraki et al., 2003). Although they were more advantageous over array-based methods, these sequence-based methods were insensitive to measuring expression levels of splice isoforms and were not able to be used for novel gene discovery. In addition, the cloning of sequence tags was very laborious, expensive, and required large amounts of RNA. This led to the development of high-throughput next-generation sequencing (NGS) in the early 2000s. NGS such as RNA-seq enabled transcriptomic analysis through the sequencing of complementary DNA (cDNA), which transformed transcriptomics analysis (Wang et al., 2009).

Following the sequencing and analysis of the sequence reads of the two chondrocyte types, differentially expressed genes between tracheal and articular chondrocytes were identified with the cuffdiff package. These 32650 genes were subjected to dimensionality reduction with PCA, which transformed the large dataset into smaller variables. Tracheal and articular chondrocyte gene expression was reduced to seven principal components with more than 50% of the data being contained within the first three principal components (**Figure 3.4A**). Clustering of the tracheal and articular gene expression revealed clear difference between the first and second principal components (**Figure 3.4B**) and the second and third principal components (**Figure 3.4C**). This indicated that tracheal and articular chondrocytes gene expression was different between the two chondrocyte types. This was validated with DESEQ2 analysis which revealed that between tracheal and articular chondrocytes 528 genes

were significantly differentially expressed by a factor of 3 or more (adjusted p-value: $p < 0.05$). It should be noted that although these data indicate that the two chondrocyte types show significant differential gene expression, the first and third principal component clustering showed that there was a slight overlap between tracheal and articular chondrocytes (**Figure 3.4D**). This could be due to the expression of genes that are essential to both chondrocyte types that make up the chondrocyte phenotype.

To gain a better insight into the role of the genes differentially expressed between tracheal and articular chondrocytes and study the reasons that drive this differential expression, IPA was used to identify the canonical pathways expressed in the RNA-Seq dataset. A total of 546 pathways were identified. The top 25 significant pathways of these were shown to relate to a variety of signalling pathways including calcium and GABA receptor signalling, implicating ion channel genes in the differential expression (**Figure 3.5A**). As well as that pathways relating to cartilage disease were shown to be amongst the top 25 pathways. These were also shown to be amongst the top 5 pathways (**Figure 3.5A**). This indicates that the population of cells used for RNA-seq was pure and further confirms the identity of these cells. Two of the top 5 pathways, the OA pathway, and the role of chondrocytes in RA were further examined and MAP analysis was conducted using IPA. MAP analysis predicts the functional effects of the genes from the RNA-seq dataset on neighbouring molecules. It also predicts genes to be activated (orange) or inhibited (blue), and their increased (red) or decreased (green) measurements and how that affects downstream molecules.

MAP analysis on the osteoarthritis pathway revealed that many of the genes that drive OA were predicted to be inhibited. This is a good indicator as the chondrocytes used for this project were isolated from healthy rats that showed no signs of OA. As the osteoarthritis progression occurs due to a variety of factors and the OA pathway is vast, the details of the OA pathway are beyond the scope of this chapter. Hence the focus will be on a few highlights observed. One of the observations was that inflammation was predicted to be inhibited from the RNA-seq dataset (**Figure 3.6A**). This is a good indication that the chondrocytes isolated were healthy. Another observation was the effect of miRNAs on the OA pathway. Several miRNAs were shown to be involved such as miR-145 and miR-140 which were predicted to be activated as well as miR-155 and miR-142 which were predicted to be inhibited (**Figure 3.6A**). The role of miRNAs in OA progression has been reviewed by (Malemud, 2018b).

Two main genes that were central to the OA pathway were Sox9 and Runx2 (**Figure 3.6A**). Perhaps this reflects the balance between genes that drive the synthesis of cartilage ECM proteins such as Col2a1 and aggrecan (Bell et al., 1997, Han and Lefebvre, 2008) and the genes that drive cartilage degradation such as osteopontin, Adamts genes and Mmps (Li et al., 2016, Yang et al., 2017). Interestingly Sox9 and its downstream targets were predicted to be inhibited however their effect on cartilage catabolism was inconclusive. Whereas Runx2 and its downstream targets were predicted to be activated, leading to ossification of cartilage tissue, degradation and hence OA (**Figure 3.6A**). Future studies would further investigate the genes that drive these predicted activations and inhibitions and elucidate their effect on tracheal

chondrocytes too as it has not been previously shown how these factors would affect tracheal chondrocytes.

Another pathway that was identified from the RNA-seq data to be amongst the top 5 pathways was the role of chondrocytes in RA (**Figure 3.6B**). MAP analysis using IPA highlighted cytokines that were shown to be involved in the activation of cartilage degradation. It indicated that IL-17 was predicted to be activated and lead to the activation of chondrocyte death, the switch from catabolic to anabolic state and proteoglycan cleavage which leads to cartilage degradation. IL-17 is the signature cytokine involved in RA (Gaffen, 2009). The predicted activation of IL-17 and the increased measurement of IL-18 receptor were predicted to inhibit glycosaminoglycans. In addition to this, IL-1 was shown to activate Mmp-8 which leads to cleavage of collagen fibres. Despite this, it was shown that the cleavage of collagen fibres and proteoglycan cleavage were predicted to be inhibited (**Figure 3.6B**). These inconsistent findings would need to be further validated in future studies. Using IPA, upstream regulators that were predicted to be driving the differential gene expression between the two chondrocyte types were also identified (**Figure 3.5C**). Interestingly many of these were found to be miRNAs. The effect of these upstream regulators would be further investigated in the next chapter.

3.4.3 Tracheal and articular chondrocyte channelome

An unbiased and comprehensive view into the ion channel genes expressed between tracheal and articular chondrocytes was investigated in this chapter and provided novel insights into the tracheal chondrocyte channelome. A closer look at the

individual ion channel families and their subtypes gives an idea of which ion channels were conserved and essential for the viability of these chondrocytes and their basic function and which ion channels were expressed specifically in relation of the chondrocyte environment and cartilage specific function. As was predicted, about 86% of ion channel genes were shared between tracheal and articular chondrocytes (**Figure 3.7**) and the heatmap of the tracheal and articular chondrocyte samples showed the ion channel gene expression to be very similar (**Figure 3.8**). This was expected as many ion channels are involved in processes that are vital for cell survival (Barrett-Jolley et al., 2010b). In addition to this ion channels regulate the RMP which in turn regulates these vital functions (Abdul Kadir et al., 2018). Despite this similarity the tracheal and articular chondrocyte samples were clustered separately, indicating that there were subtle differences in the ion channel genes that distinguish between the two chondrocyte types.

The ion channel genes expressed only in tracheal chondrocytes were found to belong to the voltage-gated calcium channel, TRPM and C channels, sodium leak channel and voltage-gated sodium channel families (**Figure 3.7**). Interestingly VGCC have been previously shown to be vital for tracheal cartilage development (Matta et al., 2015a, Wang et al., 2000, Atsuta et al., 2019, Lin et al., 2014a) as previously discussed in Chapter 1. TRP channels, sodium leak channels and voltage-gated sodium channels however have not been shown to be expressed in tracheal chondrocytes. Perhaps, the functional expression of these genes would be validated using pharmacological agents in future studies. On the other hand, the ion channel genes that were expressed in articular chondrocytes only were shown to belong to TRP channel,

calcium-activated chloride channel, voltage-gated calcium channel, voltage-gated sodium channels, inwardly-rectifying potassium channel, voltage-gated potassium channels, two-pore domain potassium channels, CIC channels, and purinergic receptor families (**Figure 3.7**). The majority of these channels have been previously shown to be expressed in articular chondrocytes (Barrett-Jolley et al., 2010b, Mobasheri et al., 2012, Lewis et al., 2011c, Mobasheri et al., 2019).

It is unclear why the expression of these ion channel genes occurs in one chondrocyte type only. Perhaps these ion channel subtypes confer specific functions to the chondrocytes which would aid in their cartilage specific roles. For example, in articular chondrocytes, TRP channels have been shown to regulate the intracellular Ca^{2+} concentration and play vital roles in nociception, temperature regulation, mechano- and osmosensation (Matta and Zakany, 2013). In addition, VGCCs have also been shown to be necessary for initiating Ca^{2+} influx in articular chondrocytes which is vital for signalling pathways that regulate ECM synthesis (Xu et al., 2009b). CaCC have been shown to be linked to cell volume and apoptosis (Hoffmann et al., 2014, Kunzelmann, 2015) as well as contribute to the volume sensitive Cl^- current in anterior cruciate ligament transection rabbit OA model as shown by my group (Kumagai et al., 2016). Ca^{2+} signalling was identified as one of the top 5 canonical pathways from the RNA-Seq dataset, highlighting its importance in chondrocytes (**Figure 3.5B**). Whereas VGSC have previously been reported in articular chondrocytes yet their functional role remains elusive (Sugimoto et al., 1996a). On the other hand, potassium channels have been well-studied in articular chondrocytes and are involved in regulation of chondrogenesis, cell volume, apoptosis and

mechanotransduction as reviewed by (Mobasheri et al., 2012). Purinergic receptors have also been found to be important in articular chondrocytes whereby they also aid in the regulation of chondrogenesis (Fodor et al., 2009). The reasons behind the expression of these ion channel genes needs to be validated in future studies through the detection of their functional ion channel subtypes in chondrocytes using specific pharmacological agents.

In addition to finding chondrocyte-specific expression of these ion channel genes many ion channel families were observed to have significantly different subtype expression between the two chondrocyte types (**Figures 9 – 13**). This also could be due to cartilage-specific roles that these two chondrocyte types are implicated in. For example, articular chondrocytes' ion channels are mainly involved in the cell volume regulation and mechanotransduction, reflecting the role of load bearing of articular cartilage. Whereas tracheal chondrocytes ion channels are more involved in the development and maintenance of cartilage, which would ensure that the structure and stability of the cartilage rings are preserved to support the trachea. This transcriptomic expression of ion channel genes has provided a more comprehensive view of the tracheal and articular chondrocyte channelome (**Figure 3.14**), enabling for the first time the comparison between the two. Future studies would further investigate the factors driving these differences in the ion channel expression between these two chondrocytes.

As chloride channels were shown to be implicated in cartilage diseases, their expression was further validated between the two chondrocyte types using qPCR

(Figure 3.15). This showed that the ion channel expression detected by qPCR was mostly correlated with that of the transcriptomic expression detected by RNA-seq. RNA-seq data and qPCR expression have been previously shown to be correlated by others (Griffith et al., 2010, Asmann et al., 2009, Wu et al., 2014, Shi and He, 2014). However, some groups have shown discrepancies, this could be due to qPCR bias as only a specific region of the cDNA can be amplified, whereas with RNA-seq the whole transcript is accessed. Implication of these chloride channels validated above in tracheal and articular chondrocytes will be investigated further in the next chapter.

4

MicroRNA regulation of
ion channels in tracheal
and articular chondrocytes

4.1 Introduction

MicroRNAs are important regulators of gene expression. They control the expression of multiple transcripts and play a significant role in various aspects of cartilage development, homeostasis, and pathology. Chondrocytes, the single cell type of cartilage, express many different miRNAs. They also express multiple ion channels that are essential for cartilage physiology, whereby the deletion of chloride channels leads to the malformation of the cartilage rings and death of mice 1 month post birth (Rock et al., 2008a). miRNAs have been associated with the development and pathogenesis of various diseases such as cardiovascular diseases, diabetes, neurodegenerative diseases, cancer, and developmental disorders (Mendell and Olson, 2012). They have also been shown to be implicated with diseases of the cartilage such as OA (Malemud, 2018a) and TM (Gradus et al., 2011). miRNAs target ion channel genes and affect a multitude of processes such as cardiac, neuro, epithelial and endocrine physiology as well as cancer biology, as reviewed by (Wang, 2013).

The expression of miRNA is dynamically regulated and hence, altered miRNA expression can render expression deregulation of ion channel genes leading to channelopathies. RNA-Seq data from chapter 3 revealed several differentially expressed ion channel and miRNA genes between tracheal and articular chondrocytes. Although miRNA induced silencing of ion channel genes was shown in several different studies, and despite the evidence of regulation of ion channels that play a role in chondrocytes (**Table 1.1**) by different miRNAs, miRNA targeting of ion channel genes in chondrocytes has not been previously shown. Hence, in this chapter

the interplay of miRNAs and ion channels in tracheal and articular chondrocyte physiology will be investigated.

4.1.1 Role of microRNAs in ion channel regulation and channelopathies

Ion channel genes functionally expressed in chondrocytes have been shown to be targeted by miRNAs in other tissues and cell types. For example, the calcium-activated potassium (BK) channel, *Kcnma* that couples membrane stretch to RVD in chondrocytes was shown to be directly targeted by miR-211 in melanoma, and has been shown to be implicated in cell proliferation and migration of various cancers (Mazar et al., 2010). miR-181a, which is expressed in chondrocytes and directly targets *Acan*, has been shown to target the glutamate receptor, *GluA2* in an epilepsy rat model and have a neuroprotective role (Ren et al., 2016). Whereas *Nav1.3*, which modulates mechanotransduction in chondrocytes and aids in the maintenance of the ECM is targeted by miR-30b. This causes downregulation of *Nav1.3* and attenuates neuropathic pain in rats (Su et al., 2017). Another sodium channel, *ENaC* is also regulated by miRNAs. miR-124-5p directly targets α -*ENaC* and downregulates its expression and function in MSCs (Ding et al., 2020).

In addition, the VGCC, *Cav1.2*, which plays a role in calcium signalling and maintenance of the RMP in chondrocytes was found to be targeted by miR-21 and miR-328 in atrial fibrillation of human atria (Barana et al., 2014, Lu et al., 2010) and by miR-221 and miR-222 in a mouse model of cardiac hypertrophy (Binas et al., 2020). This existing evidence indicates that although the interaction of miRNAs and ion channels has not been specifically shown in chondrocytes, miRNAs interplay with ion

channels expressed in chondrocytes and affect their expression and function in various tissues and diseases. This raises many different questions as to whether these ion channels would be affected in a similar manner in chondrocytes of tracheal and articular cartilage. To answer these questions, transcriptomics, and associated bioinformatic tools to predict genes targeted by miRNA in particular cell types can be used.

4.1.2 MicroRNA target prediction

There are a variety of bioinformatic tools available online that can be used for miRNA target prediction. Online databases such as miRBase (<http://www.microrna.org/>), TargetScan (<http://www.targetscan.org/>) and the microRNA Data Integration Portal (miRDIP) (<http://ophid.utoronto.ca/mirDIP/index.jsp#r>) can be used to obtain microRNA targets and sequence information (Griffiths-Jones et al., 2006, Bartel, 2004a). These bioinformatic platforms use sophisticated algorithms based on several miRNA characteristics such as the thermal stability of the miRNA:mRNA duplex and the level of complementarity of the mRNA seed sequence to predict potential miRNA targets. For instance, TargetScan uses the degree of evolutionary conservation between species to classify miRNA families into 'conserved' and 'non-conserved'. It also categorises miRNAs' targets using a 'context score' according to the predicted efficiency of the sites (van Rooij, 2011).

In addition, further analyses such as function/gene ontology analyses can be performed by databases of gene families such as the PANTHER Classification System (<http://www.pantherdb.org>). PANTHER is most widely used for the inference of gene

function for uncharacterized genes from an organism. It uses algorithms to statistically analyse gene function of a list of genes by overrepresentation or enrichment tests (Mi et al., 2013, Thomas et al., 2003). As well as that it annotates these functions with gene ontology terms as part of the GO reference genome project (Gaudet et al., 2011). Despite the availability of these tools, a more robust way of miRNA target prediction is the use of transcriptomic data in addition to these bioinformatic tools. For example, Qiagen's IPA can be used to analyse user's transcriptomic data to predict upstream regulators such as miRNAs that target a set of genes identified from the user's data.

4.1.3 IPA ingenuity upstream regulator analysis

IPA's ingenuity upstream regulator analysis is a bioinformatic tool that is used to identify a cascade of upstream regulators from the user's RNA-Seq dataset. This upstream regulator analysis uses the curated Ingenuity® Knowledge database to explain the differential gene expression in a user's dataset and identify expected effects between upstream regulators and their target genes (Calvano et al., 2005, Thomas and Bonchev, 2010). It examines the targets of each upstream regulator from the user's dataset and compares the directional change using the experimental expression in the samples. Essentially IPA uses upstream analyses to identify the upstream regulators from user's dataset.

4.1.4 Aims

In the previous chapter, RNA-Seq of tracheal and articular chondrocytes identified a number of genes relating to chondrocyte identity and function as well as ion channel

genes and miRNA genes to be differentially expressed. Several known miRNAs that regulate gene expression of ion channels in different tissues and diseases have been previously reported, however how these miRNAs and ion channels interplay in tracheal and articular chondrocytes has not been previously investigated. To gain an understanding of the mechanisms behind this differential expression, a bioinformatic approach will be used to identify upstream regulators that could be driving this differential expression. Using the RNA-Seq dataset from chapter 3, upstream regulators from the differential expression analysis between tracheal and articular chondrocytes will be identified. Function/gene ontology analysis of these regulators will be performed to identify pathways, molecular functions and biological processes linked with these upstream regulators. The expression of these upstream regulators will be validated and their effect on ion channels genes that are differentially expressed between tracheal and articular chondrocytes will be determined.

4.2 Methods

4.2.1 MicroRNA target prediction and Gene ontology analysis

IPA analysis of the RNA-seq dataset was used as previously described in chapter 3.2.3 to predict upstream regulators from tracheal and articular chondrocytes. IPA's ingenuity upstream regulator analysis was performed to identify miRNA upstream regulators and their predicted targets. Gene ontology analysed using the PANTHER classification system was carried out on these upstream regulators. Targets of miR-141-3p were also predicted using TargetScan and miRDIP and gene ontology analysis was also carried out on these genes using the PANTHER classification system.

4.2.2 qPCR quantification of microRNAs and ion channel genes

qPCR was used as previously reported in chapter 2.4, to quantify the expression of miRNAs between tracheal and articular chondrocytes. The miRNA primers were purchased from the miScript primer assays from Qiagen, UK. Primer pairs with none or few hairpins, dimers and repeat and runs were selected for quantification using qPCR. qPCR primers of the miRNAs used are listed in **Table 4.1**. qPCR was also used to quantify the expression of ion channel genes predicted to be targeted by miR-141-3p. qPCR primers of these ion channel genes are shown in **Table 4.2**.

4.2.3 Transfection of tracheal and articular chondrocytes with miR-141-3p mimic and antagomiR

Chondrocytes were seeded at 2.5×10^4 in 24-well plates and at 15×10^4 in 6-well plates. At 70% confluence, the media was changed to FCS-free DMEM, and cells were incubated for 30 minutes at 37°C and 5% CO₂ to allow the cells to adjust to the transfection conditions. Following that 3 µl of Lipofectamine 2000 (Life Technologies, UK) was added to 1000 µl of FCS-free DMEM and miR-141-3p mimic (Qiagen, UK), antagomiR (Qiagen, UK) and mimic scrambled control (Qiagen, UK) (**Table 4.3**) were diluted to a final concentrations of 50 nM, 100 nM and 200 nM and incubated at room temperature for 30 minutes. Following incubation, the media was removed from cells and the miRNA and Lipofectamine 2000 mixture was added in a dropwise manner and the cells were incubated for 6 hours. Following incubation, the media was changed to DMEM with 10% FCS and cells were further incubated for 48 hours. Following that miRNA mimic, antagomiR and scrambled control were optimised using

qPCR, which was also used to quantify target gene expression. The mimic, antagomiR and scrambled control were purchased from the miRCURY primer assays from Qiagen, UK (**Table 4.3**).

Table 4.1: miRNA primers designed by Qiagen, UK.

Gene	Mature miRNA ID	Mature miRNA Sequence (5' → 3')
miR-141-3p	rno-miR-141-3p	UAACACUGUCUGGUAAGAUGG
miR-181a-5p	mmu-miR-181a-5p	AACAUUCAACGCUGUCGGUGAGU
miR-1-2-5p	mmu-miR-1-2-5p	ACAUACUUCUUUAUGUACCCAUA
miR-29b-3p	mmu-miR-29b-3p	UAGCACCAUUUGAAAUCAGUGUU
miR-132-3p	mmu-miR-132-3p	UAACAGUCUACAGCCAUGGUCG
miR-30c-5p	mmu-miR-30c-5p	UGUAAACAUCCUACACUCUCAGC
miR-34a-5p	hsa-miR-34a-5p	UGGCAGUGUCUAGCUGGUUGU
miR-27a-3p	mmu-miR-27a-3p	UUCACAGUGGCUAAGUCCGC
miR-241-5p	mmu-miR-241-5p	UGCCUGUCUACACUUGCUGUGC
Let7a-1-3p	mmu-Let7a-1-3p	CUAUACAAUCUACUGUCUUUCC
miR-125a-5p	mmu-miR-125a-5p	UCCCUGAGACCCUUUAACCGUGA
miR-140-5p	mmu-miR-140-5p	CAGUGGUUUUACCCUAUGGUAG
RNU6	-	-
SNORD-61	-	-

Table 4.2: Ion channel gene primers for qPCR quantification designed by Primerdesign Ltd., UK and Primerblast NCBI.

Gene	Accession number	Species	Sequence (5' → 3')
Lrrc8a	NM_001127244.2	Human	F: GGGTTGAACCATGATTCCGGTGAC R: GAAGACGGCAATCATCAGCATGAC
Cacna1g	NM_001308302.1	Rat	F: ATGACAGTGAAGGTGGTGGC R: CCAGGATGTCGATGACGGAG
Ano1	NM_00110756	Rat	F: CATCCCTGCCTCCATTGTGG R: GGTGATGTTGTGTCTCTGGTCA
Hprt1	NM_012583.2	Rat	F: TCCTCCTCAGACCGCTTTTC R: ATCACTAATCACGACGCTGGG

Table 4.3: miR-141-3p negative control, mimic and antagomiR primers designed by Qiagen, UK.

miRCURY LNA miRNA (5nM)	Sequence (5' → 3')	Catalogue number	Modification
miRCURY LNA miRNA mimic hsa-miR-141-3p	UAACACUGUCUGGUAAAAGAUGG	339173 YM00471957-ADB	5'-FAM
Negative control miRCURY LNA (5)	UCACCGGGUGUAAAUCAGCUUG	339173 YM00479902-ADB	5'-FAM
miRCURY LNA miRNA inhibitor rno-miR-141-3p	CATCTTTACCAGACAGTGTT	339121 YI04100686-ADB	5'-FAM

4.3 Results

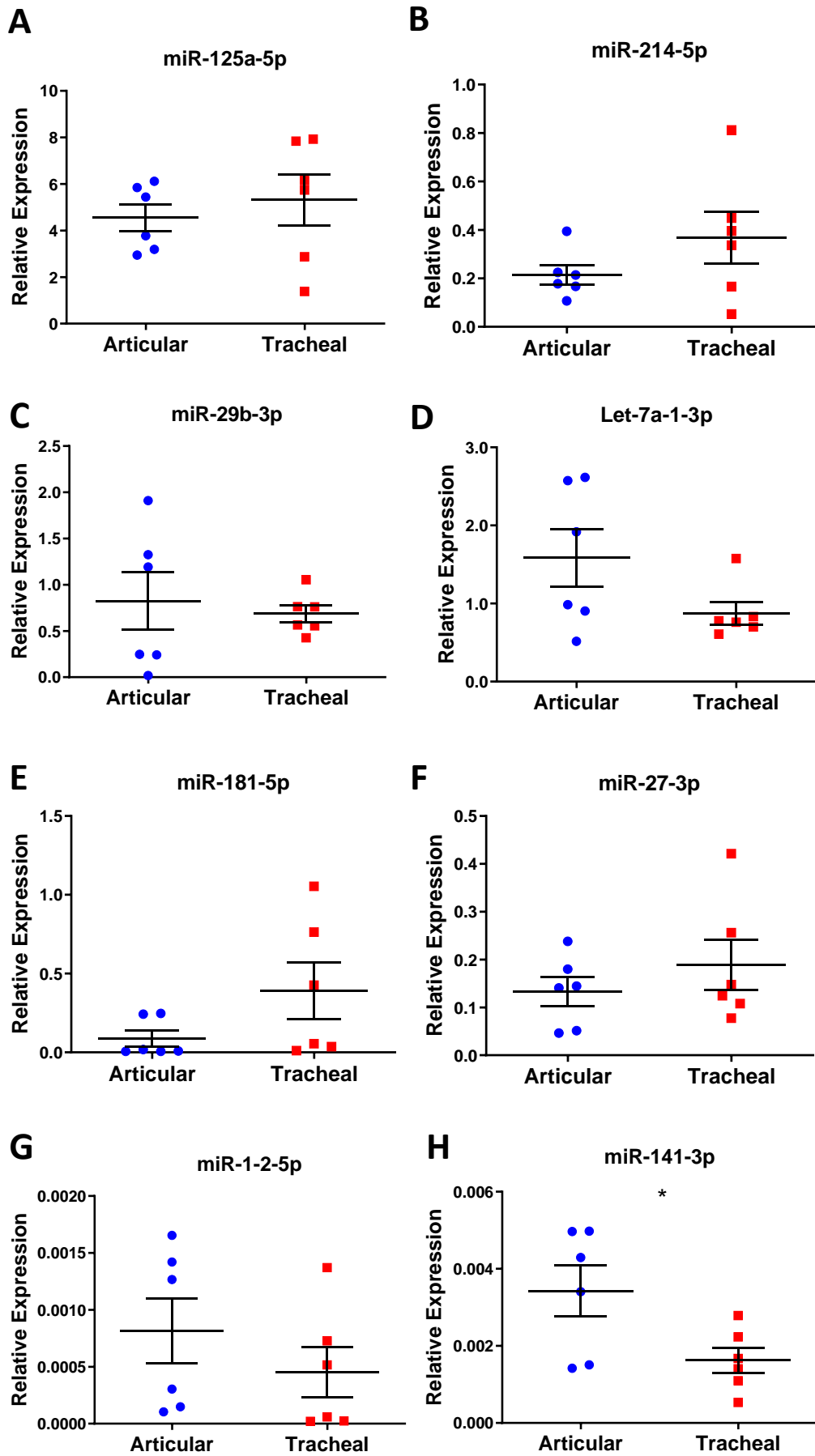
4.3.1 *MicroRNA expression between tracheal and articular chondrocytes*

IPA's ingenuity upstream analysis was used to investigate the differential gene expression of tracheal and articular chondrocytes in the RNA-Seq dataset from chapter 3. Using this transcriptomic and bioinformatic approach, 983 upstream regulators were identified of which 55 were miRNAs. From these, twelve miRNAs were selected for further investigation, ten of which were identified from IPA and two from the literature (miR-125-5p & miR-140-5p) (**Table 4.4**). For the miRNAs identified as upstream regulators, IPA was used to compute an overlap p -value using Fisher's exact test. miR-141-3p had the most significantly different overlap p -value ($p < 0.0001$) whereas miR-29b-3p and miR-34a-5p differential overlap was not found to be significant (**Table 4.4**).

To validate the expression of these predicted miRNA upstream regulators in tracheal and articular chondrocytes, qPCR quantification of the predicted miRNAs was conducted (**Figure 4.1**). Of the 12 miRNAs investigated, only two displayed significantly different expression between tracheal and articular chondrocytes; with miR-30c being more highly expressed in tracheal chondrocytes ($p < 0.05$; $n=6$) and miR-141-3p being more highly expressed in articular chondrocytes ($p < 0.05$; $n=6$) (**Figure 4.1L & H**).

Table 4.4: miRNA upstream regulators identified from RNA-seq data using IPA upstream regulator analysis (Qiagen, UK). miR-125-5p and miR-140-5p were identified from the literature. *p*-value of overlap calculated using Fisher's Exact Test.

Upstream regulators	<i>P</i>-value of overlap	Target molecule
miR-141-3p	0.00002	Cacna1g, Cdh1, Dach1, Enam, Hmx1, Irf6, Lhx6, Nanog, Pitx1, Satb1, Sox2, Tbx1 & Tbx5
miR-181a-5p	0.0002	Cdx2, Epcam, Ezh2, Gata6, Gria2, Mmp14 & Pgr
miR-1-2-5p	0.005	Cebpb, Eif4e3, Irx5, Met, Mmp9, Mrtfa, Tagln2, Trim63, Vegfa & Vegfc
miR-29b-3p	1	Mybl2, Nasp, Shroom2 & Trim9
miR-132-3p	0.02	Gria1,grin2a & Grin2b
miR-30c-5p	0.02	Cdkn1a, Gadd45a, Il6, Itga2, Runx2 & Tp53
miR-34a-5p	0.05	Birc5, Cdk1, Dhfr, Lin28a, Mcm10, Mcm3, Met, Pou5f1 & Sox2
miR-27-3p	0.03	Ephb4, Ifi16, Igf1, Pxn, Runx1 & Wee1
miR-214-5p	0.04	Alcam, Birc5 & Tfp2c
Let-7a-1-3p	0.001	Ago2, Aurkb, Bdnf, Btg2, Ccnd1, Cdc25a, Cdh2, Cebpd, Cpsf1, Dicer1, Fosl1, Gpi, Hmga1, Irs2, Itga4, Itgb3, Mcm2, Mgat1, Nfkb1, Pa2g4, Ptgs2, Rrp1b, Scd, Skp2 & Stard13
miR-125a-5p	-	-
miR-140-5p	-	-



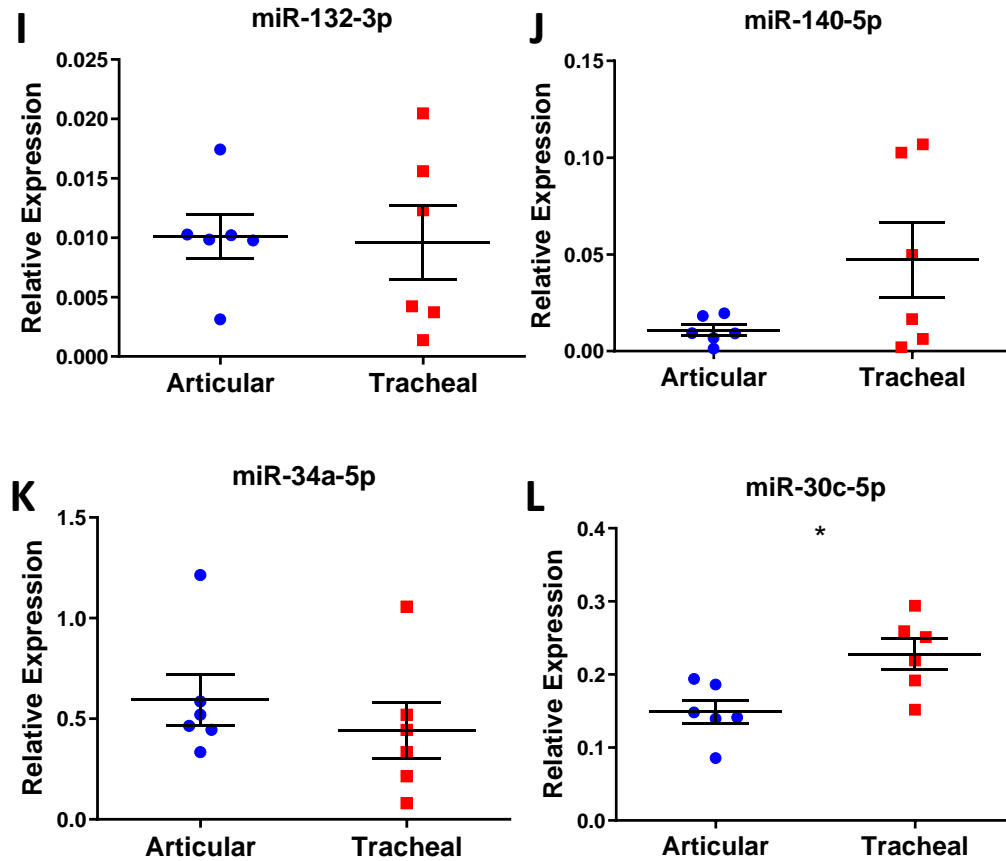


Figure 4.1: Relative expression of miRNAs identified as upstream regulators between tracheal and articular chondrocytes obtained using qPCR quantification. Expression of A) miR-125a-5p B) miR-214-5p C) miR-29b-3p D) Let-7a-1-3p E) miR-181a-5p F) miR-27-3p G) miR-1-2-5p H) miR-141-3p I) miR-132-3p J) miR-140-5p K) miR-34a-5p and L) miR-30c-5p. miRNA expression was normalised with U6 as housekeeping gene. Each point indicates a biological replicate (AC; blue; n=6. TC; red; n=6). Error bars represent SEM. Graphs were created using GraphPad Prism 8. Paired t-test was used to statistically analyse the data. * denotes $p < 0.05$.

4.3.2 Gene ontology of miR-141-3p predicted downstream targets

IPA and TargetScan were used to identify predicted downstream targets of miR-141-3p, and the PANTHER Classification System was used for multiple function/gene ontology analyses. IPA revealed 13 genes from the RNA-Seq dataset to be targets of miR-141-3p that lead to downstream effects and differential gene expression (**Table 4.4**). Whereas TargetScan revealed a total of 654 genes from the *Rattus norvegicus* genome to be targeted by miR-141-3p. Analysing the molecular function of these

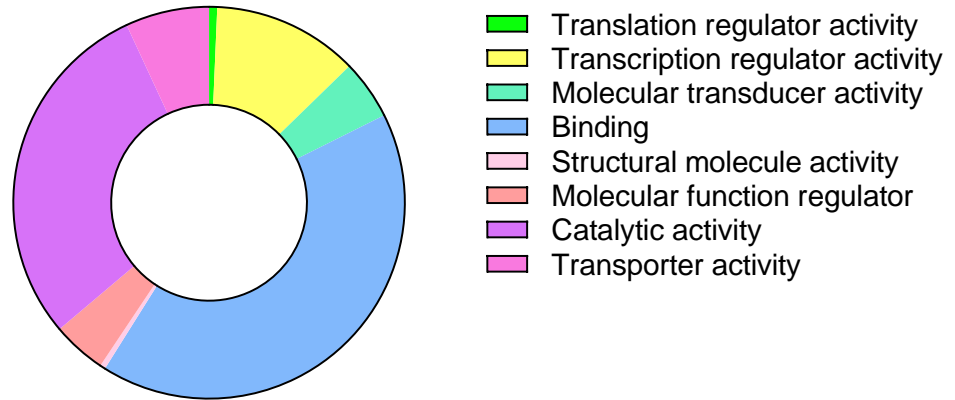
genes with PANTHER indicated that the majority of these genes identified from TargetScan, and IPA were involved in binding (**Figure 4.2A & B**), of which 32 genes were implicated in ion binding and 3 in neurotransmitter binding according to TargetScan prediction (**Figure 4.2C**). A closer inspection of the genes involved in ion binding revealed 27 genes associated with anion binding in comparison to 10 genes involved in cation binding (**Figure 4.2D**).

The biological processes linked with the targets of miR-141-3p were also analysed and these revealed links to cellular component organisation or biogenesis, developmental processes, and signalling (**Figure 4.2E**). Moreover, the cellular components such as cell junction, membrane and synapse were found to be associated with the predicated target genes of miR-141-3p (**Figure 4.2F**). The protein class of these predicted targets of miR-141-3p also gives an indication of the type of genes that could potentially be regulated by this miRNA, it revealed protein classes such as calcium-binding, cell junction, cytoskeletal, extracellular matrix, transmembrane signal receptor and transporter proteins (**Figure 4.2G**).

Finally, the pathways associated with these miR-141-3p targets included cytoskeletal regulation by Rho GTPase, FGF signalling, GABA- β receptor signalling, hedgehog signalling, IGF pathway/protein kinase β signalling cascade, ionotropic glutamate receptor pathway, metabotropic glutamate receptor pathways, muscarinic and nicotinic acetylcholine receptor signalling pathways, TGF-beta signalling, and Wnt signalling pathway (**Figure 4.2H**). In addition, upon inspecting the target genes of miR-141-3p, 15 ion channel genes were identified to be predicted targets of miR-141-3p

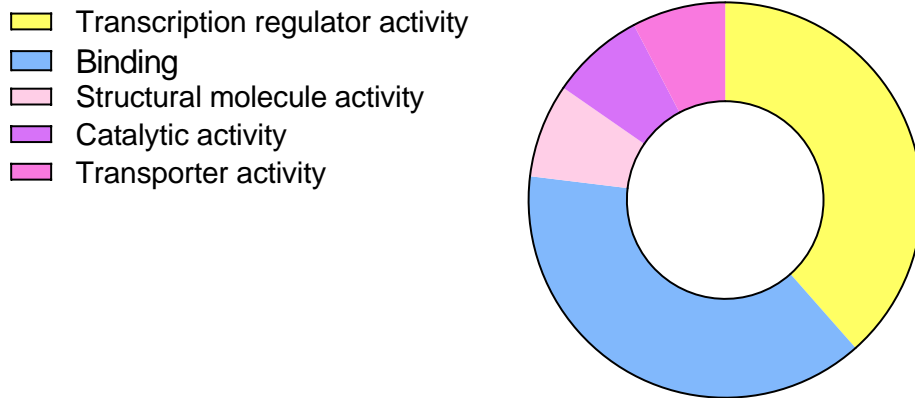
A

Molecular Functions (TargetScan)



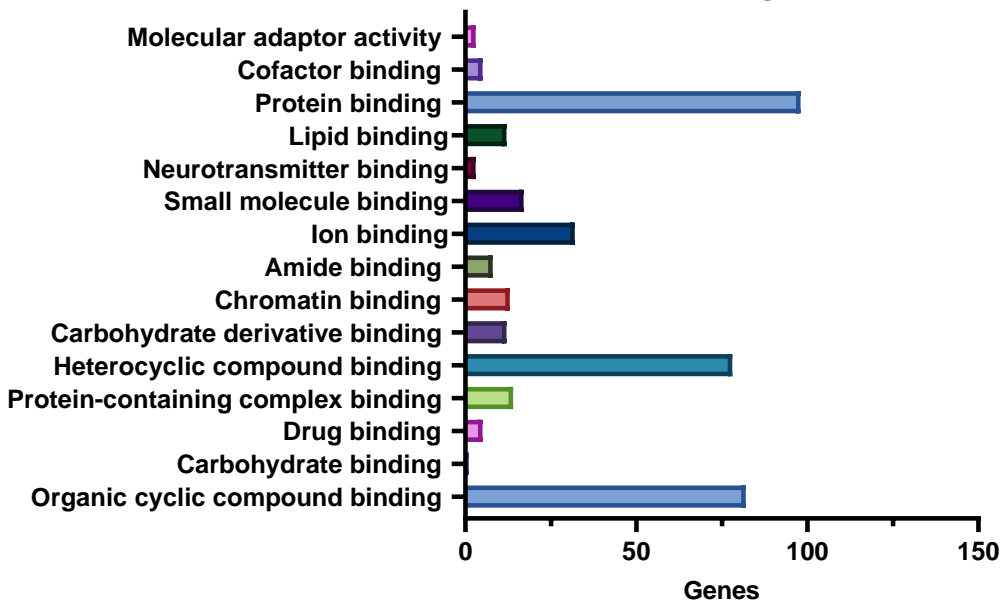
B

Molecular Functions (IPA)

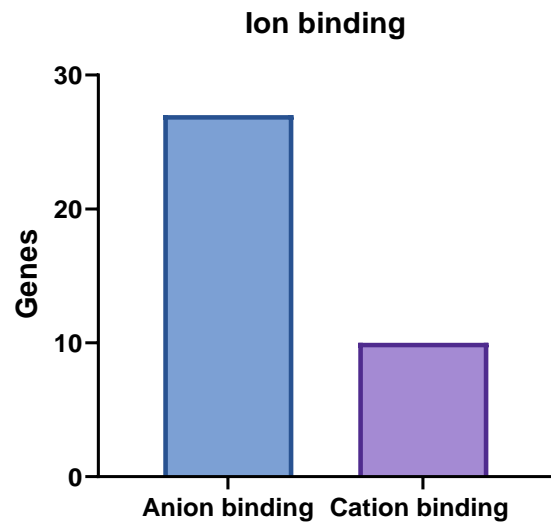


C

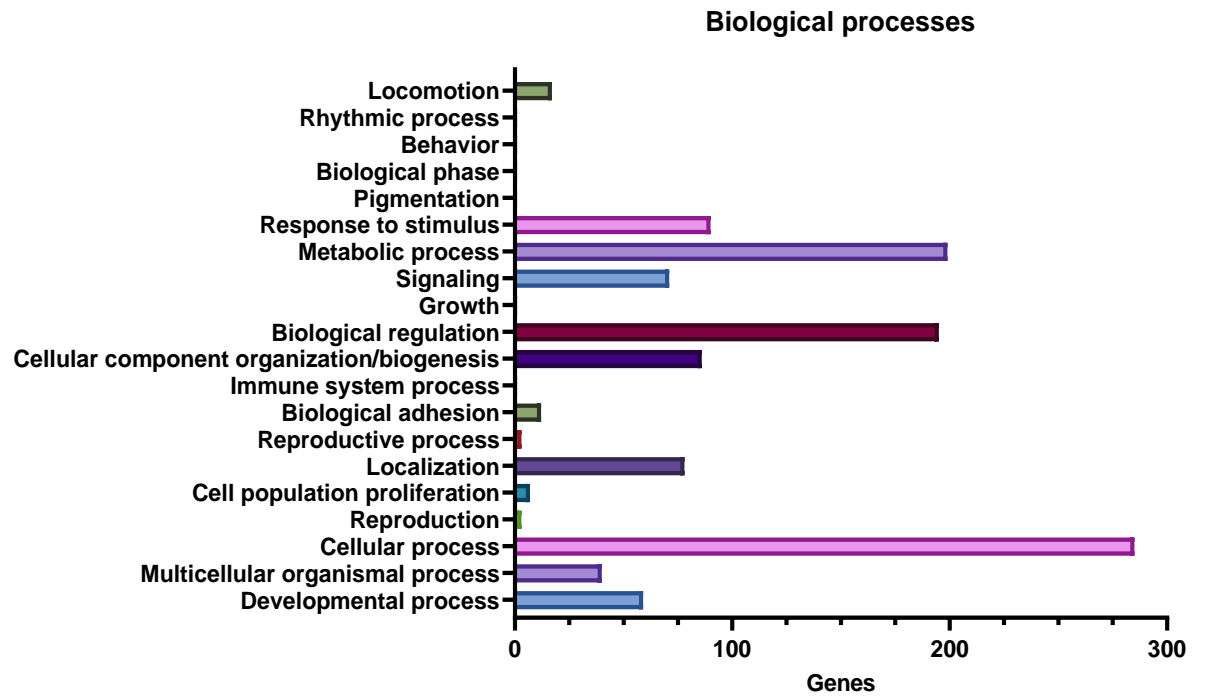
Binding



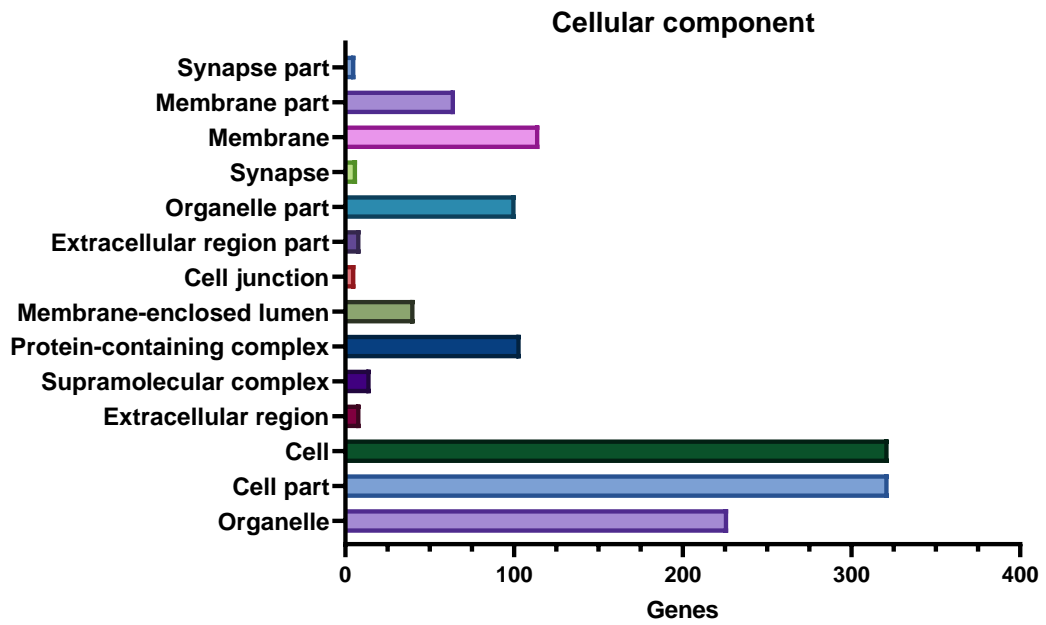
D



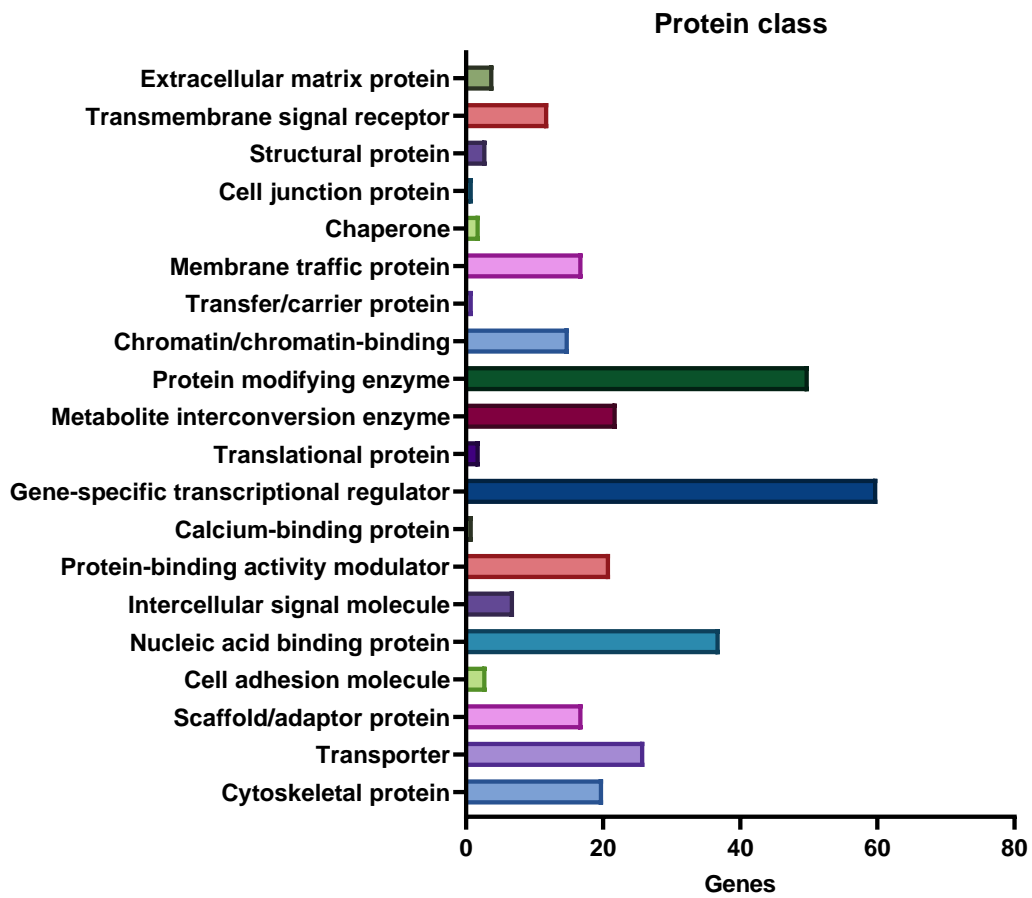
E



F



G



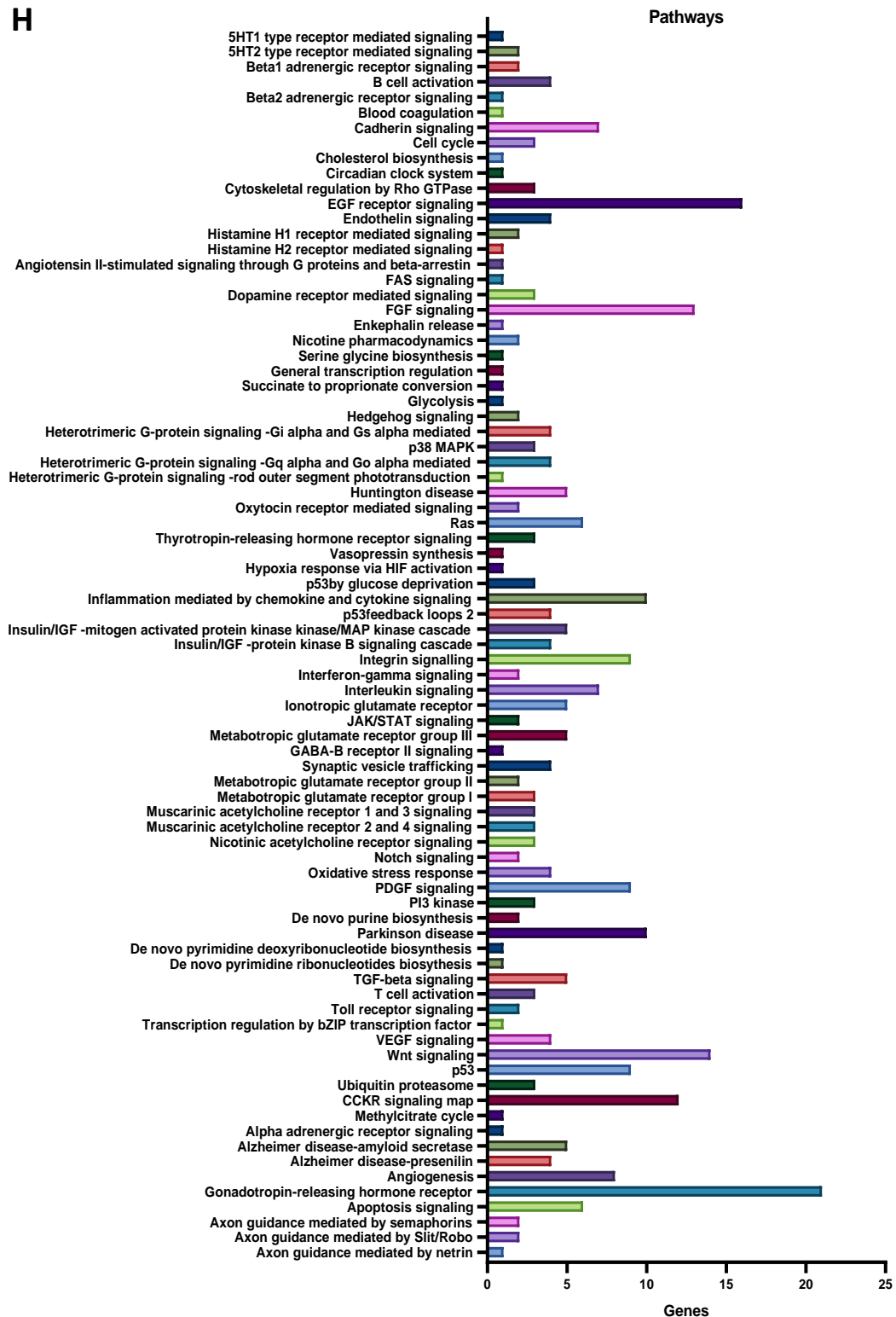


Figure 4.2: Gene ontology analysis of miR-141-3p targets. TargetScan revealed 654 targets of miR-141-3p, analysis of these targets with PANTHER classification system functional analysis identified A) Molecular functions with the majority being related to binding. B) Analysis of targets identified from IPA also revealed molecular functions largely related to binding C) A closer look into binding reveals 32 genes implicated in ion binding and 3 in neurotransmitter binding. D) Ion binding identified from C. E) Biological processes associated with miR-141-3p targets, F) Cellular components linked to miR-141-3p G) Protein class related to miR-141-3p and H) Pathways connected with miR-141-3p targets.

These ion channel genes include *Lrrc8a*, *Cacna1g* and *Ano1*. These ion channel genes were further investigated using TargetScan to explore if they are direct targets of miR-141-3p. This revealed a conserved alignment of a putative miR-141-3p target site within the 3'-UTR of *Lrrc8a* (**Figure 4.5A**) but did not show target sites for *Cacna1g* and *Ano1*.

4.3.3 Tracheal and articular chondrocyte transfection with miR-141-3p

To assess the effect of miR-141-3p on a selection of ion channel genes, both tracheal and articular chondrocytes were transfected with miR-141-3p mimic, antagomiR and scrambled control. These miRNA sequences were tagged with a 3'-FAM label (**Table 4.3**) in order to allow visualisation of transfection efficiency and facilitate transfection optimisation. Tracheal and articular chondrocytes were transfected with 50 nM, 100 nM, and 200 nM of miR-141-3p mimic, antagomiR and scrambled control to determine the optimal concentration for best transfection efficiency. Fluorescent imaging to visualise the tagged 3'-FAM labels (**Figure 4.3**) along with qPCRs of two different batches of RNA and cDNA determined 50 nM as the optimal concentration for miR-141-3p mimic and 100 nM as the optimal transfection concentrations for miR-141-3p antagomiR as at these concentrations, more chondrocytes were transfected with miR-141-3p mimic (**Figure 4.3C**) or antagomiR (**Figure 4.3D**). Two concentrations of scrambled control (50nM and 100nM) were used to allow for comparison with mimic and antagomiR (**Figure 4.3B**).

Following the transfection with the optimal concentrations, qPCR quantification of miR-141-3p expression levels was carried out to further validate the success of the

transfection. This showed that transfection of tracheal chondrocytes with miR-141-3p mimic significantly increased miR-141-3p expression compared to scrambled control ($p<0.01$) and transfection with antagomiR (AM-141-3p) significantly decreased miR-141-3p expression compared to scrambled control ($p<0.05$) (**Figure 4.4A & B**). This was also observed in articular chondrocytes transfected with miR-141-3p mimic, where the miR-141-3p levels were significantly increased compared to scrambled control ($p<0.01$), however the levels of miR-141-3p were not significantly different following antagomiR (AM-141-3p) transfection (**Figure 4.4C & D**).

4.3.4 Ion channel genes targeted by miR-141-3p following transfection

Following the successful transfection of tracheal and articular chondrocytes, qPCR quantification of *Lrrc8a*, *Cacna1g* and *Ano1* genes was performed on chondrocytes transfected with miR-141-3p mimic, antagomiR and scrambled control (**Figure 4.5 & 4.6**). The expression levels of *Lrrc8a* were significantly decreased in tracheal and articular chondrocytes ($p<0.0001$ for both) following transfection with miR-141-3p mimic (**Figure 4.5B & C**) with levels of *Lrrc8a* being significantly lower in tracheal chondrocytes in comparison with articular chondrocytes ($p<0.05$) (**Figure 4.6A**). *Lrrc8a* expression was significantly increased in tracheal chondrocytes following transfection with AM-141-3p antagomiR as well as in articular chondrocytes ($p<0.001$ for both) (**Figure 4.5D & E**). Tracheal chondrocytes had also significantly lower levels of *Lrrc8a* than articular chondrocytes ($p<0.001$) (**Figure 4.6B**).

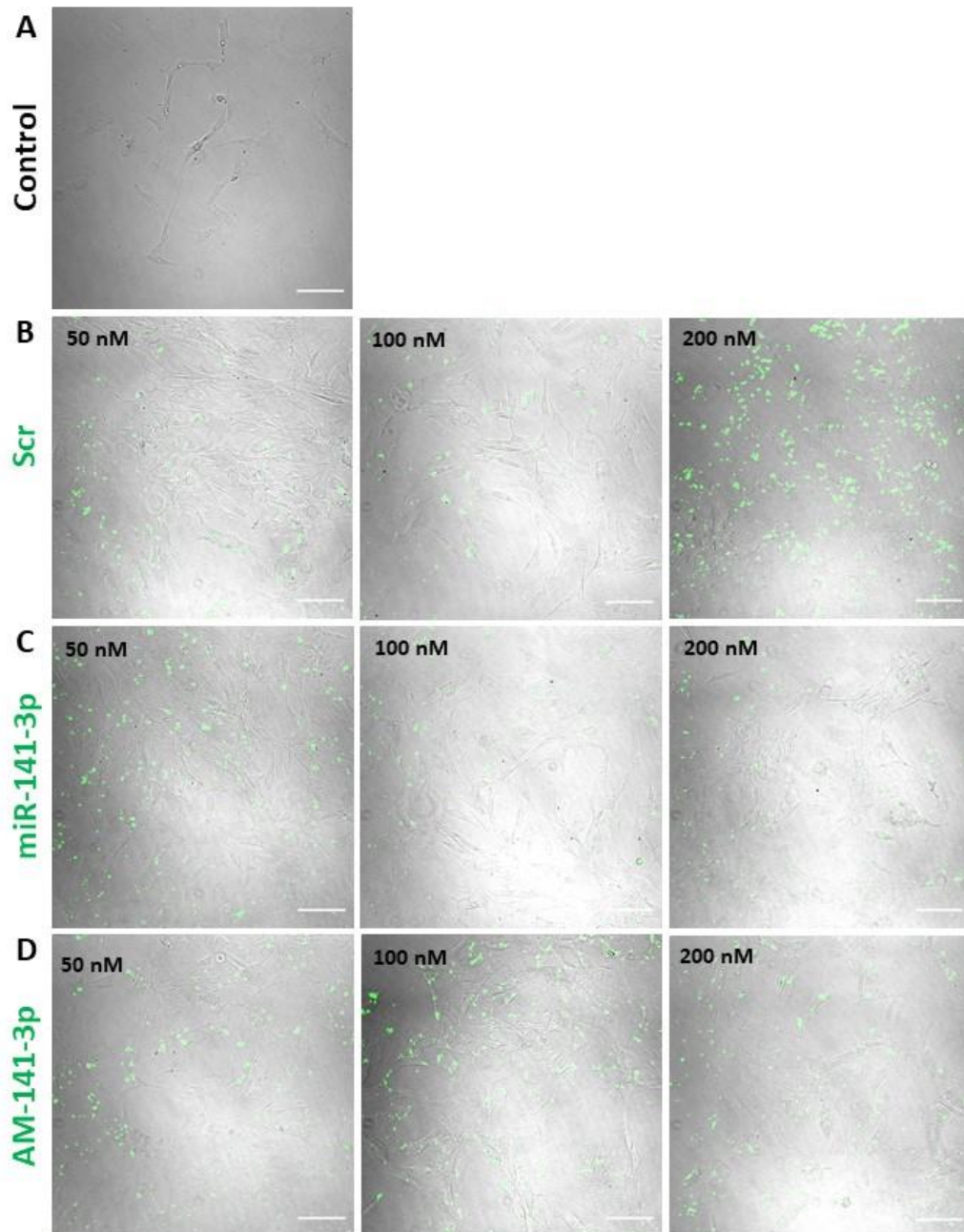


Figure 4.3: Representative immunofluorescence of tracheal chondrocytes transfected with miR-141-3p. A) vehicle control (control) and different concentrations (50, 100 and 200 nM) of B) Scramble control (Scr) C) miR-141-3p mimic (miR-141-3p) and D) AntagomiR (AM-141-3p). Images were obtained at x20 magnification with Zeiss LSM 800 confocal microscope. 3'-FAM tag was excited at 488 nm and emission spectra were recorded between 500-600 nm. Scale bar: 100 μ m.

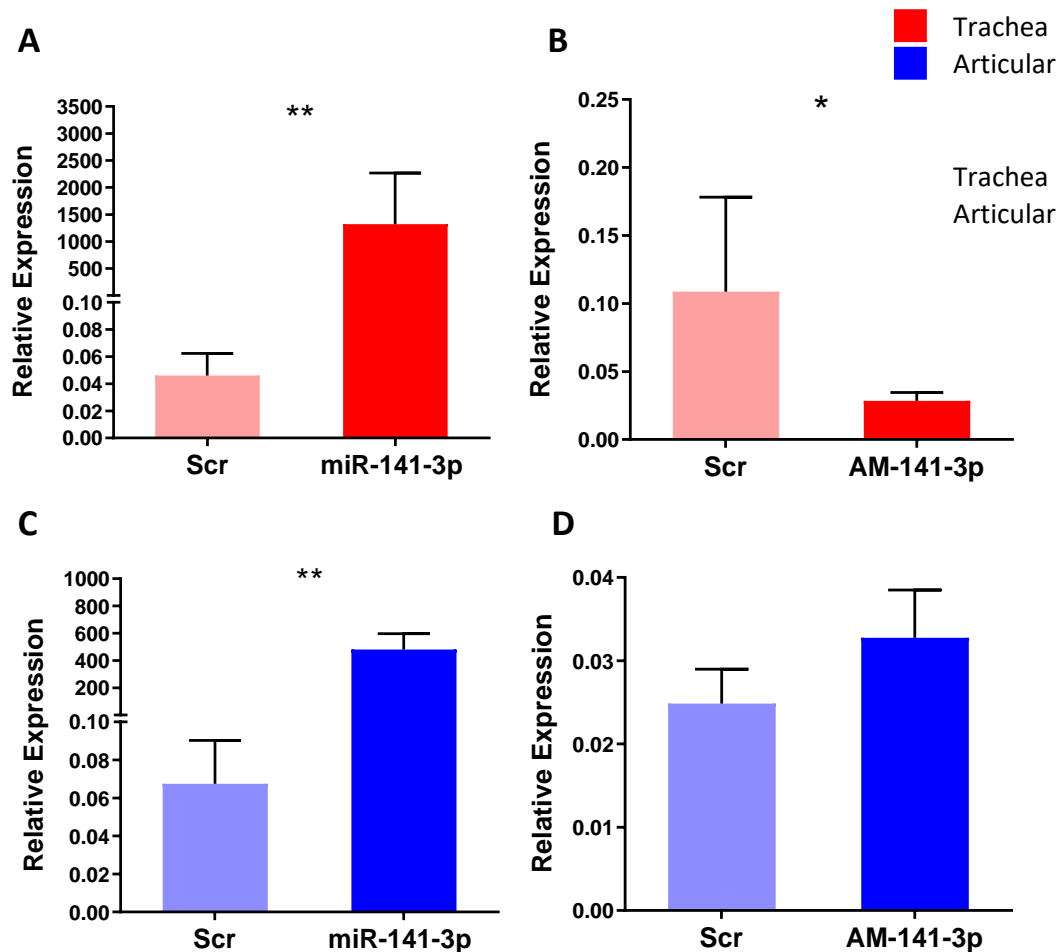


Figure 4.4: qPCR quantification of relative expression of miR-141-3p levels following transfection of tracheal and articular chondrocytes with miR-141-3p.

Expression of A) miR-141-3p in tracheal chondrocytes following transfection with scramble control (Scr) and miR-141-3p mimic. B) miR-141-3p in tracheal chondrocytes following transfection with scramble control (Scr) and miR-141-3p antagomiR. C) miR-141-3p in articular chondrocytes following transfection with scramble control (Scr) and miR-141-3p mimic. D) miR-141-3p in articular chondrocytes following transfection with scramble control (Scr) and miR-141-3p antagomiR. TC: red; n=6. AC: blue; n=6. Expression levels of miR-141-3p were normalised with SNORD61 housekeeping gene. Error bars represent SEM. Graphs were created using GraphPad Prism 8. Unpaired t-test was used to statistically analyse the data. * denotes $p < 0.05$ and ** denotes $p < 0.01$.

The expression of *Cacna1g* was also significantly decreased in tracheal chondrocytes following transfection with miR-141-3p mimic ($p < 0.001$) but not in articular chondrocytes (Figure 4.5F & G) and comparison between the two chondrocyte types also showed no significant difference (Figure 4.6C). Whereas the expression of *Cacna1g* was not different in tracheal chondrocytes post transfection with AM-141-

3p antagomiR but significantly increased in articular chondrocytes ($p < 0.001$) (**Figure 4.5H & I**) and comparison between the two cartilage types also showed no significant difference (**Figure 4.6D**).

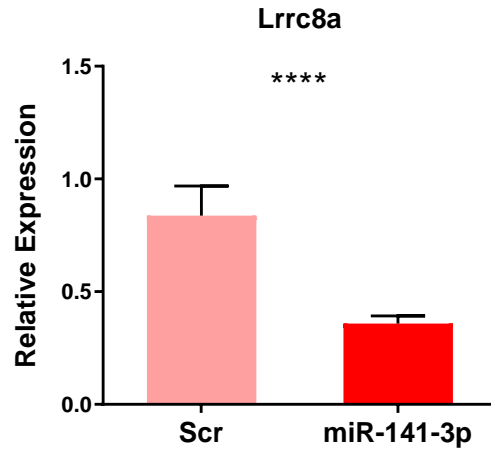
Finally, the expression levels of Ano1 post transfection with miR-141-3p mimic were not significantly different in tracheal or articular chondrocytes in comparison to scramble control (**Figure 4.5J & K**) and when comparing the expression levels of Ano1 after miR-141-3p mimic transfection there was no significant difference between trachea and articular chondrocytes (**Figure 4.6E**). However, transfection with AM-141-3p antagomiR indicated that inhibition of miR-141-3p significantly increased Ano1 expression in tracheal chondrocytes ($p < 0.05$) (**Figure 4.5L**) but not in articular chondrocytes (**Figure 4.5M**) and when the levels of Ano1 expression post AM-141-3p antagomiR transfection were compared between tracheal and articular chondrocytes there was also no significant difference (**Figure 4.6F**).

A

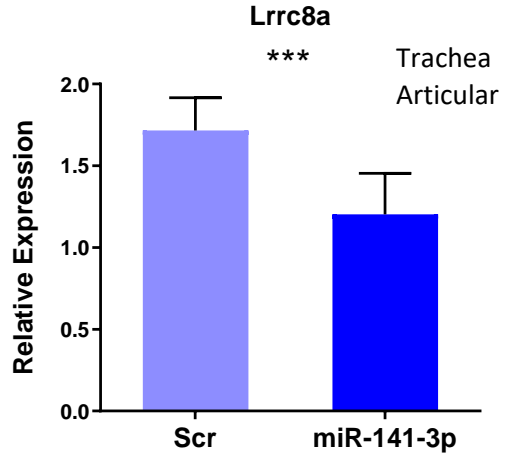
3' GGUAGAAAUGGUCUGUCACAAU 5' rno-miR-141-3p
5' AUGCCCCUCCACGCACAGUGUUA 3' rno-Lrrc8a
5' CUGCCUCUCCACGCACAGUGUUA 3' hsa-Lrrc8a

Trachea
Articular

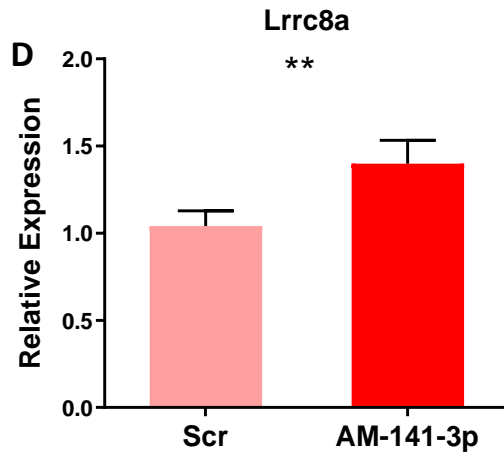
B



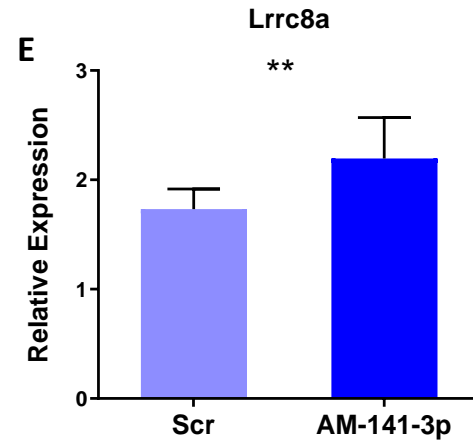
C



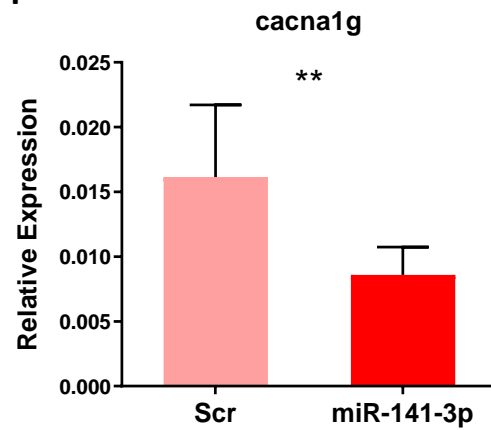
D



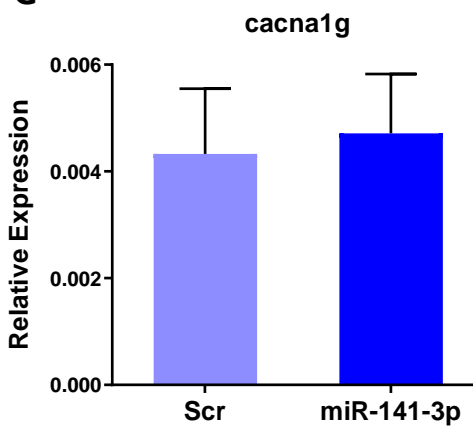
E



F



G



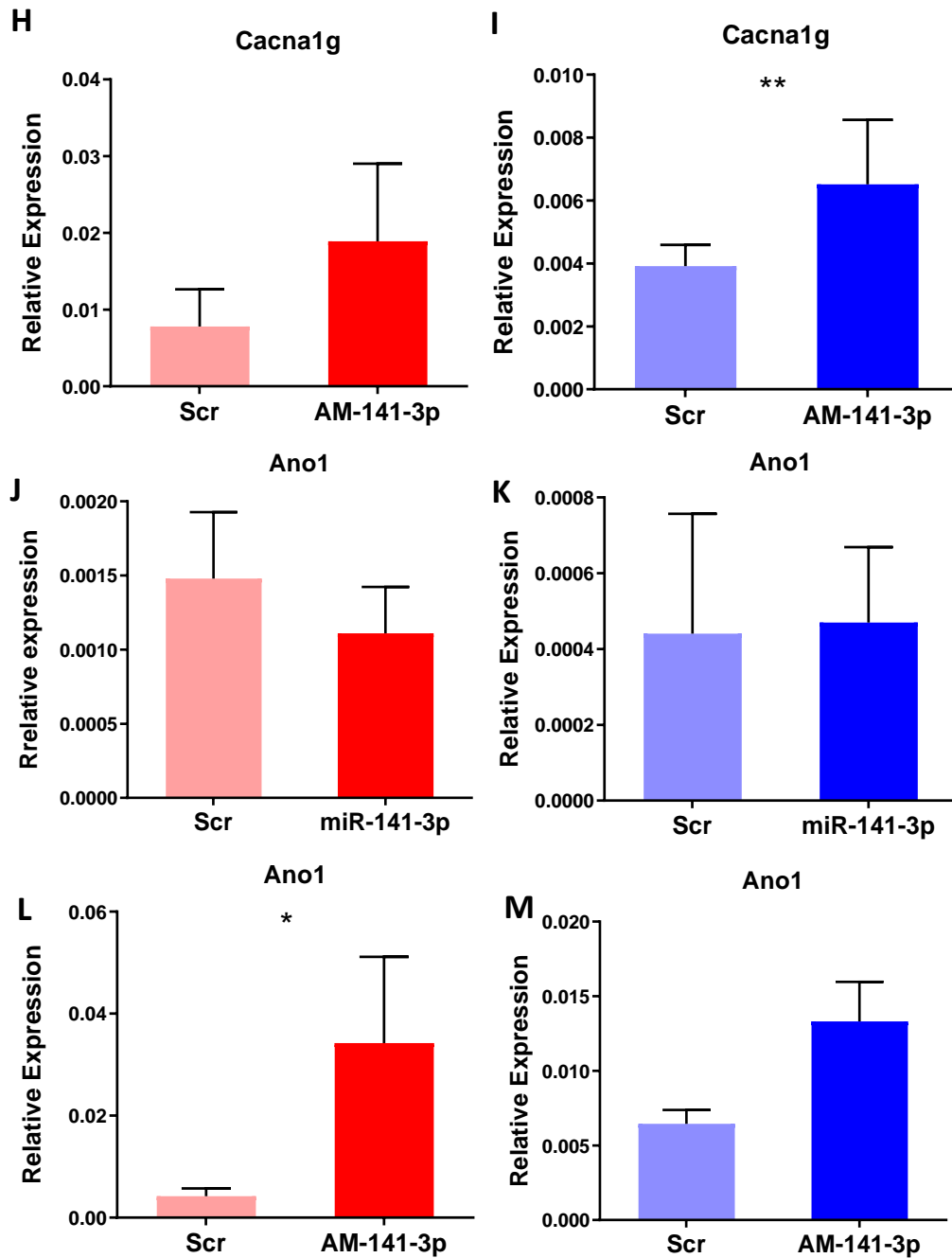


Figure 4.5: qPCR quantification of relative expression of ion channel genes in tracheal and articular chondrocytes following transfection with miR-141-3p. A) Alignment of rno-miR-141-3p sequence with putative target site in the 3'-UTR of *Lrrc8a* gene. Conserved human and rat target sites are indicated in red and miR-141-3p seed sequence is shown in blue. Expression of *Lrrc8a* following transfection of B) Tracheal chondrocytes (TC) with scramble control (Scr) and miR-141-3p mimic, C) Articular chondrocytes (AC) with Scr and miR-141-3p mimic, D) TC with Scr and miR-141-3p antagomiR and E) AC with Scr and miR-141-3p antagomiR. Expression of *Cacna1g* following transfection of F) TC with Scr and miR-141-3p mimic, G) AC with Scr and miR-141-3p mimic, H) TC with Scr and miR-141-3p antagomiR and I) AC with Scr and miR-141-3p antagomiR. Expression of *Ano1* following transfection of J) TC with Scr and miR-141-3p mimic. G) AC with Scr and miR-141-3p mimic. H) TC with Scr and miR-141-3p antagomiR and I) AC with Scr and miR-141-3p antagomiR. All genes were normalised to *Hprt1* housekeeping gene. Error bar represents SEM. Data was statistically analysed with MANOVA in Minitab. TC: red; n=5. AC: blue; n=5. * denotes $p < 0.05$, ** $p < 0.01$ *** $p < 0.001$ and **** $p < 0.0001$.

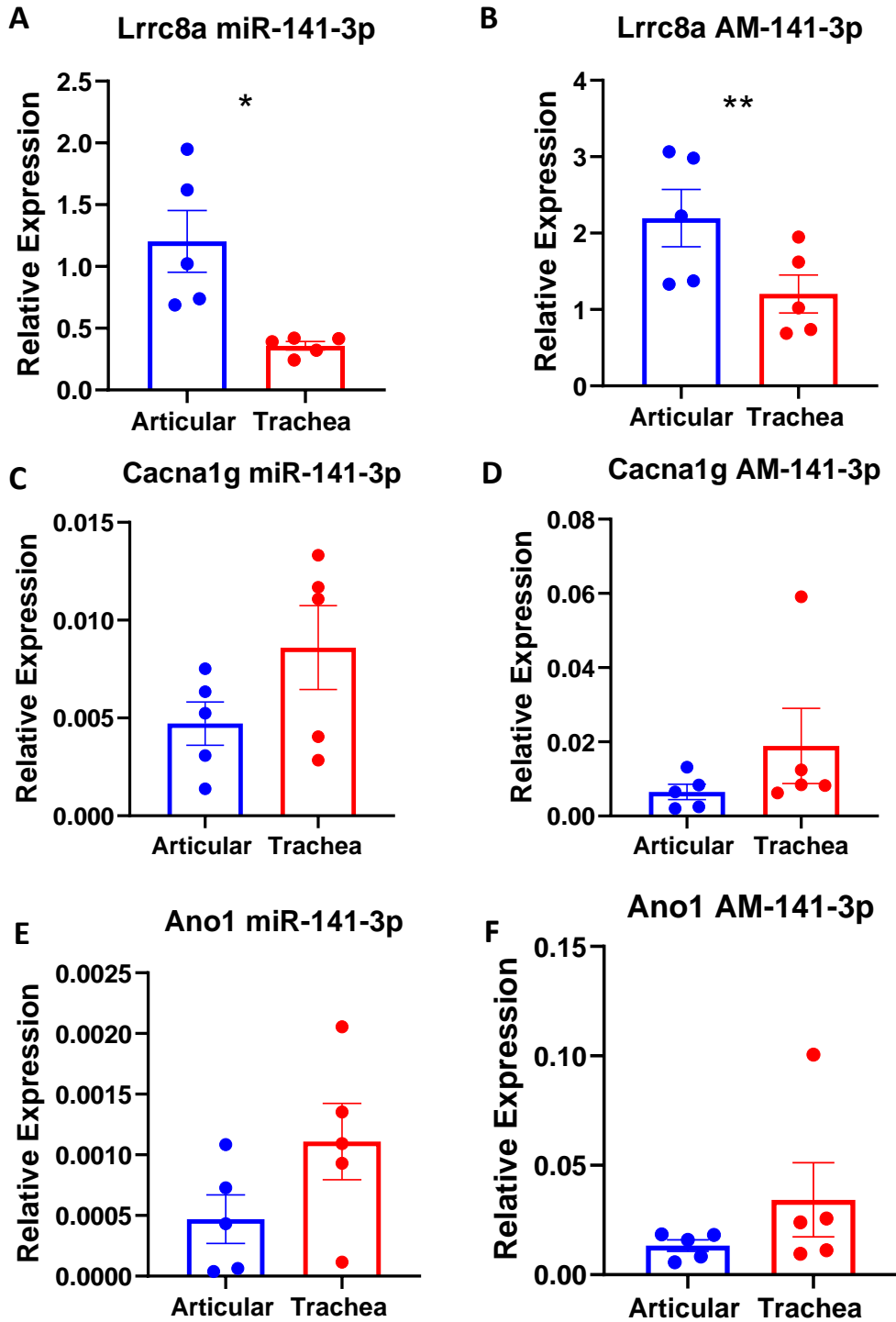


Figure 4.6: Comparison of expression levels of ion channel genes between tracheal and articular chondrocytes following transfection with miR-141-3p using qPCR quantification. Expression of Lrrc8a following transfection of tracheal and articular chondrocytes with A) miR-141-3p mimic and B) miR-141-3p antagomiR. Expression of Cacna1g following transfection of tracheal and articular chondrocytes with C) miR-141-3p mimic and D) miR-141-3p antagomiR. Expression of Ano1 following transfection of tracheal and articular chondrocytes with E) miR-141-3p mimic and F) miR-141-3p antagomiR. All genes were normalised to Hprt1 housekeeping gene. Error bars represent SEM. Graphs were created using GraphPad Prism 8. Paired t-test was used to statistically analyse the data. TC: red; n=5. AC: blue; n=5. * denotes $p < 0.05$ and ** $p < 0.01$.

4.4 Discussion

In this chapter a transcriptomic and bioinformatic approach was used to identify factors driving the differential gene expression between the trachea and articular chondrocytes. miRNA upstream regulators were identified from the transcriptomic data and their expression between tracheal and articular chondrocytes was validated with qPCRs which revealed for the first time miR-141-3p expression to be significantly increased in articular chondrocytes compared to tracheal chondrocytes. Investigation of the predicted target genes of miR-141-3p using multiple bioinformatic tools showed novel links to ion channels and chondrocyte associated signalling pathways. As well as unveiling a putative miR-141-3p target site in the 3'-UTR of *Lrrc8a* ion channel gene. Successful transfection of the two chondrocyte types with miR-141-3p showed that miR-141-3p mimic and antagomiR target ion channel genes and change their expression in both chondrocyte type.

4.4.1 Comparison of miRNA expression in tracheal and articular chondrocytes

Among the 55 miRNAs identified, 10 miRNAs were chosen from the IPA dataset based on their relation to cartilage physiology and disease and two miRNAs, miR-140-5p and miR-125a-5p, were chosen from the literature. These two miRNAs were not identified from our RNA-seq dataset to be upstream regulators; however, they have been shown to play roles in chondrogenesis, cartilage physiology and disease (Papaioannou et al., 2013, Miyaki et al., 2010, Tuddenham et al., 2006, Matsukawa et al., 2013, Yu et al., 2015b). Despite miR-140-5p not being detected as an upstream

regulator, its expression was detected in both chondrocyte type (**Figure 4.1J**). miR-140-5p was potentially not identified as an upstream regulator because it may not drive downstream changes in gene expression between trachea and articular chondrocytes, this was supported by the fact that its expression was not significantly different between the two chondrocyte type; this also was the case for miR-125a-5p.

The observed variance in the expression of miRNAs between the articular and tracheal chondrocytes could be attributed to the genetic variation between rats as primary chondrocytes were used. To ensure that the variance was minimised, RNA was extracted from cells that were at passage one. However, there was still variation between the biological replicates which could be due to miRNA expression variability which may lead to non-genetic cell to cell heterogeneity in miRNA expression (Wang et al., 2019). miRNA expression and action has also been shown to be context-dependent whereby slight differences in environmental conditions can alter miRNA expression (Erhard et al., 2014, Bartel, 2018). It was not surprising that the expression of most miRNA between trachea and articular chondrocytes did not show significant differences as miRNAs are dynamically expressed in multiple tissues and as observed in chapter 3, the two chondrocyte types showed great similarity in their transcriptome and channelome. Interestingly, two miRNAs, miR-30c and miR-141-3p, had significantly different expression between trachea and articular chondrocytes.

The increased expression of miR-30c in tracheal cartilage compared to articular cartilage coincides with the fact that miR-30 is vital for tracheal cartilage development, whereby it has been shown to repress an FGF growth factor, snail, to

enable the differentiation of chondrocytes. Deletion of miR-30c de-represses this growth factor, causing poor deposition of ECM components and malformation of cartilage rings (Gradus et al., 2011). On the other hand, the role of miR-141-3p in cartilage homeostasis has not been investigated. Hence, this chapter focused on miR-141-3p, which was shown to have significantly increased expression in articular chondrocytes compared to tracheal chondrocytes (**Figure 4.1H**).

4.4.2 Gene ontology of miR-141-3p predicted downstream targets

Gene ontology analysis of the miR-141-3p targets predicted using IPA and TargetScan indicated that the main molecular function associated with these targets was binding, of which 32 genes were involved in ion binding and 3 in neurotransmitter binding (**Figure 4.2C**). A panel of 15 ion channel genes were also shown to be targets of miR-141-3p from TargetScan. Together this data indicates that miR-141-3p may have an important role in ion channel homeostasis of chondrocytes. Interestingly the ion binding revealed that there were more genes targeted by miR-141-3p that were involved in anion binding (27 genes) than cation binding (10 genes) (**Figure 4.2D**). This is interesting as a target of miR-141-3p is the anion channel *Lrrc8a* which is a VRAC channel. Some of the notable biological processes that are associated with miR-141-3p targets such as 'signalling', 'cellular component organisation and biogenesis', 'cell population proliferation' and 'developmental processes' (**Figure 4.2E**) complement the function of miR-141-3p as it was shown to negatively regulate the proliferation, migration and apoptosis of colorectal cancer cells (Xing et al., 2020a).

miR-141-3p also had an effect on multiple signalling pathways, whereby transfection of colorectal cancer cells with miR-141-3p mimic caused E-cadherin expression to increase, and the level of N-cadherin, Snail, and Vimentin to significantly decrease (Xing et al., 2020a). The fact that miR-141-3p also targets snail and represses its expression is important as snail was shown to be targeted by miR-125 and miR-30c in tracheal chondrocytes, which also repressed its expression as previously discussed. Deletion of these miRNAs was found to lead to the malformation of cartilage rings as chondrocytes were not able to differentiate properly when snail expression was increased (Gradus et al., 2011). Thus, the expression of miR-141-3p in tracheal chondrocytes may be vital for cartilage formation and may act as a mechanism along with miR-125 and miR-30c to repress snail and regulate chondrocyte differentiation and hence cartilage formation.

Many of the cellular components identified from gene ontology analysis of miR-141-3p targets such as 'membrane', 'membrane part', 'synapse part', 'synapse' and 'cell junction' are associated with ion channels (**Figure 4.2F**). This was reflected in the protein class, which displayed links to ion channels with 'cell junction protein', 'membrane traffic protein', 'transfer carrier protein', 'calcium binding protein' and 'transporter protein' being amongst the top protein class hits (**Figure 4.2G**). Whereas 'ECM proteins' and 'cytoskeletal protein' hits indicate links to chondrocyte function (**Figure 4.2G**). One study showed that miR-141-3p targets a number of genes important in chondrogenesis such as Runx1, a transcription factor expressed during MSCs differentiation to chondrocytes and Hs2st1 (LeBlanc et al., 2015). Hs2st1 codes

for a heparin sulfate biosynthetic enzyme that also plays a role in chondrogenic differentiation (Wang et al., 2013, Zhao et al., 2015).

Most of the pathways associated with miR-141-3p targets from the gene ontology analysis were involved in chondrogenesis such as the 'cytoskeletal regulation by Rho GTPase', 'FGF signalling', 'hedgehog signalling', 'IGF pathway/protein kinase β signalling cascade', 'TGF-beta signalling', and 'Wnt signalling pathway' (**Figure 4.2H**). As well as that pathways associated with ion channels were also amongst the top pathways such as 'GABA- β receptor signalling', 'ionotropic glutamate receptor pathway', 'metabotropic glutamate receptor pathways', 'muscarinic and nicotinic acetylcholine receptor signalling pathways' (**Figure 4.2H**). These data provide evidence that miR-141-3p may be a key miRNA in chondrocyte homeostasis and normal cartilage formation.

Although mirBase and TargetScan platforms are useful, it should be noted that they are only prediction tools and that the interaction of miRNAs with their target should be verified using other means such as 3'-UTR reporter assay, northern blot, qPCR, western blot, transcriptomic and proteomic analysis (van Rooij, 2011). Recently, it was shown that miRNA mediated effects on target expression and translation can be determined using quantitative RNA-seq and sub-codon resolution ribosomal footprinting (Wessels et al., 2019). In addition, gain and loss of function analysis through the transfection of the cells with miRNA mimics and antagomiRs must also be used to validate the effect of these miRNAs on the biological function of cultured cells. Hence, tracheal and articular chondrocytes were transfected with scrambled

sequence as a control and miR-141-3p mimic and antagomiR to exogenously express or inhibit miR-141-3p.

4.4.3 Ion channels genes targeted by miR-141-3p in tracheal and articular chondrocytes

Transfection of tracheal and articular chondrocytes with miR-141-3p was shown to be successful and efficient as miR-141-3p mimic significantly increased miR-141-3p levels in both chondrocyte types (**Figure 4.4A & C**) and antagomiR significantly decreased miR-141-3p levels in tracheal chondrocyte (**Figure 4.4B**). However, it did not cause its significant decrease in articular chondrocytes (**Figure 4.4D**). This could be due to the antagomiR no longer being bound to miR-141-3p after RNA isolation. miR-141-3p also had the most significant overlap p -value amongst the upstream miRNAs. This indicates that there is a significant overlap between the RNA-Seq genes, and the genes regulated by miR-141-3p. Thus, miR-141-3p could be driving the differential gene expression between tracheal and articular chondrocytes through targeting the 13 genes predicted with IPA of amongst which *Cacna1g* was identified (**Table 4.4**).

Analysing the sequences of some of the ion channel genes predicted to be targets of miR-141-3p with TargetScan revealed that *Lrrc8a* had a putative target site of miR-141-3p in the 3'-UTR that was conserved amongst species, including human and rat (**Figure 4.5A**). This indicates that miR-141-3p may directly target *Lrrc8a* and cause changes in its expression level. Transfection of miR-141-3p mimic caused the significant decrease of *Lrrc8a* levels in both tracheal and articular chondrocytes,

indicating that the targeting of *Lrrc8a* by miR-141-3p must have an important role in cartilage physiology as not only is the target site conserved amongst species but miR-141-3p affected *Lrrc8a* levels in chondrocytes from the two different sites of cartilage (**Figure 4.5B & C**). It was observed that miR-141-3p mimic reduced *Lrrc8a* expression more in tracheal chondrocytes than articular chondrocytes. This could be because the expression of *Lrrc8a* is significantly higher in articular chondrocytes as observed from the RNA-seq and qPCR data (**Figure 3.13B & Figure 3.15B**) and hence there were more *Lrrc8a* mRNA for miR-141-3p to target in articular chondrocytes.

To further validate whether miR-141-3p targets *Lrrc8a* and decreases its expression, chondrocytes were also transfected with miR-141-3p antagomiR. This had opposite effect of what was observed with miR-141-3p mimic. The inhibition of miR-141-3p caused the significant increase in *Lrrc8a* expression, which was again more pronounced in tracheal chondrocytes as the expression of *Lrrc8a* is higher in articular chondrocytes (**Figure 4.5D & E**). This is an important finding as *Lrrc8a* is an essential subunit in the expression of functional VRAC (Syeda et al., 2016). VRAC are essential for many biological processes, one of their main functions is to regulate cell volume by modulating RVD in chondrocytes, this is important as it allows chondrocytes need to be able to change their volume as the joint moves (Lewis et al., 2011b). Cell volume regulation is also important in diseases of cartilage, as cell volume increase is associated with OA progression (Hdud et al., 2014). Future studies would further validate *Lrrc8a* targeting by miR-141-3p through luciferase gene reporter assays to determine direct binding of miR-141-3p to the 3'-UTR region of *Lrrc8a* as well as validate *Lrrc8a* protein expression using western blot analysis.

Another ion channel gene predicted to be a downstream target of miR-141-3p from IPA was *Cacna1g*. Measuring the expression levels of *Cacna1g* in chondrocytes transfected with miR-141-3p mimic indicated a significant decrease in *Cacna1g* levels in tracheal chondrocytes (**Figure 4.5F**). However, this was not observed in articular chondrocytes (**Figure 4.5G**). On the other hand, inhibiting miR-141-3p significantly increased *Cacna1g* expression in articular chondrocytes, and although it also increased it in tracheal chondrocytes, the increase in expression was not significant (**Figure 4.5H & I**). *Cacna1g* expression levels are significantly higher in tracheal chondrocytes in comparison to articular chondrocytes. This was shown in both RNA-Seq and qPCR data (**Figure 3.10G & Figure 3.15D**). Analysis of the sequences of *Cacna1g* and miR-141-3p using miRBase and TargetScan did not show a putative target site for miR-141-3p in *Cacna1g* 3'-UTR. This indicates that *Cacna1g* could be indirectly targeted by miR-141-3p, causing downstream effects on its expression levels. A luciferase gene reporter assay in future studies would determine whether there is direct binding between miR-141-3p and *Cacna1g* mRNA.

Cacna1g belongs to voltage-gated calcium channels. Its expression in cartilage is important, as intracellular transient Ca^{2+} is fundamental in differentiation initiation of MSCs into chondrocytes during chondrogenesis. Interestingly another group have shown *Cacna1g* along with its relative subtype, *Cacna1h* to be amongst genes differentially expressed in articular cartilage (Kemper et al., 2019). Although *Cacna1h* was not found to be amongst the genes targeted by miR-141-3p, it was observed to be differentially expressed in the RNA-Seq data (Appendix, **Table A.1**). *Cacna1h* had higher expression in tracheal chondrocytes compared to articular chondrocytes. This

is interesting, as another group have shown *Cacna1h* to be essential for tracheal cartilage chondrogenesis, whereby its deletion causes a reduction in *Sox9* expression and malformation of cartilage rings (Lin et al., 2014b).

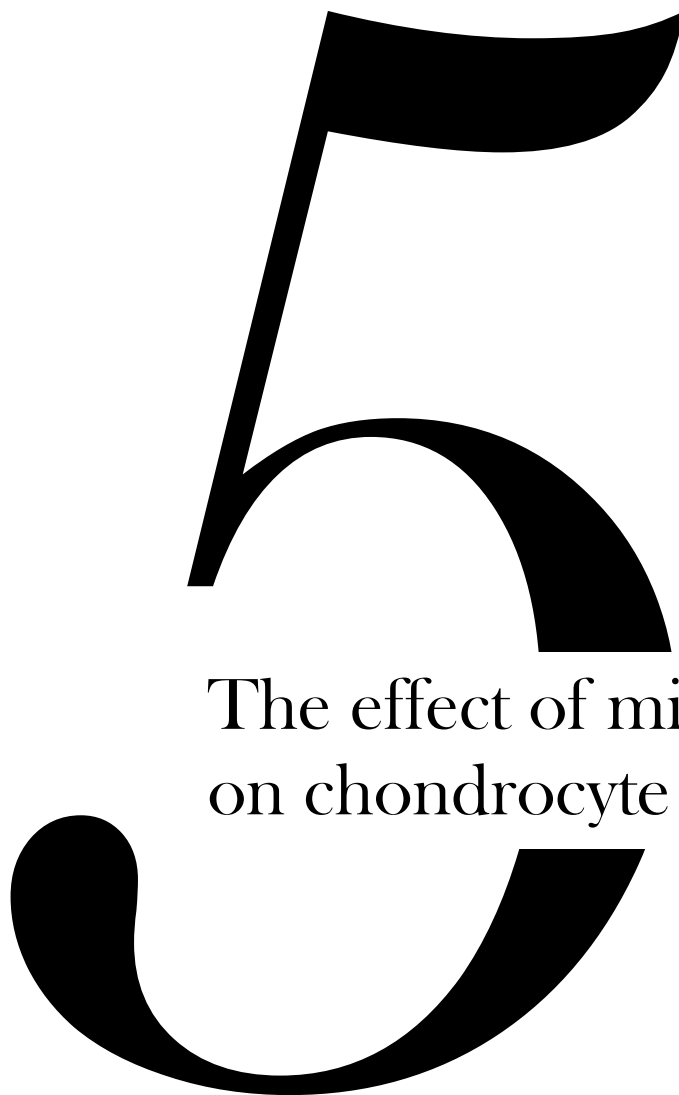
Although *Ano1* was not shown to be a target of miR-141-3p from IPA or TargetScan data, it was amongst the top 1/3 predicted targets of miR-141-3p in human when miR-141-3p targets were analysed with miRDIP. Therefore, it was interesting to investigate whether miR-141-3p affects its expression in rat as miR-141-3p is conserved amongst humans and rats. Transfection with miR-141-3p mimic did not show significant difference in either tracheal or articular chondrocytes (**Figure 4.5J & K**). However, transfection of miR-141-3p antagomiR indicated that the inhibition of miR-141-3p causes the significant increase of *Ano1* expression levels in tracheal chondrocytes (**Figure 4.5L**). This was also observed in articular chondrocytes but was not a significant increase (**Figure 4.5M**). This indicates that miR-141-3p may be targeting *Ano1* indirectly as it did not have a target site for miR-141-3p in its 3'-UTR region. To fully validate if miR-141-3p directly or indirectly targets *Ano1*, a luciferase gene reporter assay would assert the type of binding between miR-141-3p and *Ano1* mRNAs.

It remains unknown why miR-141-3p acts differently in tracheal and articular chondrocytes. Perhaps the slight differences in chondrocyte environment and the transcriptome and channelome they express affects the regulation of miRNA expression (Erhard et al., 2014). Perhaps miR-141-3p expression is used as a

mechanism to carry out the cartilage specific functions. Future studies would explore the cofactors and elements that lead to these differences.

One of the limitations encountered during this study was that the initial design of the RNA-Seq was not specific to identify miRNA. As initially, the aim of this project was to assess the gene expression between tracheal and articular chondrocytes. The number of miRNAs identified as upstream regulators was not expected. Hence in the future, RNA-seq designed to specifically quantify small RNAs should be performed. In addition, there was variation in the expression levels of ion channel genes in transfected chondrocytes. This could be because of the heterogeneity in the genetics between rats; a higher number of replicates in the future would reduce this variation and give a better indication of the effects of miR-141-3p on these genes.

Overall, using an unbiased transcriptomic and bioinformatic approach this chapter provided novel evidence that miR-141-3p is a key upstream regulator miRNA in cartilage physiology; whereby its regulation of ion channel genes may be vital for chondrocyte function and homeostasis. The impact of miR-141-3p on tracheal and articular chondrocytes function will be evaluated in the next chapter, where functional assay will be used to investigate miR-141-3p gain and loss of function on chondrocyte homeostasis.



The effect of miR-141-3p
on chondrocyte physiology

5.1 Introduction

MicroRNAs have a role in many vital cellular functions. They are able to epigenetically regulate gene expression and influence downstream cellular functions. Ion channel genes were shown in the previous chapter to be targeted and regulated by miRNA. Ion channels maintain the resting membrane potential (RMP) of cells, which regulates a variety of cellular processes including migration and proliferation (Abdul Kadir et al., 2018). Many of the mechanisms by which ion channels regulate cell migration and proliferation are related to the housekeeping functions exerted by ion transport proteins such as regulating the cell volume, intracellular Ca²⁺ levels and intra- and extracellular pH.

Studies have previously shown that miRNA can affect the proliferation and migration of chondrocytes (Song et al., 2013, Gu et al., 2017). Chondrocytes respond to stress signals, injury and external signalling factors by initiating proliferation (Adams and Shapiro, 2002). Proliferation in chondrocytes is affected by multiple cytokines, growth factors and signalling pathways (Chen et al., 2008, Enomoto-Iwamoto et al., 1997, Wuelling and Vortkamp, 2011). These factors also regulate the migration of chondrocytes, which is important during development and pathology (Morales, 2007). The endogenous expression of miR-141-3p and its inhibition was shown in the previous chapter to cause changes in *Lrrc8a*, *Cacna1g* and *Ano1* ion channel gene expression. In this chapter, the effect of miR-141-3p mimic and antagomiR on chondrocyte function is investigated, focusing on the RMP, proliferation and migration, which are all affected by changes in ion channel genes.

5.1.1 Role of Ion channels in migration and proliferation

The complement of ion channels expressed by a cell contribute to its RMP and changes in gene expression and/or function of these ion channels leads to changes in the RMP. The regulation of proliferation and migration by the RMP is well defined in non-excitabile cells such as chondrocytes (Abdul Kadir et al., 2018). The inhibition of Na⁺ and K⁺ ion channels with antagonists was shown to temporarily cause an increase in the proliferation of chondrocytes, however inhibiting these ion channels long term causes the inhibition of chondrocyte proliferation (Wohlrab et al., 2002).

The connection between free intracellular Ca²⁺ and proliferation has been well established (Al-Ani et al., 1988, Amigorena et al., 1990, Breitzkreutz et al., 1993). The block of L-type voltage-gated calcium channels by nifedipine was shown to abolish mechanically stimulated chondrocyte proliferation (Wu and Chen, 2000). This is also seen in potassium channels, whereby blocking K⁺ channels with tetraethylammonium (TEA) and 4-aminopyridine (4-AP) also decreases chondrocyte proliferation (Wohlrab et al., 2001, Wohlrab et al., 2004). It has been suggested that the mechanism through which these ion channels regulate chondrocyte proliferation is through the modulation of the RMP which would indirectly change the cell's proliferation (Mobasheri et al., 2012). In addition to regulating proliferation, ion channel have also been implicated in the regulation of cell migration.

An extensive list of ion channels involved in the regulation of migration is reviewed in (Schwab et al., 2012a). Amongst those ion channels, aquaporins have been shown to regulate the migration of chondrocytes, whereby the inhibition of Aqp1 causes the

reduction of chondrocyte migration and adhesion (Liang et al., 2008). It was also shown that an increase in intracellular Ca^{2+} through the activation of purinergic receptors with ATP, stimulates calcium-activated K^+ channels and causes a hyperpolarisation of the RMP which causes changes to the chondrocyte migration and proliferation (Suzuki et al., 2020b). There are not many studies on the effects of ion channels on chondrocyte migration. However, ion channels are known to regulate migration in different cell types. For example, VRAC which require *Lrrc8a* subunit to function, were also shown to have a role in cell migration whereby the inhibition of VRAC currents reduces the migration of glioma cells (Ransom et al., 2001, Soroceanu et al., 1999). In addition, *Ano1* was also shown to regulate cell migration in different cancer cells. It was shown that when overexpressed, *Ano1* causes an enhancement in the migration of head and neck carcinoma cells (Ayoub et al., 2010).

5.1.2 Chondrocyte proliferation and migration

In the early stages of postnatal development, chondrocyte proliferation is important and is tightly regulated to ensure normal cartilage and bone formation (Wuelling and Vortkamp, 2011). Signalling pathways and growth factors involved in chondrogenesis, such as *Ihh*, BMP, FGF, and Wnt signalling, all regulate chondrocyte proliferation as reviewed in (Wuelling and Vortkamp, 2011). *Ihh* directly activates chondrocyte proliferation by inducing the expression of Parathyroid hormone-related protein (PTHrP) (St-Jacques et al., 1999). *Ihh* signalling is mediated by Gli transcription factors, which are a family made up of *Gli1*, *Gli2* and *Gli3* (Alman, 2015). In *Gli2*^{-/-} null mice, *Gli2* was shown to activate chondrocyte proliferation whereas *Gli3* acts in the opposite manner and inhibits chondrocyte proliferation (Mau et al., 2007).

Another study showed that in *Ihh* null mice, *Gli3* restores chondrocyte proliferation (Hilton et al., 2005). Hence, the balance between the Gli receptor and activator forms is essential for the regulation of chondrocyte proliferation downstream of *Ihh*. Gli transcription factors have been shown to be targeted by miRNAs, affecting the *Ihh* signalling pathway and altering the proliferation of cells (Yu et al., 2015a, Cao et al., 2016). *Ihh* is important for chondrocyte physiology. The activation of the *Ihh* signalling pathway not only affects cell proliferation, but it also impacts cell migration. *Ihh* activates migration through the Integrin β 4 subunit (ITGB4) mediated focal adhesion kinase (FAK) pathway (Chen et al., 2014b).

Similar to proliferation, chondrocyte migration is controlled by various signalling pathways (Takebayashi et al., 1995, Maniwa et al., 2001). However, chondrocyte migration is slightly different to other cell type's migration, as chondrocytes have to migrate through the dense ECM. A number of studies have shown that chondrocytes are able to migrate under different stimuli such as Insulin-like growth factor-I, *Runx2* and fibrin (Chang et al., 2003, Fujita et al., 2004, Kirilak et al., 2006). Chondrocytes have also been shown to migrate in 3D collagen gels (Gosiewska et al., 2001, Frenkel et al., 1996). Migration is not usually taken into account for chondrocytes as once they differentiate and synthesise the ECM, they are perceived to stay put. However, chondrocyte migration is key in the repair process of cartilage post injury. It is also an important factor in tissue engineering of cartilage as regulating the migration of tissue-engineered chondrocytes would aid in the long-term restoration of the joint surface (Lu et al., 2013). Cartilage is difficult to heal, as it does not repair defects effectively. Hence manipulating the migration and proliferation of chondrocytes

would aid in the restoration of the cartilage surface post injury/damage. One approach that can be adapted to manipulate chondrocyte migration and proliferation is through epigenetic regulation with miRNAs. As well as affecting proliferation, miRNAs have also been shown to regulate chondrocyte migration (Song et al., 2013, Gu et al., 2017).

5.1.3 Role of miR-141-3p in proliferation and migration

Numerous studies have shown miRNAs to regulate cell proliferation and migration, with two miRNAs, miR-195 and miR-197, regulating chondrocyte migration and proliferation (Gu et al., 2017, Gao et al., 2020). However, the role of miR-141-3p in cartilage and chondrocytes has not yet been investigated. Despite this, miR-141-3p has been extensively studied in cancer biology and has been shown to have a dual role of being an oncogene and tumour suppressor gene as reviewed in (Gao et al., 2016). miR-141-3p plays an essential role in the migration and proliferation of different cancer types, either potentiating disease progression or posing as a possible therapeutic target (Gao et al., 2016). miR-141-3p plays a dual role in proliferation of cancer cells and was shown to inhibit the proliferation of human stromal stem cells (Qiu and Kassem, 2014) and gastric cancer cells (Griffiths-Jones S, 2006, Chen et al., 2014a). However, in pancreatic ductal adenocarcinoma cells and non-small cell lung cancer cells it was shown to enhance proliferation (Kent et al., 2009, Mei et al., 2014).

This dual effect of miR-141-3p on proliferation of cancer cells is not seen in migration. miR-141-3p has an inhibitory effect on migration of cancer cells, where it was shown to suppress migration of gastric cancer cells (Chen et al., 2014a), colorectal cancer cells

(Hu et al., 2010) and pancreatic cancer cells (Xu et al., 2014). Although the effect of miR-141-3p on chondrocyte migration and proliferation is unknown, the above evidence indicates that miR-141-3p plays a key role in cell proliferation and migration. Interestingly, miR-141-3p was identified in the previous chapter to be an important upstream regulator that targets ion channels in tracheal and articular chondrocytes.

5.1.4 Aims

Studies have shown that ion channels are involved in the regulation of proliferation and migration of chondrocytes by modulating the RMP (Schwab et al., 2012b, Wohlrab et al., 2002). miR-141-3p has been well established in regulating the proliferate and migration of different cancer cells as discussed above. However, its effect on chondrocyte function is unknown. In the previous chapter, miR-141-3p was identified as an upstream regulator that altered *Lrrc8a*, *cacna1g* and *Ano1* gene expression. This change in the expression of these ion channel genes will in turn affect the RMP of chondrocytes and hence their ability to proliferate and migrate. Hence, the aim of this chapter is to evaluate the effects of miR-141-3p transfection on the function of chondrocytes. This will be assessed by investigating the effect of miR-141-3p mimic and antagomiR on chondrocyte RMP, proliferation and migration.

5.2 Methods

5.2.1 RMP measurement

The RMP was measured using whole-cell patch clamp in current clamp mode using the Axopatch 200A amplifier (Axon Instruments, USA) as described in chapter 2.5. The glass pipettes used had slightly lower resistance than those used for cell-attached patch clamp experiments (4-8 m Ω). A standard physiological saline was used for both intracellular and extracellular solutions (**Table 2.5**). Electrophysiological data were digitized and analysed using the WinEDR program (John Dempster, University of Strathclyde) and QuB software (Qin et al., SUNY, Buffalo, NY, USA). Graphs and statistical analyses were generated using GraphPad Prism 8.

5.2.2 Ki67 proliferation assay

Following the transfection of chondrocytes with miR-141-3p mimic, antagomiR and scrambled control, the FCS-free DMEM was changed after 6 hours to DMEM with 10% FCS and cells were incubated for 48 hours. Following the incubation, cells were immunostained Ki67 (ab16667; Abcam, UK) primary antibody and AF488 (A11029; Life Technologies, UK) secondary antibody as described in chapter 2.2. Cells were left in PBS following immunocytochemistry and imaged using the Nikon Eclipse *Ti* live cell microscope. AF488 was excited at 488 nm and emission spectra were recorded between 500-600 nm. DAPI was excited at 374 nm and emission was recorded at 748 nm. Images were acquired using x40 objective and analysed using the ImageJ software where the percentage of cells expressing ki67 was determined in relation to

DAPI expression. Fisher's individual test for differences of means was used to statistically analyse the data with Minitab.

5.2.3 Migration assay

Following the transfection of chondrocytes with miR-141-3p mimic, antagomiR and scrambled control, cells were left for 48 hours to reach effective transfection efficiency and 100% confluence. To inhibit Ano1, cells were incubated with DMSO as a control and 20 μ M of 6-(1,1-Dimethylethyl)-2-[(2-furanylcarbonyl)amino]-4,5,6,7-tetrahydrobenzo[b] thiophene-3-carboxylic acid (CaCCinh-A01) (Tocris, UK) diluted in DMOS for 1 hour with DMSO being no more than 0.01% which had no effect alone. A scratch assay was conducted to measure the cell's migration. A wound was created in the middle of the culturing dish and the cells were washed with FCS-free DMEM, which was replaced with DMEM containing 10% FCS. Cells were imaged using the Nikon Eclipse *Ti* live cell microscope, every 30 minutes for 24 hours at x20 objective. Images were analysed using ImageJ software. Fisher's individual test for differences of means was used to statistically analyse the data with Minitab.

5.3 Results

5.3.1 RMP of tracheal chondrocytes transfected with miR-141-3p

In the previous chapter ion channel genes were targeted by miR-141-3p and their gene expression levels were altered. Ion channels regulate the RMP and changes in their expression levels would alter the RMP. To investigate this effect of miR-141-3p transfection, the RMP of the tracheal chondrocytes transfected with miR-141-3p

mimic and antagomiR was measured and compared to that of untreated cells (**Figure 5.1**). This revealed that the RMP was affected by the transfection of miR-141-3p and was significantly depolarised following miR-141-3p mimic ($p<0.0001$) and antagomiR ($p<0.01$) transfection, with miR-141-3p mimic causing tracheal chondrocytes to have a more positive RMP compared to the miR-141-3p antagomiR (**Figure 5.1**).

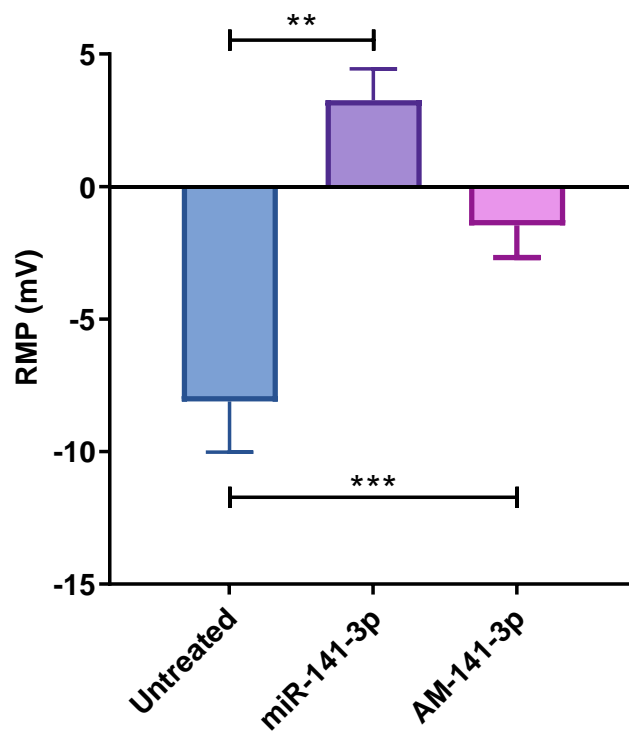
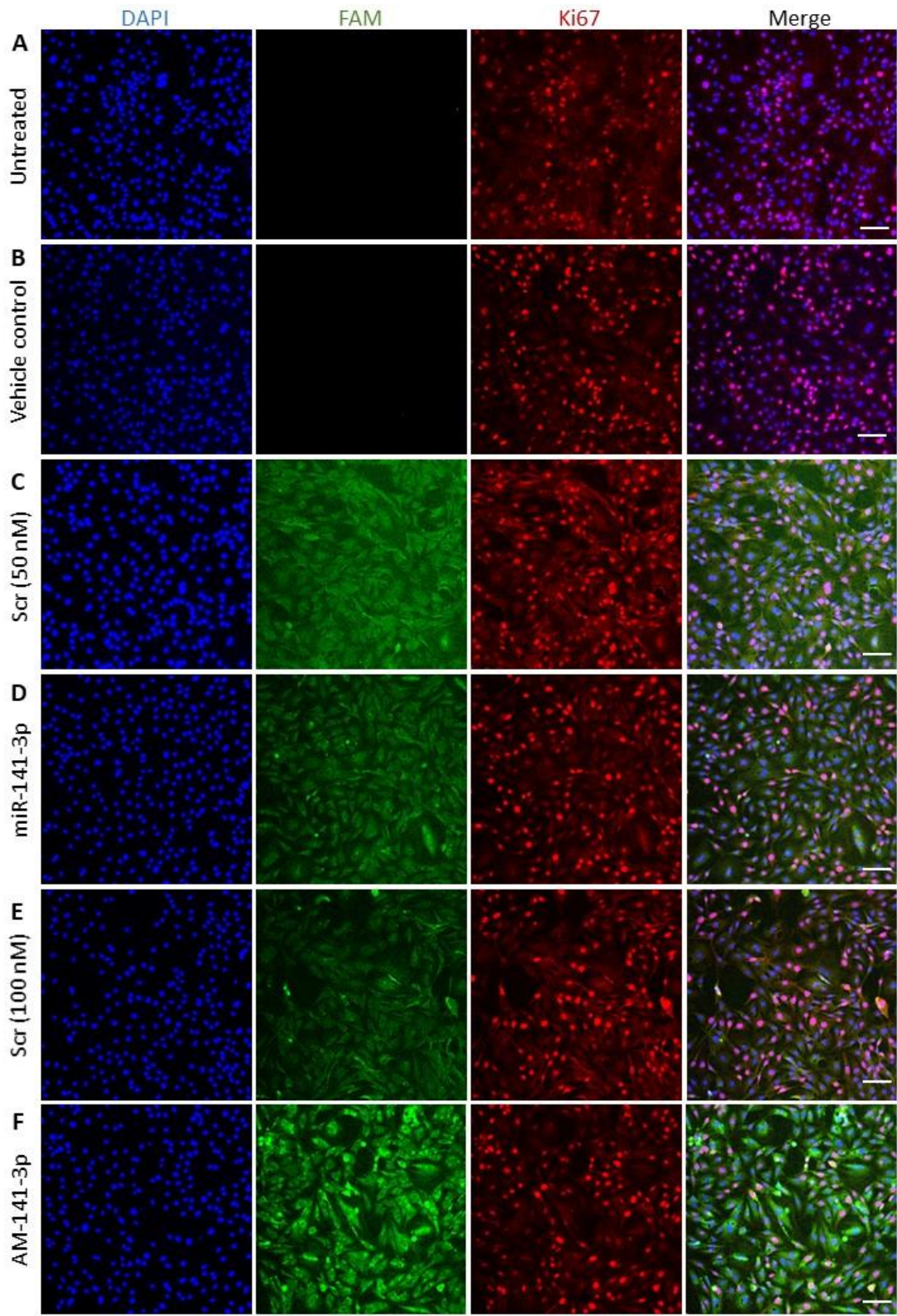


Figure 5.1: RMP measurement of tracheal chondrocytes transfected with miR-141-3p mimic and antagomiR. RMP values were recorded using whole cell patch clamp electrophysiology. Bars represent mean and error bars represent SEM. n= 18 cells used for untreated and n= 8 cells used for miR-141-3p and AM-141-3p, respectively. ** denotes $p<0.01$ and *** denotes $p<0.001$.

5.3.2 Proliferation of tracheal and articular chondrocytes transfected with miR-141-3p

The proliferation of tracheal and articular chondrocytes following the transfection with miR-141-3p was measured with the nuclear stain, Ki67, which stains the proliferating nuclei (**Figure 5.2**). Images following transfection and staining with Ki67 were analysed with ImageJ to identify the percentage of cells that were Ki67 positive, and hence proliferative in comparison to DAPI, which stained the nuclei of all chondrocytes. Two controls were used for comparison, an untreated control, and a vehicle control where the chondrocytes were treated with lipofectamine 2000 only (**Figure 5.2A& B; G& H**). Tracheal and articular chondrocytes were transfected with miR-141-3p mimic (**Figure 5.2D& J**) and antagomiR (**Figure 5.2F& L**), as well as a scrambled control at two concentrations 50 nM (**Figure 5.2C& I**) and 100 nM (**Figure 5.2E& K**) to match the concentration of the mimic and antagomiR, respectively.

In order to identify the chondrocytes transfected with miR-141-3p, the mimic, antagomiR and scrambled control were tagged with a fluorescent FAM label at the 3' end (**Figure 4.3 & 5.2**). This indicated that the transfection with miR-141-3p was successful as untreated and vehicle control showed no FAM fluorescence (**Figure 5.2A, B, G & H**). Ki67 staining revealed that in tracheal chondrocytes, proliferation was significantly decreased following transfection with miR-141-3p mimic compared to the untreated, vehicle and scrambled control ($p < 0.007$, $p < 0.01$ and $p < 0.04$ respectively) (**Figure 5.3A**) as well as that it was also significantly lower than that of chondrocytes transfected with miR-141-3p antagomiR ($p < 0.02$) (**Figure 5.3A**). Whereas in articular chondrocytes, the proliferation was significantly increased in



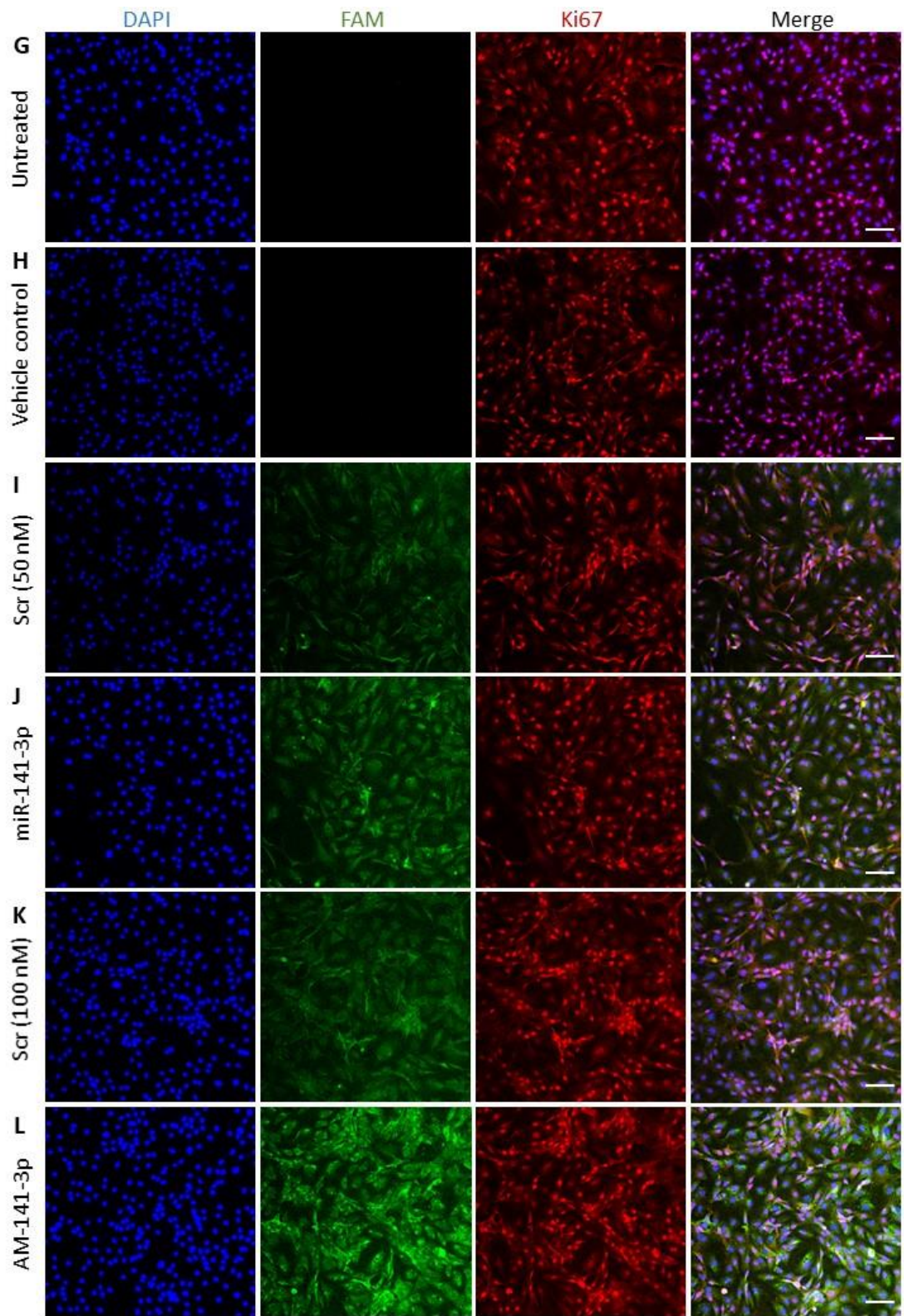


Figure 5.2: Ki67 immunocytochemistry staining of tracheal and articular chondrocytes following transfection with miR-141-3p mimic and antagomiR.

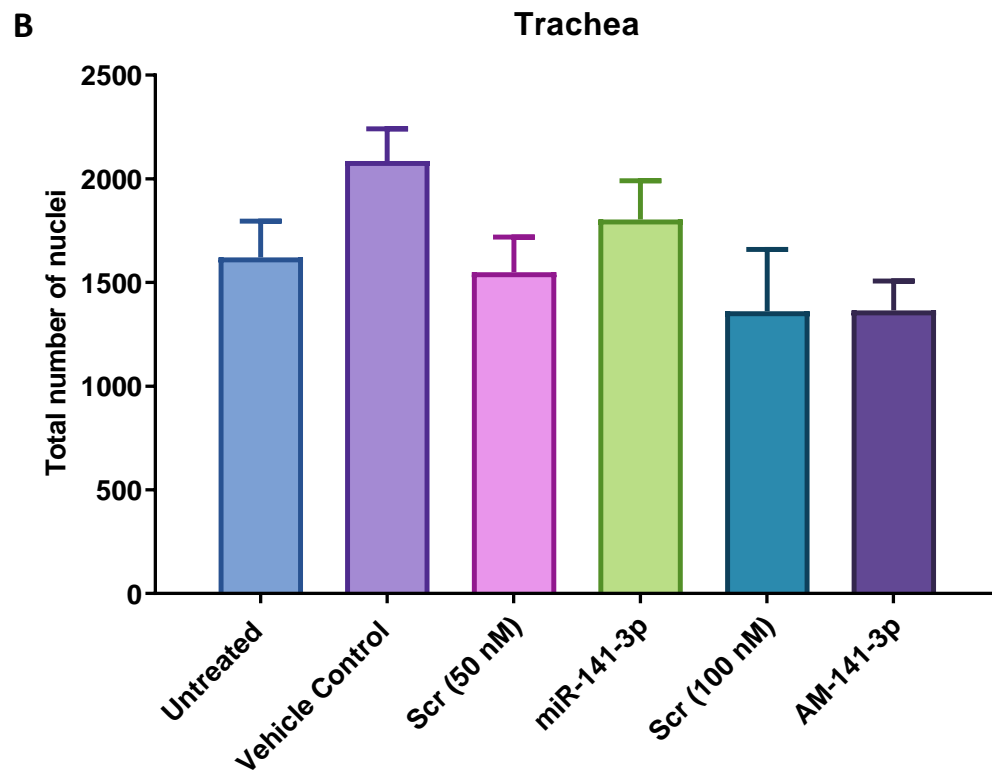
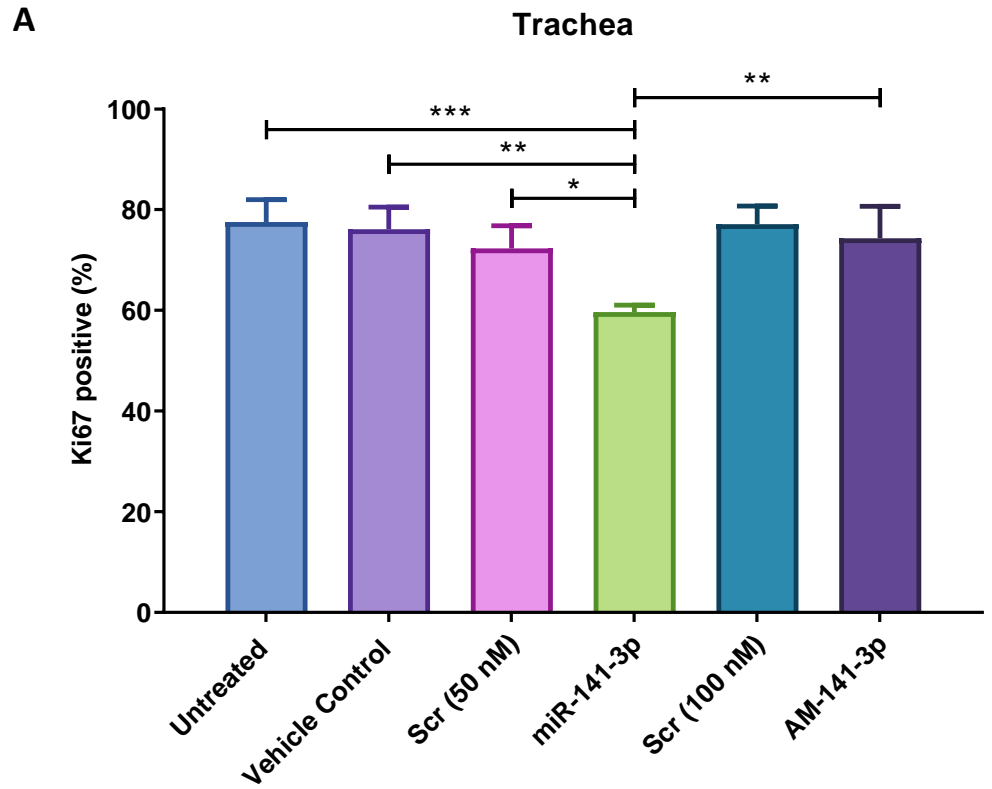
Chondrocytes were stained with DAPI (blue), FAM-miR-141-3p (green), and the nuclear stain, Ki67 antibody (Red). Ki67 staining of tracheal chondrocytes with different treatments (A-F). A) Untreated cells, B) Vehicle control, C) Scrambled control (50 nM), D) miR-141-3p mimic, E) Scrambled control (100nM) and F) miR-141-3p antagomiR. Ki67 staining of articular chondrocytes with different treatments (G-L). G) Untreated cells, H) Vehicle control, I) Scrambled control (50 nM), J) miR-141-3p mimic, K) Scrambled control (100nM) and L) miR-141-3p antagomiR. Images were taken with Nikon Eclipse Ti live cell microscope at x40 magnification. Scale bar = 100µM. Images were analysed using ImageJ.

chondrocytes transfected with miR-141-3p mimic compared to the untreated control ($p < 0.007$) (**Figure 5.3C**). The proliferation of the cells transfected with the miR-141-3p antagomiR also had significantly increased proliferation compared to untreated control ($p < 0.004$) (**Figure 5.3C**). In addition, the vehicle control in articular chondrocytes too had increased proliferation compared to untreated control ($p < 0.01$).

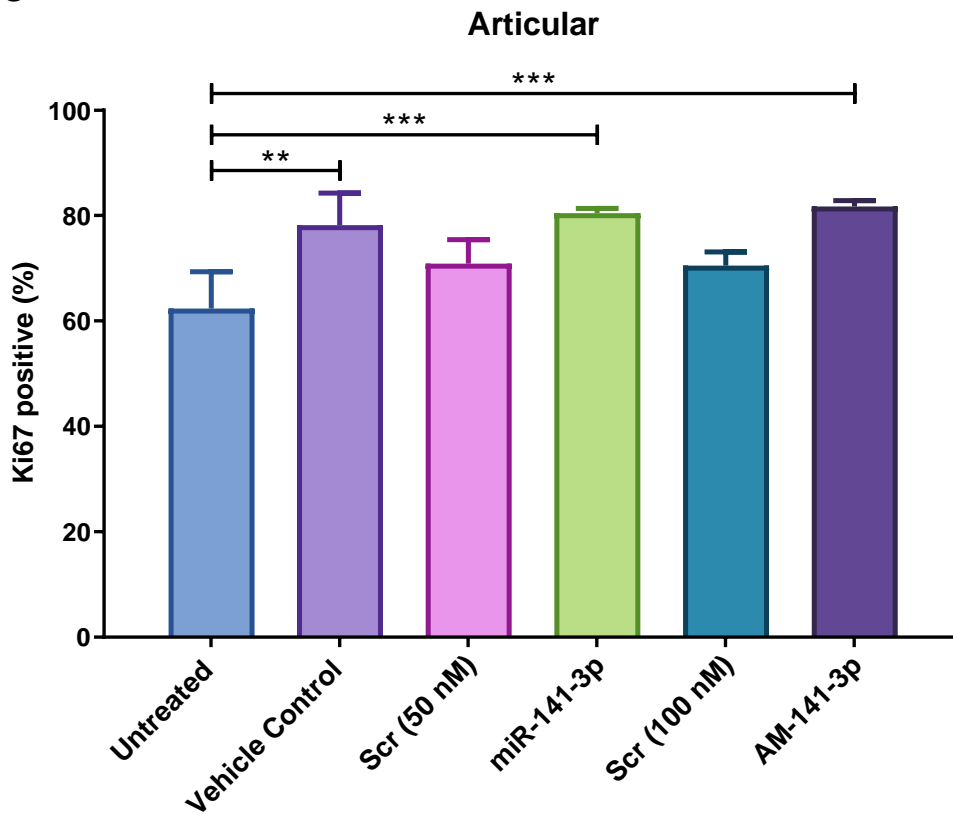
Comparison of proliferation between tracheal and articular chondrocytes following transfection with miR-141-3p showed that the proliferation of cells transfected with miR-141-3p mimic were significantly lower in tracheal chondrocytes compared to that of articular chondrocytes ($p < 0.02$) (**Figure 5.3E**). Tracheal chondrocytes transfected with miR-141-3p mimic also had significantly lower proliferation compared to articular chondrocytes transfected with miR-141-3p antagomiR ($p < 0.001$) (**Figure 5.3E**). As well as that proliferation was significantly lower in untreated articular chondrocytes compared to untreated tracheal chondrocytes ($p < 0.02$) (**Figure 5.3E**). The total number of chondrocyte nuclei between the different treatment groups in both tracheal and articular chondrocytes was not significantly

different indicating proliferation changes were not due to changes in nuclei numbers

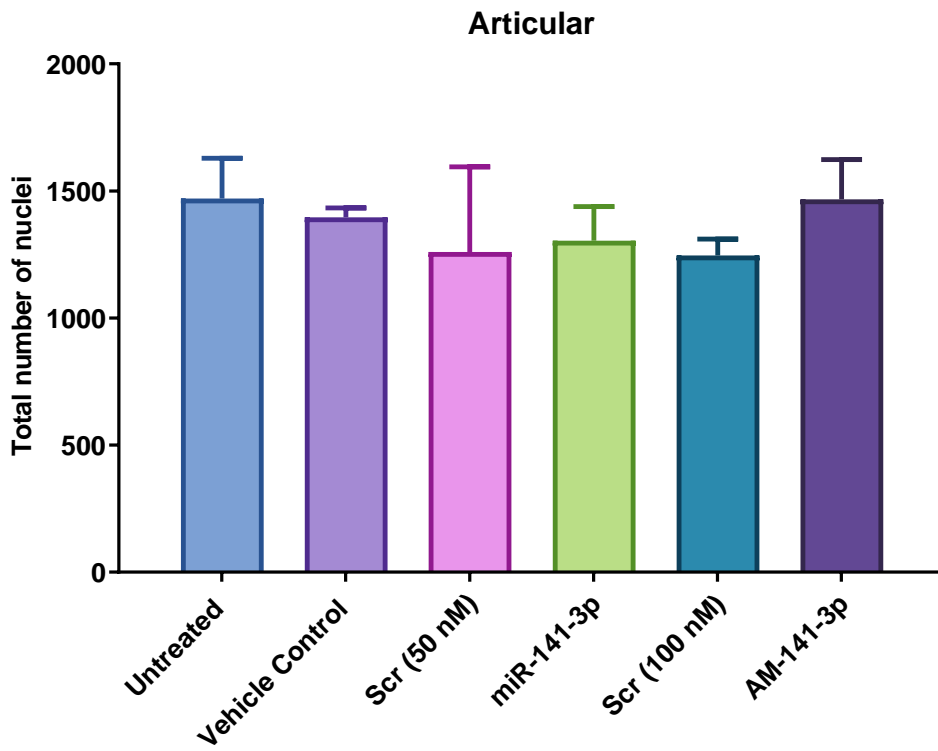
(Figure 5.3B & D).



C



D



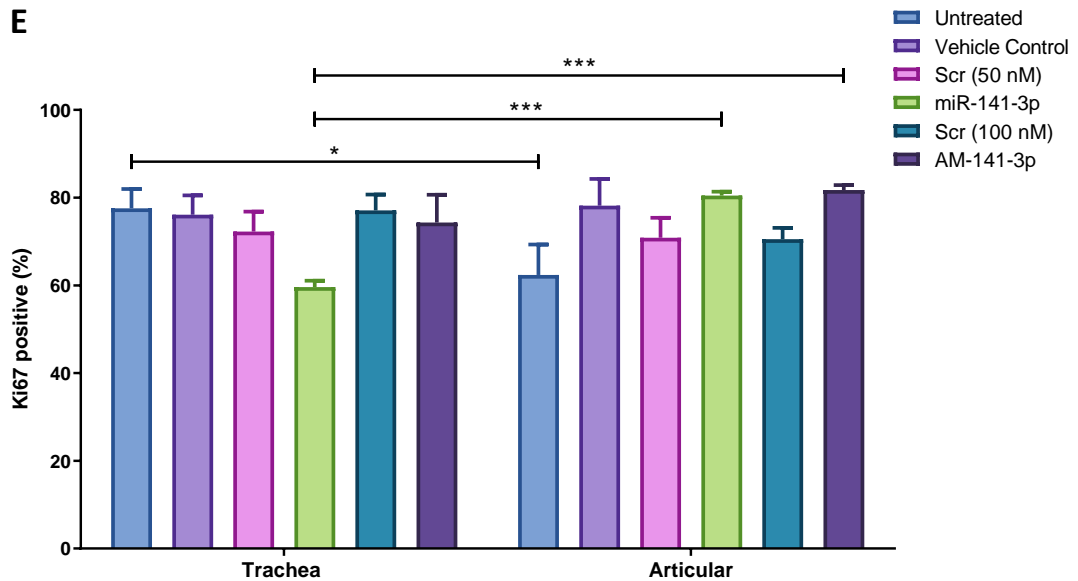


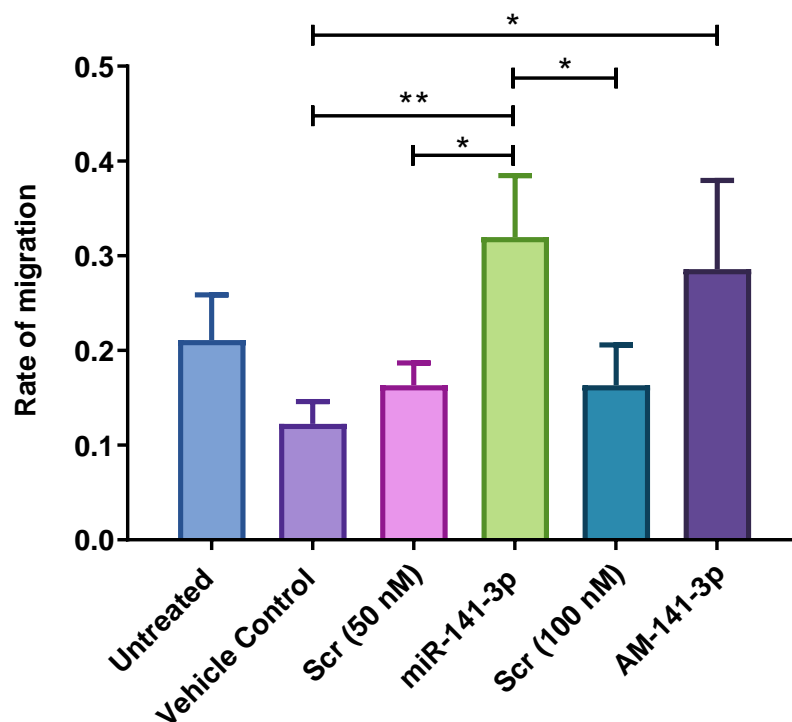
Figure 5.3: Proliferation of tracheal and articular chondrocytes assessed with Ki67 immunocytochemistry staining. Chondrocytes were stained with Ki67 antibody and the percentage of cells that were Ki67 positive were determined. A) Tracheal chondrocytes were transfected with miR-141-3p mimic and antagomiR. Untreated chondrocytes and chondrocytes transfected with lipofectamine only (vehicle control) were used as controls. Scrambled controls (Scr) at two different concentrations were used (50nM and 100nM). B) The total number of nuclei of tracheal chondrocytes for each treatment was calculated. C) Articular chondrocytes were transfected with miR-141-3p mimic and antagomiR. Untreated chondrocytes and chondrocytes transfected with lipofectamine only (vehicle control) were used as controls. Scrambled controls (Scr) at two different concentrations were used (50nM and 100nM). D) The total number of nuclei of articular chondrocytes for each treatment was calculated. E) comparison of proliferation between trachea and articular chondrocytes. Images were analysed with ImageJ. Fisher's individual test for differences of means was used to statistically analyse the data in MINITAB. n= 3 replicates, each replicate consisted of 6 images. Bars represent mean and error bars represent SEM. * denotes $p < 0.05$, ** denotes $p < 0.01$ and *** $p < 0.001$.

5.3.3 Migration of tracheal chondrocytes transfected with miR-141-3p

The migration of the tracheal chondrocytes transfected with miR-141-3p was assessed using a live migration assay over 24 hours. The images obtained were analysed using ImageJ. This revealed that tracheal chondrocytes transfected with the miR-141-3p mimic had significantly increased migration compared to vehicle and scrambled control at 50 nM and 100 nM ($p < 0.01$, $p < 0.04$ and $p < 0.04$ respectively) (Figure 5.4A). Interestingly, transfection of tracheal chondrocytes with miR-141-3p

antagomiR also caused a significant increase in migration compared to vehicle control ($p < 0.03$) (Figure 5.4A). However, although not significantly different, the migration of tracheal chondrocytes transfected with miR-141-3p mimic was higher than that of chondrocytes transfected with miR-141-3p antagomiR (Figure 5.4A). In order to elucidate the role of the ion channel Ano1 on the migration of tracheal chondrocytes, the Ano1 channel antagonist, CaCCinh-A01, was used to inhibit Ano1 and DMSO was used as a control as CaCCinh-A01 was dissolved in DMSO. This revealed that inhibition of Ano1 with channel blocker CaCCinh-A01 caused a decrease in the migration of tracheal chondrocytes compared to DMSO control, however this was not significant (Figure 5.4B).

A



B

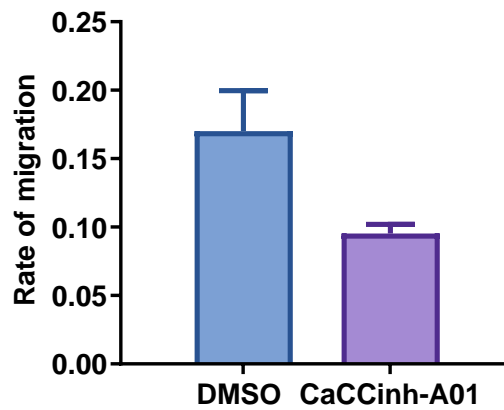


Figure 5.4: Rate of migration of tracheal chondrocytes transfected with miR-141-3p assessed with wound scratch assay. A) Rate of migration of untreated chondrocytes, chondrocytes transfected with lipofectamine only (vehicle control), chondrocytes transfected with scrambled control (Scr) used at two concentrations 50 and 100 nM and chondrocytes transfected with miR-141-3p mimic (miR-141-3p) and miR-141-3p antagomiR (AM-141-3p). B) Rate of migration of chondrocytes treated with Ano1 channel blocker, CaCCinh-A01 and DMSO as control. Data was statistically analysed with Fisher individual test for difference of mean using Minitab. Error bars represent the SEM. n=3 wells. * denotes $p < 0.05$ and ** $p < 0.01$.

5.4 Discussion

In this chapter, transfection of tracheal and articular chondrocytes with miR-141-3p was shown to lead to functional changes in chondrocytes. These are summarised in **Table 5.1**. Since many of the studies investigating the migration and RMP of chondrocytes were conducted on articular chondrocytes, the effect of miR-141-3p on migration and RMP was studied in tracheal chondrocytes only. This showed for the first time that miR-141-3p results in the depolarisation of the RMP of tracheal chondrocytes. Changes to the chondrocytes' proliferation was also observed, with tracheal chondrocytes showing a decrease in proliferation with miR-141-3p mimic and articular chondrocytes showing increased proliferation. miR-141-3p also caused an increase in tracheal chondrocyte migration, which was abrogated with Ano1

channel blocker. Cell proliferation and migration are central to tissue homeostasis in physiological and pathological conditions. Multiple factors influence the migration and proliferation of cells. Research over the past 20 years revealed that ion channels are vital in the regulation of migration and proliferation. The mechanism through which miR-141-3p mediates these changes to chondrocyte function is unknown. However, there are multiple explanations, which will be examined below.

Table 5.1: Summary of the effect of miR-141-3p mimic and antagomiR transfection on the RMP, proliferation and migration of tracheal and articular chondrocytes.

Chondrocyte function	Trachea		Articular	
	miR-141-3p mimic	miR-141-3p antagomiR	miR-141-3p mimic	miR-141-3p antagomiR
RMP	Depolarised	Depolarised	-	-
Proliferation	Decreased	No change	Increased	Increased
migration	Increased	Increased	-	-

5.4.1 Effect of miR-141-3p on RMP of tracheal chondrocytes

The RMP plays a vital role in chondrocyte homeostasis and changes in the RMP can cause changes in many biological functions (Abdul Kadir et al., 2018). The membrane potential of migrating cells indirectly affects their migration by regulating aspects such as cell volume, intracellular Ca²⁺ and pH levels. In the previous chapter, it was revealed that miR-141-3p targets and affects the expression levels of ion channel genes either directly or indirectly. miR-141-3p mimic was shown to downregulate ion channel genes and miR-141-3p antagomiR to upregulate their expression. Changes in the expression levels of ion channels can affect their function and hence the RMP, which is set and regulated by numerous ion channel families. Upon investigating the

effect of miR-141-3p transfection on the RMP, it was shown that miR-141-3p mimic and antagomiR lead to the depolarisation of the RMP of tracheal chondrocytes with miR-141-3p mimic causing a greater depolarisation than miR-141-3p antagomiR (**Figure 5.1**).

The RMP plays an important role in regulating voltage-gated Ca^{2+} channels (VGCC) (which include *Cacna1g* as a member). Depolarisation of the RMP in VGCC expressing cells causes a rise in intracellular Ca^{2+} . This coupled with Ca^{2+} -activated potassium channels can create a negative feedback loop terminating Ca^{2+} influx (Fakler and Adelman, 2008). This depolarisation of the RMP by miR-141-3p may be a factor that regulates Ca^{2+} influx, which is required for cell migration as it was shown in neutrophils that proton channels prevent the depolarisation of the membrane potential, thus sustaining the Ca^{2+} entry, which is required for the regulation of neutrophil migration (El Chemaly et al., 2010).

The modulation of the RMP could also be driving the changes to chondrocyte proliferation. It is postulated that cells' RMP determines their proliferative potential, with cells that have more hyperpolarised RMP being more quiescent (Abdul Kadir et al., 2018). Interestingly, it was shown that tracheal chondrocytes transfected with miR-141-3p mimic had decreased proliferation and those transfected with miR-141-3p antagomiR were significantly more proliferative. This may potentially be due to the depolarisation of the RMP, which is associated with higher proliferative potential (Cone Jr., 1974). Effect of miR-141-3p on chondrocyte proliferation will be discussed below.

5.4.2 Effect of miR-141-3p on tracheal and articular chondrocyte proliferation

The effect of miR-141-3p transfection on proliferation was different in tracheal and articular chondrocytes (**Table 5.1**). Transfecting tracheal chondrocytes with miR-141-3p mimic caused a significant decrease in chondrocyte proliferation compared to controls, whereas in articular chondrocytes it caused the increase in proliferation (**Figure 5.3E**). On the other hand, inhibiting miR-141-3p did not significantly change the proliferation of tracheal chondrocytes but significantly increased proliferation in articular chondrocytes (**Figure 5.3E**). These observed effects on chondrocyte proliferation were not due to changes in the total number of chondrocyte nuclei, which showed no significant difference between the different treatment groups (**Figure 5.3B & D**). It is possible that miR-141-3p modulates chondrocyte proliferation through two different mechanisms in tracheal and articular chondrocytes.

Perhaps in articular chondrocytes miR-141-3p mimic increases proliferation and antagomiR decreases proliferation but this was not observed. This could be due to miR-141-3p antagomiR in articular chondrocytes being dissociated from miR-141-3p following RNA isolation and hence not exerting its effects. One of the possible mechanisms that miR-141-3p could be operating through is the regulation of ion channel expression and hence regulation of the RMP and proliferation. Many of the mechanisms through which ion channels regulate cell proliferation are essentially related to housekeeping functions performed by ion channels such as setting the RMP, regulating volume changes, intracellular Ca²⁺ concentration and pH (Barrett-Jolley et al., 2010b). miR-141-3p was shown to target *Lrrc8a* and downregulate its

expression in the previous chapter. *Lrrc8a* is an essential subunit for the function of VRAC, which are responsible for the maintenance of volume changes in chondrocytes (Lewis et al., 2011b).

A number of studies have shown *Lrrc8a* to play a role in cell proliferation. The knockdown of *Lrrc8a* was shown to suppress cerebrovascular smooth muscle cell proliferation (Lu et al., 2019). The inhibition of *Lrrc8a* was also shown to decrease proliferation in a number of different cell types, including cervical cancer cells, fibroblasts, HeLa cells and Ehrlich Lettre ascites cells (Shen et al., 2000, Doroshenko et al., 2001, Varela et al., 2004, Klausen et al., 2010). Cell proliferation is accompanied by an increase in cell volume, which is known to be regulated by VRAC (Okumura et al., 2009). The downregulation of *Lrrc8a* is likely to lead to cell shrinkage, which impedes cell proliferation (Lang et al., 2000). Hence, the decrease in tracheal chondrocyte proliferation could be due to miR-141-3p targeting *Lrrc8a* and decreasing its expression which would lead to the dysregulation of volume changes in chondrocytes and thus the decrease in their proliferation. The inhibition of miR-141-3p in tracheal chondrocytes however did not cause a significant difference in proliferation (**Figure 5.3A**). This could be due to the number of biological replicates. Future studies would involve increasing the power of the study by increasing the biological replicates and performing knockdown of *Lrrc8a* to investigate fully the effect of miR-141-3p inhibition on tracheal chondrocytes proliferation.

Another ion channel through which miR-141-3p could be acting through is the CaCC, *Ano1*, which has been shown to regulate the proliferation of many cancerous cells. It

has been shown that Ano1 inhibition suppresses the proliferation of epithelium originated cancer cells (Guan et al., 2016) and breast cancer cells (Britschgi et al., 2013). This was also shown in interstitial cells of Cajal, where Ano1 inhibition either genetically or pharmacologically decreases cell proliferation (Stanich et al., 2011) and in oesophageal epithelial cells, where the loss of Ano1 also decreases proliferation (Vanoni et al., 2020). Hence, it is possible that the decrease in proliferation of tracheal chondrocytes could be due to the indirect miR-141-3p targeting of Ano1, which was shown in the previous chapter to decrease Ano1 expression although not significantly. To validate this, future studies would investigate the effect of miR-141-3p on protein levels of Ano1 through western blotting. Luciferase gene reporter assay would also be used to investigate whether miR-141-3p directly or indirectly targets Ano1. Other studies have shown that Ano1 downregulation can promote proliferation of different cells depending on factors that regulate its expression and function (Wang et al., 2012, Zhang et al., 2015, Wu et al., 2017). Therefore, the increase in articular chondrocyte proliferation after transfection with miR-141-3p mimic could be due to the targeting of Ano1 by miR-141-3p causing its downregulation and increase in proliferation.

In the previous chapter, miR-141-3p was also shown to downregulate the expression of *Cacna1g* (*Ca_v3.1*), which encodes the low voltage-activated T-type Ca²⁺ channels (Felix, 2005). As a result, miR-141-3p may also be acting through *Cacna1g*. As the upregulation of *Ca_v3.1* by ghrelin, a hormone involved in cell proliferation, was shown to cause the inhibition of PC-3 human prostate carcinoma cell proliferation (Díaz-Lezama et al., 2010). The upregulation of *Ca_v3.1* was also shown to inhibit

proliferation of MCF-7 human breast cancer cells (Ohkubo and Yamazaki, 2012). On the other hand knockdown of Cav3.1 suppresses the proliferation of prostate cancer cells by inhibiting AKT (Hu et al., 2018). These findings suggest that the downregulation of ion channel genes *Lrrc8a*, *Ano1* and *cacna1g* decreases cell proliferation. However, other mechanisms unrelated to ion channels could be playing a role as miR-141-3p has also been shown to modulate cell proliferation.

miR-141-3p plays a role in proliferation through modulation of the *Ihh* signalling pathway. *Gli2*, which is a primary transcriptional activator downstream of the *Ihh* pathway, is regulated by miR-141-3p, whereby miR-141-3p has a target site in the 3'-UTR region of the *Gli2* mRNA (Wang et al., 2018). The overexpression of miR-141-3p was shown to downregulate *Gli2* expression and inhibit osteosarcoma cell proliferation (Wang et al., 2018). However, in chondrocytes the downregulation of *Gli2* causes the increase in proliferation (Mau et al., 2007). It was observed from the RNA-Seq data in chapter 3, that *Gli2* expression is significantly higher in tracheal chondrocytes compared to articular chondrocytes ($p < 0.001$) (Appendix, **Table A.1**). Therefore, endogenous expression of miR-141-3p with miR-141-3p mimic could be targeting *Gli2* in articular chondrocytes and reducing its expression, hence causing the increase in proliferation of articular chondrocytes.

Interestingly, the inhibition of miR-141-3p also increased the proliferation of articular chondrocytes. The reason for this is unclear, however, it has been previously shown that inhibition of miR-141-3p increases the proliferation of colorectal cancer cells by regulating tumour necrosis factor receptor-associated factor 5 (TRAF5) (Liang et al.,

2019). Alternatively, it could be due to the fact that the inhibition of miR-141-3p causes an upregulation of ion channel genes which would result in an increase in proliferation. Future studies investigating the effect of knockdown of ion channel genes genetically and pharmacologically on chondrocyte proliferation needs to be carried out to obtain a clearer understanding of the mechanisms taking place.

5.4.3 Effect of miR-141-3p on tracheal chondrocytes migration

Cell migration is essential for cell's homeostasis in health and disease. All cells undergo migration at a given point in their life cycle including chondrocytes, which are thought to not be very motile. However, on the contrary, migration of chondrocytes is important in disease as it may be a mechanism through which the healing of cartilage can be modulated. During migration, cells undergo volume changes, with an increase in volume at the leading edge and a decrease at the trailing edge (Schwab et al., 2012b). Chondrocyte migration was investigated in tracheal chondrocytes only as articular chondrocyte migration has been previously studied (Gu et al., 2017). Following the transfection of tracheal chondrocytes with miR-141-3p mimic and antagomiR, their migration was assessed with a live wound assay, which revealed an increase in the rate of tracheal chondrocyte migration (**Figure 5.4**). One possible mechanism that this could be occurring through is the modulation of cell volume and shape with ion channels to enable cell migration (Schwab et al., 2012b).

Ion channels that were identified in the previous chapter to be regulated by miR-141-3p have been shown to play a role in cell volume and migration regulation. For

example, *Lrrc8a*, an ion channel essential for volume regulation in chondrocytes is involved in migration (Kumagai et al., 2016). VRACs regulate volume changes of cells, and their inactivation using VRAC inhibitors was shown to suppress the migration of nasopharyngeal carcinoma and glioma cells (Soroceanu et al., 1999, Mao et al., 2007). Therefore, it is possible that inhibition of miR-141-3p, which was shown in the previous chapter to increase *Lrrc8a* expression, causes changes to the cell volume, allowing chondrocytes to increase their volume and hence enabling them to be more motile and increases their migration rate. Another ion channel that was indirectly targeted by miR-141-3p in the previous chapter that could be modulating chondrocyte migration is *Ano1*.

Ano1 is not only known to be involved in the regulation of proliferation of cancerous cells as described in the previous section but also their migration. The knockdown of *Ano1* inhibits migration of lung cancer cells (Jia et al., 2015). It also significantly decreases the migration rate of pancreatic ductal adenocarcinoma cells (Sauter et al., 2015), anaplastic thyroid carcinoma cells (Kim et al., 2019) and breast carcinoma cells (Bae et al., 2017). To investigate the effect of blocking *Ano1* on the migration of chondrocytes, an *Ano1* antagonist, CaCCinh-A01 was used to pharmacologically inhibit *Ano1*. This revealed that suppression of *Ano1* decreased tracheal chondrocyte migration compared to DMSO control. This suppression of migration by *Ano1* inhibition supports the model where cell volume changes result in cell shape changes which are driven by fluxes of K^+ and Cl^- ions (Schwab et al., 2012b). Knockdown of *Ano1* was also shown to suppress the expression of *Mmp-9* and *snail1* (Bae et al., 2017). *Mmp-9* affects cell motility and is upregulated in chondrocytes by peripheral

blood derived mononuclear cell stimulation which enhances osteoarthritic human chondrocyte migration (Hopper et al., 2015). Snail1 is also known to be involved in cell migration (Cano et al., 2000).

The repression of snail1 is essential for tracheal cartilage formation. It was shown in tracheal chondrocytes to be targeted and repressed by two miRNAs, miR-125 and miR-30c. The deletion of these two miRNAs causes the upregulation of snail1, which results in poor deposition of matrix proteins and malformation of tracheal cartilage rings (Gradus et al., 2011). Interestingly miR-141-3p was also shown to also target snail1 and repress its expression (Xing et al., 2020b). Snail1 is also targeted by Cacna1g, which regulates the migration of melanoma cells through modulating snail1 expression. The Inhibition of Cacna1g with pharmacological agents and its knockdown decreases migration and represses snail1 (Maiques et al., 2018). Similar to Lrrc8a and Ano1, Cacna1g also regulates migration of cancerous cells whereby its knockdown causes the suppression of migration of prostate cancer cells (Hu et al., 2018).

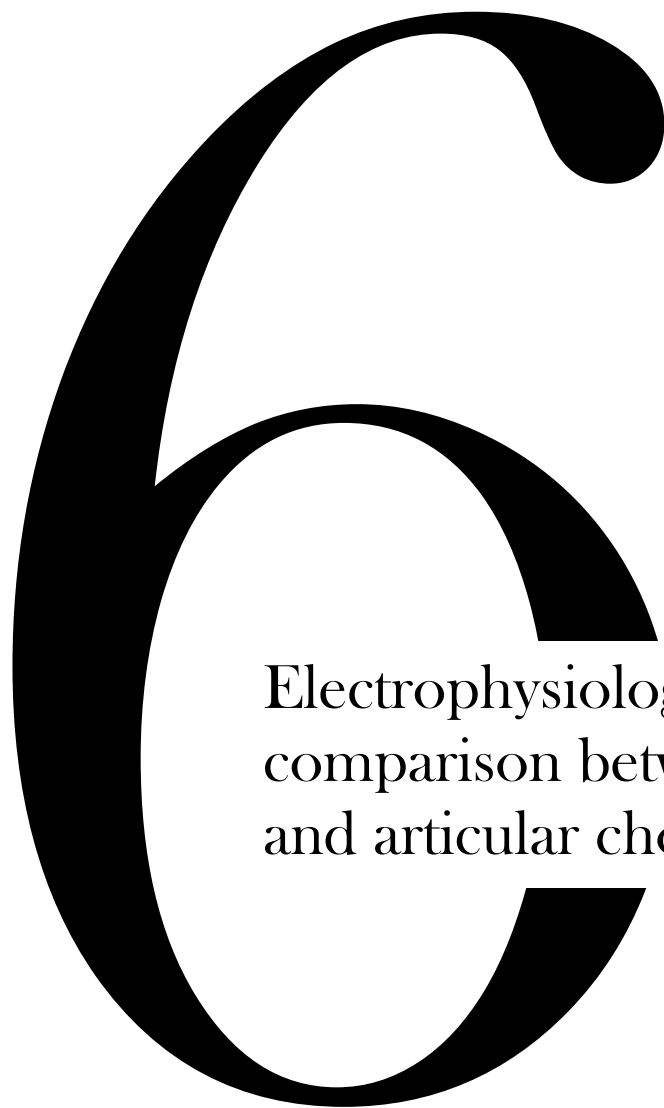
It is possible that the inhibition of miR-141-3p causes the increase in Ano1 and Cacna1g expression, as was observed in the previous chapter, which would upregulate snail1 expression and cause tracheal chondrocytes to proliferate and migrate more. This may be a mechanism to compensate for the poor matrix deposition resulting from snail1 upregulation. On the other hand, miR-141-3p mimic also increased the migration of tracheal chondrocytes (**Figure 5.4**). It is unclear why this occurs, however increasing the power of the study in the future by increasing the

biological replicates would give a clearer idea of the mechanisms taking place. It was observed from the RNA-Seq data in chapter 3 that Snail1 expression is higher in tracheal chondrocytes in comparison to articular chondrocytes (Appendix, **Table A.1**). Future studies would validate whether miR-141-3p modulates ion channel expression to regulate snail1 expression. This could be investigated by measuring the expression of snail1 post transfection with miR-141-3p mimic and antagomiR and investigating the effect of knocking down snail1 on chondrocyte migration.

A limitation of using a wound assay to assess the migration of tracheal chondrocytes is that the proliferation of these chondrocytes could have been a contributing factor to the change in migration observed. This is unlikely however as the proliferation of tracheal chondrocytes was decreased with miR-141-3p mimic transfection and unchanged with miR-141-3p antagomiR transfection (**Table 5.1**). Future studies would eliminate the contribution of proliferation by inhibiting it through serum starvation along with preincubation of the chondrocytes with Mitomycin C, which inhibits mitosis (Kang et al., 2001). It is possible that the effect of miR-141-3p on migration is also modulated through changes to the RMP.

Overall, the depolarisation of the RMP following miR-141-3p transfection may be due to changes in the expression levels of *Lrrc8a*, *Cacna1g* and *Ano1*. This modulation of the RMP could be the driving factor causing changes to proliferation and migration in chondrocytes. The depolarisation of the RMP was observed in both mimic and antagomiR, with greater depolarisation in miR-141-3p mimic transfected chondrocytes, which could be reflected by the higher migration rate in those

chondrocytes. The decreased proliferation observed in chondrocytes following miR-141-3p transfection may also potentially be due to the depolarisation of the RMP (Cone Jr., 1974). Considering the changes observed in the expression levels of ion channel genes and the RMP, the next step is to investigate the functional fingerprints of these ion channels in tracheal and articular chondrocytes and compare their electrophysiological fingerprint. This will be conducted in the next chapter.



Electrophysiological
comparison between tracheal
and articular chondrocytes

6.1 Introduction:

The ion channel fingerprint of a cell is essential for its survival. Ion channels in the past were thought to be redundant, however, the ion channel composition of a cell determines its RMP, which in turn sub-serves a large range of essential biological functions as reviewed in (Abdul Kadir et al., 2018). There are many ion channels that serve the same purpose in a cell, this is a backup mechanism in order to compensate for potential loss of certain subtypes. Relatively minor differences in the expression of ion channel genes leaves cells with distinct membrane potential properties. The modulation of the RMP is a possible new therapeutic target for a range of diseases and biological function. Changing the expression of ion channel genes changes the cell's functions, as was observed in the previous chapter where changes in the RMP of chondrocytes following the transfection with miR-141-3p and changes in their proliferation and migration was observed. In this chapter, the ion channel fingerprint of tracheal chondrocytes will be investigated under different conditions and pharmacological agents will be used to aid in the identification of the ion channels expressed. This chapter will mainly focus on tracheal chondrocytes, as articular chondrocyte electrophysiological properties are well established.

6.1.1 RMP of tracheal and articular chondrocytes

In chondrocytes, maintenance of the RMP has been demonstrated to be heavily dependent on TRP channels, with TRPV5 being a key player (Lewis et al., 2011a). Other channel subunits have also been shown to be essential contributors such as the voltage-gated $K_v1.6$ (Clark et al., 2010c) and Task-2 two-pore domain K^+ channel which confers pH sensitivity to chondrocytes (Clark et al., 2011a). Over the years, my

group has observed across different species that the RMP of chondrocytes is more positive than recorded in the literature for most other cell types. This relatively positive RMP is postulated to be due to the diverse complement of ion channels expressed by chondrocytes (Asmar et al., 2016, Barrett-Jolley et al., 2010b) that contribute to the RMP and aid in the regulation of volume changes as an adaptation to the extreme osmotic challenges these cells routinely face (Lewis et al., 2011b). My lab have shown that at negative potentials, chondrocytes exposed to higher osmotic solutions are unable to decrease their volume i.e. cell shrinkage was slower or non-existent (Lewis et al., 2011a). This supports the proposed hypothesis of why chondrocytes have a more depolarised RMP. In addition to the complement of ion channels, the extracellular environment of a cell also regulates its RMP.

6.1.2 pH in tracheal and articular chondrocytes environment

The environment that chondrocytes reside in is very different to that of most mammalian cells. It can control chondrocyte metabolism and affect their function and ability to synthesise ECM components. The avascular nature of cartilage leads to chondrocytes being as far as 3mm from the nearest blood supply. This can cause the oxygen and substrate levels to decrease to almost zero (Otte, 1991). Chondrocytes are very resilient cells that are well adapted to their environment. They are metabolically active cells and although there is a limited supply of oxygen and nutrients, chondrocytes anaerobically respire and generate ATP by substrate level phosphorylation. This results in the accumulation of lactic acid which leads to lower pH levels as lactate can only be dissipated by diffusion through the ECM (Browning and Wilkins, 2004).

In addition, the fixed negative charge caused by the high density of proteoglycans in cartilage results in an increased H^+ concentration and also attracts cation movement into the ECM which then attracts the movement of osmotically obliged water (Mobasher et al., 1998). In articular cartilage, additionally, compression of the cartilage during loading leads to the expression of water and a transient increase in the concentration of fixed negative charge, which in turn leads to further reduction of the pH of cartilage (Gray et al., 1988, Grodzinsky, 1983, Wilkins and Hall, 1995, Lee and Urban, 1997). The reported pH levels for chondrocytes are between 6.9 – 7.2 and are lower than the typical value of pH 7.4 for other cell types (Wilkins and Hall, 1995). Many ion channels are regulated by intracellular and extracellular pH and therefore, changes to the pH environment can affect their gating, which in turn would affect the RMP of cells and hence their function. Therefore, this chapter will also investigate the effect of acidic pH levels on the RMP of chondrocytes.

6.1.3 Aims

Previous chapters have shown that transfecting chondrocytes with miR-141-3p causes changes to the expression of ion channel genes which leads to changes in the RMP of chondrocytes and results in altered proliferation and migration. Since ion channels have been shown to be targeted by miR-141-3p, this chapter will investigate the functional ion channel fingerprint of tracheal chondrocytes using cell attached patch clamp electrophysiology. To validate the ion channels detected, pharmacological agents will be used. In addition, the impact of changing the cellular environment on chondrocytes will also be investigated.

6.2 Methods

6.2.1 *Single-channel cell-attached patch clamp recordings*

Single-channel electrophysiological recordings were performed by cell-attached patch clamp as previously described in chapter 2.5.

6.2.2 *RMP recordings under normal and acidic pH conditions*

The RMP was measured using whole-cell patch clamp in current clamp mode as described in Chapter 5.2.1. For RMP measurements under normal pH conditions, a standard physiological saline was used for both intracellular and extracellular solutions (**Table 2.5**). For recordings under low pH conditions, a standard physiological saline was also used for intracellular and extracellular solutions, however the HEPES buffer was replaced with 10 mM MES buffer (**Table 2.5**), and the pH was set at 6.5 with HCl for both solutions. Membrane potential (V_m) was calculated by subtracting the holding potential from the measured RMP.

6.2.3 *Pharmacological agents*

The selective VRAC blocker, 4-[(2-Butyl-6,7-dichloro-2-cyclopentyl-2,3-dihydro-1-oxo-1H-inden-5-yl)oxy]butanoic acid (DCPIB) was sourced from Tocris, UK. It was dissolved in DMSO and diluted to a final working concentration of 40 μ M, with DMSO being no more than 0.01% which had no observable effects alone. Tracheal chondrocytes were perfused with 40 μ M DCPIB and current was measured as previously reported.

6.2.4 Statistical Analysis

Electrophysiology graphs were created in GraphPad Prism 8 and statistically analysed for difference with a t-test and for similarity with an equivalence and noninferiority test using the EQUIVNONINF package (Wellek and Ziegler, 2017) in R 4.0.3 (R, 2020). To group ion channels with similar electrophysiological properties, the V_{Rev} and slope conductance of the channels were plotted against each other. These ion channel properties were clustered with *K*-means clustering performed with python 3.9.0 (Van Rossum and Drake Jr, 1995).

6.3 Results

6.3.1 Comparison of the RMP between tracheal and articular chondrocytes

As the RMP of tracheal chondrocytes was shown to be affected by the transfection of miR-141-3p in the previous chapter, one of the first parameters to investigate and compare between tracheal and articular chondrocytes was the RMP under normal physiological conditions. Whole-cell measurements of the RMP revealed a RMP of -8.1 ± 6.9 mV ($n=18$) in tracheal chondrocytes and -10.6 ± 6.9 mV ($n=13$) in articular chondrocytes (**Figure 6.1**). Comparison of these RMPs showed no significant difference with an unpaired t-test. An equivalence and noninferiority test (Wellek and Ziegler, 2017) also failed to reject a null hypothesis that they were different. These RMPs as previously observed by my group were more depolarised than reported for other cell types (Barrett-Jolley et al., 2010b, Lewis et al., 2011a, Maleckar et al., 2018).

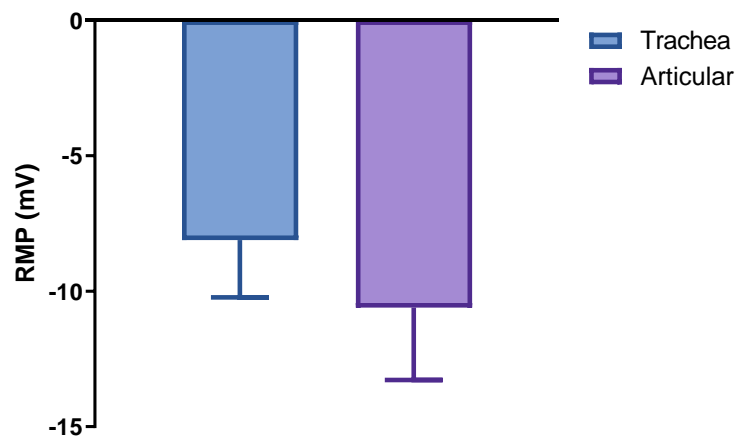


Figure 6.1: Comparison of the RMP between tracheal and articular chondrocytes under normal physiological conditions. RMP values were recorded using whole cell patch clamp electrophysiology. Bars represent mean of n=18 tracheal chondrocytes and n=13 articular chondrocytes. Error bars represent SEM. Unpaired t-test conducted with GraphPad Prism 8 did not show significant difference and equivalence and noninferiority test conducted with R showed no significant similarity.

6.3.2 Ion channels functionally expressed in tracheal chondrocytes

In order to investigate the functional ion channel fingerprints of tracheal chondrocytes, cell attached patch-clamp electrophysiology was used. Pharmacological agents were used to confirm functional ion channel families. A variety of different ion channels with different electrophysiological properties were recorded. For example, analysing these recordings revealed a slow gated ion channel that was commonly observed in the tracheal chondrocyte traces (**Figure 6.2**). Holding the cell at different voltages shows that the ion channel's current increases as the voltage increases (**Figure 6.2A**). In addition, all points amplitude histograms for each trace along with calculated open probabilities of the channel indicate that the channel is more active at more positive voltages (**Figure 6.2B-E**). A representative IV curve shows that the channel had a V_{Rev} of -25.5 ± 2.8 mV and a slope conductance of 203 ± 12 pS (**Figure 6.2F**). These properties indicate that it could be a chloride channel.

However, pharmacological agents are needed to further validate the ion channel identity.

As there was a wide variety of ion channels recorded from the tracheal chondrocytes with a range of V_{Rev} and slope conductance, a non-biased approach was used in order to classify these channels to gain a better understanding of their identity. The V_{Rev} was plotted against the slope conductance and the channels were clustered with *k*-means clustering (**Figure 6.3**). Under physiological conditions, 28 ion channels were grouped into 10 clusters (**Figure 6.3A**). The equilibrium potentials for Na^+ , Ca^{2+} , Cl^- , and K^+ were calculated based on their concentrations in the physiological recording solutions (**Table 2.5**). The V_{Rev} from the IV curves reflects the equilibrium potential and aids in the identification of the type of ion channel being shown. This enabled the classification of the clusters into sodium channels, non-specific cations, chloride channels and potassium channels based on their V_{Rev} (**Figure 6.3A**). Using the *k*-means clustering enabled the identification of a non-specific cation-like channel that was slow-gated (**Figure 6.4A**). All amplitude histograms and open probabilities indicated that the channel was mostly in the closed state (**Figure 6.4B-E**) and the IV curve indicated that the channel had a V_{Rev} of 8.8 ± 6.9 mV and a slope conductance of 33.5 ± 2.6 pS (**Figure 6.4F**), indicative of a non-specific cation.

A fast-gated sodium-like channel (**Figure 6.5A**) was also identified; where the channel is activated and its 'gates' are open for shorter periods of time and close very quickly. All points amplitude histograms indicated that at low voltages, the channel is predominantly in the closed state and at high voltages it is predominantly in the open

state (**Figure 6.5B & C**). IV curve showed a conductance of 22.7 ± 1.1 pS and a V_{Rev} of 18.6 ± 4.8 mV (**Figure 6.5D**), indicating that it may be a sodium channel. As well as that a fast-gated potassium-like channel was also observed from the tracheal chondrocyte recordings (**Figure 6.6A**). All points amplitude histogram and open probabilities also revealed that at high voltages it is predominantly in the open state and is in the closed state at low voltages (**Figure 6.6B & C**). IV curve showed a conductance of 115 ± 0 pS and a V_{Rev} of -64.7 ± 0 mV (**Figure 6.6D**) which are properties of a potassium channel according to the concentrations used in our physiological recording solutions.

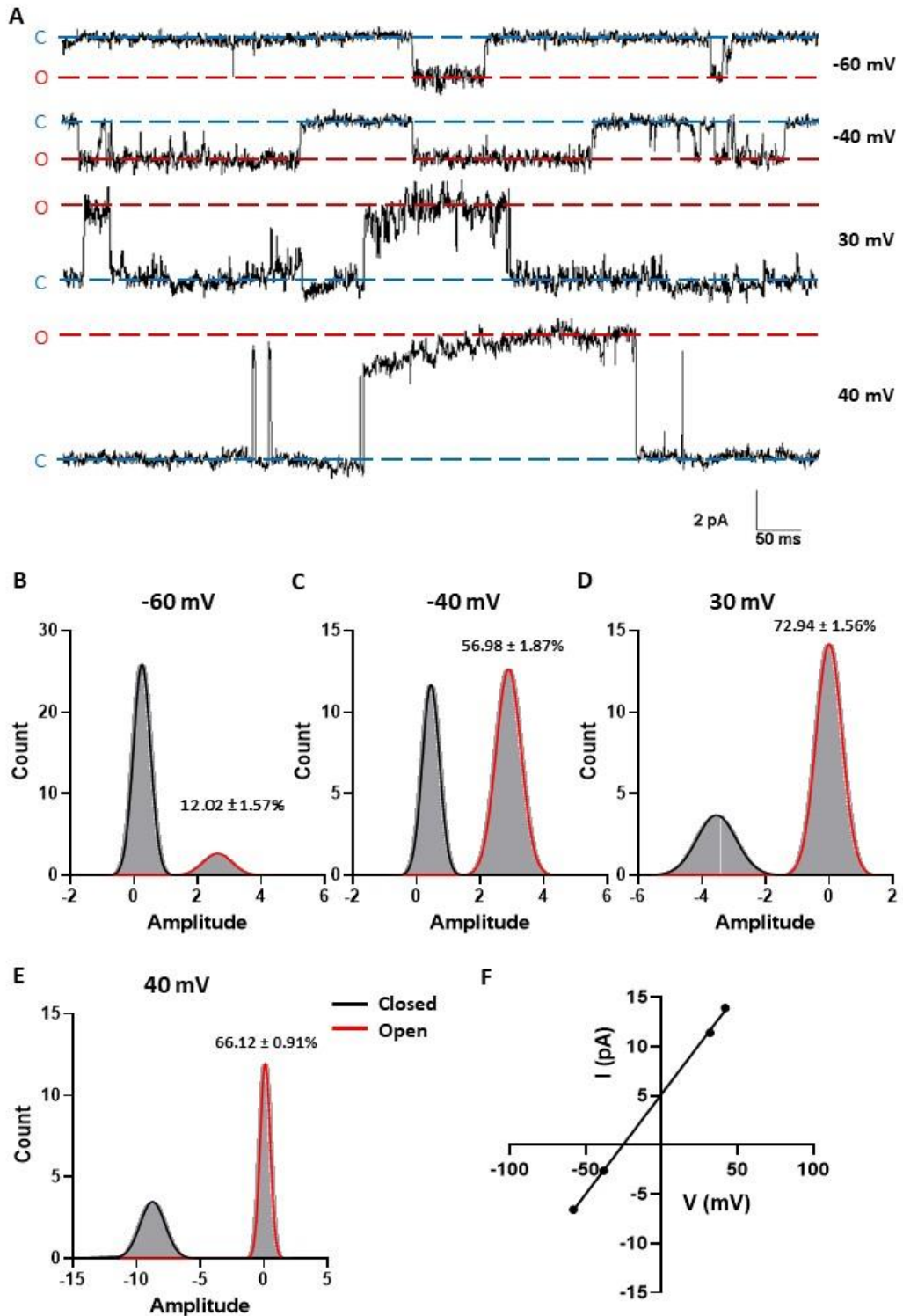


Figure 6.2: Representative single channel activity of a chloride-like ion channel in cell-attached patch-clamp mode. A) Representative raw single channel recordings at different holding potentials. B-E) All points amplitude histograms for ion channel recordings at different holding potentials. Open probabilities (P_o) shown for each histogram. D) Representative current-voltage (IV) curve for chloride-like single-channel. IV curve shows a slope conductance of 203 ± 12 pS and reversal potential of -25.5 ± 2.8 mV. Indicative of a chloride channel. O and red dashed line represents open state; C and blue dashed line represents closed state.

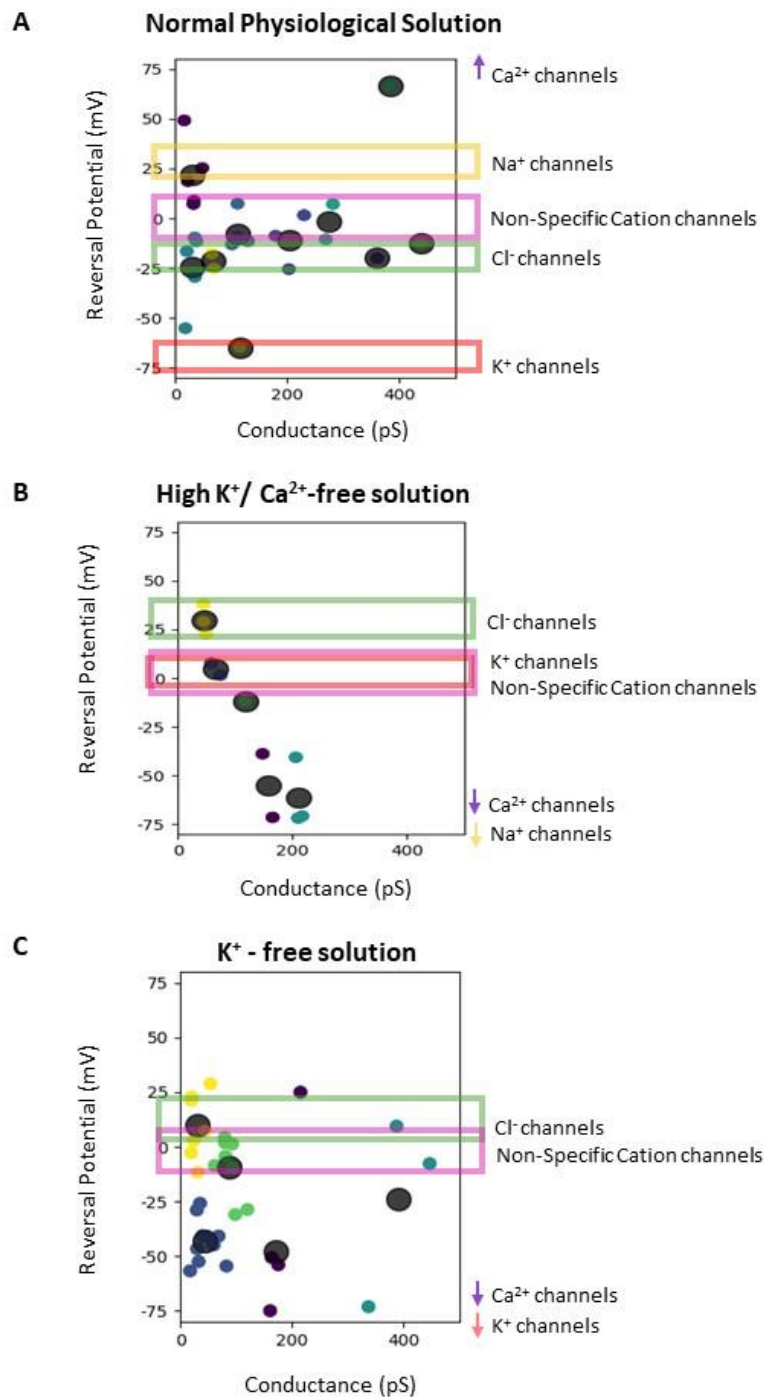


Figure 6.3: K-means clustering of single channels measured using different recording solutions. A) Channels recorded with normal physiological solution. B) Channels recorded with High K⁺/ Ca²⁺-free solution. C) Channels recorded with K⁺-free Solution. Predicted channel equilibrium potentials are indicated with different coloured bands. Yellow: sodium channels ; Green: chloride channels; Magenta: non-specific cations; Purple: calcium channels; Red: potassium channels.

To further confirm the type of channels being expressed in tracheal chondrocytes, recording solutions with different ion compositions were used (**Table 2.5**) and ion channel expression was recorded. This would cause a shift in the ions' equilibrium potential and hence a shift in the V_{Rev} . Using a high K^+ / Ca^{2+} -free solution caused a shift in the ion channels' V_{Rev} whereby potassium and chloride ions V_{Rev} shifted up and sodium ions V_{Rev} shifted down (**Figure 6.3B**). Using this solution, 11 channels were identified, which were clustered into 5 groups (**Figure 6.3B**). A K^+ - free solution was also used and this caused a shift in the sodium and chloride ions V_{Rev} as well as that it eliminated the potassium ions V_{Rev} from the range (**Figure 6.3C**). Using the K^+ - free solution, 33 ion channels were identified and clustered into 5 groups (**Figure 6.3C**).

6.3.3 Expression of VRAC in tracheal chondrocytes

As *Lrrc8a* was previously shown to be differentially expressed between the two chondrocyte types in chapter 3, targeted by miR-141-3p in chapter 4 and potentially drive changes in the function of chondrocytes as observed in chapter 5, determining its functional expression in tracheal chondrocytes was important. A commonly observed channel in the tracheal chondrocyte recordings was a fast-gated channel that was active at around -100 mV holding potential (**Figure 6.7A**). This channel had high open probabilities at these low holding potentials as observed from the all-points amplitude histograms (**Figure 6.7C & D**) and had a slope conductance of 49 ± 34.3 pS ($n=7$) and a V_{Rev} of -54.9 ± 5.7 mV ($n=7$) (**Figure 6.7E**). These findings were similar to those observed in the literature and implicate this channel as a strong VRAC candidate. However, to fully validate this channel's identity, DCPIB, a selective VRAC

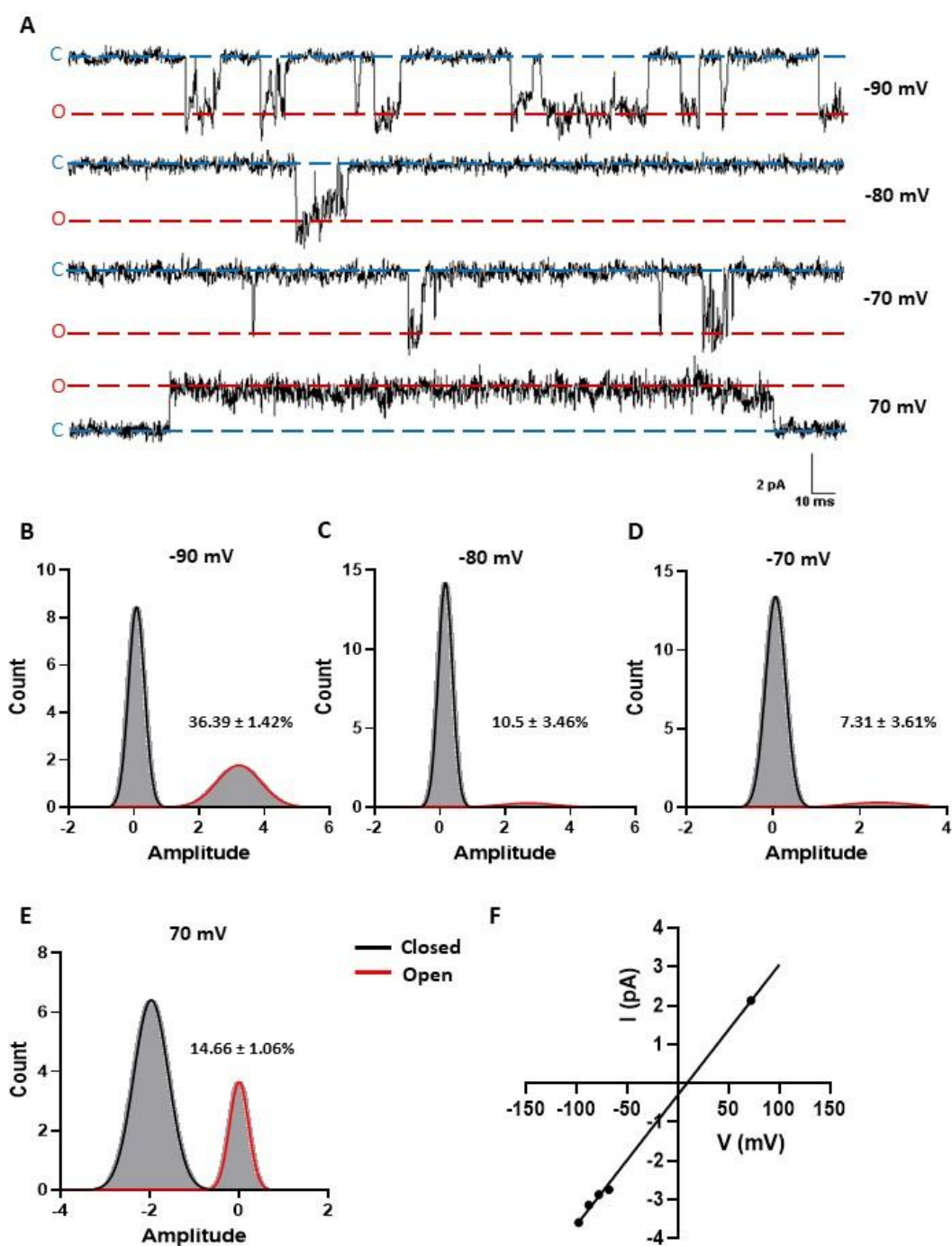


Figure 6.4: Representative Single channel activity of a non-specific cation-like ion channel in cell-attached patch-clamp mode. A) Representative raw single channel recordings at different holding potentials. B-E) All points amplitude histograms for ion channel recordings at different holding potentials. Open probabilities (P_o) shown for each histogram. D) Representative current-voltage (IV) curve for non-specific cation-like single-channel. IV curve shows a slope conductance of 33.5 ± 2.6 pS and reversal potential of 8.8 ± 6.9 mV. Indicative of a non-specific cation channel. O and red dashed line represents open state; C and blue dashed line represents closed state.

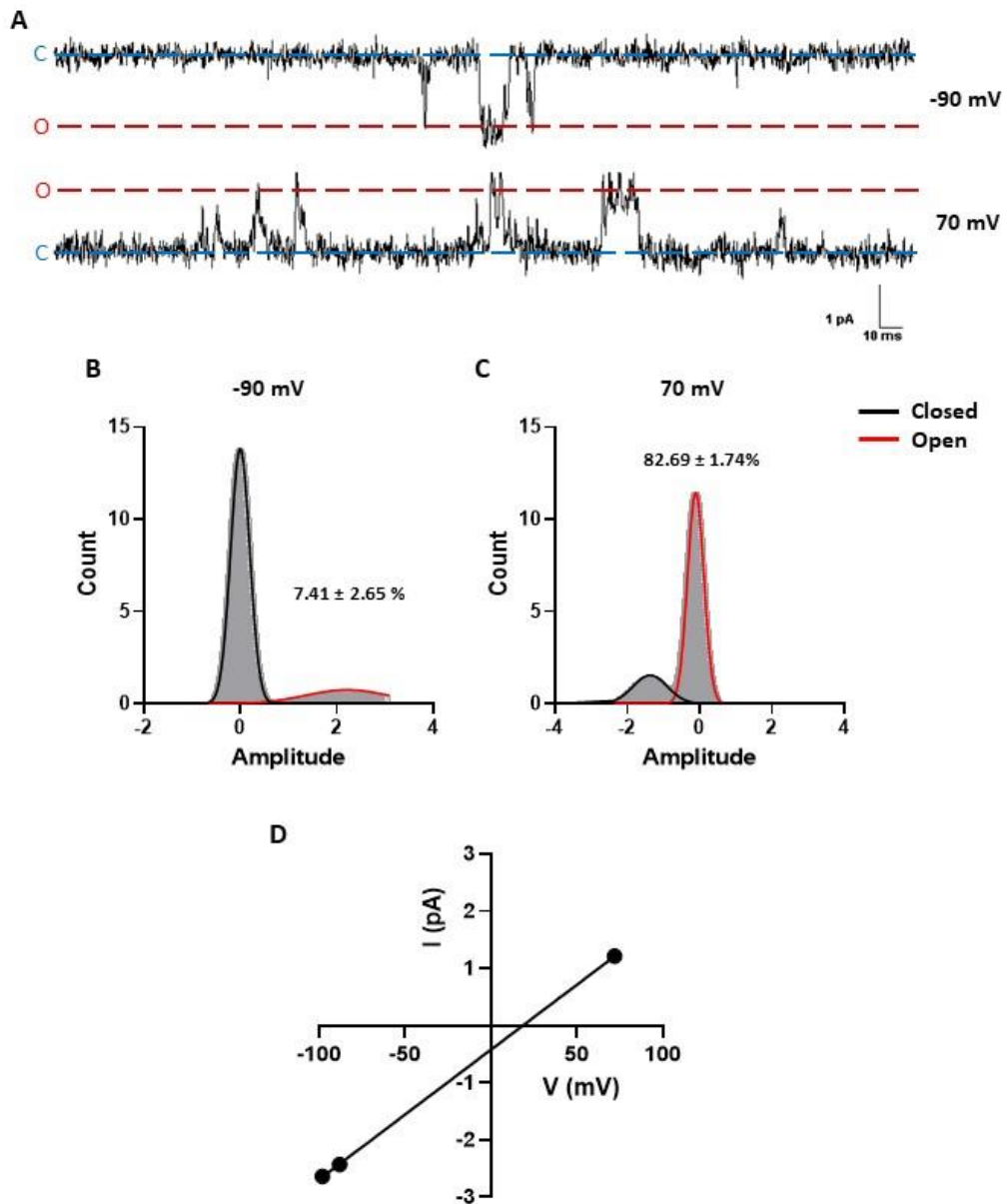


Figure 6.5: Representative Single channel activity of a sodium-like ion channel in cell-attached patch-clamp mode. A) Representative raw single channel recordings at different holding potentials. B-E) All points amplitude histograms for ion channel recordings at different holding potentials. Open probabilities (P_o) shown for each histogram. D) Representative current-voltage (IV) curve for sodium-like single-channel. IV curve shows a slope conductance of 22.7 ± 1.1 pS and reversal potential of 18.6 ± 4.8 mV. Indicative of a sodium channel. O and red dashed line represents open state; C and blue dashed line represents closed state.

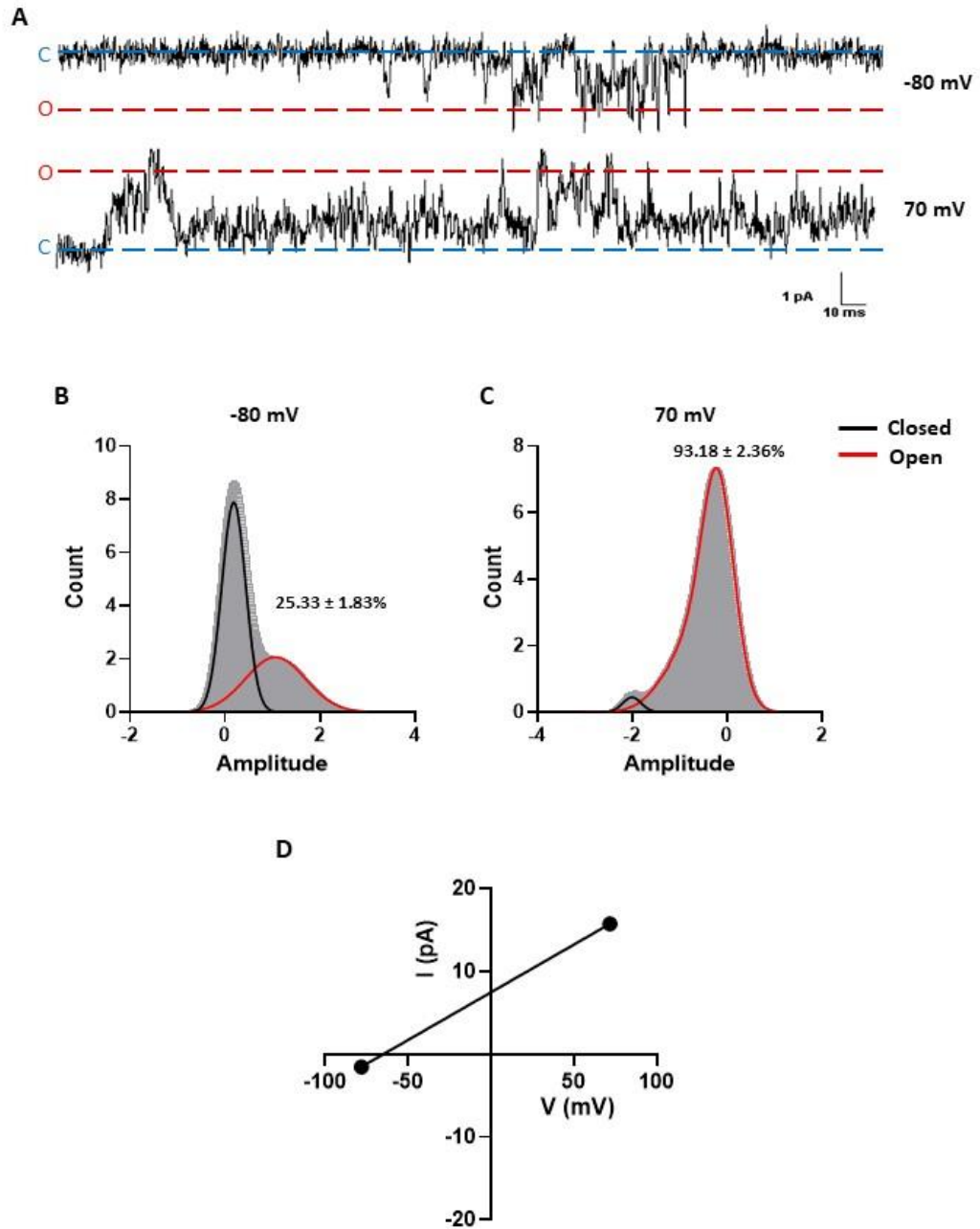


Figure 6.6: Representative Single channel activity of a potassium-like ion channel in cell-attached patch-clamp mode. A) Representative raw single channel recordings at different holding potentials. B-E) All points amplitude histograms for ion channel recordings at different holding potentials. Open probabilities (P_o) shown for each histogram. D) Representative current-voltage (IV) curve for potassium-like single-channel. IV curve shows a slope conductance of 115 ± 0 pS and reversal potential of $-64.7 \pm$ mV. Indicative of a potassium channel. O and red dashed line represents open state; C and blue dashed line represents closed state.

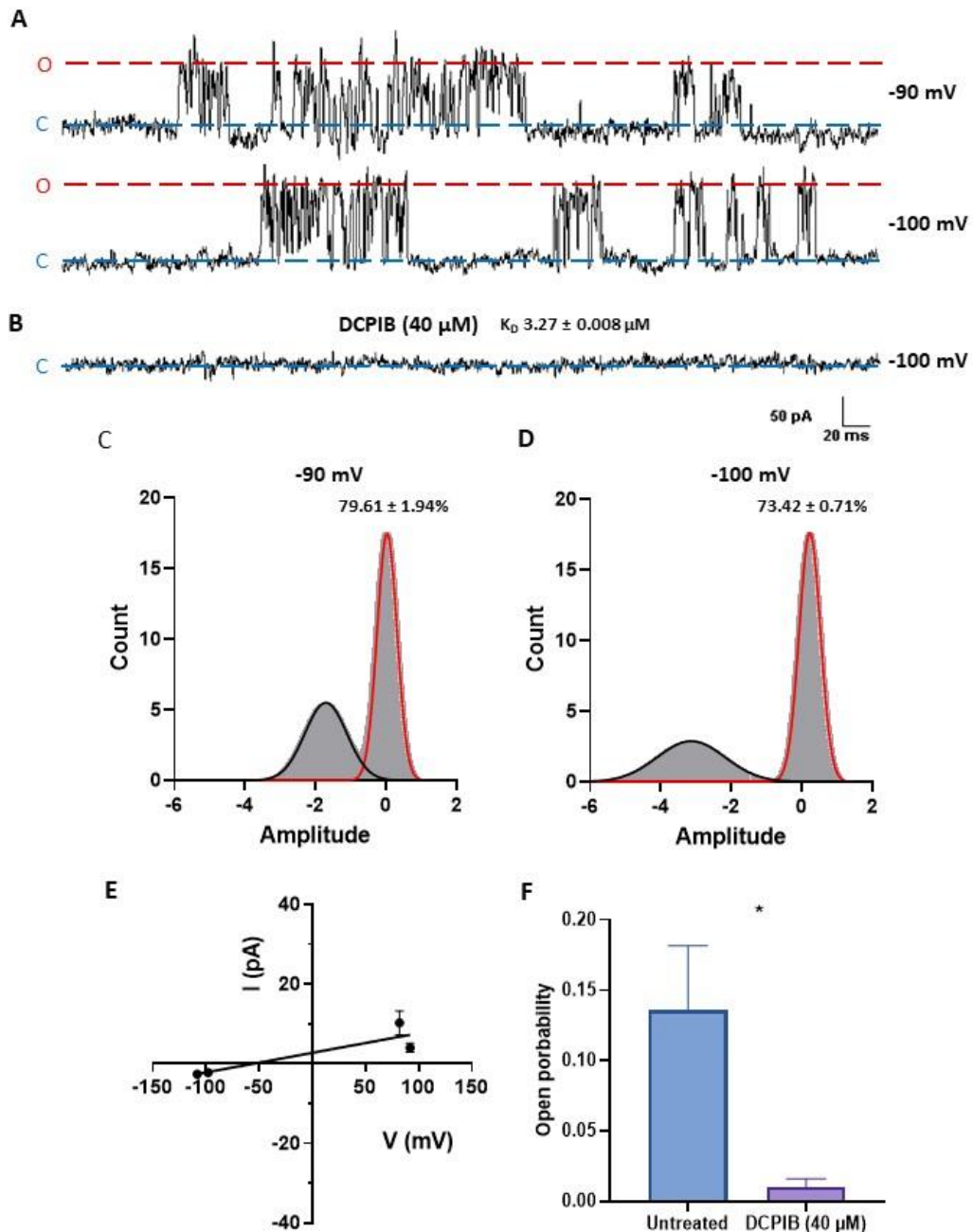


Figure 6.7: Representative Single channel activity of VRAC channel in cell-attached patch-clamp mode. A) Representative raw single channel recordings at different holding potentials. B) Representative single-channel trace following addition of VRAC blocker, DCPIB (40 μ M). Equilibrium dissociation constant (K_D) was calculated to be $3.27 \pm 0.008 \mu$ M ($n=3$). C-D) All points amplitude histograms for ion channel recordings at different holding potentials. Open probabilities (P_o) shown for each histogram. E) Current-voltage (IV) curve for VRAC single-channel. IV curve showed a mean slope conductance of 49 ± 34.8 pS and reversal potential of -54.9 ± 5.7 mV ($n=7$). F) open probability of channels following VRAC inhibition with DCPIB. Bar indicates mean open probability. Error bars represent SEM. T-test was used to statistically analyse data in GraphPad Prism 8. * denotes $p < 0.05$. O and red dashed line represents open state; C and blue dashed line represents closed state.

antagonist was used. At 40 μM , DCPIB abolished the channels current at a holding potential of -100 mV (**Figure 6.7B**) and significantly decreased the channel's open probability ($p < 0.05$) (**Figure 6.7F**). DCPIB had a dissociation constant (K_D) of $3.27 \pm 0.008 \mu\text{M}$, indicating that DCPIB potently blocks VRAC currents in tracheal chondrocytes.

6.3.4 The effect of pH on the RMP in both tracheal and articular chondrocytes.

Upon investigating the ion channels that were identified to be functionally expressed in tracheal chondrocytes, it was revealed from the literature that many of these ion channels are regulated by pH. It was also observed from the RNA-seq data from chapter 3 that most of the highly differentially expressed ion channels in tracheal chondrocytes compared to articular chondrocytes are also regulated by pH (**Table 6.1**). Some of these channels such as Nicotinic Acetylcholine Receptors and Aquaporins are not predicted to be functionally present in the recordings from tracheal chondrocytes as ligands were not used that would enable their activation and in the case of aquaporins, they conduct water through their pore and hence would not be identified under the electrophysiological recording conditions used in this chapter.

As pH is important in maintaining the homeostasis of chondrocytes and essential for functions such as volume control, migration and proliferation, the effect of changing the extracellular pH on the RMP of tracheal and articular chondrocytes was investigated. Chondrocytes' RMPs were recorded using whole-cell patch clamp and

an extracellular solution with physiological pH 7.4 or low pH 6.5 was perfused onto the cells. This showed that both tracheal and articular chondrocytes had a biphasic response to the pH change (**Figure 6.8A**). The addition of the acidic pH extracellular solution caused a significant depolarisation of the RMP from -8.1 ± 6.9 mV ($n=18$) at pH 7.4 to 5.9 ± 6.8 mV ($n=11$) at pH 6.5 ($p < 0.001$) in tracheal chondrocytes (**Figure 6.8B**) and from -10.6 ± 6.9 mV ($n=13$) at pH 7.4 to 5.1 ± 6.8 mV ($n=10$) at pH 6.5 ($p < 0.0001$) in articular chondrocytes (**Figure 6.8C**). The RMP hyperpolarised back to physiological levels with the perfusion of physiological pH 7.4 extracellular solution (**Figure 6.8A**).

Table 6.1: pH-sensitive ion channels significantly differentially expressed in tracheal chondrocytes in comparison to articular chondrocytes. Subtypes with – would not be identified to be functionally expressed under the recording conditions used.

Gene	Ion channel Family	Prediction of functional expression
Asic2	Acid Sensing Ion channels	+
Scnn1b	Epithelial Sodium Channels	+
Chrna1	Nicotinic Acetylcholine Receptors	-
Chrnb4	Nicotinic Acetylcholine Receptors	-
P2rx2	P2X Receptors	+
Catsper4	Catsper ion channels	+
Kcnk1	Two-pore potassium channels	+
Kcnk16	Two-pore potassium channels	+
Kcnh8	Voltage-activated potassium channels	+
Trpc4	Transient Potential Channels	+
Trpc5	Transient Potential Channels	+
Pkd2l1	Transient Potential Channels	+
Cacna1g	Voltage-gated Calcium channels	+
Scn2a	Voltage-gated Sodium channels	+
Aqp5	Aquaporins	-
Aqp7	Aquaporins	-
Clcn3	ClC family	+
Clcnka	ClC family	+
Panx1	Pannexins	+

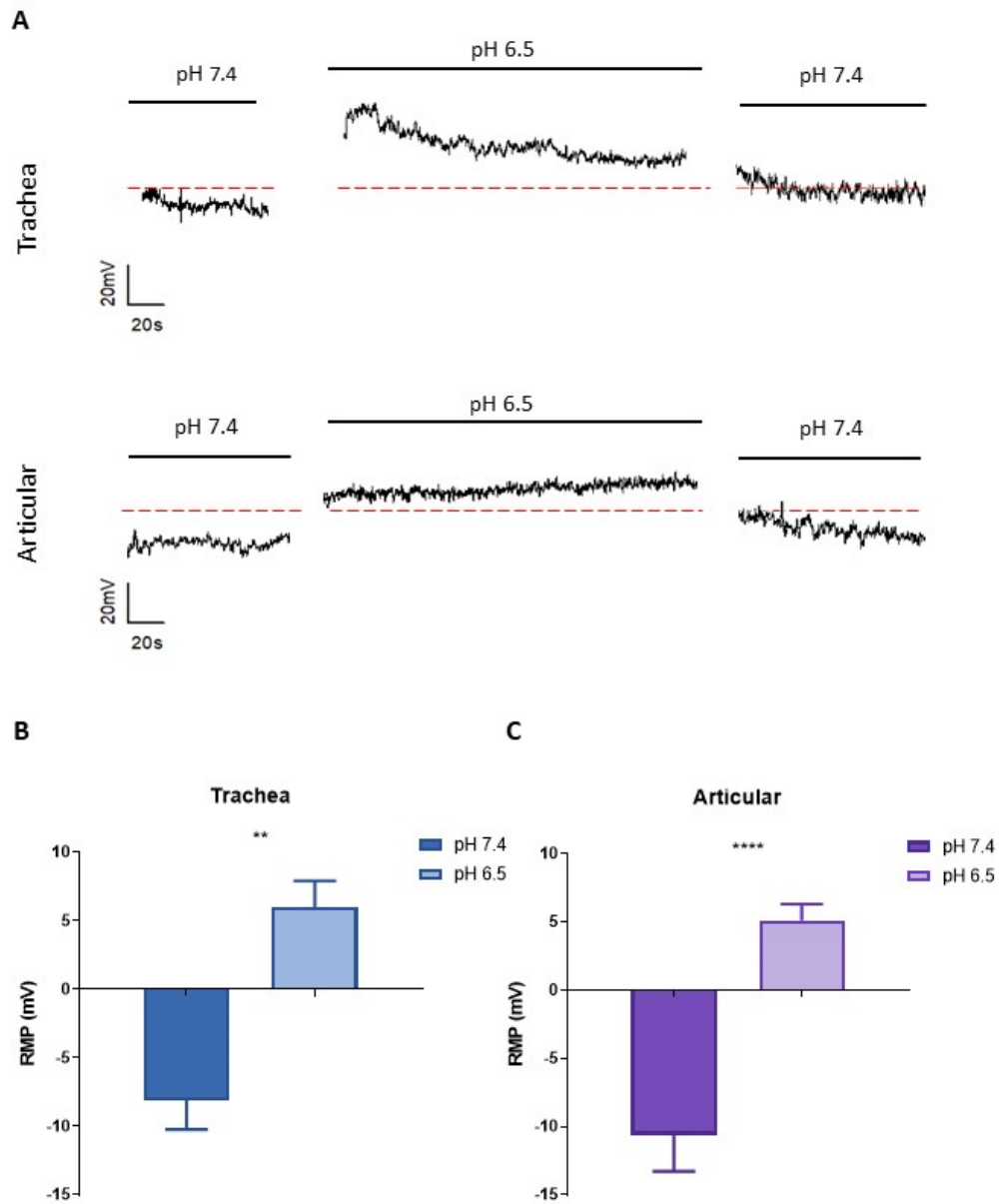


Figure 6.8: The effect of low pH on RMP of tracheal and articular chondrocytes.

A) Representative raw trace recording of the RMP of tracheal chondrocytes under low pH (6.5) and physiological pH (7.4) for tracheal and articular chondrocytes. Summary of chondrocyte RMP at low and physiological pH in B) tracheal chondrocytes and C) articular chondrocytes. Bars represent mean of n=18 pH 7.4 and n=11 pH 6.5 for tracheal chondrocytes and n=13 pH 7.4 and n=10 pH 6.5 for articular chondrocytes. Error bars represent SEM. Unpaired t-test was used to statistically analyse the data using GraphPad Prism 8. ** denotes $p < 0.001$ and **** denotes $p < 0.0001$. Dashed red line indicates 0 mV.

6.4 Discussion

In this chapter, tracheal chondrocytes were shown to express a diverse complement of ion channels comparable to the articular chondrocytes 'channelome' (Barrett-Jolley et al., 2010b, Mobasheri et al., 2019). Together these ion channels set the tracheal chondrocyte RMP, which was found to be similar to that of articular chondrocytes and not significantly different. Using different extracellular solution, numerous functional ion channel families were identified in tracheal chondrocytes that were further identified using pharmacological agents, which inhibited channel currents when applied. Many of the ion channels identified from the RNA-Seq data and functionally expressed in tracheal chondrocytes were pH sensitive (Holzer, 2009). Changing the extracellular pH caused a shift in the RMP to a more depolarised potential which was biphasic and hyperpolarised back to normal levels with physiological pH extracellular solutions. The implications of pH changes on ion channels and the physiological importance in tracheal chondrocytes will be discussed below.

6.4.1 RMP of tracheal and articular chondrocytes

The RMP of tracheal and articular chondrocytes as initially hypothesised was similar between the two chondrocyte types and fell between -8 to -10 mV (**Figure 6.1**). This was expected as the two chondrocyte types express the same ion channel families as observed in Chapter 3 from the RNA-seq data. Although the two chondrocyte types express the same ion channel families, there are still difference in ion channel subtype expression and abundance as previously observed from the RNA-seq data.

The 'channelome' expressed in a cell ensures that ion channels function in synchronicity to ensure that the RMP of the cell remains within normal physiological ranges, hence why there are many different ion channels that carry out the same function. This may be to have redundancies, should one subtype fail, the effect it provides could be compensated for by other ion channels.

Determining an accurate RMP recording in chondrocytes is very challenging as there are multiple technical limits associated with chondrocytes' biophysics when conventional patch-clamp techniques are applied (Wilson et al., 2004). These are the following: the small size of chondrocytes ~ 6 pF together with the chondrocyte's very high input resistance of ~ 10 G Ω , require optimisation of the patch-clamp conditions in which a very high seal resistance that is consistent is achieved. Otherwise, a 'seal leak current' contaminates the true RMP value. Capacitance measurement is used to assess the cell's size as the cell membrane acts as a capacitor where the lipid bilayer composition acts as an insulating layer that separates two electrically charged media, the extracellular and intracellular space (Golowasch and Nadim, 2015). The total membrane capacitance is directly proportional to the cell surface area and hence reflects the cell size of a typical spherical cell (Streit and Lux, 1987). The cell capacitance along with the membrane resistance (arising from ion channels embedded in the lipid bilayer) determine how fast the RMP responds to the flow of current from ion channels by determining the membrane time constant (Lempka and McIntyre, 2015).

In this study, the RMP of chondrocytes was more positive than values reported for other cell types. The values observed were in line with data from my group and others that also found the RMP of chondrocytes to be more positive than other cell types (Barrett-Jolley et al., 2010b, Lewis et al., 2011a, Maleckar et al., 2018). Perhaps the basis of this more positive RMP in chondrocytes is to provide an adaptive mechanism to modulate dramatic osmotic changes that these cells routinely face with minimum changes to the cell volume (Lewis et al., 2011a). However, due to the limitations explained above, this more positive RMP could be due to leak current through the seal resistance, and a more representative value of ~ -40 mV to -50 mV could be more accurate although not completely correct (Suzuki et al., 2020a). This value is also more positive than usual compared to other cell types. However other groups have shown it to be more negative (Maleckar et al., 2020). The RMP of chondrocytes will continue to be debated amongst electrophysiologists. Future studies would involve further optimising the electrophysiological conditions to accurately report the RMP of chondrocytes as well as using 3D cultured chondrocytes to mimic as much as possible the physiological environment that chondrocytes reside in. Determining the ion channel composition of a cell can also give a better indication of their role and contribution to the RMP.

6.4.2 Tracheal chondrocyte channelome

The differential gene expression of the main ion channel families between tracheal and articular chondrocytes was observed in chapter 3 from the RNA-seq data. However, although these ion channel genes were identified in both chondrocyte types, the functional expression of these ion channels has not been shown in tracheal

chondrocytes and the tracheal chondrocyte 'channelome' has not yet been well characterised unlike that of articular cartilage. Cell-attached patch clamp of single channels enabled the identification of a variety of ion channels with different electrophysiological properties in tracheal chondrocytes.

One of the most commonly observed channels was a slow-gated chloride-like channel (**Figure 6.2**); where the channel is activated and its 'gates' are open for longer and close more slowly. Interestingly, this channel showed current relaxation at depolarised voltages, where the current changes at different holding potentials, in this case it increases. According to some electrophysiologists this is an 'artifact'. However, one possible explanation is that the concentrations of the permeable ion inside the cell changes as the recording is taking place and hence the current changes. Another possible explanation as to why this occurs was first described by (Fenwick et al., 1982). Where change in current occurs due to the change in the cell's membrane potential, which changes due to the activation of the channel. This change in the membrane potential cannot be clamped in the cell-attached mode because of the cell's high membrane resistance (Barry and Lynch, 1991a, Fenwick et al., 1982) and hence a change in current is observed. The properties observed for this channel such as its V_{Rev} and high open probabilities at depolarised holding potentials, along with its slow-gating indicate that it could belong to the ClC chloride channel family (Pusch et al., 1999). However, further validation with ClC channel blockers such as methanesulfonate and cyclamate (Rychkov et al., 1998) needs to be used in future studies to elucidate the channel's identity.

As many ion channels with varied electrophysiological properties were observed in tracheal chondrocytes, a non-biased method was used to group these channels based on their V_{Rev} and slope conductance with K -means clustering. Essentially the algorithm for K -means clustering groups the data points so that the distance between the groups is maximised, but the total distance between the points within a 'cluster' is kept to a minimum. As the equilibrium potential of the ions passing through a channel lead to the V_{Rev} , the equilibrium potentials of common ions was calculated using the Nernst equation (**Equation 2.1**, Chapter 2.5). This was used as a guide to identify the ion channel families observed in the clustering (**Figure 6.3**). Using this method not only enabled the prediction of where the different ion channel families would lie on the V_{Rev} scale but also identified clusters of different sized ion channels within the same ion channel family.

Using the K -means clustering of channels recorded with physiological solutions along with equilibrium potentials, a large population of non-specific cation channels were identified to be expressed in tracheal chondrocytes. This expression of non-specific cations such as TRP channels was previously shown in articular chondrocytes by my lab group (Feetham et al., 2015, Lewis et al., 2013b, Feetham et al., 2018). However, TRP channels expression in tracheal chondrocytes has not previously been reported. A representative example of a TRP-like channel is shown in **Figure 6.4**. This channel had a slope conductance of 33.5 ± 2.6 pS and reversal potential of 8.8 ± 6.9 mV and did not show voltage sensitivity, indicative of a TRP channel. However, to fully validate the channel's identity pharmacological agents that block TRP channels would need to

be used (Alexander et al., 2011). Sodium channels and potassium channels were also identified in recordings using physiological solutions and *K*-means clustering.

Voltage-gated sodium channels share hallmark properties of voltage-dependent activation, rapid inactivation, and selective ion conductance as identified by the seminal work of (Hodgkin and Huxley, 1952b). The properties of the sodium-like channel identified in tracheal chondrocytes (**Figure 6.5**) with a V_{Rev} of 18.6 ± 4.8 mV and slope conductance of 22.7 ± 1.1 pS, indicates that it may be a voltage-gated ion channel. This sodium-like channel was fast-gated, whereby the channel is open for shorter periods of time and gets inactivated quickly. Voltage-gated sodium channels are important in articular chondrocytes (**Table 1.1**), yet their functional expression has not been previously reported in tracheal chondrocytes. Future studies would use the neurotoxins tetrodotoxin and saxitoxin that block voltage-gated sodium channels (Yu and Catterall, 2003), to validate and report this novel finding in tracheal chondrocytes.

Surprisingly, potassium channels were not as commonly observed in the tracheal chondrocytes however a few potassium channels were functionally expressed as shown in (**Figure 6.6**). This potassium-like channel was fast-gated and had a slope conductance of 115 ± 0 pS and reversal potential of -64.7 ± 0 mV, properties indicative of a large conductance calcium-activated potassium channel (BK) (Ishii et al., 1997, Latorre et al., 1989). Likewise, as there are many different types of potassium channels and different groups of calcium-activated potassium channels,

pharmacological agents will need to be used in order to fully confirm the channel's identity (Alexander et al., 2019).

Despite clustering the ion channels into groups based on equilibrium potentials and size, it was still difficult to discern between the ion channels observed (**Figure 6.3A**). One approach to distinguish between the channels was applied through changing the ion concentrations in the recording solutions. This led to a shift in the equilibrium potentials of ions and hence changed the activation of the ion channels they are permeable through. Initially, a high K^+ / Ca^{2+} -free recording solution was used (**Figure 6.3B**). Recording the channels with physiological solutions, sodium channels and chloride channels were observed to be clustered closely together. Through the use of a high K^+ / Ca^{2+} -free solution, the possibility of sodium channels being active was eliminated as sodium's equilibrium potential was outside of the V_{Rev} range.

However, using this recording solution, potassium channels were still observed and overlapped with non-specific cations, to eliminate the possibility of potassium channel activation a K^+ -free solution was used (**Figure 6.3C**). This indeed changed the equilibrium potential of K^+ ion to be outside the V_{Rev} range, giving a clearer idea of the channels being activated using this K^+ - free solution. Future studies would involve increasing the number of channels recorded and using other specific solutions to distinguish between the channels. Nevertheless, the gold-standard validation of the ion channels identities involves using pharmacological agents that would activate or inhibit channels, this is also an approach that would need to be investigated in future studies.

6.4.3 *The expression of VRAC in tracheal chondrocytes*

Due to the sheer number of different channels recorded and the tedious process of patch-clamp cell attached recording and analysis as well as the time constraints of this project, a focus on chloride channels was adopted. As not only were chloride channels frequently observed but also because in previous chapters, they were shown to be key in the interplay of miRNAs and ion channels. The chloride channel *Lrrc8a*, an essential subunit of VRAC was shown to be differentially expressed between tracheal and articular chondrocytes and a target of miR-141-3p which potentially drives the observed functional changes in chondrocytes following miR-141-3p transfection.

Using the literature as a guide, *K*-means clustering and observing the phenotypes of chloride-like channels, a fast-gated channel was identified as a potential target for VRAC identity (**Figure 6.8**). VRAC have been previously shown to be active at -100 mV with conductance ranging from ~ 10 pS to 50 pS (Syeda et al., 2016). The VRAC-like channel identified in (**Figure 6.8**) had a slope conductance of 49 ± 34.3 pS ($n=7$) and its gating phenotype resembled that observed by (Syeda et al., 2016), with similar open probabilities at -100mV. Its reversal potential was -54.9 ± 5.7 mV ($n=7$), indicating that it was a chloride channel as it belong to the chloride channel cluster.

Finally, to verify the identity of this channel, a selective VRAC antagonist DCPIB was used as it has been previously shown by many groups to selectively block VRAC channels (Ponce et al., 2012, Abdullaev et al., 2006, Decher et al., 2001). Perfusion of 40 μ M of DCPIB onto the tracheal chondrocytes inhibited the VRAC current (**Figure**

6.7B &F). In order to assess the potency of this block of DCPIB on VRAC current, the dissociation constant (K_D) of the reaction between the ion channel and DCPIB was calculated. K_D is the concentration of when 50% of receptors of the ion channel are occupied by DCPIB, this was determined to be $3.27 \pm 0.008 \mu\text{M}$ ($n=3$). This indicates that less DCPIB is required to occupy 50% of the channel's receptors, implying that each molecule of DCPIB is tightly associated with the channel's receptor (Salahudeen and Nishtala, 2017). Together these findings indicate that this channel is a strong candidate for VRAC channel. Future studies would further investigate this VRAC current by using different hypotonic solutions, as different osmolality gradients are known to regulate VRAC current (Trothe et al., 2018). VRAC have also been involved in pH sensing and hence the effect of changing the pH environment of chondrocytes will be discussed below.

6.4.4 The effect of extracellular acidic pH on tracheal and articular chondrocytes

The extracellular environment of the chondrocyte plays a major role in the ion channel gating and modulation of the RMP which impacts its cellular function. The chondrocyte extracellular environment is unusual compared to other cell types, in particular its osmotic and ionic gradients. The low extracellular pH environment in cartilage constantly exposes the chondrocytes to the risk of intracellular acidification as the extracellular pH and intracellular pH in chondrocytes are closely linked whereby slight reductions of extracellular pH leads to reductions in intracellular pH (Wilkins and Hall, 1995, Falchuk et al., 1970). Since many ion channels that were differentially expressed between tracheal and articular chondrocytes in chapter 3

and targeted by miR-141-3p in chapter 5 and 6 such as *Lrrc8a*, were pH sensitive, in this chapter, the RMP of chondrocytes was measured at acidic pH conditions and compared to the RMP at normal physiological conditions. This showed that in an acidic pH environment of 6.5 (lower than the values reported for cartilage) the RMP becomes significantly depolarised to $\sim 5\text{mV}$ for both chondrocyte types. This depolarisation was biphasic and reversed back to physiological RMP under normal pH conditions. This indicates that the acidic pH environment modulates the ion channel gating leading to changes in the RMP that were reversible once the extracellular conditions were restored back to normal.

Some of the possible ion channels that could be driving this reversible RMP change could be chloride channels. Recently, the structure and pH-sensing mechanism of the proton-activated chloride channel (PAC) was elucidated by (Ruan et al., 2020). PAC mediates the influx of Cl^- as well as cell swelling, it is also implicated in acid-induced cell death (Ruan et al., 2020). The novel PAC gene TMEM206 was identified in the RNA-seq dataset and hence could be driving these RMP changes (**Table A.1**). Another chloride channel that could be mediating this RMP change is the VRAC, which was functionally expressed in tracheal chondrocytes as shown in **Figure 6.7**. It has been shown that VRAC are not only involved in osmoregulation but also in pH sensing, in particular low extracellular pH (Wang et al., 2017). Sustained low pH environments have been shown to activate *Lrrc8a* currents, an essential component of VRAC, and lead to an increase in intracellular alkalinity and depolarisation of nodose neurones (Wang et al., 2017). In addition, extracellular acidity has also been shown to activate Ano1, a CaCC (Faria et al., 2014). Ano1 activation has been known to cause

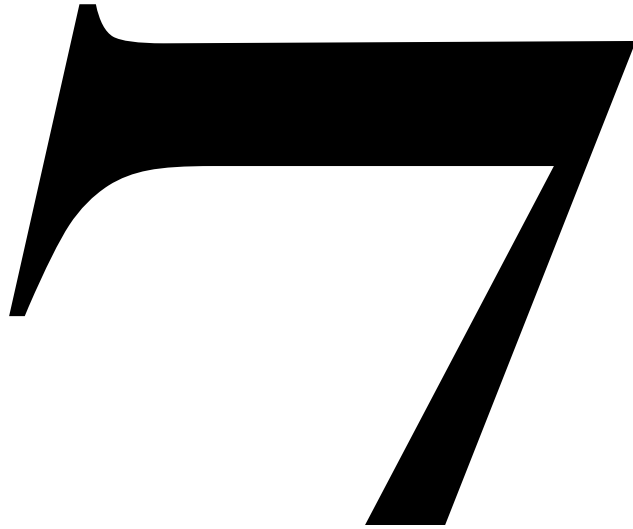
depolarisation in neurones and other cell types (Cho and Oh, 2013, Liu et al., 2010, Cho et al., 2012, Hartzell et al., 2009). However, its role in chondrocyte's RMP is unknown. Therefore, to validate whether these channels are mediating the RMP depolarisation caused by low pH, future studies would involve measuring the RMP in the presence of channel antagonists such as DCPIB and CaCCinh-A01 which are VRAC and Ano1 inhibitors respectively, at low extracellular pH conditions.

It is important to maintain the overall extracellular pH environment of cartilage as it can affect the metabolism of chondrocytes and their ability to synthesise ECM proteins which are sensitive to extracellular pH. This provides a negative feedback mechanism that regulates the production of matrix proteins. Although low pH reduces the lactate production, it has been shown to significantly inhibit cartilage production by around 75% at acidic pH levels (Wilkins and Hall, 1995). Whereas in physiological conditions at extracellular pH values of 7.1 – 7.2, cartilage turnover was found to be upregulated by 50%. This effect of pH was also shown by (Wu et al., 2007) whereby glycosaminoglycans synthesis was reduced by 80% at acidic environments. Glycosaminoglycans are needed to attract water to cartilage to maintain its physiological role (Wu et al., 2007).

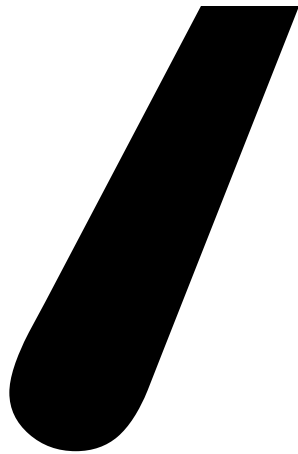
However, some ECM proteins were shown to be pH independent. For example, an acidic pH environment in chondrocytes does not affect the rate of collagen production (Wu et al., 2007). Aside from ECM turnover, other physiological functions that are affected by an acidic pH environment are proliferation and migration. This is due to the fact that an acidic pH environment promotes the degradation of the ECM,

thus allowing cells to be more migratory (Stock and Schwab, 2009). On the other hand, an alkaline pH environment affects the cell's proliferation whereby high intracellular pH is a permissive signal for proliferation (Denker et al., 2000, Pouysségur et al., 1985). Regulating the pH environment of chondrocytes is important as dysregulation of the intracellular and/or extracellular pH can occur in disease states. This will be further discussed in chapter 7.

Overall, in this chapter, novel functional ion channels belonging to different families were observed in tracheal chondrocytes, giving a clearer image of the tracheal chondrocyte channelome. Of these channels, VRAC currents were identified and were shown to be blocked with the potent VRAC inhibitor DCPIB. Seeing as VRAC is also involved in pH sensing, the effect of pH on the RMP of chondrocytes was investigated and was observed to lead to the depolarisation of the membrane potential. Since RMP is important in the maintenance of many cellular functions in cartilage, the pH environment is an important consideration in relation to cartilage disease.



General Discussion



7.1 Main findings

This study used an unbiased approach that combined molecular biology and electrophysiology to investigate the interplay of miRNAs and ion channels in tracheal and articular chondrocyte physiology. The main novel findings of this doctoral study are as follows:

- (1) Tracheal and articular chondrocytes share a similar transcriptome and channelome. They express most ion channel families with distinct differences in ion channel subtypes.
- (2) miRNA upstream regulators drive downstream changes in gene expression between tracheal and articular chondrocytes with miR-141-3p being amongst the top regulators identified. miR-141-3p expression was significantly higher in articular chondrocytes in comparison to tracheal chondrocytes. Gene ontology analysis of miR-141-3p target genes indicated important links to ion channels. Transcriptomic analysis also implicated miR-141-3p as a key miRNA in chondrocyte homeostasis and normal cartilage function.
- (3) miR-141-3p targets ion channel genes and alters their expression. It has a putative target site in the 3'-UTR of *Lrrc8a* ion channel gene. Transfecting tracheal and articular chondrocytes with miR-141-3p caused the downregulation of *Lrrc8a* expression whereas the inhibition of miR-141-3p caused the upregulation of *Lrrc8a* levels. miR-141-3p affects chondrocytes' function, possibly through the targeting of ion channel genes. Transfecting chondrocytes with miR-141-3p resulted in the depolarisation of tracheal chondrocytes RMP and decreased their proliferation. Whereas in articular chondrocytes it increased their proliferation. Tracheal chondrocyte migration

was increased with miR-141-3p transfection, which was decreased with the addition of a CaCC channel blocker, CaCCinh-A01.

- (4) Tracheal chondrocytes express a diverse range of ion channel genes that contribute to their channelome. The functional fingerprint of a variety of ion channels was observed in tracheal chondrocytes. Novel VRAC currents were observed in tracheal chondrocytes which were inhibited with the VRAC antagonist DCPIB.
- (5) Tracheal and articular chondrocytes share similar RMP values that were more positive than reported for other cell types but firmly in line with values reported for chondrocytes. An acidic pH environment in tracheal and articular chondrocytes led to a biphasic depolarisation of the RMP that reverts to physiological levels under normal pH conditions.

In summary, for the first time, this study has shown that miRNAs and ion channels interplay in chondrocytes and lead to functional changes that affect these cells' RMP, proliferation and migration. Transcriptomic studies revealed novel ion channel gene expression in tracheal and articular chondrocytes, which aided in the elucidation of the tracheal chondrocyte channelome and added to the established articular chondrocyte channelome.

7.1.1 Tracheal and articular chondrocytes: similar or different?

Tracheal and articular chondrocytes as previously hypothesised were shown to be very similar. However, this study identified distinct differences in their transcriptome, channelome and response to epigenetic regulation by miRNA. It was intriguing to find

that the hierarchical clustering of ion channel genes between the two chondrocyte types in chapter 3 grouped the tracheal chondrocyte samples and articular chondrocyte samples separately – distinguishing the differences between the two chondrocytes' ion channel expression.

My group have previously shown that there were no species variations between articular chondrocytes isolated from canine, bovine, ovine, equine and human cartilage in terms of their RMP (Lewis et al., 2011a). However, other groups have reported differences in chondrocytes sourced from different tissues and locations within those tissues as reviewed by (Grad and Salzman, 2009). Most of these studies sourced chondrocytes from different cartilages for use in tissue engineering to compensate for the limited availability of autologous articular cartilage. One group compared chondrocytes isolated from elastic, hyaline and fibrocartilage and found differences in their ability to form cartilage on collagen scaffolds with elastic cartilage chondrocytes having increased cartilage production compared to hyaline and fibrocartilage (Zhang and Spector, 2009).

These studies provide evidence that chondrocytes from different sources of cartilage may be physiologically different as observed in the present study. Many of these studies indicate that chondrocytes have the ability to adapt to their milieu. These findings lead to the proposition that tracheal and articular chondrocytes are similar but perhaps have evolutionarily become adapted to their environment. Hence, they may have subtly tailored the expression of ion channel subtypes to facilitate the functional needs of the cartilage they are expressed in. As observed in chapter 3 the

ion channels expressed in specifically one chondrocyte type were related to the function of cartilage that the chondrocyte was isolated from; with ion channels related to cartilage formation and support being expressed in tracheal chondrocytes only and ion channels related to volume regulation and mechanotransduction being expressed in articular chondrocytes only.

In this study passaged chondrocytes were used to investigate the similarities or differences between chondrocytes isolated from tracheal and articular cartilage. There are advantages and disadvantages of using passaged chondrocytes. One of the advantages is that chondrocytes once isolated can be expanded to overcome their low density in cartilage (Melero-Martin et al., 2009). However this can result in dedifferentiation of chondrocytes as the passage number increases and hence affects chondrocytes' phenotype.

Studies examining the production of matrix proteins have shown that after passage four, chondrocytes start to undergo apoptosis and fail to produce type II collagen and proteoglycans (Schulze-Tanzil et al., 2004, Kang et al., 2007). This can be overcome by limiting the passage number of chondrocytes used. It has been shown that dedifferentiated chondrocytes at passage 1 – 4 when introduced to high density cultures were able to regain a chondrocyte phenotype and form cartilage nodules. Whereas chondrocytes at passage 5 – 8 were unable to redifferentiate and did not express extracellular matrix proteins (Schulze-Tanzil et al., 2002). Hence to eliminate this factor, chondrocytes from the two cartilage types in this study were isolated from

the same animals and were kept at the same passage numbers to minimise the variability and ensure that they retain their chondrocyte phenotype.

Although chondrocytes were used up to passage four, minimal Col10a1 expression was observed in both chondrocyte types with tracheal chondrocytes expressing more Col10a1 than articular chondrocytes. Col10a1 is a marker of chondrocyte maturity and hypertrophy (Kirsch et al., 2000). Col10a1 expression was also observed by different groups that showed Col10a1 expression in low passage numbers (lower than passage 4) (Stokes et al., 2001, Cha et al., 2013). It is only after passage 6 that the chondrocytes express high Col10a1 and low Col2a1 levels which reflects cartilage hypertrophy (Ashraf et al., 2016). Perhaps this minimal expression of Col10a1 represents the chondrocytes of the deep zone as they are terminally differentiated and express Col10a1 (Akkiraju and Nohe, 2015b, Schmid and Linsenmayer, 1985). In addition, Col10a1 expression may be required in chondrocytes to facilitate normal function as Col10a1 is important for organisation of the ECM (Kwan et al., 1991).

Overall chondrocytes as hypothesised are not different, yet they are not entirely similar. They adapt to their environment by regulating the expression levels of ECM proteins, ion channels and miRNAs to adapt to the cartilage that they are expressed in and facilitate its function within the body.

7.1.2 miRNA and ion channel interplay in chondrocytes

This study shows for the first time the regulation of chondrocyte ion channels by miRNAs. miR-141-3p endogenously expressed in chondrocytes was shown for the

first time to target ion channel genes and downregulate their expression, whereas the inhibition of miR-141-3p was shown to upregulate their expression. Until very recently, the expression of miR-141-3p in chondrocytes was not previously shown (Yang et al., 2019, Zhang et al., 2020). In this study, analysing the predicted targets of miR-141-3p using different bioinformatic tools revealed links to ion channels, chondrocyte homeostasis and normal cartilage function (Chapter 3). miR-141-3p was also observed to have significantly higher levels in articular chondrocytes in comparison to tracheal chondrocytes (Chapter 4). This may be due to the fact that miR-141-3p has been recently shown to be implicated in OA, which affects articular chondrocytes. Two studies have recently shown that long non-coding RNAs (lncRNA) interact with miR-141-3p and act as protective mechanisms in OA cartilage (Yang et al., 2019, Zhang et al., 2020).

The lncRNA SNHG15, was shown to be decreased in OA cartilage and IL-1 β -treated chondrocytes. It has protective properties, whereby its overexpression ameliorated articular cartilage destruction by decreasing chondrocyte apoptosis, increasing chondrocyte proliferation, and decreasing ECM degradation (Zhang et al., 2020). miR-141-3p expression was shown to be enhanced in OA cartilage and its overexpression reduces the function of SNHG15 on chondrocyte proliferation, apoptosis, and ECM degradation. SNHG15 binds to miR-141-3p and suppresses its expression (Zhang et al., 2020). It does this by acting as a competing endogenous RNA (ceRNA) or miRNA 'sponge'. ceRNAs modulate the level of transcription and translation of their miRNA target genes (Xiong et al., 2019).

Another lncRNA LINC00341, was shown to suppress the action of miR-141-3p on YAF2 which is an antiapoptotic factor. LINC00341 promotes chondrocyte survival and inhibition of OA progression (Yang et al., 2019). miR-141-3p has also been shown to modulate inflammation and apoptosis (Pan et al., 2019, Qin et al., 2019). Evidence for this was observed in chapter 4 in the pathways associated with miR-141-3p targets, which included: 'cell cycle', 'hypoxia response via HIF activation', 'inflammation mediated by cytokine and chemokine signalling', and 'apoptosis signalling'. These findings further implicate miR-141-3p in OA progression as inflammation was shown to be one of the upstream stimuli for OA initiation in the OA pathway identified amongst the top canonical pathways in chondrocytes in chapter 3.

miR-141-3p is a well-established regulator in cancer biology where it has been shown to regulate proliferation, migration and apoptosis as reviewed by (Gao et al., 2016). However, its role in chondrocytes remains unclear. Recently, miR-141 was shown to be a regulator of cartilage catabolism during the progression of OA (Ji et al., 2020). Increased levels of miR-141/200c were shown to be associated with cartilage degradation whereby it correlated with decreased expression of ECM anabolic markers in OA patients (Ji et al., 2020). miR-141/200c inhibitors were administered via a nanocarrier through local intra-articular injection which was observed to cause the reversal of cartilage degradation (Ji et al., 2020). These findings are promising as they indicate that positively charged chondrocyte-homing nanocarriers can be used for sustained drug delivery to the highly negatively charged cartilage and provide a unique delivery system to chondrocytes in the middle and deep zone which are rarely targeted by conventional drug methods (Rothenfluh et al., 2008).

Regenerative medicine advances in cartilage restoration have proved to be difficult (Lammi et al., 2018). Many different scaffold-based and scaffold-free culture models have been developed (Chen and Kawazoe, 2018, Tekin et al., 2011). However, the challenge remains in reconstructing models that would retain the chondrocyte viability as well increase their proliferation and migration in order to achieve correct distribution of embedded cells. Decellularized tissues have also been used as scaffolds as they have the correct structure for tissue assembly of the macromolecules. The first transplantation of a tissue-engineered trachea was conducted by (Macchiarini et al., 2008, Hollander et al., 2009). This was a major breakthrough for regenerative medicine. However, it was based on a donor tracheal graft. This leads to an even higher demand of donor tissue, whereby with each passing year the shortage of donor tissue and organs increases.

In addition, it also raises difficult ethical questions about organ donations, definition of human death and distributive justice. Hence, fully tissue-engineered models would provide a better solution once their limitations are overcome. For example, the nanotechnology-based strategy above can be used to deliver miRNA mimics or inhibitors to chondrocytes. This can be used to increase chondrocyte viability, proliferation, and migration. It can also be used to deliver miRNA that would target ion channels in chondrocytes to alter their expression. For example, miRNAs can be delivered to chondrocytes that would target *Ano1* and *Cav3.2* which are essential for tracheal cartilage formation (Lin et al., 2014b, Rock et al., 2008b) and enhance their expression to prevent cartilage deformation resulting from their loss.

The expression of functional VRAC currents in tracheal chondrocytes was shown for the first time in this study. miR-141-3p targets the VRAC, *Lrrc8a* in both chondrocyte types and decreases its expression. miR-141-3p has a putative target site in the 3'-UTR of *Lrrc8a*, indicating that it may be targeting *Lrrc8a* directly. However, this has to be validated in future studies with luciferase gene reporter assays. The VRAC currents in tracheal chondrocytes were inhibited by the VRAC antagonist DCPIB. DCPIB is one of the most potent VRAC inhibitors with an IC_{50} of approximately 5 μ M (Decher et al., 2001). Thus, the inhibition of the VRAC current with DCPIB validates the channel's identity. Although VRAC are well-known for cell volume control (Strange et al., 2019) and would be anticipated to be more important in articular chondrocytes, their expression and function would be vital for tracheal chondrocytes too. As VRAC are important for RMP regulation, cell cycle regulation and transport of osmolytes (Strange et al., 1996, Okada, 1997, Nilius et al., 1997, Strange et al., 2019). The expression of *Lrrc8a* and its regulation by miR-141-3p in chondrocytes is an important finding as VRAC are essential in proliferation, migration, and apoptosis regulation (Hoffmann et al., 2015). My group have shown that changes in chloride ion channels such as *Ano1* and *Lrrc8a* occurs prior to the onset of apparent cartilage loss (Kumagai et al., 2016). Thus, targeting *Lrrc8a* with miRNAs can be used as mechanism to manipulate its expression and chondrocyte function which can aid in the inhibition of cartilage disease progression such as OA.

In addition to the regulation of ion channels, miR-141-3p also altered the RMP of tracheal chondrocytes, causing its depolarisation. As the RMP is regulated by ion channels, it is most likely that miR-141-3p is acting through ion channels identified in

chapter 4 (Lrrc8a, Cacna1g or Ano1) either directly or non-directly to change the RMP. Hyperpolarisation of chondrocytes has been recently proposed to be a positive feedback loop that can enhance Ca^{2+} entry into chondrocytes (Suzuki et al., 2020b). The influx of Ca^{2+} into chondrocytes can enhance the secretion of cytokines and catabolic factors (Yoo et al., 2007, Little et al., 2002). Hence this may be a mechanism through which miR-141-3p enhances OA progression by changing the RMP of chondrocytes, regulating Ca^{2+} entry and cytokine secretion. miR-141-3p was also shown to decrease proliferation of tracheal chondrocytes in this study as well as increase their migration. Some of the variability of the effect of miR-141-3p on chondrocyte function for example the discrepancies in proliferation and migration needs to be further validated in future studies, which will be discussed in the future directions section.

7.1.3 Importance of maintaining the physiological chondrocyte environment

It was demonstrated in this study that an acidic pH environment in chondrocytes results in a biphasic depolarisation of both chondrocyte types that is reversed back to normal levels in the presence of physiological pH. Maintaining the physiological environment of chondrocytes is essential and plays a role in cartilage diseases. For example, in articular cartilage, extracellular acidosis can occur in OA and RA and is a clinical feature of these diseases that correlates with disease severity (Levick, 1990). This was observed in both patients (Farr et al., 1985, Goetzl et al., 1974) and animal models mimicking joint disease (Kofoed, 1986). This acidosis in articular cartilage affects the articular chondrocytes and can lead to the dysregulation in the production

of ECM proteins as discussed in chapter 6 which leads to worse disease outcomes. However, clever strategies have been employed to utilise the acidosis in OA, whereby novel pH-responsive drug therapies have been proposed that disseminate in a low pH environment and release anti-inflammatory drugs for OA treatment (Chung et al., 2015, Chen et al., 2019, Tao et al., 2019).

In tracheal cartilage, chondrocytes can be indirectly exposed to acidic pH due to the acidic environment of the trachea, which has been reported to be around pH 6.1 – 7.9 (Fischer and Widdicombe, 2006). Chondrocytes can also be indirectly exposed to acidic pH levels through Gastroesophageal reflux disease (GERD) which is a condition where acid from the stomach gets backed up to the oesophagus causing it to become irritated and/or inflamed. GERD has been shown to cause acidosis of the trachea which occurs due to the acid aspiration from the stomach into the trachea. Studies have shown that once the trachea becomes acidified and the pH decreases, airway resistance and broncho-constriction occurs (Vaezi, 2005, Mathew et al., 2004). This acidosis due to GERD has been shown to lead to and exacerbate bronchial asthma, chronic persistent cough and chronic obstructive pulmonary disease among others (Gaude, 2009). Hence the regulation of the extracellular pH environment of chondrocytes is essential as they reside in a harsh environment and are constantly exposed to the risk of acidosis which could cause changes in the ion channel activation and thus the RMP leading to the malfunctioning of vital cellular functions such as volume regulation, proliferation, migration, and ECM synthesis.

7.2 Future perspectives

As with many scientific projects addressing one question leads to additional questions to be investigated. In this study, I investigated whether tracheal and articular chondrocytes were similar or different and whether miRNAs and ion channels interplay in chondrocytes using a molecular biology and electrophysiology approach. Through investigating these questions one of the limitations that was encountered was that the RNA-seq was not designed with miRNA detection in mind. Despite this miRNA expression was still detected. However, future studies would use single-cell RNA-seq to identify heterogenous populations of chondrocytes and small RNA-seq which would capture the complete range of small RNAs and miRNA species which is difficult to do with conventional RNA-seq. In addition, the miRNA target filter analysis in IPA can also be used alongside small RNA-seq to fully identify the relationships most biologically relevant from the small RNA-seq dataset. As well as that further analysis of the vast RNA-seq data obtained in chapter 3 can be used in future studies to further understand in depth the physiology of tracheal and articular chondrocytes.

Moreover, in order to identify whether miR-141-3p is mediating its effect on chondrocyte function through targeting ion channel genes directly or indirectly, luciferase gene reporter assays would be used to determine if miR-141-3p binds to the 3'-UTR region of *Lrrc8a*, *Cacna1g* and *Ano1* genes. As well as that western blotting would be used post miR-141-3p transfection to investigate the effect of miR-141-3p on protein levels of the ion channel genes above.

Furthermore, as miR-141-3p has been recently shown to play a role in OA and affect the ECM catabolism in cartilage (Zhang et al., 2020), future studies would investigate the effect of miR-141-3p transfection on chondrocytes' ability to synthesise ECM proteins by measuring the ECM protein deposition. Also, the effect of miR-141-3p on VRAC current in chondrocytes can be investigated in future studies to determine whether miR-141-3p would block VRAC currents. VRAC currents can be activated in future studies through the use of hypotonic solutions as VRAC currents are triggered by a hypotonic challenge (Qiu et al., 2014, Voss et al., 2014). The effect of miR-141-3p on Ano1 and Cacna1g currents in chondrocytes can also be investigated once their identity has been confirmed with pharmacological agents. Finally, in vivo studies to determine the effect of miR-141-3p on chondrocyte function and ion channel functional expression can be carried out by injecting miR-141-3p mimics and inhibitors into rats. This would enable the full elucidation of the role of miR-141-3p in chondrocyte physiology.

7.3 Conclusion

Overall, this study has shown that tracheal and articular chondrocytes, although very similar, have distinct differences in their channelome and response to epigenetic regulation by miRNAs. This is an important discovery that needs to be considered for the treatment of cartilage diseases. OA is a long term incurable condition that affects approximately one in ten adults in the UK (Swain et al., 2020). It can lead to severe physical impairment that affects patients' quality of life. Hence uncovering possible treatments for OA is important to lessen the burden of OA.

Here, I have shown that miR-141-3p targets ion channels genes, alters their expression and affects the function of both tracheal and articular chondrocytes. In light of the evidence above it seems likely that miR-141-3p may play a role in OA progression. Hence elucidating the effect of miR-141-3p on chondrocytes and manipulating its expression can be used as a potentially treatment of cartilage diseases such as OA and TM. The inhibition of miR-141-3p would enhance ion channel expression, chondrocyte proliferation as well as migration and restoration of the RMP to physiological values.

8

Appendix

Table A.1: Genes differentially expressed between tracheal and articular chondrocytes.

Gene	Articular (FPKM)	Trachea (FPKM)	<i>p</i> -value
Cacna1h	59.5763	185.603	-
Gli2	14240.5	28301.8	0.00115
Snai1	45492.7	61819.5	0.11095
Tmem206	14220.7	9352.85	0.0655

Table A.2: Top 50 significantly differentially expressed genes identified using DESEQ2 analysis between tracheal and articular chondrocytes.

Gene	Mean	Log2 fold change	<i>p</i> -value	Adjusted <i>p</i> -value
Tbx15	1526.963242	-4.074213768	2.91E-123	4.63E-119
Tenm3	12632.91212	4.368843504	1.41E-120	1.12E-116
Foxf1	1113.648837	7.649618233	3.27E-113	1.74E-109
Mab21l2	648.8821734	-9.441078154	4.35E-84	1.73E-80
LOC100911668	743.1835903	-7.747695793	1.45E-71	4.63E-68
Pitx1	491.7895719	-8.063532191	2.12E-56	5.63E-53
Gsc	298.7112708	-4.853589045	7.13E-51	1.62E-47
Hoxc10	1153.598345	-14.08444262	2.67E-49	5.32E-46
Tsen34	659.0467064	-13.27691329	1.21E-45	2.14E-42
Ephb6	741.6897928	-2.684085796	4.57E-45	7.28E-42
Hoxb3	466.9307262	4.200139564	1.25E-43	1.82E-40
Card6	525.9215499	3.882929455	4.14E-43	5.50E-40
NA	1092.927388	4.311686797	3.19E-41	3.91E-38
Hoxd9	519.5481931	-11.24837365	2.41E-39	2.75E-36
Sim2	3438.011004	2.319781428	3.95E-38	4.19E-35
Arid4b	273.5424148	-12.00790653	2.51E-37	2.50E-34
NA	1148.586529	-2.087611664	7.22E-37	6.76E-34

Slc2a12	1001.22409	-2.977886366	4.53E-34	4.01E-31
Hoxc6	305.7595639	-12.16887519	1.51E-33	1.26E-30
Hoxc8	210.7522219	-11.6325321	7.72E-32	6.15E-29
Asb4	173.078881	-11.34859352	5.45E-31	4.14E-28
Irx5	437.3793417	-4.080966166	2.07E-30	1.50E-27
LOC103692128	126.5688733	-10.89707315	2.05E-29	1.42E-26
Adgra3	4202.765752	-1.521548533	2.40E-28	1.59E-25
Met	3037.517679	3.929762784	3.33E-28	2.12E-25
Hoxc9	177.114193	-9.69546525	5.33E-28	3.26E-25
Foxd1	218.4613228	-5.030527909	6.06E-28	3.58E-25
LOC100909443	137.1097835	-10.4332402	7.01E-28	3.99E-25
Hoxb2	590.1931242	3.447478707	2.81E-27	1.55E-24
Alx1	923.5251963	12.88806939	5.30E-27	2.82E-24
Wscd2	1197.448961	3.52830261	2.44E-26	1.25E-23
LOC103689925	119.3169487	-10.23335924	3.00E-26	1.49E-23
Plekhg4	523.4664449	-3.751483835	4.80E-26	2.32E-23
Tbx5	226.2438409	8.024899526	1.07E-25	5.03E-23
NA	4033.282976	-1.709743092	4.88E-25	2.22E-22
Islr	3306.163699	-3.876430859	7.31E-25	3.23E-22
Srgn	488.2816517	3.966330594	1.04E-24	4.37E-22
Hspa4l	248.3832379	2.638662067	1.02E-24	4.37E-22
Rassf9	1025.819582	2.896770712	2.29E-24	9.34E-22
Csmd2	85.27206218	-10.32647534	8.69E-24	3.46E-21
Col9a2	5044.503384	4.651053301	1.21E-23	4.71E-21
Upk3b	517.368675	4.031746251	1.26E-23	4.77E-21
Kif26a	148.5779914	4.343689839	1.94E-23	7.18E-21
Prdm16	941.5490883	1.3747259	2.66E-23	9.64E-21
Loxl2	13749.04161	-1.169576623	3.05E-23	1.08E-20
Tbx3	810.149348	5.171716138	3.86E-23	1.34E-20
Pth1r	699.460512	-2.216407261	4.10E-23	1.39E-20
Hoxb4	374.1074475	3.489794055	4.44E-23	1.47E-20

Prima1	1384.833102	-7.171731549	7.67E-23	2.45E-20
Hoxa11	57.65315287	-9.761713803	7.57E-23	2.45E-20

Q

References

Q

- ABDUL KADIR, L., STACEY, M. & BARRETT-JOLLEY, R. 2018. Emerging Roles of the Membrane Potential: Action Beyond the Action Potential. *Frontiers in Physiology*, 9.
- ABDULLAEV, I. F., RUDKOUSKAYA, A., SCHOOLS, G. P., KIMELBERG, H. K. & MONGIN, A. A. 2006. Pharmacological comparison of swelling-activated excitatory amino acid release and Cl⁻ currents in cultured rat astrocytes. *The Journal of physiology*, 572, 677-689.
- ABOUHEIF, M. M., NAKASA, T., SHIBUYA, H., NIIMOTO, T., KONGCHAROENSOMBAT, W. & OCHI, M. 2010. Silencing microRNA-34a inhibits chondrocyte apoptosis in a rat osteoarthritis model in vitro. *Rheumatology (Oxford)*, 49, 2054-60.
- ADAMS, C. S. & SHAPIRO, I. M. 2002. The Fate of the Terminally Differentiated Chondrocyte: Evidence for Microenvironmental Regulation of Chondrocyte Apoptosis. *Critical Reviews in Oral Biology & Medicine*, 13, 465-473.
- AKKIRAJU, H. & NOHE, A. 2015a. Role of Chondrocytes in Cartilage Formation, Progression of Osteoarthritis and Cartilage Regeneration. *Journal of developmental biology*, 3, 177-192.
- AKKIRAJU, H. & NOHE, A. 2015b. Role of Chondrocytes in Cartilage Formation, Progression of Osteoarthritis and Cartilage Regeneration. *Journal of Developmental Biology*, 3.
- AL-ANI, A. M., MESSENGER, A. G., LAWRY, J., BLEEHEN, S. S. & MACNEIL, S. 1988. Calcium/calmodulin regulation of the proliferation of human epidermal keratinocytes, dermal fibroblasts and mouse B16 melanoma cells in culture. *Br J Dermatol*, 119, 295-306.
- ALEXANDER, S. P. H., MATHIE, A. & PETERS, J. A. 2011. Guide to Receptors and Channels (GRAC), 5th edition. *British journal of pharmacology*, 164 Suppl 1, S1-S324.
- ALEXANDER, S. P. H., MATHIE, A., PETERS, J. A., VEALE, E. L., STRIESSNIG, J., KELLY, E., ARMSTRONG, J. F., FACCENDA, E., HARDING, S. D., PAWSON, A. J., SHARMAN, J. L., SOUTHAN, C., DAVIES, J. A. & COLLABORATORS, C. 2019. THE CONCISE GUIDE TO PHARMACOLOGY 2019/20: Ion channels. *British journal of pharmacology*, 176 Suppl 1, S142-S228.
- ALMAN, B. A. 2015. The role of hedgehog signalling in skeletal health and disease. *Nat Rev Rheumatol*, 11, 552-60.
- AMERES, S. L., HORWICH, M. D., HUNG, J. H., XU, J., GHILDIYAL, M., WENG, Z. & ZAMORE, P. D. 2010. Target RNA-directed trimming and tailing of small silencing RNAs. *Science*, 328, 1534-9.
- AMIGORENA, S., CHOQUET, D., TEILLAUD, J. L., KORN, H. & FRIDMAN, W. H. 1990. Ion channels and b cell mitogenesis. *Molecular Immunology*, 27, 1259-1268.
- ANDERSON, D. R. 1964. The ultrastructure of elastic and hyaline cartilage of the rat. 114, 403-433.
- ARAVIN, A. A., LAGOS-QUINTANA, M., YALCIN, A., ZAVOLAN, M., MARKS, D., SNYDER, B., GAASTERLAND, T., MEYER, J. & TUSCHL, T. 2003. The small RNA profile during *Drosophila melanogaster* development. *Dev Cell*, 5, 337-50.
- ARCHER, C. W. & FRANCIS-WEST, P. 2003. The chondrocyte. *Int J Biochem Cell Biol*, 35, 401-4.
- ASHRAF, S., CHA, B. H., KIM, J. S., AHN, J., HAN, I., PARK, H. & LEE, S. H. 2016. Regulation of senescence associated signaling mechanisms in chondrocytes for cartilage tissue regeneration. *Osteoarthritis and Cartilage*, 24, 196-205.
- ASKEW, M. J. & MOW, V. C. 1978. The Biomechanical Function of the Collagen Fibril Ultrastructure of Articular Cartilage. *Journal of Biomechanical Engineering*, 100, 105-115.

- ASMANN, Y. W., KLEE, E. W., THOMPSON, E. A., PEREZ, E. A., MIDDHA, S., OBERG, A. L., THERNEAU, T. M., SMITH, D. I., POLAND, G. A., WIEBEN, E. D. & KOCHER, J.-P. A. 2009. 3' tag digital gene expression profiling of human brain and universal reference RNA using Illumina Genome Analyzer. *BMC Genomics*, 10, 531.
- ASMAR, A., BARRETT-JOLLEY, R., WERNER, A., KELLY JR, R. & STACEY, M. 2016. Membrane channel gene expression in human costal and articular chondrocytes. *Organogenesis* [Online].
- ASMAR, A. J. 2017. The Chondrocyte Channelome: A Novel Ion Channel Candidate in the Pathogenesis of Pectus Deformities.
- ATSUTA, Y., TOMIZAWA, R. R., LEVIN, M. & TABIN, C. J. 2019. L-type voltage-gated Ca²⁺ channel Ca_v1.2 regulates chondrogenesis during limb development. *Proceedings of the National Academy of Sciences*, 116, 21592.
- AYDELOTTE, M. B., GREENHILL, R. R. & KUETTNER, K. E. 1988. Differences between sub-populations of cultured bovine articular chondrocytes. II. Proteoglycan metabolism. *Connect Tissue Res*, 18, 223-34.
- AYDELOTTE, M. B. & KUETTNER, K. E. 1988. Differences between sub-populations of cultured bovine articular chondrocytes. I. Morphology and cartilage matrix production. *Connect Tissue Res*, 18, 205-22.
- AYOUB, C., WASYLYK, C., LI, Y., THOMAS, E., MARISA, L., ROBÉ, A., ROUX, M., ABECASSIS, J., DE REYNIÈS, A. & WASYLYK, B. 2010. ANO1 amplification and expression in HNSCC with a high propensity for future distant metastasis and its functions in HNSCC cell lines. *Br J Cancer*, 103, 715-26.
- BACCARINI, A., CHAUHAN, H., GARDNER, T. J., JAYAPRAKASH, A. D., SACHIDANANDAM, R. & BROWN, B. D. 2011. Kinetic analysis reveals the fate of a microRNA following target regulation in mammalian cells. *Curr Biol*, 21, 369-76.
- BAE, J. S., PARK, J. Y., PARK, S.-H., HA, S. H., AN, A. R., NOH, S. J., KWON, K. S., JUNG, S. H., PARK, H. S., KANG, M. J. & JANG, K. Y. 2017. Expression of ANO1/DOG1 is associated with shorter survival and progression of breast carcinomas. *Oncotarget*, 9, 607-621.
- BAIRATI, A., COMAZZI, M. & GIORIA, M. 1996. A comparative study of perichondrial tissue in mammalian cartilages. *Tissue and Cell*, 28, 455-468.
- BARANA, A., MATAMOROS, M., DOLZ-GAITÓN, P., PÉREZ-HERNÁNDEZ, M., AMORÓS, I., NÚÑEZ, M., SACRISTÁN, S., PEDRAZ, Á., PINTO, Á., FERNÁNDEZ-AVILÉS, F., TAMARGO, J., DELPÓN, E. & CABALLERO, R. 2014. Chronic atrial fibrillation increases microRNA-21 in human atrial myocytes decreasing L-type calcium current. *Circ Arrhythm Electrophysiol*, 7, 861-8.
- BARISH, M. E. 1983. A transient calcium-dependent chloride current in the immature *Xenopus* oocyte. *The Journal of physiology*, 342, 309-325.
- BARRETT-JOLLEY, R., LEWIS, R., FALLMAN, R. & MOBASHERI, A. 2010a. The emerging chondrocyte channelome. *Frontiers in physiology*, 1, 135-135.
- BARRETT-JOLLEY, R., LEWIS, R., FALLMAN, R. & MOBASHERI, A. 2010b. The emerging chondrocyte channelome. *Frontiers in Physiology*, 1.
- BARRY, P. H. & LYNCH, J. W. 1991a. Liquid junction potentials and small cell effects in patch-clamp analysis. *J Membr Biol*, 121, 101-17.
- BARRY, P. H. & LYNCH, J. W. 1991b. Liquid junction potentials and small cell effects in patch-clamp analysis. *The Journal of Membrane Biology*, 121, 101-117.
- BARTEL, D. P. 2004a. MicroRNAs: Genomics, Biogenesis, Mechanism, and Function. *Cell*, 116, 281-297.
- BARTEL, D. P. 2004b. MicroRNAs: genomics, biogenesis, mechanism, and function. *Cell*, 116.

- BARTEL, D. P. 2018. Metazoan MicroRNAs. *Cell*, 173, 20-51.
- BAXTER, J. D. & DUNBAR, J. S. 1963. TRACHEOMALACIA. *Ann Otol Rhinol Laryngol*, 72, 1013-23.
- BECKER, D., BLASE, C., BEREITER-HAHN, J. & JENDRACH, M. 2005. TRPV4 exhibits a functional role in cell-volume regulation. *J Cell Sci*, 118, 2435-40.
- BEECH, D. J. & XIAO, B. 2018. Piezo channel mechanisms in health and disease. *J Physiol*, 596, 965-967.
- BELL, D. M., LEUNG, K. K. H., WHEATLEY, S. C., NG, L. J., ZHOU, S., WING LING, K., HAR SHAM, M., KOOPMAN, P., TAM, P. P. L. & CHEAH, K. S. E. 1997. SOX9 directly regulates the type-II collagen gene. *Nature Genetics*, 16, 174-178.
- BENJAMIN, M. & EVANS, E. J. 1990. Fibrocartilage. *Journal of anatomy*, 171, 1-15.
- BHOSALE, A. M. & RICHARDSON, J. B. 2008a. Articular cartilage: structure, injuries and review of management. *British Medical Bulletin*, 87, 77-95.
- BHOSALE, A. M. & RICHARDSON, J. B. 2008b. Articular cartilage: structure, injuries and review of management. *Br Med Bull*, 87, 77-95.
- BI, W., DENG, J. M., ZHANG, Z., BEHRINGER, R. R. & DE CROMBRUGGHE, B. 1999. Sox9 is required for cartilage formation. *Nature Genetics*, 22, 85-89.
- BI, X. 2018. Correlation of serum cartilage oligomeric matrix protein with knee osteoarthritis diagnosis: a meta-analysis. *Journal of Orthopaedic Surgery and Research*, 13, 262.
- BINAS, S., KNYRIM, M., HUPFELD, J., KLOECKNER, U., RABE, S., MILDENBERGER, S., QUARCH, K., STRÄTZ, N., MISIAK, D., GEKLE, M., GROSSMANN, C. & SCHREIER, B. 2020. miR-221 and -222 target CACNA1C and KCNJ5 leading to altered cardiac ion channel expression and current density. *Cellular and Molecular Life Sciences*, 77, 903-918.
- BOHNSACK, M. T., CZAPLINSKI, K. & GORLICH, D. 2004. Exportin 5 is a RanGTP-dependent dsRNA-binding protein that mediates nuclear export of pre-miRNAs. *Rna*, 10, 185-91.
- BOILEAU, C., MARTEL-PELLETIER, J., BRUNET, J., TARDIF, G., SCHRIER, D., FLORY, C., EL-KATTAN, A., BOILY, M. & PELLETIER, J. P. 2005. Oral treatment with PD-0200347, an alpha2delta ligand, reduces the development of experimental osteoarthritis by inhibiting metalloproteinases and inducible nitric oxide synthase gene expression and synthesis in cartilage chondrocytes. *Arthritis Rheum*, 52, 488-500.
- BONDARAVA, M., LI, T., ENDL, E. & WEHNER, F. 2009. alpha-ENaC is a functional element of the hypertonicity-induced cation channel in HepG2 cells and it mediates proliferation. *Pflugers Arch*, 458, 675-87.
- BOUTELL, J., MACIEWICZ, R. A. & PARKER, A. E. 2000. Cartilage ECM molecules are differentially expressed between nasal and articular bovine chondrocytes. *International Journal of Experimental Pathology*, 81, A7-A8.
- BREITKREUTZ, D., STARK, H. J., PLEIN, P., BAUR, M. & FUSENIG, N. E. 1993. Differential modulation of epidermal keratinization in immortalized (HaCaT) and tumorigenic human skin keratinocytes (HaCaT-ras) by retinoic acid and extracellular Ca2+. *Differentiation; research in biological diversity*, 54, 201-217.
- BRITSCHGI, A., BILL, A., BRINKHAUS, H., ROTHWELL, C., CLAY, I., DUSS, S., REBHAN, M., RAMAN, P., GUY, C. T., WETZEL, K., GEORGE, E., POPA, M. O., LILLEY, S., CHOUDHURY, H., GOSLING, M., WANG, L., FITZGERALD, S., BORAWSKI, J., BAFFOE, J., LABOW, M., GAITHER, L. A. & BENTIREES-ALJ, M. 2013. Calcium-activated chloride channel ANO1 promotes breast cancer progression by activating EGFR and CAMK signaling. *Proc Natl Acad Sci U S A*, 110, E1026-34.

- BROWNING, J. A. & WILKINS, R. J. 2004. Mechanisms contributing to intracellular pH homeostasis in an immortalised human chondrocyte cell line. *Comp Biochem Physiol A Mol Integr Physiol*, 137, 409-18.
- BUCKWALTER, J., MANKIN, H. J. J. O. B. & SURGERY, J. 1997. Articular cartilage: part I. 79, 600.
- BUCKWALTER, J. A. & MANKIN, H. J. 1998. Articular cartilage: tissue design and chondrocyte-matrix interactions. *Instr Course Lect*, 47, 477-86.
- CALVANO, S. E., XIAO, W., RICHARDS, D. R., FELCIANO, R. M., BAKER, H. V., CHO, R. J., CHEN, R. O., BROWNSTEIN, B. H., COBB, J. P., TSCHOEKE, S. K., MILLER-GRAZIANO, C., MOLDAWER, L. L., MINDRINOS, M. N., DAVIS, R. W., TOMPKINS, R. G., LOWRY, S. F., INFLAMMATION & HOST RESPONSE TO INJURY LARGE SCALE COLLABORATIVE RESEARCH, P. 2005. A network-based analysis of systemic inflammation in humans. *Nature*, 437, 1032-1037.
- CANESSA, C. M., SCHILD, L., BUELL, G., THORENS, B., GAUTSCHI, I., HORISBERGER, J.-D. & ROSSIER, B. C. 1994. Amiloride-sensitive epithelial Na⁺ channel is made of three homologous subunits. *Nature*, 367, 463-467.
- CANO, A., PÉREZ-MORENO, M. A., RODRIGO, I., LOCASCIO, A., BLANCO, M. J., DEL BARRIO, M. G., PORTILLO, F. & NIETO, M. A. 2000. The transcription factor Snail controls epithelial–mesenchymal transitions by repressing E-cadherin expression. *Nature Cell Biology*, 2, 76-83.
- CAO, D., YU, T. & OU, X. 2016. MiR-873-5P controls gastric cancer progression by targeting hedgehog-Gli signaling. *Die Pharmazie - An International Journal of Pharmaceutical Sciences*, 71, 603-606.
- CAPUTO, A., CACI, E., FERRERA, L., PEDEMONTE, N., BARSANTI, C., SONDO, E., PFEFFER, U., RAVAZZOLO, R., ZEGARRA-MORAN, O. & GALIETTA, L. J. 2008. TMEM16A, a membrane protein associated with calcium-dependent chloride channel activity. *Science*, 322, 590-4.
- CARTHEW, R. W. & SONTHEIMER, E. J. 2009. Origins and Mechanisms of miRNAs and siRNAs. *Cell*, 136, 642-55.
- CATTERALL, W. A. 1995. Structure and function of voltage-gated ion channels. *Annu Rev Biochem*, 64, 493-531.
- CHA, B. H., LEE, J. S., KIM, S. W., CHA, H. J. & LEE, S. H. 2013. The modulation of the oxidative stress response in chondrocytes by Wip1 and its effect on senescence and dedifferentiation during in vitro expansion. *Biomaterials*, 34, 2380-8.
- CHANG, C., LAUFFENBURGER, D. A. & MORALES, T. I. 2003. Motile chondrocytes from newborn calf: migration properties and synthesis of collagen II. *Osteoarthritis Cartilage*, 11, 603-12.
- CHANGEUX, J. P. 2010. Allosteric receptors: from electric organ to cognition. *Annu Rev Pharmacol Toxicol*, 50, 1-38.
- CHEN, B., HUANG, T., JIANG, J., LV, L., LI, H. & XIA, S. 2014a. miR-141 suppresses proliferation and motility of gastric cancer cells by targeting HDGF. *Mol Cell Biochem*, 388, 211-8.
- CHEN, D., KIM, D. J., SHEN, J., ZOU, Z. & O'KEEFE, R. J. 2020. Runx2 plays a central role in Osteoarthritis development. *Journal of Orthopaedic Translation*, 23, 132-139.
- CHEN, D., SHEN, J., ZHAO, W., WANG, T., HAN, L., HAMILTON, J. L. & IM, H.-J. 2017. Osteoarthritis: toward a comprehensive understanding of pathological mechanism. *Bone research*, 5, 16044-16044.
- CHEN, G. & KAWAZOE, N. 2018. Porous Scaffolds for Regeneration of Cartilage, Bone and Osteochondral Tissue. *Adv Exp Med Biol*, 1058, 171-191.

- CHEN, H., QIN, Z., ZHAO, J., HE, Y., REN, E., ZHU, Y., LIU, G., MAO, C. & ZHENG, L. 2019. Cartilage-targeting and dual MMP-13/pH responsive theranostic nanoprobe for osteoarthritis imaging and precision therapy. *Biomaterials*, 225, 119520.
- CHEN, Q., XU, R., ZENG, C., LU, Q., HUANG, D., SHI, C., ZHANG, W., DENG, L., YAN, R., RAO, H., GAO, G. & LUO, S. 2014b. Down-regulation of Gli transcription factor leads to the inhibition of migration and invasion of ovarian cancer cells via integrin β 4-mediated FAK signaling. *PLoS one*, 9, e88386-e88386.
- CHEN, X., MACICA, C. M., NASIRI, A. & BROADUS, A. E. 2008. Regulation of articular chondrocyte proliferation and differentiation by indian hedgehog and parathyroid hormone-related protein in mice. *Arthritis and rheumatism*, 58, 3788-3797.
- CHO, H. & OH, U. 2013. Anoctamin 1 mediates thermal pain as a heat sensor. *Current neuropharmacology*, 11, 641-651.
- CHO, H., YANG, Y. D., LEE, J., LEE, B., KIM, T., JANG, Y., BACK, S. K., NA, H. S., HARFE, B. D., WANG, F., RAOUF, R., WOOD, J. N. & OH, U. 2012. The calcium-activated chloride channel anoctamin 1 acts as a heat sensor in nociceptive neurons. *Nat Neurosci*, 15, 1015-21.
- CHUNG, M.-F., CHIA, W.-T., WAN, W.-L., LIN, Y.-J. & SUNG, H.-W. 2015. Controlled Release of an Anti-inflammatory Drug Using an Ultrasensitive ROS-Responsive Gas-Generating Carrier for Localized Inflammation Inhibition. *Journal of the American Chemical Society*, 137, 12462-12465.
- CLARK, A. L., VOTTA, B. J., KUMAR, S., LIEDTKE, W. & GUILAK, F. 2010a. Chondroprotective role of the osmotically sensitive ion channel transient receptor potential vanilloid 4: age- and sex-dependent progression of osteoarthritis in Trpv4-deficient mice. *Arthritis Rheum*, 62, 2973-83.
- CLARK, R. B., HATANO, N., KONDO, C., BELKE, D. D., BROWN, B. S., KUMAR, S., VOTTA, B. J. & GILES, W. R. 2010b. Voltage-gated K⁺ currents in mouse articular chondrocytes regulate membrane potential. *Channels (Austin, Tex.)*, 4, 179-191.
- CLARK, R. B., HATANO, N., KONDO, C., BELKE, D. D., BROWN, B. S., KUMAR, S., VOTTA, B. J. & GILES, W. R. 2010c. Voltage-gated K⁺ currents in mouse articular chondrocytes regulate membrane potential. *Channels*, 4, 179-191.
- CLARK, R. B., KONDO, C., BELKE, D. D. & GILES, W. R. 2011a. Two-pore domain K⁺ channels regulate membrane potential of isolated human articular chondrocytes. *Journal of Physiology-London*, 589, 5071-5089.
- CLARK, R. B., KONDO, C., BELKE, D. D. & GILES, W. R. 2011b. Two-pore domain K⁺ channels regulate membrane potential of isolated human articular chondrocytes. *The Journal of physiology*, 589, 5071-5089.
- CONE JR., C. D. 1974. THE ROLE OF THE SURFACE ELECTRICAL TRANSMEMBRANE POTENTIAL IN NORMAL AND MALIGNANT MITOGENESIS. 238, 420-435.
- DAHESHIA, M. & YAO, J. Q. 2008. The interleukin 1beta pathway in the pathogenesis of osteoarthritis. *J Rheumatol*, 35, 2306-12.
- DE, N., YOUNG, L., LAU, P. W., MEISNER, N. C., MORRISSEY, D. V. & MACRAE, I. J. 2013. Highly complementary target RNAs promote release of guide RNAs from human Argonaute2. *Mol Cell*, 50, 344-55.
- DECHER, N., LANG, H. J., NILIUS, B., BRÜGGEMANN, A., BUSCH, A. E. & STEINMEYER, K. 2001. DCPIB is a novel selective blocker of I(Cl,swell) and prevents swelling-induced shortening of guinea-pig atrial action potential duration. *British journal of pharmacology*, 134, 1467-1479.
- DENKER, S. P., HUANG, D. C., ORLOWSKI, J., FURTHMAYR, H. & BARBER, D. L. 2000. Direct binding of the Na⁺-H exchanger NHE1 to ERM proteins regulates the cortical cytoskeleton and cell shape independently of H(+) translocation. *Mol Cell*, 6, 1425-36.

- DESSAU, W., SASSE, J., TIMPL, R., JILEK, F. & VON DER MARK, K. 1978. Synthesis and extracellular deposition of fibronectin in chondrocyte cultures. Response to the removal of extracellular cartilage matrix. *J Cell Biol*, 79, 342-55.
- DESSAU, W., VON DER MARK, H., VON DER MARK, K. & FISCHER, S. 1980. Changes in the patterns of collagens and fibronectin during limb-bud chondrogenesis. *J Embryol Exp Morphol*, 57, 51-60.
- DÍAZ-LEZAMA, N., HERNÁNDEZ-ELVIRA, M., SANDOVAL, A., MONROY, A., FELIX, R. & MONJARAZ, E. 2010. Ghrelin inhibits proliferation and increases T-type Ca²⁺ channel expression in PC-3 human prostate carcinoma cells. *Biochemical and Biophysical Research Communications*, 403, 24-29.
- DING, Y., CUI, Y., ZHOU, Z., HOU, Y., PANG, X. & NIE, H. 2020. Lipopolysaccharide Inhibits Alpha Epithelial Sodium Channel Expression via MiR-124-5p in Alveolar Type 2 Epithelial Cells. *BioMed Research International*, 2020, 8150780.
- DOROSHENKO, P., SABANOV, V. & DOROSHENKO, N. 2001. Cell cycle-related changes in regulatory volume decrease and volume-sensitive chloride conductance in mouse fibroblasts. 187, 65-72.
- DRISSI, H., ZUSCIK, M., ROSIER, R. & O'KEEFE, R. 2005. Transcriptional regulation of chondrocyte maturation: potential involvement of transcription factors in OA pathogenesis. *Mol Aspects Med*, 26, 169-79.
- DUDEK, K. A., LAFONT, J. E., MARTINEZ-SANCHEZ, A. & MURPHY, C. L. 2010. Type II collagen expression is regulated by tissue-specific miR-675 in human articular chondrocytes. *J Biol Chem*, 285, 24381-7.
- EAMES, B. F., DE LA FUENTE, L. & HELMS, J. A. 2003. Molecular ontogeny of the skeleton. *Birth Defects Res C Embryo Today*, 69, 93-101.
- EBERHART, J. K., HE, X., SWARTZ, M. E., YAN, Y. L., SONG, H., BOLING, T. C., KUNERTH, A. K., WALKER, M. B., KIMMEL, C. B. & POSTLETHWAIT, J. H. 2008. MicroRNA Mirn140 modulates Pdgf signaling during palatogenesis. *Nat Genet*, 40, 290-8.
- ECKSTEIN, F., TIESCHKY, M., FABER, S., ENGLMEIER, K. H. & REISER, M. 1999. Functional analysis of articular cartilage deformation, recovery, and fluid flow following dynamic exercise in vivo. *Anat Embryol (Berl)*, 200, 419-24.
- EL CHEMALY, A., OKOCHI, Y., SASAKI, M., ARNAUDEAU, S., OKAMURA, Y. & DEMAUREX, N. 2010. VSOP/Hv1 proton channels sustain calcium entry, neutrophil migration, and superoxide production by limiting cell depolarization and acidification. *The Journal of experimental medicine*, 207, 129-139.
- ENOMOTO-IWAMOTO, M., IWAMOTO, M., NAKASHIMA, K., MUKUDAI, Y., BOETTIGER, D., PACIFICI, M., KURISU, K. & SUZUKI, F. 1997. Involvement of $\alpha 5\beta 1$ Integrin in Matrix Interactions and Proliferation of Chondrocytes. *Journal of Bone and Mineral Research*, 12, 1124-1132.
- ERHARD, F., HAAS, J., LIEBER, D., MALTERER, G., JASKIEWICZ, L., ZAVOLAN, M., DÖLKEN, L. & ZIMMER, R. 2014. Widespread context dependency of microRNA-mediated regulation. *Genome research*, 24, 906-919.
- EYRE, D. R. 2004. Collagens and cartilage matrix homeostasis. *Clin Orthop Relat Res*, S118-22.
- EYRE, D. R., WEIS, M. A. & WU, J. J. 2006. Articular cartilage collagen: an irreplaceable framework? *Eur Cell Mater*, 12, 57-63.
- FAKLER, B. & ADELMAN, J. P. 2008. Control of K⁺ Channels by Calcium Nano/Microdomains. *Neuron*, 59, 873-881.
- FALCHUK, K. H., GOETZL, E. J. & KULKA, J. P. 1970. Respiratory gases of synovial fluids. An approach to synovial tissue circulatory-metabolic imbalance in rheumatoid arthritis. *Am J Med*, 49, 223-31.

- FARIA, D., ROCK, J. R., ROMAO, A. M., SCHWEDA, F., BANDULIK, S., WITZGALL, R., SCHLATTER, E., HEITZMANN, D., PAVENSTÄDT, H., HERRMANN, E., KUNZELMANN, K. & SCHREIBER, R. 2014. The calcium-activated chloride channel Anoctamin 1 contributes to the regulation of renal function. *Kidney International*, 85, 1369-1381.
- FARR, M., GARVEY, K., BOLD, A. M., KENDALL, M. J. & BACON, P. A. 1985. Significance of the hydrogen ion concentration in synovial fluid in rheumatoid arthritis. *Clin Exp Rheumatol*, 3, 99-104.
- FEETHAM, C., NUNN, N., LEWIS, R., DART, C. & BARRETT-JOLLEY, R. 2014. TRPV4 and KCa functionally couple as osmosensors in the PVN. *British Journal of Pharmacology*, 172.
- FEETHAM, C. H., NUNN, N., LEWIS, R., DART, C. & BARRETT-JOLLEY, R. 2015. TRPV4 and K(Ca) ion channels functionally couple as osmosensors in the paraventricular nucleus. *Br J Pharmacol*, 172, 1753-68.
- FEETHAM, C. H., O'BRIEN, F. & BARRETT-JOLLEY, R. 2018. Ion Channels in the Paraventricular Hypothalamic Nucleus (PVN); Emerging Diversity and Functional Roles. 9.
- FELIX, R. 2005. Molecular Regulation of Voltage-Gated Ca²⁺ Channels. *Journal of Receptors and Signal Transduction*, 25, 57-71.
- FELL, H. B. 1925. The histogenesis of cartilage and bone in the long bones of the embryonic fowl. *Journal of Morphology*, 40, 417-459.
- FENWICK, E. M., MARTY, A. & NEHER, E. 1982. A patch-clamp study of bovine chromaffin cells and of their sensitivity to acetylcholine. *J Physiol*, 331, 577-97.
- FILLER, R. M., BUCK, J. R., BAHORIC, A. & STEWARD, D. J. 1982. Treatment of segmental tracheomalacia and bronchomalacia by implantation of an airway splint. *Journal of Pediatric Surgery*, 17, 597-603.
- FINDLAY, D. M. & ATKINS, G. J. 2014. Osteoblast-chondrocyte interactions in osteoarthritis. *Curr Osteoporos Rep*, 12, 127-34.
- FISCHER, H. & WIDDICOMBE, J. H. 2006. Mechanisms of acid and base secretion by the airway epithelium. *The Journal of membrane biology*, 211, 139-150.
- FODOR, J., MATTA, C., JUHÁSZ, T., OLÁH, T., GÖNCZI, M., SZÍJGYÁRTÓ, Z., GERGELY, P., CSERNOCH, L. & ZÁKÁNY, R. 2009. Ionotropic purinergic receptor P2X4 is involved in the regulation of chondrogenesis in chicken micromass cell cultures. *Cell Calcium*, 45, 421-430.
- FODOR, J., MATTA, C., OLÁH, T., JUHÁSZ, T., TAKÁCS, R., TÓTH, A., DIENES, B., CSERNOCH, L. & ZÁKÁNY, R. 2013. Store-operated calcium entry and calcium influx via voltage-operated calcium channels regulate intracellular calcium oscillations in chondrogenic cells. *Cell Calcium*, 54, 1-16.
- FRENKEL, S. R., CLANCY, R. M., RICCI, J. L., DI CESARE, P. E., REDISKE, J. J. & ABRAMSON, S. B. 1996. Effects of nitric oxide on chondrocyte migration, adhesion, and cytoskeletal assembly. *Arthritis & Rheumatism*, 39, 1905-1912.
- FUJITA, T., AZUMA, Y., FUKUYAMA, R., HATTORI, Y., YOSHIDA, C., KOIDA, M., OGITA, K. & KOMORI, T. 2004. Runx2 induces osteoblast and chondrocyte differentiation and enhances their migration by coupling with PI3K-Akt signaling. *J Cell Biol*, 166, 85-95.
- FUJITA, Y., SHIOMI, T., YANAGIMOTO, S., MATSUMOTO, H., TOYAMA, Y. & OKADA, Y. 2006. Tetraspanin CD151 is expressed in osteoarthritic cartilage and is involved in pericellular activation of pro-matrix metalloproteinase 7 in osteoarthritic chondrocytes. *Arthritis Rheum*, 54, 3233-43.
- FUKUMOTO, T., SPERLING, J. W., SANYAL, A., FITZSIMMONS, J. S., REINHOLZ, G. G., CONOVER, C. A. & O'DRISCOLL, S. W. 2003. Combined effects of insulin-like growth

factor-1 and transforming growth factor-beta1 on periosteal mesenchymal cells during chondrogenesis in vitro. *Osteoarthritis Cartilage*, 11, 55-64.

- GAFFEN, S. L. 2009. The role of interleukin-17 in the pathogenesis of rheumatoid arthritis. *Current rheumatology reports*, 11, 365-370.
- GAO, S., LIU, L., ZHU, S., WANG, D., WU, Q., NING, G. & FENG, S. 2020. MicroRNA-197 regulates chondrocyte proliferation, migration, and inflammation in pathogenesis of osteoarthritis by targeting EIF4G2. *Bioscience reports*, 40, BSR20192095.
- GAO, Y., FENG, B., HAN, S., ZHANG, K., CHEN, J., LI, C., WANG, R. & CHEN, L. 2016. The Roles of MicroRNA-141 in Human Cancers: From Diagnosis to Treatment. *Cellular Physiology and Biochemistry*, 38, 427-448.
- GAUDE, G. S. 2009. Pulmonary manifestations of gastroesophageal reflux disease. *Annals of thoracic medicine*, 4, 115-123.
- GAUDET, P., LIVSTONE, M. S., LEWIS, S. E. & THOMAS, P. D. 2011. Phylogenetic-based propagation of functional annotations within the Gene Ontology consortium. *Brief Bioinform*, 12, 449-62.
- GAVENIS, K., SCHUMACHER, C., SCHNEIDER, U., EISFELD, J., MOLLENHAUER, J. & SCHMIDT-ROHLFING, B. 2009. Expression of ion channels of the TRP family in articular chondrocytes from osteoarthritic patients: changes between native and in vitro propagated chondrocytes. *Mol Cell Biochem*, 321, 135-43.
- GHINI, F., RUBOLINO, C., CLIMENT, M., SIMEONE, I., MARZI, M. J. & NICASSIO, F. 2018. Endogenous transcripts control miRNA levels and activity in mammalian cells by target-directed miRNA degradation. *Nature Communications*, 9, 3119.
- GIBSON, G. & ASAHARA, H. 2013. microRNAs and cartilage. *J Orthop Res*, 31, 1333-44.
- GOETZL, E. J., RYNES, R. I. & STILLMAN, J. S. 1974. Abnormalities of respiratory gases in synovial fluid of patients with juvenile rheumatoid arthritis. 17, 450-454.
- GOLDRING, M. B., TSUCHIMOCHI, K. & IJIRI, K. 2006a. The control of chondrogenesis. 97, 33-44.
- GOLDRING, M. B., TSUCHIMOCHI, K. & IJIRI, K. 2006b. The control of chondrogenesis. *J Cell Biochem*, 97, 33-44.
- GOLOWASCH, J. & NADIM, F. 2015. Capacitance, Membrane. In: JAEGER, D. & JUNG, R. (eds.) *Encyclopedia of Computational Neuroscience*. New York, NY: Springer New York.
- GOSIEWSKA, A., REZANIA, A., DHANARAJ, S., VYAKARNAM, M., ZHOU, J., BURTIS, D., BROWN, L., KONG, W., ZIMMERMAN, M. & GEESIN, J. C. 2001. Development of a Three-Dimensional Transmigration Assay for Testing Cell–Polymer Interactions for Tissue Engineering Applications. *Tissue Engineering*, 7, 267-277.
- GRAD, S. & SALZMANN, G. M. 2009. Chondrozyten – ein Zelltyp, verschiedene Subpopulationen. *Der Orthopäde*, 38, 1038.
- GRADUS, B., ALON, I. & HORNSTEIN, E. 2011. miRNAs control tracheal chondrocyte differentiation. *Dev Biol*, 360, 58-65.
- GRAY, M. L., PIZZANELLI, A. M., GRODZINSKY, A. J. & LEE, R. C. 1988. Mechanical and physicochemical determinants of the chondrocyte biosynthetic response. 6, 777-792.
- GRIFFITH, M., GRIFFITH, O. L., MWENIFUMBO, J., GOYA, R., MORRISSY, A. S., MORIN, R. D., CORBETT, R., TANG, M. J., HOU, Y.-C., PUGH, T. J., ROBERTSON, G., CHITTARANJAN, S., ALLY, A., ASANO, J. K., CHAN, S. Y., LI, H. I., MCDONALD, H., TEAGUE, K., ZHAO, Y., ZENG, T., DELANEY, A., HIRST, M., MORIN, G. B., JONES, S. J. M., TAI, I. T. & MARRA, M. A. 2010. Alternative expression analysis by RNA sequencing. *Nature Methods*, 7, 843-847.

- GRIFFITHS-JONES S, G. R., VAN DONGEN S, BATEMAN A, ENRIGHT AJ 2006. miRBase: microRNA sequences, targets and gene nomenclature. *Nucleic Acids Res.* 2006, D140-144. 10.1093/nar/gkj112. 34 Database.
- GRIFFITHS-JONES, S., GROCOCK, R. J., VAN DONGEN, S., BATEMAN, A. & ENRIGHT, A. J. 2006. miRBase: microRNA sequences, targets and gene nomenclature. *Nucleic Acids Res*, 34, D140-4.
- GRIFFITHS-JONES, S., SAINI, H. K., VAN DONGEN, S. & ENRIGHT, A. J. 2008. miRBase: tools for microRNA genomics. *Nucleic Acids Res*, 36, D154-8.
- GRIFFITHS-JONES S, S. H., VAN DONGEN S, ENRIGHT AJ miRBase: tools for microRNA genomics. *Nucleic Acids Res.* 2008, D154-158. 36 Database.
- GRODZINSKY, A. J. 1983. Electromechanical and physicochemical properties of connective tissue. *Crit Rev Biomed Eng*, 9, 133-99.
- GU, Y. L., RONG, X. X., WEN, L. T., ZHU, G. X. & QIAN, M. Q. 2017. miR-195 inhibits the proliferation and migration of chondrocytes by targeting GIT1. *Mol Med Rep*, 15, 194-200.
- GUAN, L., SONG, Y., GAO, J., GAO, J. & WANG, K. 2016. Inhibition of calcium-activated chloride channel ANO1 suppresses proliferation and induces apoptosis of epithelium originated cancer cells. *Oncotarget*, 7, 78619-78630.
- GUENTHER, H. L., GUENTHER, H. E., FROESCH, E. R. & FLEISCH, H. 1982. Effect of insulin-like growth factor on collagen and glycosaminoglycan synthesis by rabbit articular chondrocytes in culture. *Experientia*, 38, 979-81.
- GULYAEVA, L. F. & KUSHLINSKIY, N. E. 2016. Regulatory mechanisms of microRNA expression. *Journal of translational medicine*, 14, 143-143.
- HAIDAR, O., O'NEILL, N., STAUNTON, C. A., BAVAN, S., O'BRIEN, F., ZOUGGARI, S., SHARIF, U., MOBASHERI, A., KUMAGAI, K. & BARRETT-JOLLEY, R. 2020. Pro-inflammatory Cytokines Drive Deregulation of Potassium Channel Expression in Primary Synovial Fibroblasts. *Frontiers in physiology*, 11, 226-226.
- HAMADA, T., SAKAI, T., HIRAIWA, H., NAKASHIMA, M., ONO, Y., MITSUYAMA, H. & ISHIGURO, N. 2013. Surface markers and gene expression to characterize the differentiation of monolayer expanded human articular chondrocytes. *Nagoya journal of medical science*, 75, 101-111.
- HAN, Y. & LEFEBVRE, V. 2008. L-Sox5 and Sox6 Drive Expression of the Aggrecan Gene in Cartilage by Securing Binding of Sox9 to a Far-Upstream Enhancer. *Molecular and Cellular Biology*, 28, 4999.
- HARTZELL, H. C., YU, K., XIAO, Q., CHIEN, L.-T. & QU, Z. 2009. Anoctamin/TMEM16 family members are Ca²⁺-activated Cl⁻ channels. *The Journal of physiology*, 587, 2127-2139.
- HASHIMOTO, M., NAKASA, T., HIKATA, T. & ASAHARA, H. 2008. Molecular network of cartilage homeostasis and osteoarthritis. *Med Res Rev*, 28, 464-81.
- HASHIMOTO, S., CREIGHTON-ACHERMANN, L., TAKAHASHI, K., AMIEL, D., COUTTS, R. D. & LOTZ, M. 2002. Development and regulation of osteophyte formation during experimental osteoarthritis. *Osteoarthritis Cartilage*, 10, 180-7.
- HDUD, I. M., MOBASHERI, A. & LOUGHNA, P. T. 2014. Effect of osmotic stress on the expression of TRPV4 and BKCa channels and possible interaction with ERK1/2 and p38 in cultured equine chondrocytes. *Am J Physiol Cell Physiol*, 306, C1050-7.
- HENRY, S. P., LIANG, S. D., AKDEMIR, K. C. & DE CROMBRUGGHE, B. 2012. The Postnatal Role of Sox9 in Cartilage. *Journal of Bone and Mineral Research*, 27, 2511-2525.
- HILTON, M. J., TU, X., COOK, J., HU, H. & LONG, F. 2005. Ihh controls cartilage development by antagonizing Gli3, but requires additional effectors to regulate osteoblast and vascular development. *Development*, 132, 4339.

- HODGKIN, A. L. & HUXLEY, A. F. 1952a. The components of membrane conductance in the giant axon of *Loligo*. *The Journal of physiology*, 116, 473-496.
- HODGKIN, A. L. & HUXLEY, A. F. 1952b. A quantitative description of membrane current and its application to conduction and excitation in nerve. 117, 500-544.
- HOFFMANN, E. K., HOLM, N. B. & LAMBERT, I. H. 2014. Functions of volume-sensitive and calcium-activated chloride channels. *IUBMB Life*, 66, 257-67.
- HOFFMANN, E. K., SØRENSEN, B. H., SAUTER, D. P. R. & LAMBERT, I. H. 2015. Role of volume-regulated and calcium-activated anion channels in cell volume homeostasis, cancer and drug resistance. *Channels (Austin, Tex.)*, 9, 380-396.
- HOLLANDER, A., MACCHIARINI, P., GORDIJJN, B. & BIRCHALL, M. 2009. The first stem cell-based tissue-engineered organ replacement: implications for regenerative medicine and society. *Regenerative Medicine*, 4, 147-148.
- HOLZER, P. 2009. Acid-sensitive ion channels and receptors. *Handbook of experimental pharmacology*, 283-332.
- HOPPER, N., HENSON, F., BROOKS, R., ALI, E., RUSHTON, N. & WARDALE, J. 2015. Peripheral blood derived mononuclear cells enhance osteoarthritic human chondrocyte migration. *Arthritis Research & Therapy*, 17, 199.
- HU, M., XIA, M., CHEN, X., LIN, Z., XU, Y., MA, Y. & SU, L. 2010. MicroRNA-141 regulates Smad interacting protein 1 (SIP1) and inhibits migration and invasion of colorectal cancer cells. *Dig Dis Sci*, 55, 2365-72.
- HU, S., LI, L., HUANG, W., LIU, J., LAN, G., YU, S., PENG, L., XIE, X., YANG, L., NIAN, Y. & WANG, Y. 2018. CAV3.1 knockdown suppresses cell proliferation, migration and invasion of prostate cancer cells by inhibiting AKT. *Cancer management and research*, 10, 4603-4614.
- HUGHES, A. L., PAKHOMOVA, A. & BROWN, P. D. 2010. Regulatory volume increase in epithelial cells isolated from the mouse fourth ventricle choroid plexus involves Na(+)-H(+) exchange but not Na(+)-K(+)-2Cl(-) cotransport. *Brain Res*, 1323, 1-10.
- HWANG, H. W. & MENDELL, J. T. 2006. MicroRNAs in cell proliferation, cell death, and tumorigenesis. *British journal of cancer*, 94, 776-780.
- INDRAWATTANA, N., CHEN, G., TADOKORO, M., SHANN, L. H., OHGUSHI, H., TATEISHI, T., TANAKA, J. & BUNYARATVEJ, A. 2004. Growth factor combination for chondrogenic induction from human mesenchymal stem cell. *Biochem Biophys Res Commun*, 320, 914-9.
- ISHII, T. M., SILVIA, C., HIRSCHBERG, B., BOND, C. T., ADELMAN, J. P. & MAYLIE, J. 1997. A human intermediate conductance calcium-activated potassium channel. *Proceedings of the National Academy of Sciences of the United States of America*, 94, 11651-11656.
- JAY, G. D., TANTRAVAHU, U., BRITT, D. E., BARRACH, H. J. & CHA, C. J. 2001. Homology of lubricin and superficial zone protein (SZP): products of megakaryocyte stimulating factor (MSF) gene expression by human synovial fibroblasts and articular chondrocytes localized to chromosome 1q25. *J Orthop Res*, 19, 677-87.
- JEREMIASSE, B., MATTA, C., FELLOWS, C. R., BOOCOOCK, D. J., SMITH, J. R., LIDDELL, S., LAFEBER, F., VAN SPIL, W. E. & MOBASHERI, A. 2020. Alterations in the chondrocyte surfaceome in response to pro-inflammatory cytokines. *BMC Molecular and Cell Biology*, 21, 47.
- JI, M.-L., JIANG, H., WU, F., GENG, R., YA, L. K., LIN, Y. C., XU, J. H., WU, X. T. & LU, J. 2020. Precise targeting of miR-141/200c cluster in chondrocytes attenuates osteoarthritis development. *Annals of the Rheumatic Diseases*, annrheumdis-2020-218469.

- JI, Q., XU, X., XU, Y., FAN, Z., KANG, L., LI, L., LIANG, Y., GUO, J., HONG, T., LI, Z., ZHANG, Q., YE, Q. & WANG, Y. 2016. miR-105/Runx2 axis mediates FGF2-induced ADAMTS expression in osteoarthritis cartilage. *J Mol Med (Berl)*, 94, 681-94.
- JIA, L., LIU, W., GUAN, L., LU, M. & WANG, K. 2015. Inhibition of Calcium-Activated Chloride Channel ANO1/TMEM16A Suppresses Tumor Growth and Invasion in Human Lung Cancer. *PLoS one*, 10, e0136584-e0136584.
- JIN, L., ZHAO, J., JING, W., YAN, S., WANG, X., XIAO, C. & MA, B. 2014. Role of miR-146a in human chondrocyte apoptosis in response to mechanical pressure injury in vitro. *Int J Mol Med*, 34, 451-63.
- JONES, S. W., WATKINS, G., LE GOOD, N., ROBERTS, S., MURPHY, C. L., BROCKBANK, S. M., NEEDHAM, M. R., READ, S. J. & NEWHAM, P. 2009. The identification of differentially expressed microRNA in osteoarthritic tissue that modulate the production of TNF-alpha and MMP13. *Osteoarthritis Cartilage*, 17, 464-72.
- KANG, S. G., CHUNG, H., YOO, Y. D., LEE, J. G., CHOI, Y. I. & YU, Y. S. 2001. Mechanism of growth inhibitory effect of Mitomycin-C on cultured human retinal pigment epithelial cells: apoptosis and cell cycle arrest. *Curr Eye Res*, 22, 174-81.
- KANG, S. W., YOO, S. P. & KIM, B. S. 2007. Effect of chondrocyte passage number on histological aspects of tissue-engineered cartilage. *Biomed Mater Eng*, 17, 269-76.
- KEMPER, A. M., DRNEVICH, J., MCCUE, M. E. & MCCOY, A. M. 2019. Differential Gene Expression in Articular Cartilage and Subchondral Bone of Neonatal and Adult Horses. *Genes*, 10, 745.
- KENIRY, A., OXLEY, D., MONNIER, P., KYBA, M., DANDOLO, L., SMITS, G. & REIK, W. 2012. The H19 lincRNA is a developmental reservoir of miR-675 that suppresses growth and Igf1r. *Nat Cell Biol*, 14, 659-65.
- KENT, O. A., MULLENDORE, M., WENTZEL, E. A., LÓPEZ-ROMERO, P., TAN, A. C., ALVAREZ, H., WEST, K., OCHS, M. F., HIDALGO, M., ARKING, D. E., MAITRA, A. & MENDELL, J. T. 2009. A resource for analysis of microRNA expression and function in pancreatic ductal adenocarcinoma cells. *Cancer biology & therapy*, 8, 2013-2024.
- KIANI, C., CHEN, L., WU, Y. J., YEE, A. J. & YANG, B. B. 2002. Structure and function of aggrecan. *Cell Research*, 12, 19-32.
- KIM, D., SONG, J., HAN, J., KIM, Y., CHUN, C. H. & JIN, E. J. 2013. Two non-coding RNAs, MicroRNA-101 and HOTTIP contribute cartilage integrity by epigenetic and homeotic regulation of integrin- α 1. *Cell Signal*, 25, 2878-87.
- KIM, J.-Y., YOUN, H. Y., CHOI, J., BAEK, S. K., KWON, S. Y., EUN, B. K., PARK, J.-Y. & OH, K. H. 2019. Anoctamin-1 affects the migration and invasion of anaplastic thyroid carcinoma cells. *Animal Cells and Systems*, 23, 294-301.
- KIRILAK, Y., PAVLOS, N. J., WILLERS, C. R., HAN, R., FENG, H., XU, J., ASOKANANTHAN, N., STEWART, G. A., HENRY, P., WOOD, D. & ZHENG, M. H. 2006. Fibrin sealant promotes migration and proliferation of human articular chondrocytes: possible involvement of thrombin and protease-activated receptors. *Int J Mol Med*, 17, 551-8.
- KIRSCH, T., SWOBODA, B. & NAH, H. D. 2000. Activation of annexin II and V expression, terminal differentiation, mineralization and apoptosis in human osteoarthritic cartilage. *Osteoarthritis and Cartilage*, 8, 294-302.
- KLAUSEN, T. K., PREISLER, S., PEDERSEN, S. F. & HOFFMANN, E. K. 2010. Monovalent ions control proliferation of Ehrlich Lettre ascites cells. 299, C714-C725.
- KNIGHT, M. M., MCGLASHAN, S. R., GARCIA, M., JENSEN, C. G. & POOLE, C. A. 2009. Articular chondrocytes express connexin 43 hemichannels and P2 receptors - a

putative mechanoreceptor complex involving the primary cilium? *J Anat*, 214, 275-83.

- KOBAYASHI, M., SQUIRES, G. R., MOUSA, A., TANZER, M., ZUKOR, D. J., ANTONIOU, J., FEIGE, U. & POOLE, A. R. 2005. Role of interleukin-1 and tumor necrosis factor alpha in matrix degradation of human osteoarthritic cartilage. *Arthritis Rheum*, 52, 128-35.
- KOBAYASHI, T., LU, J., COBB, B. S., RODDA, S. J., MCMAHON, A. P., SCHIPANI, E., MERKENSCHLAGER, M. & KRONENBERG, H. M. 2008. Dicer-dependent pathways regulate chondrocyte proliferation and differentiation. *Proc Natl Acad Sci U S A*, 105, 1949-54.
- KOFOED, H. 1986. Synovitis causes hypoxia and acidity in synovial fluid and subchondral bone. *Injury*, 17, 391-4.
- KUKURBA, K. R. & MONTGOMERY, S. B. 2015. RNA Sequencing and Analysis. 2015, [pdb.top084970](https://pubmed.ncbi.nlm.nih.gov/26084970/).
- KUMAGAI, K., TOYODA, F., STAUNTON, C. A., MAEDA, T., OKUMURA, N., MATSUURA, H., MATSUSUE, Y., IMAI, S. & BARRETT-JOLLEY, R. 2016. Activation of a chondrocyte volume-sensitive Cl(-) conductance prior to macroscopic cartilage lesion formation in the rabbit knee anterior cruciate ligament transection osteoarthritis model. *Osteoarthritis and cartilage*, 24, 1786-1794.
- KUNZELMANN, K. 2015. TMEM16, LRRC8A, bestrophin: chloride channels controlled by Ca(2+) and cell volume. *Trends Biochem Sci*, 40, 535-43.
- KUNZELMANN, K., TIAN, Y., MARTINS, J. R., FARIA, D., KONGSUPHOL, P., OUSINGSAWAT, J., THEVENOD, F., ROUSSA, E., ROCK, J. & SCHREIBER, R. 2011. Anoctamins. *Pflugers Arch*, 462, 195-208.
- KURITA, K., SHINOMURA, T., UJITA, M., ZAKO, M., KIDA, D., IWATA, H. & KIMATA, K. 1996. Occurrence of PG-Lb, a leucine-rich small chondroitin/dermatan sulphate proteoglycan in mammalian epiphyseal cartilage: molecular cloning and sequence analysis of the mouse cDNA. *Biochem J*, 318 (Pt 3), 909-14.
- KURITA, T., YAMAMURA, H., SUZUKI, Y., GILES, W. R. & IMAIZUMI, Y. 2015. The CIC-7 Chloride Channel Is Downregulated by Hypoosmotic Stress in Human Chondrocytes. *Mol Pharmacol*, 88, 113-20.
- KWAN, A. P., CUMMINGS, C. E., CHAPMAN, J. A. & GRANT, M. E. 1991. Macromolecular organization of chicken type X collagen in vitro. *J Cell Biol*, 114, 597-604.
- LAGOS-QUINTANA, M., RAUHUT, R., LENDECKEL, W. & TUSCHL, T. 2001. Identification of novel genes coding for small expressed RNAs. *Science*, 294, 853-8.
- LAMMI, M. J., PILTTI, J., PRITTINEN, J. & QU, C. 2018. Challenges in Fabrication of Tissue-Engineered Cartilage with Correct Cellular Colonization and Extracellular Matrix Assembly. *International journal of molecular sciences*, 19, 2700.
- LANG, F., RITTER, M., GAMPER, N., HUBER, S., FILLON, S., TANNEUR, V., LEPPLE-WIENHUES, A., SZABO, I. & GULBINS, E. 2000. Cell volume in the regulation of cell proliferation and apoptotic cell death. *Cell Physiol Biochem*, 10, 417-28.
- LATORRE, R., OBERHAUSER, A., LABARCA, P. & ALVAREZ, O. 1989. Varieties of calcium-activated potassium channels. *Annu Rev Physiol*, 51, 385-99.
- LAUING, K. L., CORTES, M., DOMOWICZ, M. S., HENRY, J. G., BARIA, A. T. & SCHWARTZ, N. B. 2014. Aggrecan is required for growth plate cytoarchitecture and differentiation. *Developmental biology*, 396, 224-236.
- LEBLANC, K. T., WALCOTT, M. E., GAUR, T., O'CONNELL, S. L., BASIL, K., TADIRI, C. P., MASON-SAVAS, A., SILVA, J. A., VAN WIJNEN, A. J., STEIN, J. L., STEIN, G. S., AYERS, D. C., LIAN, J. B. & FANNING, P. J. 2015. Runx1 Activities in Superficial Zone

Chondrocytes, Osteoarthritic Chondrocyte Clones and Response to Mechanical Loading. 230, 440-448.

- LEDDY, H. A., MCNULTY, A. L., GUILAK, F. & LIEDTKE, W. 2014. Unraveling the mechanism by which TRPV4 mutations cause skeletal dysplasias. *Rare Dis*, 2, e962971.
- LEE, R. B. & URBAN, J. P. 1997. Evidence for a negative Pasteur effect in articular cartilage. *Biochem J*, 321 (Pt 1), 95-102.
- LEE, R. C., FEINBAUM, R. L. & AMBROS, V. 1993. The *C. elegans* heterochronic gene *lin-4* encodes small RNAs with antisense complementarity to *lin-14*. *Cell*, 75.
- LEE, W., GUILAK, F. & LIEDTKE, W. 2017. Role of Piezo Channels in Joint Health and Injury. *Curr Top Membr*, 79, 263-273.
- LEE, Y., AHN, C., HAN, J., CHOI, H., KIM, J., YIM, J., LEE, J., PROVOST, P., RÅDMARK, O., KIM, S. & KIM, V. N. 2003. The nuclear RNase III Drosha initiates microRNA processing. *Nature*, 425, 415-9.
- LEE, Y., JEON, K., LEE, J. T., KIM, S. & KIM, V. N. 2002. MicroRNA maturation: stepwise processing and subcellular localization. *Embo j*, 21, 4663-70.
- LEFEBVRE, V., BEHRINGER, R. R. & DE CROMBRUGGHE, B. 2001. L-Sox5, Sox6 and Sox9 control essential steps of the chondrocyte differentiation pathway. *Osteoarthritis Cartilage*, 9 Suppl A, S69-75.
- LEFEBVRE, V., LI, P. & DE CROMBRUGGHE, B. 1998a. A new long form of Sox5 (L-Sox5), Sox6 and Sox9 are coexpressed in chondrogenesis and cooperatively activate the type II collagen gene. *The EMBO Journal*, 17, 5718-5733.
- LEFEBVRE, V., LI, P. & DE CROMBRUGGHE, B. 1998b. A new long form of Sox5 (L-Sox5), Sox6 and Sox9 are coexpressed in chondrogenesis and cooperatively activate the type II collagen gene. *Embo j*, 17, 5718-33.
- LEMPKA, S. & MCINTYRE, C. 2015. Resistivity/Conductivity of Extracellular Medium. In: JAEGER, D. & JUNG, R. (eds.) *Encyclopedia of Computational Neuroscience*. New York, NY: Springer New York.
- LEVICK, J. R. 1990. Hypoxia and acidosis in chronic inflammatory arthritis; relation to vascular supply and dynamic effusion pressure. *The Journal of rheumatology*, 17, 579-582.
- LEWIS, R., ASPLIN, K. E., BRUCE, G., DART, C., MOBASHERI, A. & BARRETT-JOLLEY, R. 2011a. The Role of the Membrane Potential in Chondrocyte Volume Regulation. *Journal of Cellular Physiology*, 226, 2979-2986.
- LEWIS, R., FEETHAM, C. & BARRETT-JOLLEY, R. 2011b. Cell volume control in chondrocytes. *Cellular Physiology and Biochemistry*, 28, 1111-1122.
- LEWIS, R., FEETHAM, C. H. & BARRETT-JOLLEY, R. 2011c. Cell Volume Regulation in Chondrocytes. *Cellular Physiology and Biochemistry*, 28, 1111-1122.
- LEWIS, R., FEETHAM, C. H., GENTLES, L., PENNY, J., TREGILGAS, L., TOHAMI, W., MOBASHERI, A. & BARRETT-JOLLEY, R. 2013a. Benzamil sensitive ion channels contribute to volume regulation in canine chondrocytes. *Br J Pharmacol*, 168, 1584-96.
- LEWIS, R., MAY, H., MOBASHERI, A. & BARRETT-JOLLEY, R. 2013b. Chondrocyte channel transcriptomics: do microarray data fit with expression and functional data? *Channels (Austin, Tex.)*, 7, 459-467.
- LI, C., HU, Q., CHEN, Z., SHEN, B., YANG, J., KANG, P., ZHOU, Z. & PEI, F. 2018a. MicroRNA-140 Suppresses Human Chondrocytes Hypertrophy by Targeting SMAD1 and Controlling the Bone Morphogenetic Protein Pathway in Osteoarthritis. *Am J Med Sci*, 355, 477-487.

- LI, J., HUANG, J., DAI, L., YU, D., CHEN, Q., ZHANG, X. & DAI, K. 2012. miR-146a, an IL-1 β responsive miRNA, induces vascular endothelial growth factor and chondrocyte apoptosis by targeting Smad4. *Arthritis Res Ther*, 14, R75.
- LI, X., HE, P., LI, Z., WANG, H., LIU, M., XIAO, Y., XU, D., KANG, Y. & WANG, H. 2018b. Interleukin-1 β -mediated suppression of microRNA-27a-3p activity in human cartilage via MAPK and NF- κ B pathways: A potential mechanism of osteoarthritis pathogenesis. *Mol Med Rep*, 18, 541-549.
- LI, Y., JIANG, W., WANG, H., DENG, Z., ZENG, C., TU, M., LI, L., XIAO, W., GAO, S., LUO, W. & LEI, G. 2016. Osteopontin Promotes Expression of Matrix Metalloproteinase 13 through NF- κ B Signaling in Osteoarthritis. *BioMed Research International*, 2016, 6345656.
- LIANG, H. T., FENG, X. C. & MA, T. H. 2008. Water channel activity of plasma membrane affects chondrocyte migration and adhesion. *Clin Exp Pharmacol Physiol*, 35, 7-10.
- LIANG, Z., LI, X., LIU, S., LI, C., WANG, X. & XING, J. 2019. MiR-141-3p inhibits cell proliferation, migration and invasion by targeting TRAF5 in colorectal cancer. *Biochemical and Biophysical Research Communications*, 514, 699-705.
- LIN, S.-S., TZENG, B.-H., LEE, K.-R., SMITH, R. J. H., CAMPBELL, K. P. & CHEN, C.-C. 2014a. Ca²⁺-activated Cl⁻ channels are required for the NFAT-dependent Sox9 expression in tracheal cartilage. *Proceedings of the National Academy of Sciences*, 111, E1990.
- LIN, S. S., TZENG, B. H., LEE, K. R., SMITH, R. J., CAMPBELL, K. P. & CHEN, C. C. 2014b. Cav3.2 T-type calcium channel is required for the NFAT-dependent Sox9 expression in tracheal cartilage. *Proc Natl Acad Sci U S A*, 111, E1990-8.
- LITTLE, C. B., HUGHES, C. E., CURTIS, C. L., JONES, S. A., CATERSON, B. & FLANNERY, C. R. 2002. Cyclosporin A inhibition of aggrecanase-mediated proteoglycan catabolism in articular cartilage. *Arthritis & Rheumatism*, 46, 124-129.
- LIU, B., LINLEY, J. E., DU, X., ZHANG, X., OOI, L., ZHANG, H. & GAMPER, N. 2010. The acute nociceptive signals induced by bradykinin in rat sensory neurons are mediated by inhibition of M-type K⁺ channels and activation of Ca²⁺-activated Cl⁻ channels. *The Journal of clinical investigation*, 120, 1240-1252.
- LONG, K. J. & WALSH, K. B. 1994. A calcium-activated potassium channel in growth plate chondrocytes: regulation by protein kinase A. *Biochem Biophys Res Commun*, 201, 776-81.
- LOVE, M. I., HUBER, W. & ANDERS, S. 2014. Moderated estimation of fold change and dispersion for RNA-seq data with DESeq2. *Genome Biology*, 15, 550.
- LU, J., XU, F. & ZHANG, J. 2019. Inhibition of angiotensin II-induced cerebrovascular smooth muscle cell proliferation by LRRc8A downregulation through suppressing PI3K/AKT activation. *Hum Cell*, 32, 316-325.
- LU, Y., XU, Y., YIN, Z., YANG, X., JIANG, Y. & GUI, J. 2013. Chondrocyte migration affects tissue-engineered cartilage integration by activating the signal transduction pathways involving Src, PLC γ 1, and ERK1/2. *Tissue Eng Part A*, 19, 2506-16.
- LU, Y., ZHANG, Y., WANG, N., PAN, Z., GAO, X., ZHANG, F., ZHANG, Y., SHAN, H., LUO, X., BAI, Y., SUN, L., SONG, W., XU, C., WANG, Z. & YANG, B. 2010. MicroRNA-328 contributes to adverse electrical remodeling in atrial fibrillation. *Circulation*, 122, 2378-87.
- LUND, E., GÜTTINGER, S., CALADO, A., DAHLBERG, J. E. & KUTAY, U. 2004. Nuclear export of microRNA precursors. *Science*, 303, 95-8.
- LUYTEN, F. P., HASCALL, V. C., NISSLEY, S. P., MORALES, T. I. & REDDI, A. H. 1988. Insulin-like growth factors maintain steady-state metabolism of proteoglycans in bovine articular cartilage explants. *Arch Biochem Biophys*, 267, 416-25.

- LYTLE, C. 1997. Activation of the Avian Erythrocyte Na-K-Cl Cotransport Protein by Cell Shrinkage, cAMP, Fluoride, and Calyculin-A Involves Phosphorylation at Common Sites. *272*, 15069-15077.
- MACCHIARINI, P., JUNGEBLUTH, P., GO, T., ASNAGHI, M. A., REES, L. E., COGAN, T. A., DODSON, A., MARTORELL, J., BELLINI, S., PARNIGOTTO, P. P., DICKINSON, S. C., HOLLANDER, A. P., MANTERO, S., CONCONI, M. T. & BIRCHALL, M. A. 2008. Clinical transplantation of a tissue-engineered airway. *The Lancet*, *372*, 2023-2030.
- MAIQUES, O., BARCELÓ, C., PANOSA, A., PIJUAN, J., ORGAZ, J. L., RODRIGUEZ-HERNANDEZ, I., MATAS-NADAL, C., TELL, G., VILELLA, R., FABRA, A., PUIG, S., SANZ-MORENO, V., MATIAS-GUIU, X., CANTI, C., HERREROS, J., MARTI, R. M. & MACIÀ, A. 2018. T-type calcium channels drive migration/invasion in BRAFV600E melanoma cells through Snail1. *Pigment Cell & Melanoma Research*, *31*, 484-495.
- MALECKAR, M., MARTÍN-VASALLO, P., GILES, W. & MOBASHERI, A. 2020. Physiological Effects of the Electrogenic Current Generated by the Na⁺/K⁺ Pump in Mammalian Articular Chondrocytes. *2*, 258-268.
- MALECKAR, M. M., CLARK, R. B., VOTTA, B. & GILES, W. R. 2018. The Resting Potential and K⁺ Currents in Primary Human Articular Chondrocytes. *9*.
- MALEMUD, C. J. 2018a. MicroRNAs and Osteoarthritis. *Cells*, *7*.
- MALEMUD, C. J. 2018b. MicroRNAs and Osteoarthritis. *Cells*, *7*, 92.
- MANIWA, S., OCHI, M., MOTOMURA, T., NISHIKORI, T., CHEN, J. & NAORA, H. 2001. Effects of hyaluronic acid and basic fibroblast growth factor on motility of chondrocytes and synovial cells in culture. *Acta Orthop Scand*, *72*, 299-303.
- MANKIN, H. J. & THRASHER, A. Z. 1975. Water content and binding in normal and osteoarthritic human cartilage. *J Bone Joint Surg Am*, *57*, 76-80.
- MAO, J., WANG, L., FAN, A., WANG, J., XU, B., JACOB, T. J. & CHEN, L. 2007. Blockage of volume-activated chloride channels inhibits migration of nasopharyngeal carcinoma cells. *Cell Physiol Biochem*, *19*, 249-58.
- MARCINOWSKI, L., TANGUY, M., KRMPOTIC, A., RÄDLE, B., LISNIĆ, V. J., TUDDENHAM, L., CHANE-WOON-MING, B., RUZSICS, Z., ERHARD, F., BENKARTEK, C., BABIC, M., ZIMMER, R., TRGOVCICH, J., KOSZINOWSKI, U. H., JONJIC, S., PFEFFER, S. & DÖLKEN, L. 2012. Degradation of cellular mir-27 by a novel, highly abundant viral transcript is important for efficient virus replication in vivo. *PLoS Pathog*, *8*, e1002510.
- MARLOVITS, S., HOMBAUER, M., TRUPPE, M., VÈCSEI, V. & SCHLEGEL, W. 2004. Changes in the ratio of type-I and type-II collagen expression during monolayer culture of human chondrocytes. *J Bone Joint Surg Br*, *86*, 286-95.
- MARTINEZ-SANCHEZ, A., DUDEK, K. A. & MURPHY, C. L. 2012. Regulation of human chondrocyte function through direct inhibition of cartilage master regulator SOX9 by microRNA-145 (miRNA-145). *J Biol Chem*, *287*, 916-24.
- MATHEW, J. L., SINGH, M. & MITTAL, S. K. 2004. Gastro-oesophageal reflux and bronchial asthma: current status and future directions. *Postgrad Med J*, *80*, 701-5.
- MATSUKAWA, T., SAKAI, T., YONEZAWA, T., HIRAIWA, H., HAMADA, T., NAKASHIMA, M., ONO, Y., ISHIZUKA, S., NAKAHARA, H., LOTZ, M. K., ASAHARA, H. & ISHIGURO, N. 2013. MicroRNA-125b regulates the expression of aggrecanase-1 (ADAMTS-4) in human osteoarthritic chondrocytes. *Arthritis Research & Therapy*, *15*, R28.
- MATTA, C. & ZAKANY, R. 2013. Calcium signalling in chondrogenesis: implications for cartilage repair. *Front Biosci (Schol Ed)*, *5*, 305-24.
- MATTA, C., ZÁKÁNY, R. & MOBASHERI, A. 2015a. Voltage-Dependent Calcium Channels in Chondrocytes: Roles in Health and Disease. *Current Rheumatology Reports*, *17*, 43.

- MATTA, C., ZÁKÁNY, R. & MOBASHERI, A. 2015b. Voltage-dependent calcium channels in chondrocytes: roles in health and disease. *Curr Rheumatol Rep*, 17, 43.
- MAU, E., WHETSTONE, H., YU, C., HOPYAN, S., WUNDER, J. S. & ALMAN, B. A. 2007. PTHrP regulates growth plate chondrocyte differentiation and proliferation in a Gli3 dependent manner utilizing hedgehog ligand dependent and independent mechanisms. *Developmental Biology*, 305, 28-39.
- MAZAR, J., DEYOUNG, K., KHAITAN, D., MEISTER, E., ALMODOVAR, A., GOYDOS, J., RAY, A. & PERERA, R. J. 2010. The regulation of miRNA-211 expression and its role in melanoma cell invasiveness. *PLoS One*, 5, e13779.
- MCCUTCHEN, C. W. 1962. The frictional properties of animal joints. *Wear*, 5, 1-17.
- MCKEE, T. J., PERLMAN, G., MORRIS, M. & KOMAROVA, S. V. 2019. Extracellular matrix composition of connective tissues: a systematic review and meta-analysis. *Scientific Reports*, 9, 10542.
- MEI, Z., HE, Y., FENG, J., SHI, J., DU, Y., QIAN, L., HUANG, Q. & JIE, Z. 2014. MicroRNA-141 promotes the proliferation of non-small cell lung cancer cells by regulating expression of PHLPP1 and PHLPP2. *FEBS letters*, 588, 3055-3061.
- MEIJER, H. A., KONG, Y. W., LU, W. T., WILCZYNSKA, A., SPRIGGS, R. V., ROBINSON, S. W., GODFREY, J. D., WILLIS, A. E. & BUSHELL, M. 2013. Translational Repression and eIF4A2 Activity Are Critical for MicroRNA-Mediated Gene Regulation. 340, 82-85.
- MELERO-MARTIN, J. M., SANTHALINGAM, S. & AL-RUBEAI, M. 2009. Methodology for optimal in vitro cell expansion in tissue engineering. *Adv Biochem Eng Biotechnol*, 112, 209-29.
- MENDELL, J. T. & OLSON, E. N. 2012. MicroRNAs in stress signaling and human disease. *Cell*, 148, 1172-87.
- MENDLER, M., EICH-BENDER, S. G., VAUGHAN, L., WINTERHALTER, K. H. & BRUCKNER, P. 1989. Cartilage contains mixed fibrils of collagen types II, IX, and XI. *J Cell Biol*, 108, 191-7.
- MI, H., MURUGANUJAN, A. & THOMAS, P. D. 2013. PANTHER in 2013: modeling the evolution of gene function, and other gene attributes, in the context of phylogenetic trees. *Nucleic Acids Res*, 41, D377-86.
- MILEDI, R. 1982. A calcium-dependent transient outward current in *Xenopus laevis* oocytes. 215, 491-497.
- MILLWARD-SADLER, S. J., WRIGHT, M. O. & SALTER, D. 2001. The NMDA receptor is involved in the response of normal human articular chondrocytes to mechanical stimulation. *The Journal of Pathology*, 193, 32A-32A.
- MININA, E., KRESCHER, C., NASKI, M. C., ORNITZ, D. M. & VORTKAMP, A. 2002. Interaction of FGF, Ihh/Pthlh, and BMP signaling integrates chondrocyte proliferation and hypertrophic differentiation. *Dev Cell*, 3, 439-49.
- MIYAKI, S., SATO, T., INOUE, A., OTSUKI, S., ITO, Y., YOKOYAMA, S., KATO, Y., TAKEMOTO, F., NAKASA, T., YAMASHITA, S., TAKADA, S., LOTZ, M. K., UENO-KUDO, H. & ASAHARA, H. 2010. MicroRNA-140 plays dual roles in both cartilage development and homeostasis. *Genes Dev*, 24, 1173-85.
- MOBASHERI, A., GENT, T. C., NASH, A. I., WOMACK, M. D., MOSKALUK, C. A. & BARRETT-JOLLEY, R. 2007. Evidence for functional ATP-sensitive (K(ATP)) potassium channels in human and equine articular chondrocytes. *Osteoarthritis Cartilage*, 15, 1-8.
- MOBASHERI, A., GENT, T. C., WOMACK, M. D., CARTER, S. D., CLEGG, P. D. & BARRETT-JOLLEY, R. 2005. Quantitative analysis of voltage-gated potassium currents from primary equine (*Equus caballus*) and elephant (*Loxodonta africana*) articular chondrocytes. *Am J Physiol Regul Integr Comp Physiol*, 289, R172-80.

- MOBASHERI, A., LEWIS, R., FERREIRA-MENDES, A., RUFINO, A., DART, C. & BARRETT-JOLLEY, R. 2012. Potassium channels in articular chondrocytes. *Channels (Austin, Tex.)*, 6, 416-425.
- MOBASHERI, A., LEWIS, R., MAXWELL, J. E., HILL, C., WOMACK, M. & BARRETT-JOLLEY, R. 2010. Characterization of a stretch-activated potassium channel in chondrocytes. *J Cell Physiol*, 223, 511-8.
- MOBASHERI, A. & MARPLES, D. 2004. Expression of the AQP-1 water channel in normal human tissues: a semiquantitative study using tissue microarray technology. *Am J Physiol Cell Physiol*, 286, C529-37.
- MOBASHERI, A., MATTA, C., UZIELIENÈ, I., BUDD, E., MARTÍN-VASALLO, P. & BERNOTIENE, E. 2019. The chondrocyte channelome: A narrative review. *Joint Bone Spine*, 86, 29-35.
- MOBASHERI, A., MOBASHERI, R., FRANCIS, M. J., TRUJILLO, E., ALVAREZ DE LA ROSA, D. & MARTÍN-VASALLO, P. 1998. Ion transport in chondrocytes: membrane transporters involved in intracellular ion homeostasis and the regulation of cell volume, free [Ca²⁺] and pH. *Histol Histopathol*, 13, 893-910.
- MOBASHERI, A., TRUJILLO, E., BELL, S., CARTER, S. D., CLEGG, P. D., MARTÍN-VASALLO, P. & MARPLES, D. 2004. Aquaporin water channels AQP1 and AQP3, are expressed in equine articular chondrocytes. *Vet J*, 168, 143-50.
- MOILANEN, L. J., HÄMÄLÄINEN, M., NUMMENMAA, E., ILMARINEN, P., VUOLTEENAHO, K., NIEMINEN, R. M., LEHTIMÄKI, L. & MOILANEN, E. 2015. Monosodium iodoacetate-induced inflammation and joint pain are reduced in TRPA1 deficient mice--potential role of TRPA1 in osteoarthritis. *Osteoarthritis Cartilage*, 23, 2017-26.
- MONSORO-BURQ, A. H. 2005. Sclerotome development and morphogenesis: when experimental embryology meets genetics. *Int J Dev Biol*, 49, 301-8.
- MORALES, T. I. 1991. Transforming growth factor-beta 1 stimulates synthesis of proteoglycan aggregates in calf articular cartilage organ cultures. *Arch Biochem Biophys*, 286, 99-106.
- MORALES, T. I. 2007. Chondrocyte moves: clever strategies? *Osteoarthritis Cartilage*, 15, 861-71.
- MORAN, Y., BARZILAI, M. G., LIEBESKIND, B. J. & ZAKON, H. H. 2015. Evolution of voltage-gated ion channels at the emergence of Metazoa. *The Journal of Experimental Biology*, 218, 515-525.
- MORTAZAVI, A., WILLIAMS, B. A., MCCUE, K., SCHAEFFER, L. & WOLD, B. 2008. Mapping and quantifying mammalian transcriptomes by RNA-Seq. *Nat Methods*, 5, 621-8.
- MOUW, J. K., IMLER, S. M. & LEVENSTON, M. E. 2007. Ion-channel regulation of chondrocyte matrix synthesis in 3D culture under static and dynamic compression. *Biomech Model Mechanobiol*, 6, 33-41.
- MOW, V. C., RATCLIFFE, A. & POOLE, A. R. 1992. Cartilage and diarthrodial joints as paradigms for hierarchical materials and structures. *Biomaterials*, 13, 67-97.
- MOW, V. C., WANG, C. C. & HUNG, C. T. 1999. The extracellular matrix, interstitial fluid and ions as a mechanical signal transducer in articular cartilage. *Osteoarthritis Cartilage*, 7, 41-58.
- MURAMATSU, S., WAKABAYASHI, M., OHNO, T., AMANO, K., OISHI, R., SUGAHARA, T., SHIOJIRI, S., TASHIRO, K., SUZUKI, Y., NISHIMURA, R., KUHARA, S., SUGANO, S., YONEDA, T. & MATSUDA, A. 2007. Functional gene screening system identified TRPV4 as a regulator of chondrogenic differentiation. *J Biol Chem*, 282, 32158-67.

- MURPHY, G. & LEE, M. H. 2005. What are the roles of metalloproteinases in cartilage and bone damage? *Annals of the Rheumatic Diseases*, 64, iv44.
- NAKAMURA, Y., HE, X., KATO, H., WAKITANI, S., KOBAYASHI, T., WATANABE, S., IIDA, A., TAHARA, H., WARMAN, M. L., WATANAPOKASIN, R. & POSTLETHWAIT, J. H. 2012. Sox9 is upstream of microRNA-140 in cartilage. *Appl Biochem Biotechnol*, 166, 64-71.
- NAKAMURA, Y., INLOES, J. B., KATAGIRI, T. & KOBAYASHI, T. 2011. Chondrocyte-specific microRNA-140 regulates endochondral bone development and targets Dnpep to modulate bone morphogenetic protein signaling. *Mol Cell Biol*, 31, 3019-28.
- NG, L. J., WHEATLEY, S., MUSCAT, G. E., CONWAY-CAMPBELL, J., BOWLES, J., WRIGHT, E., BELL, D. M., TAM, P. P., CHEAH, K. S. & KOOPMAN, P. 1997. SOX9 binds DNA, activates transcription, and coexpresses with type II collagen during chondrogenesis in the mouse. *Dev Biol*, 183, 108-21.
- NILIUS, B., EGGERMONT, J., VOETS, T., BUYSE, G., MANOLOPOULOS, V. & DROOGMANS, G. 1997. Properties of volume-regulated anion channels in mammalian cells. *Prog Biophys Mol Biol*, 68, 69-119.
- NUKA, S., ZHOU, W., HENRY, S. P., GENDRON, C. M., SCHULTZ, J. B., SHINOMURA, T., JOHNSON, J., WANG, Y., KEENE, D. R., RAMÍREZ-SOLIS, R., BEHRINGER, R. R., YOUNG, M. F. & HÖÖK, M. 2010. Phenotypic characterization of epiphycan-deficient and epiphycan/biglycan double-deficient mice. *Osteoarthritis and cartilage*, 18, 88-96.
- O'CONNOR, C. J., LEDDY, H. A., BENEFIELD, H. C., LIEDTKE, W. B. & GUILAK, F. 2014. TRPV4-mediated mechanotransduction regulates the metabolic response of chondrocytes to dynamic loading. *Proc Natl Acad Sci U S A*, 111, 1316-21.
- OHKUBO, T. & YAMAZAKI, J. 2012. T-type voltage-activated calcium channel Cav3.1, but not Cav3.2, is involved in the inhibition of proliferation and apoptosis in MCF-7 human breast cancer cells. *Int J Oncol*, 41, 267-75.
- OKADA, Y. 1997. Volume expansion-sensing outward-rectifier Cl⁻ channel: fresh start to the molecular identity and volume sensor. *Am J Physiol*, 273, C755-89.
- OKAMURA, K., HAGEN, J. W., DUAN, H., TYLER, D. M. & LAI, E. C. 2007. The mirtron pathway generates microRNA-class regulatory RNAs in Drosophila. *Cell*, 130, 89-100.
- OKUMURA, N., IMAI, S., TOYODA, F., ISOYA, E., KUMAGAI, K., MATSUURA, H. & MATSUSUE, Y. 2009. Regulatory role of tyrosine phosphorylation in the swelling-activated chloride current in isolated rabbit articular chondrocytes. *The Journal of physiology*, 587, 3761-3776.
- ONNERFJORD, P., KHABUT, A., REINHOLT, F. P., SVENSSON, O. & HEINEGARD, D. 2012. Quantitative proteomic analysis of eight cartilaginous tissues reveals characteristic differences as well as similarities between subgroups. *J Biol Chem*, 287, 18913-24.
- OSBORN, K. D., TRIPPEL, S. B. & MANKIN, H. J. 1989. Growth factor stimulation of adult articular cartilage. *J Orthop Res*, 7, 35-42.
- OTTE, P. 1991. Basic cell metabolism of articular cartilage. Manometric studies. *Z Rheumatol*, 50, 304-12.
- OZATA, D. M., GAINETDINOV, I., ZOCH, A., O'CARROLL, D. & ZAMORE, P. D. 2019. PIWI-interacting RNAs: small RNAs with big functions. *Nature Reviews Genetics*, 20, 89-108.
- PAN, A., TAN, Y., WANG, Z. & XU, G. 2019. STAT4 silencing underlies a novel inhibitory role of microRNA-141-3p in inflammation response of mice with experimental autoimmune myocarditis. 317, H531-H540.

- PAPAIOANNOU, G., INLOES, J. B., NAKAMURA, Y., PALTRINIERI, E. & KOBAYASHI, T. 2013. let-7 and miR-140 microRNAs coordinately regulate skeletal development. *Proc Natl Acad Sci U S A*, 110, E3291-300.
- PHAN, M. N., LEDDY, H. A., VOTTA, B. J., KUMAR, S., LEVY, D. S., LIPSHUTZ, D. B., LEE, S. H., LIEDTKE, W. & GUILAK, F. 2009. Functional characterization of TRPV4 as an osmotically sensitive ion channel in porcine articular chondrocytes. *Arthritis Rheum*, 60, 3028-37.
- POIRAUDEAU, S., LIEBERHERR, M., KERGOSIE, N. & CORVOL, M. T. 1997a. Different mechanisms are involved in intracellular calcium increase by insulin-like growth factors 1 and 2 in articular chondrocytes: voltage-gated calcium channels, and/or phospholipase C coupled to a pertussis-sensitive G-protein. *J Cell Biochem*, 64, 414-22.
- POIRAUDEAU, S., LIEBERHERR, M., KERGOSIE, N. & CORVOL, M. T. 1997b. Different mechanisms are involved in intracellular calcium increase by insulin-like growth factors 1 and 2 in articular chondrocytes: voltage-gated calcium channels, and/or phospholipase C coupled to a pertussis-sensitive G-protein. *Journal of cellular biochemistry*, 64, 414-422.
- PONCE, A., JIMENEZ-PEÑA, L. & TEJEDA-GUZMAN, C. 2012. The Role of Swelling-Activated Chloride Currents ($I_{CL,swell}$) in the Regulatory Volume Decrease Response of Freshly Dissociated Rat Articular Chondrocytes. *Cellular Physiology and Biochemistry*, 30, 1254-1270.
- POOLE, C. A. 1997. Review. Articular cartilage chondrons: form, function and failure. 191, 1-13.
- POROCA, D. R., PELIS, R. M. & CHAPPE, V. M. 2017. CIC Channels and Transporters: Structure, Physiological Functions, and Implications in Human Chloride Channelopathies. *Frontiers in pharmacology*, 8, 151-151.
- PORTER, S., CLARK, I. M., KEVORKIAN, L. & EDWARDS, D. R. 2005. The ADAMTS metalloproteinases. *The Biochemical journal*, 386, 15-27.
- POUYSSÉGUR, J., FRANCHI, A., L'ALLEMAIN, G. & PARIS, S. 1985. Cytoplasmic pH, a key determinant of growth factor-induced DNA synthesis in quiescent fibroblasts. *FEBS Lett*, 190, 115-9.
- PULLIG, O., WESELOH, G., RONNEBERGER, D., KÄKÖNEN, S. & SWOBODA, B. 2000. Chondrocyte differentiation in human osteoarthritis: expression of osteocalcin in normal and osteoarthritic cartilage and bone. *Calcif Tissue Int*, 67, 230-40.
- PUSCH, M., JORDT, S. E., STEIN, V. & JENTSCH, T. J. 1999. Chloride dependence of hyperpolarization-activated chloride channel gates. *The Journal of physiology*, 515 (Pt 2), 341-353.
- QIN, Q., CUI, L., ZHOU, Z., ZHANG, Z., WANG, Y. & ZHOU, C. 2019. Inhibition of microRNA-141-3p Reduces Hypoxia-Induced Apoptosis in H9c2 Rat Cardiomyocytes by Activating the RP105-Dependent PI3K/AKT Signaling Pathway. *Medical science monitor : international medical journal of experimental and clinical research*, 25, 7016-7025.
- QIU, W. & KASSEM, M. 2014. miR-141-3p inhibits human stromal (mesenchymal) stem cell proliferation and differentiation. *Biochimica et Biophysica Acta (BBA) - Molecular Cell Research*, 1843, 2114-2121.
- QIU, Z., DUBIN, A. E., MATHUR, J., TU, B., REDDY, K., MIRAGLIA, L. J., REINHARDT, J., ORTH, A. P. & PATAPOUTIAN, A. 2014. SWELL1, a plasma membrane protein, is an essential component of volume-regulated anion channel. *Cell*, 157, 447-458.
- R 2020. R: A language and environment for statistical computing. Vienna, Austria: R Foundation for Statistical Computing <https://www.R-project.org/>.

- RAMACHANDRAN, V. & CHEN, X. 2008. Degradation of microRNAs by a family of exoribonucleases in Arabidopsis. *Science*, 321, 1490-2.
- RANSOM, C. B., O'NEAL, J. T. & SONTHEIMER, H. 2001. Volume-activated chloride currents contribute to the resting conductance and invasive migration of human glioma cells. *J Neurosci*, 21, 7674-83.
- RATTANASOPHA, S., TONGKOBPETCH, S., SRICHOMTHONG, C., SIRIWAN, P., SUPHAPEETIPORN, K. & SHOTELERSUK, V. 2012. PDGFRa mutations in humans with isolated cleft palate. *Eur J Hum Genet*, 20, 1058-62.
- REINHART, B. J., SLACK, F. J., BASSON, M., PASQUINELLI, A. E., BETTINGER, J. C., ROUGVIE, A. E., HORVITZ, H. R. & RUVKUN, G. 2000. The 21-nucleotide let-7 RNA regulates developmental timing in *Caenorhabditis elegans*. *Nature*, 403, 901-6.
- REMST, D. F., BLANEY DAVIDSON, E. N. & VAN DER KRAAN, P. M. 2015. Unravelling osteoarthritis-related synovial fibrosis: a step closer to solving joint stiffness. *Rheumatology (Oxford)*, 54, 1954-63.
- REN, L., ZHU, R. & LI, X. 2016. Silencing miR-181a produces neuroprotection against hippocampus neuron cell apoptosis post-status epilepticus in a rat model and in children with temporal lobe epilepsy. *Genet Mol Res*, 15.
- ROBERTS, C. R., RAINS, J. K., PARÉ, P. D., WALKER, D. C., WIGGS, B. & BERT, J. L. 1997. Ultrastructure and tensile properties of human tracheal cartilage. *Journal of Biomechanics*, 31, 81-86.
- ROCK, J. R., FUTTNER, C. R. & HARFE, B. D. 2008a. The transmembrane protein TMEM16A is required for normal development of the murine trachea. *Developmental Biology*, 321, 141-149.
- ROCK, J. R., FUTTNER, C. R. & HARFE, B. D. 2008b. The transmembrane protein TMEM16A is required for normal development of the murine trachea. *Dev Biol*, 321, 141-9.
- ROCK, J. R., O'NEAL, W. K., GABRIEL, S. E., RANDELL, S. H., HARFE, B. D., BOUCHER, R. C. & GRUBB, B. R. 2009. Transmembrane protein 16A (TMEM16A) is a Ca²⁺-regulated Cl⁻ secretory channel in mouse airways. *The Journal of biological chemistry*, 284, 14875-14880.
- ROMAN-BLAS, J. A., STOKES, D. G. & JIMENEZ, S. A. 2007. Modulation of TGF-beta signaling by proinflammatory cytokines in articular chondrocytes. *Osteoarthritis Cartilage*, 15, 1367-77.
- ROSSIER, B. C., PRADERVAND, S., SCHILD, L. & HUMMLER, E. 2002. Epithelial sodium channel and the control of sodium balance: interaction between genetic and environmental factors. *Annu Rev Physiol*, 64, 877-97.
- ROTHENFLUH, D. A., BERMUDEZ, H., O'NEIL, C. P. & HUBBELL, J. A. 2008. Biofunctional polymer nanoparticles for intra-articular targeting and retention in cartilage. *Nature Materials*, 7, 248-254.
- RUAN, Z., OSEI-OWUSU, J., DU, J., QIU, Z. & LÜ, W. 2020. Structures and pH-sensing mechanism of the proton-activated chloride channel. *Nature*.
- RUBY, J. G., JAN, C. H. & BARTEL, D. P. 2007. Intronic microRNA precursors that bypass Drosha processing. *Nature*, 448, 83-6.
- RÜEGGER, S. & GROßHANS, H. 2012. MicroRNA turnover: when, how, and why. *Trends Biochem Sci*, 37, 436-46.
- RYCHKOV, G. Y., PUSCH, M., ROBERTS, M. L., JENTSCH, T. J. & BRETAG, A. H. 1998. Permeation and block of the skeletal muscle chloride channel, ClC-1, by foreign anions. *The Journal of general physiology*, 111, 653-665.
- SACHS, F. 1991. Mechanical transduction by membrane ion channels: a mini review. *Mol Cell Biochem*, 104, 57-60.

- SALAHUDEEN, M. S. & NISHTALA, P. S. 2017. An overview of pharmacodynamic modelling, ligand-binding approach and its application in clinical practice. *Saudi pharmaceutical journal : SPJ : the official publication of the Saudi Pharmaceutical Society*, 25, 165-175.
- SALTER, D. M., WRIGHT, M. O. & MILLWARD-SADLER, S. J. 2004. NMDA receptor expression and roles in human articular chondrocyte mechanotransduction. *Biorheology*, 41, 273-281.
- SANCHEZ-ADAMS, J., LEDDY, H. A., MCNULTY, A. L., O'CONNOR, C. J. & GUILAK, F. 2014. The mechanobiology of articular cartilage: bearing the burden of osteoarthritis. *Current rheumatology reports*, 16, 451-451.
- SÁNCHEZ, J. C., POWELL, T., STAINES, H. M. & WILKINS, R. J. 2006. Electrophysiological demonstration of voltage- activated H⁺ channels in bovine articular chondrocytes. *Cell Physiol Biochem*, 18, 85-90.
- SANDELL, L. J., NALIN, A. M. & REIFE, R. A. 1994. Alternative splice form of type II procollagen mRNA (IIA) is predominant in skeletal precursors and non-cartilaginous tissues during early mouse development. *Dev Dyn*, 199, 129-40.
- SAUTER, D. R. P., NOVAK, I., PEDERSEN, S. F., LARSEN, E. H. & HOFFMANN, E. K. 2015. ANO1 (TMEM16A) in pancreatic ductal adenocarcinoma (PDAC). *Pflugers Archiv : European journal of physiology*, 467, 1495-1508.
- SCHENA, M., SHALON, D., DAVIS, R. W. & BROWN, P. O. 1995. Quantitative monitoring of gene expression patterns with a complementary DNA microarray. *Science*, 270, 467-70.
- SCHMID, T. M. & LINSENMAYER, T. F. 1985. Immunohistochemical localization of short chain cartilage collagen (type X) in avian tissues. *J Cell Biol*, 100, 598-605.
- SCHREIBER, R., ULIYAKINA, I., KONGSUPHOL, P., WARTH, R., MIRZA, M., MARTINS, J. R. & KUNZELMANN, K. 2010. Expression and function of epithelial anoctamins. *J Biol Chem*, 285, 7838-45.
- SCHROEDER, B. C., CHENG, T., JAN, Y. N. & JAN, L. Y. 2008. Expression cloning of TMEM16A as a calcium-activated chloride channel subunit. *Cell*, 134, 1019-29.
- SCHULZE-TANZIL, G., DE SOUZA, P., VILLEGAS CASTREJON, H., JOHN, T., MERKER, H. J., SCHEID, A. & SHAKIBAEI, M. 2002. Redifferentiation of dedifferentiated human chondrocytes in high-density cultures. *Cell and Tissue Research*, 308, 371-379.
- SCHULZE-TANZIL, G., MOBASHERI, A., DE SOUZA, P., JOHN, T. & SHAKIBAEI, M. 2004. Loss of chondrogenic potential in dedifferentiated chondrocytes correlates with deficient Shc-Erk interaction and apoptosis. *Osteoarthritis Cartilage*, 12, 448-58.
- SCHWAB, A., FABIAN, A., HANLEY, P. J. & STOCK, C. 2012a. Role of Ion Channels and Transporters in Cell Migration. 92, 1865-1913.
- SCHWAB, A., FABIAN, A., HANLEY, P. J. & STOCK, C. 2012b. Role of ion channels and transporters in cell migration. *Physiol Rev*, 92, 1865-913.
- SHAKIBAEI, M. & MOBASHERI, A. 2003. Beta1-integrins co-localize with Na, K-ATPase, epithelial sodium channels (ENaC) and voltage activated calcium channels (VACC) in mechanoreceptor complexes of mouse limb-bud chondrocytes. *Histol Histopathol*, 18, 343-51.
- SHAKIBAEI, M., SCHULZE-TANZIL, G., DE SOUZA, P., JOHN, T., RAHMANZADEH, M., RAHMANZADEH, R. & MERKER, H.-J. 2001. Inhibition of Mitogen-activated Protein Kinase Kinase Induces Apoptosis of Human Chondrocytes. 276, 13289-13294.
- SHAO, Y., ALICKNAVITCH, M. & FARACH-CARSON, M. C. 2005. Expression of voltage sensitive calcium channel (VSCC) L-type Cav1.2 (alpha1C) and T-type Cav3.2 (alpha1H) subunits during mouse bone development. *Dev Dyn*, 234, 54-62.

- SHARMAN, J., HALE, V., HILLS, R., ROSSER, E., JONES, M., GREENHILL, S., HARMAR, A. & IUPHAR, N. C. 2009. IUPHAR-DB: An Expert-Curated, Peer-Reviewed Database of Receptors and Ion Channels. *Nature Precedings*.
- SHEN, M. R., DROOGMANS, G., EGGERMONT, J., VOETS, T., ELLORY, J. C. & NILIUS, B. 2000. Differential expression of volume-regulated anion channels during cell cycle progression of human cervical cancer cells. *The Journal of physiology*, 529 Pt 2, 385-394.
- SHENDURE, J. & JI, H. 2008. Next-generation DNA sequencing. *Nat Biotechnol*, 26, 1135-45.
- SHI, Y. & HE, M. 2014. Differential gene expression identified by RNA-Seq and qPCR in two sizes of pearl oyster (*Pinctada fucata*). *Gene*, 538, 313-322.
- SHINOMURA, T. & KIMATA, K. 1992. Proteoglycan-Lb, a small dermatan sulfate proteoglycan expressed in embryonic chick epiphyseal cartilage, is structurally related to osteoinductive factor. *J Biol Chem*, 267, 1265-70.
- SHIRAKI, T., KONDO, S., KATAYAMA, S., WAKI, K., KASUKAWA, T., KAWAJI, H., KODZIUS, R., WATAHIKI, A., NAKAMURA, M., ARAKAWA, T., FUKUDA, S., SASAKI, D., PODHAJSKA, A., HARBERS, M., KAWAI, J., CARNINCI, P. & HAYASHIZAKI, Y. 2003. Cap analysis gene expression for high-throughput analysis of transcriptional starting point and identification of promoter usage. *Proceedings of the National Academy of Sciences*, 100, 15776.
- SIVAN, S., NEIDLINGER-WILKE, C., WÜRTZ, K., MAROUDAS, A. & URBAN, J. P. 2006. Diurnal fluid expression and activity of intervertebral disc cells. *Biorheology*, 43, 283-91.
- SMITS, P., LI, P., MANDEL, J., ZHANG, Z., DENG, J. M., BEHRINGER, R. R., DE CROMBRUGGHE, B. & LEFEBVRE, V. 2001. The transcription factors L-Sox5 and Sox6 are essential for cartilage formation. *Dev Cell*, 1, 277-90.
- SONG, J., KIM, D., CHUN, C. H. & JIN, E. J. 2013. MicroRNA-375, a new regulator of cadherin-7, suppresses the migration of chondrogenic progenitors. *Cell Signal*, 25, 698-706.
- SONG, S.-J., TAO, J.-J., LI, S.-F., QIAN, X.-W., NIU, R.-W., WANG, C., ZHANG, Y.-H., CHEN, Y., WANG, K., ZHU, F., ZHU, C.-J., MA, G.-G., YANG, Y., PENG, X.-Q., ZHOU, R.-P. & CHEN, F.-H. 2020. 17 β -estradiol attenuates rat articular chondrocyte injury by targeting ASIC1a-mediated apoptosis. *Molecular and Cellular Endocrinology*, 505, 110742.
- SONG, T., MA, J., GUO, L., YANG, P., ZHOU, X. & YE, T. 2017. Regulation of chondrocyte functions by transient receptor potential cation channel V6 in osteoarthritis. 232, 3170-3181.
- SOPHIA FOX, A. J., BEDI, A. & RODEO, S. A. 2009. The Basic Science of Articular Cartilage: Structure, Composition, and Function. *Sports Health*, 1, 461-468.
- SOROCEANU, L., MANNING, T. J., JR. & SONTHEIMER, H. 1999. Modulation of glioma cell migration and invasion using Cl(-) and K(+) ion channel blockers. *J Neurosci*, 19, 5942-54.
- ST-JACQUES, B., HAMMERSCHMIDT, M. & MCMAHON, A. P. 1999. Indian hedgehog signaling regulates proliferation and differentiation of chondrocytes and is essential for bone formation. *Genes & development*, 13, 2072-2086.
- STANICH, J. E., GIBBONS, S. J., EISENMAN, S. T., BARDSLEY, M. R., ROCK, J. R., HARFE, B. D., ORDOG, T. & FARRUGIA, G. 2011. Ano1 as a regulator of proliferation. *American journal of physiology. Gastrointestinal and liver physiology*, 301, G1044-G1051.
- STOCK, C. & SCHWAB, A. 2009. Protons make tumor cells move like clockwork. *Pflugers Arch*, 458, 981-92.

- STOKES, D. G., LIU, G., DHARMAVARAM, R., HAWKINS, D., PIERA-VELAZQUEZ, S. & JIMENEZ, S. A. 2001. Regulation of type-II collagen gene expression during human chondrocyte de-differentiation and recovery of chondrocyte-specific phenotype in culture involves Sry-type high-mobility-group box (SOX) transcription factors. *Biochem J*, 360, 461-70.
- STRANGE, K., EMMA, F. & JACKSON, P. S. 1996. Cellular and molecular physiology of volume-sensitive anion channels. *Am J Physiol*, 270, C711-30.
- STRANGE, K., YAMADA, T. & DENTON, J. S. 2019. A 30-year journey from volume-regulated anion currents to molecular structure of the LRRC8 channel. *Journal of General Physiology*, 151, 100-117.
- STREIT, J. & LUX, H. D. 1987. Voltage dependent calcium currents in PC12 growth cones and cells during NGF-induced cell growth. *Pflügers Archiv*, 408, 634-641.
- SU, S., SHAO, J., ZHAO, Q., REN, X., CAI, W., LI, L., BAI, Q., CHEN, X., XU, B., WANG, J., CAO, J. & ZANG, W. 2017. MiR-30b Attenuates Neuropathic Pain by Regulating Voltage-Gated Sodium Channel Nav1.3 in Rats. 10.
- SUGIMOTO, T., YOSHINO, M., NAGAO, M., ISHII, S. & YABU, H. 1996a. Voltage-gated ionic channels in cultured rabbit articular chondrocytes. *Comparative Biochemistry and Physiology Part C: Pharmacology, Toxicology and Endocrinology*, 115, 223-232.
- SUGIMOTO, T., YOSHINO, M., NAGAO, M., ISHII, S. & YABU, H. 1996b. Voltage-gated ionic channels in cultured rabbit articular chondrocytes. *Comp Biochem Physiol C Pharmacol Toxicol Endocrinol*, 115, 223-32.
- SUMIYOSHI, K., KUBOTA, S., OHGAWARA, T., KAWATA, K., ABD EL KADER, T., NISHIDA, T., IKEDA, N., SHIMO, T., YAMASHIRO, T. & TAKIGAWA, M. 2013. Novel role of miR-181a in cartilage metabolism. *J Cell Biochem*, 114, 2094-100.
- SUMIYOSHI, K., KUBOTA, S., OHGAWARA, T., KAWATA, K., NISHIDA, T., SHIMO, T., YAMASHIRO, T. & TAKIGAWA, M. 2010. Identification of miR-1 as a micro RNA that supports late-stage differentiation of growth cartilage cells. *Biochem Biophys Res Commun*, 402, 286-90.
- SUMIYOSHI, N., ISHITOBI, H., MIYAKI, S., MIYADO, K., ADACHI, N. & OCHI, M. 2016. The role of tetraspanin CD9 in osteoarthritis using three different mouse models. *Biomed Res*, 37, 283-291.
- SUZUKI, Y., YAMAMURA, H., IMAIZUMI, Y., CLARK, R. B. & GILES, W. R. 2020a. K(+) and Ca(2+) Channels Regulate Ca(2+) Signaling in Chondrocytes: An Illustrated Review. *Cells*, 9.
- SUZUKI, Y., YAMAMURA, H., IMAIZUMI, Y., CLARK, R. B. & GILES, W. R. 2020b. K(+) and Ca(2+) Channels Regulate Ca(2+) Signaling in Chondrocytes: An Illustrated Review. *Cells*, 9, 1577.
- SWAIN, S., SARMANOVA, A., MALLEEN, C., KUO, C. F., COUPLAND, C., DOHERTY, M. & ZHANG, W. 2020. Trends in incidence and prevalence of osteoarthritis in the United Kingdom: findings from the Clinical Practice Research Datalink (CPRD). *Osteoarthritis and Cartilage*, 28, 792-801.
- SWINGLER, T. E., WHEELER, G., CARMONT, V., ELLIOTT, H. R., BARTER, M. J., ABU-ELMAGD, M., DONELL, S. T., BOOT-HANDFORD, R. P., HAJIHOSSEINI, M. K., MÜNSTERBERG, A., DALMAY, T., YOUNG, D. A. & CLARK, I. M. 2012. The expression and function of microRNAs in chondrogenesis and osteoarthritis. *Arthritis Rheum*, 64, 1909-19.
- SYEDA, R., QIU, Z., DUBIN, A. E., MURTHY, S. E., FLORENDO, M. N., MASON, D. E., MATHUR, J., CAHALAN, S. M., PETERS, E. C., MONTAL, M. & PATAPOUTIAN, A. 2016. LRRC8 Proteins Form Volume-Regulated Anion Channels that Sense Ionic Strength. *Cell*, 164, 499-511.

- TAKAHASHI, N., RIENECK, K., VAN DER KRAAN, P. M., VAN BEUNINGEN, H. M., VITTERS, E. L., BENDTZEN, K. & VAN DEN BERG, W. B. 2005. Elucidation of IL-1/TGF-beta interactions in mouse chondrocyte cell line by genome-wide gene expression. *Osteoarthritis Cartilage*, 13, 426-38.
- TAKEBAYASHI, T., IWAMOTO, M., JIKKO, A., MATSUMURA, T., ENOMOTO-IWAMOTO, M., MYOUKAI, F., KOYAMA, E., YAMAAI, T., MATSUMOTO, K., NAKAMURA, T. & ET AL. 1995. Hepatocyte growth factor/scatter factor modulates cell motility, proliferation, and proteoglycan synthesis of chondrocytes. *J Cell Biol*, 129, 1411-9.
- TAO, W., WANG, J., PARAK, W. J., FAROKHZAD, O. C. & SHI, J. 2019. Nanobuffering of pH-Responsive Polymers: A Known but Sometimes Overlooked Phenomenon and Its Biological Applications. *ACS Nano*, 13, 4876-4882.
- TARDIF, G., HUM, D., PELLETIER, J. P., DUVAL, N. & MARTEL-PELLETIER, J. 2009. Regulation of the IGFBP-5 and MMP-13 genes by the microRNAs miR-140 and miR-27a in human osteoarthritic chondrocytes. *BMC Musculoskelet Disord*, 10, 148.
- TEKIN, H., SANCHEZ, J. G., TSINMAN, T., LANGER, R. & KHADEMHOSEINI, A. 2011. Thermoresponsive Platforms for Tissue Engineering and Regenerative Medicine. *AIChE J*, 57, 3249-3258.
- THOMAS, P. D., CAMPBELL, M. J., KEJARIWAL, A., MI, H., KARLAK, B., DAVERMAN, R., DIEMER, K., MURUGANUJAN, A. & NARECHANIA, A. 2003. PANTHER: A Library of Protein Families and Subfamilies Indexed by Function. 13, 2129-2141.
- THOMAS, S. & BONCHEV, D. 2010. A survey of current software for network analysis in molecular biology. *Human Genomics*, 4, 353.
- THOMSON, D. W. & DINGER, M. E. 2016. Endogenous microRNA sponges: evidence and controversy. *Nat Rev Genet*, 17, 272-83.
- TROTTE, J., RITZMANN, D., LANG, V., SCHOLZ, P., PUL, Ü., KAUFMANN, R., BUERGER, C. & ERTONGUR-FAUTH, T. 2018. Hypotonic stress response of human keratinocytes involves LRRC8A as component of volume-regulated anion channels. 27, 1352-1360.
- TRUJILLO, E., ALVAREZ DE LA ROSA, D., MOBASHERI, A., AVILA, J., GONZÁLEZ, T. & MARTÍN-VASALLO, P. 1999a. Sodium transport systems in human chondrocytes. I. Morphological and functional expression of the Na⁺,K⁽⁺⁾-ATPase alpha and beta subunit isoforms in healthy and arthritic chondrocytes. *Histol Histopathol*, 14, 1011-22.
- TRUJILLO, E., ALVAREZ DE LA ROSA, D., MOBASHERI, A., GONZÁLEZ, T., CANESSA, C. M. & MARTÍN-VASALLO, P. 1999b. Sodium transport systems in human chondrocytes. II. Expression of ENaC, Na⁺/K⁺/2Cl⁻ cotransporter and Na⁺/H⁺ exchangers in healthy and arthritic chondrocytes. *Histology and histopathology*, 14, 1023-1031.
- TSUGA, K., TOHSE, N., YOSHINO, M., SUGIMOTO, T., YAMASHITA, T., ISHII, S. & YABU, H. 2002. Chloride conductance determining membrane potential of rabbit articular chondrocytes. *Journal of Membrane Biology*, 185, 75-81.
- TUDDENHAM, L., WHEELER, G., NTOUNIA-FOUSARA, S., WATERS, J., HAJIHOSEINI, M. K., CLARK, I. & DALMAY, T. 2006. The cartilage specific microRNA-140 targets histone deacetylase 4 in mouse cells. *FEBS Lett*, 580, 4214-7.
- UKAI, T., SATO, M., AKUTSU, H., UMEZAWA, A. & MOCHIDA, J. 2012. MicroRNA-199a-3p, microRNA-193b, and microRNA-320c are correlated to aging and regulate human cartilage metabolism. *J Orthop Res*, 30, 1915-22.
- UNWIN, N. 1993. Neurotransmitter action: opening of ligand-gated ion channels. *Cell*, 72 Suppl, 31-41.

- URBAN, J. P., HALL, A. C. & GEHL, K. A. 1993. Regulation of matrix synthesis rates by the ionic and osmotic environment of articular chondrocytes. *J Cell Physiol*, 154, 262-70.
- VAEZI, M. F. 2005. Atypical manifestations of gastroesophageal reflux disease. *MedGenMed*, 7, 25.
- VAN DEN BERG, W. B. 1999. The role of cytokines and growth factors in cartilage destruction in osteoarthritis and rheumatoid arthritis. *Z Rheumatol*, 58, 136-41.
- VAN ROOIJ, E. 2011. The art of microRNA research. *Circ Res*, 108, 219-34.
- VAN ROSSUM, G. & DRAKE JR, F. L. 1995. Python tutorial. Amsterdam, The Netherlands: Centrum voor Wiskunde en Informatica.
- VANONI, S., ZENG, C., MARELLA, S., UDDIN, J., WU, D., ARORA, K., PTASCHINSKI, C., QUE, J., NOAH, T., WAGGONER, L., BARSKI, A., KARTASHOV, A., ROCHMAN, M., WEN, T., MARTIN, L., SPENCE, J., COLLINS, M., MUKKADA, V., PUTNAM, P., NAREN, A., CHEHADE, M., ROTHENBERG, M. E. & HOGAN, S. P. 2020. Identification of anoctamin 1 (ANO1) as a key driver of esophageal epithelial proliferation in eosinophilic esophagitis. *Journal of Allergy and Clinical Immunology*, 145, 239-254.e2.
- VARELA, D., SIMON, F., RIVEROS, A., JØRGENSEN, F. & STUTZIN, A. 2004. NAD(P)H Oxidase-derived H₂O₂ Signals Chloride Channel Activation in Cell Volume Regulation and Cell Proliferation. 279, 13301-13304.
- VELCULESCU, V. E., ZHANG, L., VOGELSTEIN, B. & KINZLER, K. W. 1995. Serial analysis of gene expression. *Science*, 270, 484-7.
- VENN, M. & MAROUDAS, A. 1977. Chemical composition and swelling of normal and osteoarthrotic femoral head cartilage. I. Chemical composition. *Annals of the rheumatic diseases*, 36, 121-129.
- VON DER MARK, K., GAUSS, V., VON DER MARK, H. & MÜLLER, P. 1977. Relationship between cell shape and type of collagen synthesised as chondrocytes lose their cartilage phenotype in culture. *Nature*, 267, 531-532.
- VOSS, F. K., ULLRICH, F., MÜNCH, J., LAZAROW, K., LUTTER, D., MAH, N., ANDRADE-NAVARRO, M. A., VON KRIES, J. P., STAUBER, T. & JENTSCH, T. J. 2014. Identification of LRRC8 heteromers as an essential component of the volume-regulated anion channel VRAC. *Science*, 344, 634-8.
- WANG, J., WANG, X., HOLZ, J. D., RUTKOWSKI, T., WANG, Y., ZHU, Z. & DONG, Y. 2013. Runx1 Is Critical for PTH-induced Onset of Mesenchymal Progenitor Cell Chondrogenic Differentiation. *PLOS ONE*, 8, e74255.
- WANG, M., YANG, H., ZHENG, L. Y., ZHANG, Z., TANG, Y. B., WANG, G. L., DU, Y. H., LV, X. F., LIU, J., ZHOU, J. G. & GUAN, Y. Y. 2012. Downregulation of TMEM16A calcium-activated chloride channel contributes to cerebrovascular remodeling during hypertension by promoting basilar smooth muscle cell proliferation. *Circulation*, 125, 697-707.
- WANG, N., LI, P., LIU, W., WANG, N., LU, Z., FENG, J., ZENG, X., YANG, J., WANG, Y. & ZHAO, W. 2018. miR-141-3p suppresses proliferation and promotes apoptosis by targeting GLI2 in osteosarcoma cells. *Oncol Rep*, 39, 747-754.
- WANG, N., ZHENG, J., CHEN, Z., LIU, Y., DURA, B., KWAK, M., XAVIER-FERRUCIO, J., LU, Y.-C., ZHANG, M., RODEN, C., CHENG, J., KRAUSE, D. S., DING, Y., FAN, R. & LU, J. 2019. Single-cell microRNA-mRNA co-sequencing reveals non-genetic heterogeneity and mechanisms of microRNA regulation. *Nature Communications*, 10, 95.
- WANG, R., LU, Y., GUNASEKAR, S., ZHANG, Y., BENSON, C. J., CHAPLEAU, M. W., SAH, R. & ABOUD, F. M. 2017. The volume-regulated anion channel (LRRC8) in nodose neurons is sensitive to acidic pH. *JCI Insight*, 2.

- WANG, X. T., NAGABA, S., NAGABA, Y., LEUNG, S. W., WANG, J., QIU, W., ZHAO, P. L. & GUGGINO, S. E. 2000. Cardiac L-type calcium channel alpha 1-subunit is increased by cyclic adenosine monophosphate: messenger RNA and protein expression in intact bone. *J Bone Miner Res*, 15, 1275-85.
- WANG, Z. 2013. miRNA in the Regulation of Ion Channel/Transporter Expression. *Comprehensive Physiology*.
- WANG, Z., GERSTEIN, M. & SNYDER, M. 2009. RNA-Seq: a revolutionary tool for transcriptomics. *Nature reviews. Genetics*, 10, 57-63.
- WATANABE, H., KIMATA, K., LINE, S., STRONG, D., GAO, L. Y., KOZAK, C. A. & YAMADA, Y. 1994. Mouse cartilage matrix deficiency (cmd) caused by a 7 bp deletion in the aggrecan gene. *Nat Genet*, 7, 154-7.
- WATANABE, T., SATO, T., AMANO, T., KAWAMURA, Y., KAWAMURA, N., KAWAGUCHI, H., YAMASHITA, N., KURIHARA, H. & NAKAOKA, T. 2008. Dnm3os, a non-coding RNA, is required for normal growth and skeletal development in mice. *Dev Dyn*, 237, 3738-48.
- WEI, Y., WANG, Y., WANG, Y. & BAI, L. 2017. Transient Receptor Potential Vanilloid 5 Mediates Ca²⁺ Influx and Inhibits Chondrocyte Autophagy in a Rat Osteoarthritis Model. *Cell Physiol Biochem*, 42, 319-332.
- WELLEK, S. & ZIEGLER, P. 2017. EQUIVNONINF: Testing for Equivalence and Noninferiority. <https://CRAN.R-project.org/package=EQUIVNONINF>.
- WESSELS, H.-H., LEBEDEVA, S., HIRSEKORN, A., WURMUS, R., AKALIN, A., MUKHERJEE, N. & OHLER, U. 2019. Global identification of functional microRNA-mRNA interactions in Drosophila. *Nature Communications*, 10, 1626.
- WESTHOLM, J. O. & LAI, E. C. 2011. Mirtrons: microRNA biogenesis via splicing. *Biochimie*, 93, 1897-904.
- WIENHOLDS, E., KLOOSTERMAN, W. P., MISKA, E., ALVAREZ-SAAVEDRA, E., BEREZIKOV, E., DE BRUIJN, E., HORVITZ, H. R., KAUPPINEN, S. & PLASTERK, R. H. 2005. MicroRNA expression in zebrafish embryonic development. *Science*, 309, 310-1.
- WILHELM, B. T., MARGUERAT, S., WATT, S., SCHUBERT, F., WOOD, V., GOODHEAD, I., PENKETT, C. J., ROGERS, J. & BÄHLER, J. 2008. Dynamic repertoire of a eukaryotic transcriptome surveyed at single-nucleotide resolution. *Nature*, 453, 1239-43.
- WILKINS, R. J. & HALL, A. C. 1995. Control of matrix synthesis in isolated bovine chondrocytes by extracellular and intracellular pH. *Journal of cellular physiology*, 164, 474-481.
- WILSON, J. R., DUNCAN, N. A., GILES, W. R. & CLARK, R. B. 2004. A voltage-dependent K⁺ current contributes to membrane potential of acutely isolated canine articular chondrocytes. 557, 93-104.
- WINTER, J., JUNG, S., KELLER, S., GREGORY, R. I. & DIEDERICHS, S. 2009. Many roads to maturity: microRNA biogenesis pathways and their regulation. *Nat Cell Biol*, 11, 228-34.
- WOHLRAB, D., LEBEK, S., KRÜGER, T. & REICHEL, H. 2002. Influence of ion channels on the proliferation of human chondrocytes. *Biorheology*, 39, 55-61.
- WOHLRAB, D., VOCKE, M., KLAPPERSTÜCK, T. & HEIN, W. 2004. Effects of potassium and anion channel blockers on the cellular response of human osteoarthritic chondrocytes. *J Orthop Sci*, 9, 364-71.
- WOHLRAB, D., WOHLRAB, J., REICHEL, H. & HEIN, W. 2001. Is the proliferation of human chondrocytes regulated by ionic channels? *J Orthop Sci*, 6, 155-9.
- WOJDASIEWICZ, P., PONIATOWSKI, Ł. A. & SZUKIEWICZ, D. 2014. The Role of Inflammatory and Anti-Inflammatory Cytokines in the Pathogenesis of Osteoarthritis. *Mediators of Inflammation*, 2014, 561459.

- WRIGHT, M., JOBANPUTRA, P., BAVINGTON, C., SALTER, D. M. & NUKI, G. 1996. Effects of intermittent pressure-induced strain on the electrophysiology of cultured human chondrocytes: evidence for the presence of stretch-activated membrane ion channels. *Clin Sci (Lond)*, 90, 61-71.
- WU, A. R., NEFF, N. F., KALISKY, T., DALERBA, P., TREUTLEIN, B., ROTHENBERG, M. E., MBURU, F. M., MANTALAS, G. L., SIM, S., CLARKE, M. F. & QUAKE, S. R. 2014. Quantitative assessment of single-cell RNA-sequencing methods. *Nature Methods*, 11, 41-46.
- WU, H., WANG, H., GUAN, S., ZHANG, J., CHEN, Q., WANG, X., MA, K., ZHAO, P., ZHAO, H., YAO, W., JIN, F., XIAO, Q. & WEI, M. 2017. Cell-specific regulation of proliferation by Ano1/TMEM16A in breast cancer with different ER, PR, and HER2 status. *Oncotarget*, 8, 84996-85013.
- WU, M. H., URBAN, J. P., CUI, Z. F., CUI, Z. & XU, X. 2007. Effect of extracellular pH on matrix synthesis by chondrocytes in 3D agarose gel. *Biotechnol Prog*, 23, 430-4.
- WU, Q. Q. & CHEN, Q. 2000. Mechanoregulation of chondrocyte proliferation, maturation, and hypertrophy: ion-channel dependent transduction of matrix deformation signals. *Exp Cell Res*, 256, 383-91.
- WUELING, M. & VORTKAMP, A. 2011. Chondrocyte proliferation and differentiation. *Endocr Dev*, 21, 1-11.
- XING, Y., JING, H., ZHANG, Y., SUO, J. & QIAN, M. 2020a. MicroRNA-141-3p affected proliferation, chemosensitivity, migration and invasion of colorectal cancer cells by targeting EGFR. *The International Journal of Biochemistry & Cell Biology*, 118, 105643.
- XING, Y., JING, H., ZHANG, Y., SUO, J. & QIAN, M. 2020b. MicroRNA-141-3p affected proliferation, chemosensitivity, migration and invasion of colorectal cancer cells by targeting EGFR. *The international journal of biochemistry & cell biology*, 118, 105643.
- XIONG, G., LIU, C., YANG, G., FENG, M., XU, J., ZHAO, F., YOU, L., ZHOU, L., ZHENG, L., HU, Y., WANG, X., ZHANG, T. & ZHAO, Y. 2019. Long noncoding RNA GSTM3TV2 upregulates LAT2 and OLR1 by competitively sponging let-7 to promote gemcitabine resistance in pancreatic cancer. *Journal of Hematology & Oncology*, 12, 97.
- XU, J., WANG, W., CLARK, C. C. & BRIGHTON, C. T. 2009a. Signal transduction in electrically stimulated articular chondrocytes involves translocation of extracellular calcium through voltage-gated channels. *Osteoarthritis Cartilage*, 17, 397-405.
- XU, J., WANG, W., CLARK, C. C. & BRIGHTON, C. T. 2009b. Signal transduction in electrically stimulated articular chondrocytes involves translocation of extracellular calcium through voltage-gated channels. *Osteoarthritis and Cartilage*, 17, 397-405.
- XU, L., LI, Q., XU, D., WANG, Q., AN, Y., DU, Q., ZHANG, J., ZHU, Y. & MIAO, Y. 2014. hsa-miR-141 downregulates TM4SF1 to inhibit pancreatic cancer cell invasion and migration. *Int J Oncol*, 44, 459-466.
- XU, Y., WANG, Y. Q., WANG, A. T., YU, C. Y., LUO, Y., LIU, R. M., ZHAO, Y. J. & XIAO, J. H. 2020. Effect of CD44 on differentiation of human amniotic mesenchymal stem cells into chondrocytes via Smad and ERK signaling pathways. *Mol Med Rep*, 21, 2357-2366.
- YAMASAKI, K., NAKASA, T., MIYAKI, S., ISHIKAWA, M., DEIE, M., ADACHI, N., YASUNAGA, Y., ASAHARA, H. & OCHI, M. 2009. Expression of MicroRNA-146a in osteoarthritis cartilage. *Arthritis Rheum*, 60, 1035-41.
- YAMASHITA, S., MIYAKI, S., KATO, Y., YOKOYAMA, S., SATO, T., BARRIONUEVO, F., AKIYAMA, H., SCHERER, G., TAKADA, S. & ASAHARA, H. 2012. L-Sox5 and Sox6

proteins enhance chondrogenic miR-140 microRNA expression by strengthening dimeric Sox9 activity. *J Biol Chem*, 287, 22206-15.

- YAN, C., WANG, Y., SHEN, X. Y., YANG, G., JIAN, J., WANG, H. S., CHEN, G. Q. & WU, Q. 2011. MicroRNA regulation associated chondrogenesis of mouse MSCs grown on polyhydroxyalkanoates. *Biomaterials*, 32, 6435-44.
- YANG, B., GUO, H., ZHANG, Y., CHEN, L., YING, D. & DONG, S. 2011a. MicroRNA-145 regulates chondrogenic differentiation of mesenchymal stem cells by targeting Sox9. *PLoS One*, 6, e21679.
- YANG, C. Y., CHANALARIS, A. & TROEBERG, L. 2017. ADAMTS and ADAM metalloproteinases in osteoarthritis - looking beyond the 'usual suspects'. *Osteoarthritis and cartilage*, 25, 1000-1009.
- YANG, J., QIN, S., YI, C., MA, G., ZHU, H., ZHOU, W., XIONG, Y., ZHU, X., WANG, Y., HE, L. & GUO, X. 2011b. MiR-140 is co-expressed with Wwp2-C transcript and activated by Sox9 to target Sp1 in maintaining the chondrocyte proliferation. *FEBS Lett*, 585, 2992-7.
- YANG, J. S., PHILLIPS, M. D., BETEL, D., MU, P., VENTURA, A., SIEPEL, A. C., CHEN, K. C. & LAI, E. C. 2011c. Widespread regulatory activity of vertebrate microRNA* species. *Rna*, 17, 312-26.
- YANG, Q., LI, X., ZHOU, Y., FU, W., WANG, J. & WEI, Q. 2019. A LINC00341-mediated regulatory pathway supports chondrocyte survival and may prevent osteoarthritis progression. 120, 10812-10820.
- YANG, Y. D., CHO, H., KOO, J. Y., TAK, M. H., CHO, Y., SHIM, W. S., PARK, S. P., LEE, J., LEE, B., KIM, B. M., RAOUF, R., SHIN, Y. K. & OH, U. 2008. TMEM16A confers receptor-activated calcium-dependent chloride conductance. *Nature*, 455, 1210-5.
- YOO, S.-A., PARK, B.-H., YOON, H.-J., LEE, J.-Y., SONG, J.-H., KIM, H. A., CHO, C.-S. & KIM, W.-U. 2007. Calcineurin modulates the catabolic and anabolic activity of chondrocytes and participates in the progression of experimental osteoarthritis. *Arthritis & Rheumatism*, 56, 2299-2311.
- YU, F., ZHENG, Y., HONG, W., CHEN, B., DONG, P. & ZHENG, J. 2015a. MicroRNA-200a suppresses epithelial-to-mesenchymal transition in rat hepatic stellate cells via GLI family zinc finger 2. *Mol Med Rep*, 12, 8121-8128.
- YU, F. H. & CATTERALL, W. A. 2003. Overview of the voltage-gated sodium channel family. *Genome Biology*, 4, 207.
- YU, F. H. & CATTERALL, W. A. 2004. The VGL-Chanome: A Protein Superfamily Specialized for Electrical Signaling and Ionic Homeostasis. *Science's STKE*, 2004, re15.
- YU, F. H., YAROV-YAROVOY, V., GUTMAN, G. A. & CATTERALL, W. A. 2005. Overview of molecular relationships in the voltage-gated ion channel superfamily. *Pharmacol Rev*, 57, 387-95.
- YU, X., WEI, F., YU, J., ZHAO, H., JIA, L., YE, Y., DU, R., REN, X. & LI, H. 2015b. Matrix metalloproteinase 13: a potential intermediate between low expression of microRNA-125b and increasing metastatic potential of non-small cell lung cancer. *Cancer Genetics*, 208, 76-84.
- ZHANG, J., ZHANG, H. Y., ZHANG, M., QIU, Z. Y., WU, Y. P., CALLAWAY, D. A., JIANG, J. X., LU, L., JING, L., YANG, T. & WANG, M. Q. 2014. Connexin43 hemichannels mediate small molecule exchange between chondrocytes and matrix in biomechanically-stimulated temporomandibular joint cartilage. *Osteoarthritis Cartilage*, 22, 822-30.
- ZHANG, L. & SPECTOR, M. 2009. Comparison of three types of chondrocytes in collagen scaffolds for cartilage tissue engineering. *Biomedical Materials*, 4, 045012.

- ZHANG, X., HUANG, C.-R., PAN, S., PANG, Y., CHEN, Y.-S., ZHA, G.-C., GUO, K.-J. & ZHENG, X. 2020. Long non-coding RNA SNHG15 is a competing endogenous RNA of miR-141-3p that prevents osteoarthritis progression by upregulating BCL2L13 expression. *International Immunopharmacology*, 83, 106425.
- ZHANG, X. H., ZHENG, B., YANG, Z., HE, M., YUE, L. Y., ZHANG, R. N., ZHANG, M., ZHANG, W., ZHANG, X. & WEN, J. K. 2015. TMEM16A and myocardin form a positive feedback loop that is disrupted by KLF5 during Ang II-induced vascular remodeling. *Hypertension*, 66, 412-21.
- ZHANG, Z., QIN, Y.-W., BREWER, G. & JING, Q. 2012. MicroRNA degradation and turnover: regulating the regulators. *Wiley interdisciplinary reviews. RNA*, 3, 593-600.
- ZHAO, S., WANG, Z., CHEN, J. & CHEN, J. 2015. Preparation of heparan sulfate-like polysaccharide and application in stem cell chondrogenic differentiation. *Carbohydrate Research*, 401, 32-38.
- ZHENG, Q., ZHOU, G., MORELLO, R., CHEN, Y., GARCIA-ROJAS, X. & LEE, B. 2003. Type X collagen gene regulation by Runx2 contributes directly to its hypertrophic chondrocyte-specific expression in vivo. *The Journal of cell biology*, 162, 833-842.
- ZHOU, S., CUI, Z. & URBAN, J. P. G. 2004. Factors influencing the oxygen concentration gradient from the synovial surface of articular cartilage to the cartilage–bone interface: A modeling study. 50, 3915-3924.